

## **ABSTRACT**

Title of Document: **RELEASE OF INORGANIC AND ORGANIC CONTAMINANTS FROM FLY ASH AMENDED PERMEABLE REACTIVE BARRIERS**

Doina Lorena Morar, Master of Science, 2008

Directed By: Dr. Ahmet H. Aydilek, Department of Civil and Environmental Engineering  
Dr. Eric A. Seagren, Department of Civil and Environmental Engineering

Large quantities of fly ash are generated in the United States via coal combustion, most of which is disposed of in lagoons or landfills. The overall goal of this research was to assess the feasibility of using high carbon content (HCC) fly ashes as a reactive medium in permeable reactive barriers (PRBs) for remediation of petroleum hydrocarbon contaminated groundwater. A series of column and batch tests were performed to evaluate the leaching of selected metals from the fly ash, and adsorption/desorption of two target hydrocarbons (naphthalene and *o*-xylene) onto/from this PRB medium. Leaching of metals in the column experiments exhibited a first-flush, followed by a tailing slope elution pattern for all fly ashes. The naphthalene and *o*-xylene adsorption/desorption on/from the fly ashes were directly correlated with the organic carbon of the fly ash as measured by loss in ignition. Adsorption/desorption hysteresis was obvious in column and batch tests, suggesting that the adsorption/desorption was not completely reversible during the testing.

**RELEASE OF INORGANIC AND ORGANIC CONTAMINANTS FROM  
FLY ASH AMENDED PERMEABLE REACTIVE BARRIERS**

By

**Doina Lorena Morar**

**Thesis submitted to the Faculty of the Graduate School of the  
University of Maryland, College Park, in partial fulfillment  
of the requirements for the degree of  
Master of Science  
2008**

**Advisory Committee:**

**Dr. Ahmet H. Aydilek, Advisor**

**Dr. Eric A. Seagren, Advisor**

**Dr. Allen P. Davis, Committee member**

**© Copyright by  
Doina Lorena Morar  
2008**

## ACKNOWLEDGEMENTS

I would like to gratefully acknowledge the Maryland Department of Natural Resources, who offered the grant which made this research possible. Then I would like to express my gratitude toward few academic constituencies who offered their support on different aspects of the project. Most importantly, I would like to manifest my gratitude toward my two advisors, Dr. Ahmet Aydilek and Dr. Eric Seagren, for their excellent guidance, support, advice and extensive patience, during my time as graduate research assistant. I am also grateful to Dr. Allen Davis for serving on the examination committee at the defense of my thesis, and for his invaluable advice during the research, and to Dr. Bruce James for his advice and assistance in demonstrating lab equipment and procedures. I deeply appreciate the emotional and intellectual support provided by my dear friend, office colleague and lab-mate Joan, who made my graduate life bearable. I would like to also express my gratitude toward my lab-mates who kindly shared with me and demonstrated to me the procedures for using the lab equipment: Melih, Lan, Hounq Li, Phil, Eliea, and Eunyoung. My appreciation extends to our department administrative staff; without their support none of this would have been possible.

My love and appreciation extend to my wonderful family, especially to my mom and my brother who although they missed me enormously during this time, they motivated, supported, and encouraged me when it was most needed. My father would be very proud of me too, and I am sure that from above he watched over me at all times. I want to thank him for his love and guidance through which I got to be who I am today. I am forever indebted to my American host family: Jim, Amanda and their three lovely daughters: Samantha, Elizabeth and Jessica, for their love and moral, motivational, and financial support. Without them I probably would not even be here. Also I would like to express my love and appreciation toward my wonderful friends for their understanding, moral support, and encouragements.

Not lastly, but firstly I would like to express my gratitude to the marvelous Creator, who enabled me to explore and understand a minuscule part of his creation.

## TABLE OF CONTENTS

<b>LIST OF FIGURES .....</b>	<b>V</b>
<b>LIST OF TABLES .....</b>	<b>II X</b>
<b>CHAPTER 1. INTRODUCTION .....</b>	<b>1</b>
<b>CHAPTER 2. LITERATURE REVIEW .....</b>	<b>5</b>
2.1. PETROLEUM SPILLS AS AN ENVIRONMENTAL PROBLEM AND REMEDICATION TECHNOLOGIES .....	5
2.2. FLY ASH .....	10
2.3. LEACHING MECHANISM AND FACTORS INFLUENCING LEACHING OF METALS .....	14
2.4. LABORATORY LEACHING STUDIES .....	19
2.4.1. Batch Water Leach Tests (WLT).....	20
2.4.2. Column leaching tests .....	24
2.5. LEACHING MECHANISM AND FACTORS INFLUENCING DESORPTION OF ORGANICS .....	26
2.6. LABORATORY DESORPTION TESTS.....	30
2.6.1. Batch desorption of organics tests .....	31
2.6.2. Column leaching of organics tests .....	33
<b>CHAPTER 3. MATERIALS AND METHODS.....</b>	<b>35</b>
3.1. MATERIALS.....	35
3.1.1. Solid materials .....	35

3.1.1.1. Fly ashes.....	35
3.1.1.1.a. Sources of fly ashes.....	35
3.1.1.1.b. Chemistry and physical properties of fly ashes .....	37
3.1.1.2. Sand.....	42
3.1.1.3. Powder Activated Carbon (PAC): .....	42
3.1.2. Aqueous phase .....	44
3.1.2.1. Synthetic groundwater recipe .....	44
3.2. REACTOR SYSTEMS.....	46
3.2.1. Batch test experimental set up .....	46
3.2.2. Column tests and experimental set up .....	46
3.3. METAL LEACH TESTS.....	53
3.3.1. Batch–Water Leach Test (WLT) .....	53
3.3.2. Column leach tests .....	55
3.4. ORGANIC CONTAMINANTS DESORPTION TESTS.....	55
3.4.1. Sequential desorption of organics – Batch test.....	56
3.4.2. Column for desorption of organics test.....	59
3.5. ANALYTICAL METHODS .....	60
3.5.1. pH determination .....	60
3.5.2. Bromide analysis in tracer test samples.....	61
3.5.3. Determination of metal concentrations by Atomic Absorption Spectrophotometry .....	62
3.5.4. Organics determination by fluorescence analysis.....	67
3.6. MATHEMATICAL MODELS.....	67

<b>CHAPTER 4. EVALUATION OF TRANSPORT PARAMETERS IN COLUMN TESTS .....</b>	<b>75</b>
<b>CHAPTER 5. METAL CONTAMINANTS - RESULTS AND DISCUSSIONS</b>	<b>86</b>
5.1. BATCH WATER LEACHING TESTS.....	86
5.2. COLUMN LEACHING TESTS RESULTS.....	103
5.2.1. pH measurements.....	103
5.2.2. van Genuchten (1981) and Fry et al. (1993) models .....	105
5.2.2.1. Metal Concentrations.....	108
5.3. RELATIONSHIP BETWEEN WLTS AND CLTS RESULTS .....	117
<b>CHAPTER 6. ORGANIC CONTAMINANTS - RESULTS AND DISCUSSIONS</b>	<b>127</b>
.....	
6.1. BATCH TESTS – RESULTS AND DISCUSSIONS .....	127
6.1.1. Batch adsorption tests .....	127
6.1.2. Batch sequential desorption tests.....	137
6.2. COLUMN ADSORPTION/DESORPTION TESTS .....	148
6.2.1. Column Adsorption Test Results.....	149
6.2.2 Column Desorption Test Results .....	152
6.3. COMPARISON OF RESULTS FROM BATCH AND COLUMN TESTS .	162
<b>CHAPTER 7. CONCLUSIONS AND RECOMMENDATIONS .....</b>	<b>166</b>
7.1. SUMMARY AND CONCLUSIONS .....	166
7.2. PRACTICAL IMPLICATIONS .....	169_Toc188942696
<b>APPENDIX 1 .....</b>	<b>172</b>
<b>REFERENCES.....</b>	<b>183</b>

## LIST OF FIGURES

Figure 2. 1. Schematic representation of a PRB .....	9
Figure 2. 2. pe-pH diagrams for aqueous (a) arsenic and (b) selenium species .....	17
Figure 2. 3. pE-pH relationship for dissolved aqueous Cr species .....	18
Figure 2. 4. Aluminum solubility vs pH .....	18
Figure 3. 1. Locations of power plants .....	36
Figure 3. 2. Grain size distribution of the seven fly ashes and sand .....	41
Figure 3. 3. Image of a packed column with the three porous media layers .....	48
Figure 3. 4. Schematic of the column experiment set up.....	48
Figure 3. 5. Transversal section through the mixture layer of column specimens .....	52
Figure 4. 1. Observed and modeled bromide tracer breakthrough and washout curves for the 40% Potomac River fly ash/60% sand column. ....	78
Figure 4. 2. Observed and modeled bromide tracer breakthrough and washout curves for the 40% Dickerson Precipitator fly ash/60% sand column. ....	79
Figure 4. 3. The bromide tracer input and inverted washout curves for the 40% Potomac River fly ash/60% sand mixture column.....	80
Figure 4. 4. The bromide tracer input and inverted washout curves for the 40% Dickerson Precipitator fly ash/60% sand mixture column. ....	81
Figure 5. 1. Aluminum aqueous concentrations in WLTs conducted with deionized water with ionic strength fixed (IS=0.02M) on different sand-fly ash mixtures.....	88
Figure 5. 2. Aluminum aqueous concentrations in WLTs conducted with artificial groundwater solution on different sand-fly ash mixtures. ....	89
Figure 5. 3. Arsenic aqueous concentrations in WLTs conducted with deionized water with ionic strength fixed (IS=0.02M) on different sand-fly ash mixture	90



Figure 5. 4. Arsenic aqueous concentrations in WLTs conducted with artificial groundwater solution on different sand-fly ash mixtures. ....	91
Figure 5. 5. Chromium aqueous concentrations in WLTs conducted with deionized water with ionic strength fixed (IS=0.02M) on different sand-fly ash mixtures.....	92
Figure 5. 6. Chromium aqueous concentrations in WLTs conducted with artificial groundwater solution on different sand-fly ash mixtures .....	93
Figure 5. 7. Selenium aqueous concentrations in WLTs conducted with deionized water with ionic strength fixed (IS=0.02M) on different sand-fly ash mixtures.....	94
Figure 5. 8. Selenium aqueous concentrations in WLTs conducted with artificial groundwater solution on different sand-fly ash mixtures. ....	95
Figure 5. 9. pC – pH diagram for aluminum from WLTs with a) deionized water and b) groundwater .....	98
Figure 5. 10. Relationship between the WLTs conducted with groundwater and with deionized water for aluminum.. ....	99
Figure 5. 11. Relationship between the WLTs conducted with groundwater and with deionized water for arsenic. ....	100
Figure 5. 12. Relationship between the WLTs conducted with groundwater and with deionized water for chromium. ....	101
Figure 5. 13. Relationship between the WLTs conducted with groundwater and with deionized water for selenium. ....	102
Figure 5. 14. pH in the CLTs.. ....	104
Figure 5. 15. Predictions of the two analytical solutions for a) 40% Potomac River / 60% Sand and b) 40% Brandon Shores / 60% Sand column data. ....	107
Figure 5. 16. Elution curves for aluminum from CLTs.. ....	111
Figure 5. 17. Elution curves for arsenic from CLTs. ....	112
Figure 5. 18. Elution curves for chromium from CLTs.....	113
Figure 5. 19. Elution curves for selenium from CLTs.....	114

Figure 5. 20. Comparison of the peak initial effluent concentrations from CLTs and aqueous concentrations from WLTs for 60% sand + 40% fly ash mixtures: (a) Al, (b)As, (c) Cr, and (d) Se.....	119
Figure 5.20. (Continued) Comparison of the peak initial effluent concentrations from CLTs and aqueous concentrations from WLTs for 60% sand + 40% fly ash mixtures: (a) Al, (b)As, (c) Cr, and (d) Se.....	120
Figure 5. 21. Comparison of the actual leached amounts from CLTs to the predicted ones from .... WLTs for 60% sand + 40% fly ash mixtures: (a) Al, (b)As, (c) Cr, and (d) Se.....	123
Figure 5. 21. (Continued) Comparison of the actual leached amounts from CLTs to the predicted ones from WLTs for 60% sand + 40% fly ash mixtures: (a) Al, (b)As, (c) Cr, and (d) Se. ....	124
Figure 6. 1. Schematic of possible pathways for sorption of an organic molecule onto the organic matrices of a sorbing material.....	131
Figure 6. 2. Grain size distribution for Dickerson Precipitator, Paul Smith and Morgantown fly ash.....	132
Figure 6. 3. Adsorption isotherms with best fit models after a) naphthalene and b) o-xylene adsorption experiments with Dickerson Precipitator, Paul Smith and Morgantown fly ash. ....	133
Figure 6. 4. Change in solid phase concentration of a) naphthalene and b) o-xylene after each desorption step.....	142
Figure 6. 5. Total solute desorbed from successive desorption steps from a) Dickerson Precipitator; b) Paul Smith; c) Morgantown fly ashes.....	143
Figure 6. 6. Desorption isotherms with best fit models after a) naphthalene and b) o-xylene sequential desorption experiments with Dickerson Precipitator, Paul Smith and Morgantown fly ash.....	144
Figure 6. 7. Adsorption/desorption scheme of organic compounds on solid sorbent	147
Figure 6. 8. Sorption-desorption elution curves for a) naphthalene, and b) o-xylene from the 40% Morgantown fly ash + 60% sand column. ....	155
Figure 6. 9 Sorption-desorption elution curves for of a) naphthalene, and b) o-xylene from the 40% Paul Smith fly ash + 60% sand column. ....	156
Figure 6. 10. Sorption-desorption elution curves for a) naphthalene, and b) o-xylene from the 40% Dickerson Precipitator fly ash + 60% sand column.....	157

Figure 6. 11. Sorption-desorption elution curves for of a) naphthalene, and b) o-xylene from the 6% PAC fly ash + 94% sand column. ....	158
Figure 6. 12. Sorption-desorption elution curves for naphthalene from the sand column.....	159
Figure 6. 13. Effluent concentrations for a) naphthalene, and b) o-xylene from the fly ash and PAC columns.. ....	160
Figure 6. 14. $K_d - f_{oc}$ correlations in batch adsorption, desorption and column adsorption/desorption tests with a) naphthalene and b) o-xylene. ....	165
Figure A. 3. Observed and modeled bromide tracer breakthrough and washout curves for the 40% Morgantown fly ash / 60% sand column. ....	179
Figure A. 4. Observed and modeled bromide tracer breakthrough and washout curves for the 6% PAC / 96% sand column. ....	179
Figure A. 5. Observed and modeled bromide tracer breakthrough and washout curves for the 40% Paul Smith fly ash / 60% sand column. ....	180
Figure A. 7. Observed and modeled bromide tracer breakthrough and washout curves for the 40% Potomac River fly ash / 60% sand column. The sampling was conducted at the effluent port only. ....	181
Figure A. 8. Observed and modeled bromide tracer breakthrough and washout curves for the 40% Brandon Shores fly ash / 60% sand column.. ....	181
Figure A. 9. Observed and modeled bromide tracer breakthrough and washout curves for the 40% Chalk Point fly ash / 60% sand column. ....	182
Figure A. 10. Observed and modeled bromide tracer breakthrough and washout curves for the 40% Dickerson Baghouse fly ash / 60% sand column..	182

## LIST OF TABLES

Table 2. 1. Chemical Requirements for Fly Ash Classification .....	11
Table 3. 1 Major minerals and their concentrations determined by X-ray diffraction	38
Table 3. 2. Specific gravity of the seven fly ashes.....	40
Table 3. 3. pH of the seven fly ashes .....	40
Table 3. 4. Chemical composition of the sand used in the study.....	43
Table 3. 5. Grain size distribution of PAC particles.....	43
Table 3. 6. Mineral composition of the groundwater (from Murphy et al. 1997) .....	45
Table 3. 7. Operating parameters for arsenic determination on HGAAS.....	65
Table 4. 1. Flow and transport related properties of specimens used in column experiments.....	83
Table 4. 2. Constant – head hydraulic conductivity test results.....	85
Table 5. 1. Aqueous concentrations of metals from WLTs with fly ash alone and sand-fly ash mixtures .....	87
Table 5. 2. Metals leaching parameters from CLTs.....	110
Table 5. 3. Peak initial metal concentrations from column leaching tests.....	115
Table 5. 4. Comparison of the peak CLTs concentrations and corresponding aqueous WLTs concentration against the EPA MCL and WQL .....	126
Table 6. 1. Summary of results from batch adsorption experiments .....	128
Table 6. 2. Correlation between carbon content and specific surface area of fly ash	132
Table 6. 3. Adsorption isotherms parameters from batch adsorption tests.....	134
Table 6. 4. Physicochemical properties of naphthalene and o-xylene .....	136

Table 6. 5. Summary of results from batch sequential desorption experiments .....	140
Table 6. 6. Desorption isotherm parameters from batch sequential desorption tests	145
Table 6. 7 Summary of column adsorption/desorption test results.....	151
Table 6. 8. Sorption/Desorption isotherm parameters from column tests .....	164

# **CHAPTER 1**

## **INTRODUCTION**

Over 60% of the electricity generated in United States is produced by coal combustion, with resulting abundant quantities of fly ash (about 68 million tons in 2001) as residue. Of that fly ash only about 38% is currently recycled or reused in different beneficial applications (Sajwan et al. 2006), and the remainder is disposed in lagoons or stockpiled on landfills.

Taking a closer look at the local scale, the amount of unburned carbon constituent present in Maryland fly ashes has been increasing in the last decade due to introduction of low nitrogen oxide burners to coal-burning power plants. The twelve power plants in Maryland produce about 600,000 tons of high carbon content (HCC) Class F fly ash annually. Unfortunately Class F fly ash cannot be used in construction applications because it has no value as a concrete additive, lacking the required pozzolanic properties due to its high carbon content. As a result it is currently land-filled or impounded, consuming valuable landfill space and imposing serious concerns related to the effects on the environment. For example, some concerns have been expressed vis-à-vis detrimental leachability of heavy metals from the disposed ash into the environment (soils, water bodies, groundwater). Such leaching of metals could create potential human health hazards, and negative impacts on the

environment related to their potential for cumulative build-up and their long life in the environment.

In their concerted efforts to solve this problem, the Maryland Department of Natural Resources Power Plant Research Program (MDNR PPRP) initiated a series of demonstration projects to facilitate and encourage the reuse of this abundantly available residual material, HCC fly ash. The present study is one of their attempts to increase awareness and renew emphasis on beneficial reuse of fly ashes in different applications. In addition, legislation has been promulgated to remove barriers to large-scale beneficial reuse of fly ashes. A regulatory framework was implemented by which fly ash was excluded from the waste definition in the Resource Conservation and Recovery Act (RCRA) (1976), authorizing the reuse of fly ash with no special handling requirements, but in environmentally safe conditions.

Another contemporary environmental challenge is posted by petroleum spills from leaking underground storage tanks or from accidental releases, which are considered to be major threats to groundwater quality (Meegoda 1999). Finding efficient and cost effective remediation strategies for groundwater contaminated with petroleum products has been a challenging task in the recent years. Recently, there has been strong interest in using industrial by-products as part of reactive media in permeable reactive barriers (PRBs) applications for remediation of groundwater plumes contaminated with different organic pollutants (Blowes and Ptacek 1992, Powell and Puls 1997, Powell and Powell 1998).

These two serious environmental issues – production of fly ash residues and petroleum hydrocarbon contamination of groundwater – can be coupled together to

result in beneficial outcomes. Specifically, the mechanism of action in PRBs is based on the phenomenon of surface-related adsorption of organic contaminants. The major source of surface area in the fly ash is represented by its carbon content. Hence, the higher unburned carbon content (e.g., loss on ignition, LOI %) in the HCC fly ashes generally results in larger surface area available for adsorption of organics. Therefore, high carbon content fly ash is a good candidate as an adsorbent for organics. Moreover, it can be used as reactive media in PRBs for purification of contaminated waters, as an alternative clean-up treatment for remediation of groundwater polluted with organic contaminants.

The primary goal of this research program was to assess the feasibility of using HCC Maryland fly ashes for PRB applications in remediation of contaminated groundwater bodies with petroleum hydrocarbon products. To evaluate the suitability of this abundantly available waste material for use as a reactive/sorptive media in construction of PRBs, several key issues need to be addressed. First, the metals leaching behavior from HCC fly ashes must be evaluated. In other words, what fraction of metals present in the fly ash can be removed by leaching. Although there are numerous studies focused on leaching of metals behavior from fly ashes designated to be used in geotechnical, construction applications, not much literature exists on leaching of metals from HCC fly ash in a PRB application. Second, information is lacking regarding the efficiency of HCC in retarding the movement of organic pollutants in petroleum-contaminated soils and the suitability of HCC for use in PRBs. Generally, the key desirable characteristics of the reactive media in a PRB are that it should: have a long lasting and high sorption capacity for organics,



maintain consistent porosity and permeability over its lifetime, not cause adverse chemical reactions, and not act as a potential source of contaminants itself. In order to address and achieve the goals of this project, several different tasks were conducted: 1) short term batch water leaching of metals tests, 2) bench scale sequential batch desorption of organics tests, 3) long term column leaching of metals experiments, 4) laboratory column experiments for desorption of organics, 5) tracer studies on the column experiments for evaluation of transport parameters, and 6) numerical modeling of column data for the metal leaching.

The details of this project are described in the following chapters. In Chapter 2, the literature is reviewed regarding the following key topics relevant to this research: petroleum spills as an environmental problem and remediation technologies proposed; the origin, properties and beneficial use of fly ashes; leaching mechanisms, factors influencing leaching of metals and laboratory leaching studies; and desorption mechanisms, factors influencing desorption of organic contaminants from sorptive barriers, and laboratory studies on desorption of organics. Chapter 3 includes the materials used in the testing process, describes in a detailed manner the methodologies used and experimental set-ups, and presents the analytical solutions used for modeling of the column leaching data. In Chapter 4, the evaluation of transport parameters in the column tests is described. The results of the tests for the leaching of metals and desorption of organic contaminants from fly ash are presented and discussed in Chapters 5 and 6, respectively. Finally, a summary of the findings and the conclusions of the current investigation, along with the recommendations for further research, are presented in Chapter 7.

## **CHAPTER 2**

### **LITERATURE REVIEW**

#### **2.1. PETROLEUM SPILLS AS AN ENVIRONMENTAL PROBLEM AND REMEDIATION TECHNOLOGIES**

Accidental releases of petroleum products occur frequently throughout highly populated urban areas around the world. Petroleum spills from leaking underground storage tanks is considered to be one of the main threats to groundwater quality in nowadays. Mismanagement, improper installation, inadequate design, poor maintenance, corrosion and overfilling of the tanks storing petroleum products and piping failures can result in leaks and spills, posing serious threats to the human health, wildlife, and environment. Numerous drinking water supplies were closed because of excessive contamination with petroleum products. Statistically, it has been estimated that about 25-30% of the underground storage tanks on the United States territory are leaking (Meegoda et al. 1999). Most of these tanks were installed prior to the new EPA regulations (1988) which, in order to prevent eventual leaks, require that all buried underground storage tanks to be replaced with tanks with double-lining, or to be upgraded to meet minimum design standards established by EPA. However, since this has not happened everywhere yet, serious environmental damages from such releases still occur, and hazardous products seep through the soil, eventually reaching groundwater. As a result, the water is contaminated with

chemicals very difficult to clean to the minimum contaminant level (MCL) required by EPA, making water supplies unsafe to drink.

Federal law and regulatory agencies require the responsible party for the spill to select a clean-up technology and to take the correction action for the removal or treatment of the contamination. Heavier components of petroleum products such as organics like benzene, toluene, xylenes, naphthalene, appear to cause the most damage because, although they are less toxic, they persist in the environment longer than volatile organic components, requiring costly remediation strategies. Several remediation technologies were developed over the years for contamination cleanup and they can be divided into two broad categories: remediation technologies designed to treat or remove contaminants and technologies designed to restrict movement of contaminants in soil (e.g., Permeable Reactive Barriers) (Singh and Naik 1997).

Ex-situ clean-up technologies are part of the first category and involve excavation and removal of vast volumes of contaminated soils, followed by ex-situ treatments like thermal desorption of organics (Smith et al. 2001), microbial remediation (bioremediation) (Aislabie et al. 2006), soil washing (Shiw and Naik 1997, Berselli et al. 2006), and biopiles and composting (Jorgensen et al. 2000, Li et al. 2002). Several in-situ remediation technologies are included as well in this first category, such as bioventing (Origgi et al. 1997, Vallejo et al. 2001, Lee et al. 2006), air sparging (Braida and Ong 2001), phytoremediation (plant-assisted bioremediation) (Chang and Corapcioglu 1998, Macek et al. 2000, Alkorta and Garbisu 2001), bioremediation (Parker and Burgos 1999), landfarming (McCarthy et al. 2004), and monitored natural attenuation. Because many of this strategies have proven to be inefficient in some cases and/or very expensive, and/or not to be technically feasible,

lately, serious emphasis has been placed on encouraging researchers for technological advancement in the assessment of strategies to use the solid wastes (by-products) resulted from different industries in construction of in-situ permeable reactive barriers (PRBs) designed for the uptake and adoption of contaminants (Powell and Puls 1997; Powell and Powell 1998). Precisely to encourage this action, laws have been enacted to eliminate barriers regarding beneficial and safe re-use of solid residues in geotechnical applications (constructions) and environmental applications (remediation strategies). This action brings several benefits including the development of beneficial reuse applications for the abundant solid residues produced by industries which currently represent a challenge in terms of storage in environmentally safe conditions.

The use of permeable reactive barriers (PRBs) (Figure 2.1) in remediation of a plume of contaminated groundwater has been recognized by U.S. EPA to be one of the most promising innovative solutions with high potential to efficiently restrict the movement of contaminants in soils and remove contamination at significant cost savings as compared to other remediation strategies. The concept of PRB involves the emplacement of a permeable barrier in the subsurface in the pathway of a plume of contaminated groundwater and as it flows through the barrier wall under its natural gradient the contaminants are either immobilized or chemically transformed into environmentally friendly (harmless) compounds (Powell and Puls 1997, Powell and Powell 1998). The main desirable characteristics of the reactive media are: the material should not be easily soluble, it should be compatible with the contaminant remediated having the ability to either immobilize it or to transform it into harmless

form, it should persist over long times, it should allow the groundwater flow to perform at its natural gradient, it should not cause adverse chemical reactions, and it should not act as a potential source of contaminants itself.

The very first full-scale PRB system constructed as in-situ remediation strategy was in 1994 in California, being approved for construction by the San Francisco Regional Water Quality Control Board. Since then, many other PRBs were installed in the field for treatment of plumes polluted with different organic compounds, and toxic heavy metals using zero-valent iron as reactive medium (Blowes et al. 1995, Robert et al. 1996, Benner et al. 1997, Eykholt and Davenport 1998, Francis and Dodge 1998, Shokes and Moller 1999, Su and Puls 2001).

As mentioned above, there is a strong interest in using industrial by-products as part of reactive media in PRBs. A variety of by-products such as foundry sand, wood chips, tire chips, compost have been used as sorptive/reactive media for remediation of plumes contaminated with different organics (Kim et al. 1997, Lee et al. 2002, Edil et al. 2004,). Most of these materials include significant amounts of organic carbon which act as a good sorptive medium for the contaminant of interest.

The high levels of carbon contents may offer new opportunities for ash re-utilization and a particular attention is oriented in this study toward the potential for high carbon content fly ashes to be utilized as barrier material in remediation and treatment of groundwater contaminated with organic compounds. "It is the "organic" portion of the ash, the unburned carbon, which may be the key to success in many new utilization schemes" (Hurt and Suuberg 1997).

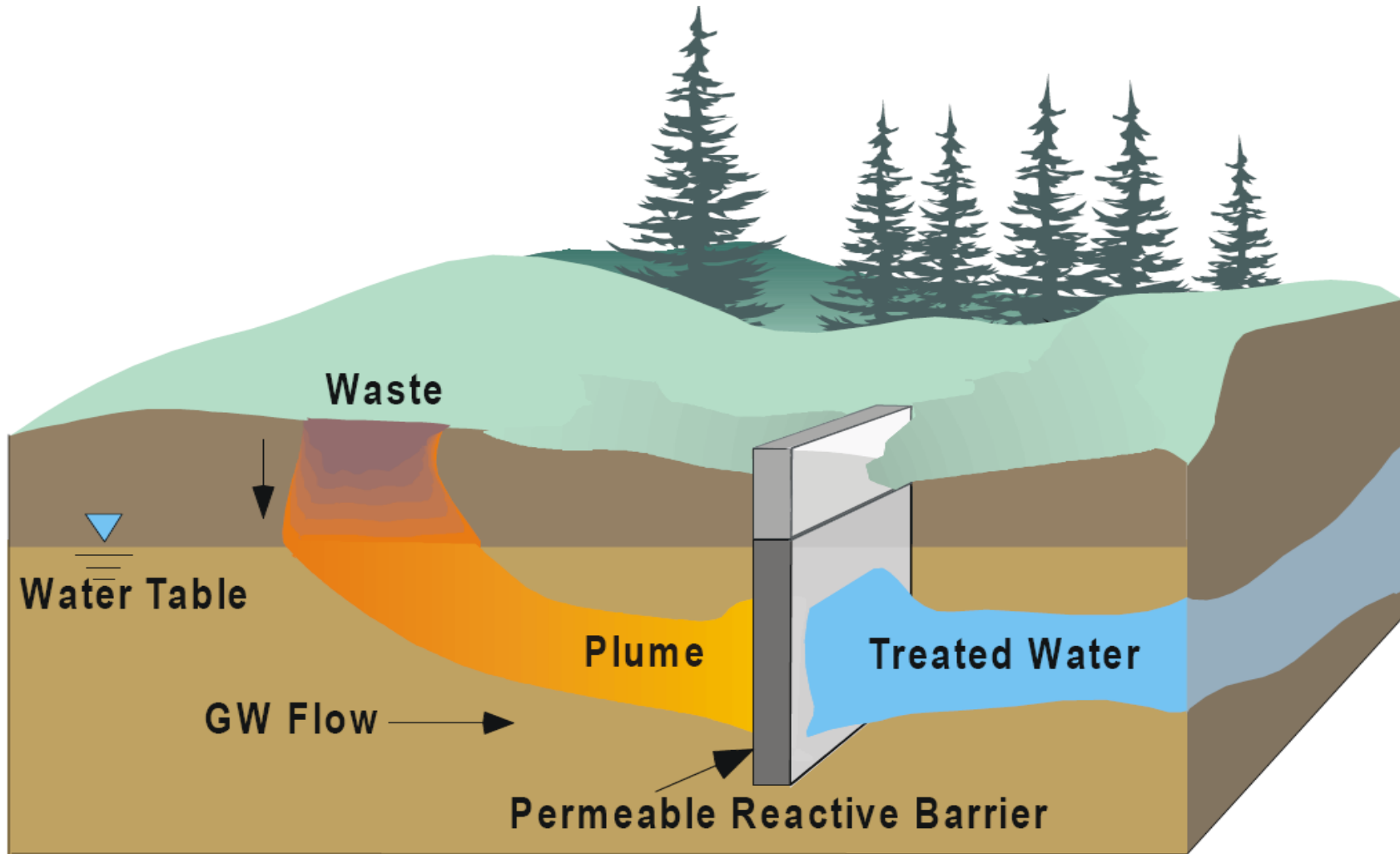


Figure 2. 1. Schematic representation of a PRB ( <http://www.powellassociates.com/sciserv>).

## 2.2. FLY ASH

Fly ash is the by-product carried off in the stack gasses generated during the burning of coal in electrical power plants. Over 110.4 millions metric tons of coal combustion by-products (Sajwan et al. 2006) of which 68 millions tons of fly ash, were produced in 2001, according to the American Coal Association (ACA) and is considered to be the fourth largest mineral resource produced in US. Only about 38.1% of it is currently recycled or reused in different beneficial applications (road embankments, restoration of eroded terrains, agriculture, waste stabilization/solidification), and the remainder (~ 62%) is disposed in lagoons or stockpiled on landfills (Punshon et al. 1999, Sajwan et al. 2006). To facilitate and encourage the reuse of this residual material, a regulatory framework was enforced by which fly ash was exempted from the waste definition in the Resource Conservation and Recovery Act (RCRA) (1976), subtitle C, section 3001, permitting the reuse of fly ash with no special handling requirements, but in environmentally safe conditions (Twardowska and Stefaniak 2006).

According to ASTM C 618, fly ashes can be classified in two categories (classes) based on their chemical composition: class F fly ash and class C fly ash, the difference between them being evidenced by the weight percentage concentration of the mixture of silicon dioxide ( $\text{SiO}_2$ ), aluminum oxide ( $\text{Al}_2\text{O}_3$ ), and iron oxide ( $\text{Fe}_2\text{O}_3$ ), and by the concentration of calcium (as  $\text{CaO}$ ) (typically higher in type C fly ashes (Cockrell et. al. 1970). Table 2.1 lists the most important chemical requirements for fly ash classification. Type F fly ash is generated in combustion of anthracite and

**Table 2. 1. Chemical Requirements for Fly Ash Classification**  
 ([http://geoserver.cee.wisc.edu/fauga/new\\_page\\_1.htm](http://geoserver.cee.wisc.edu/fauga/new_page_1.htm))

Properties	Fly Ash Class	
	Class F	Class C
Silicon dioxide (SiO <sub>2</sub> ) plus aluminum oxide (Al <sub>2</sub> O <sub>3</sub> ) plus iron oxide (Fe <sub>2</sub> O <sub>3</sub> ), min, %	70.0	50.0
Sulfur trioxide (SO <sub>3</sub> ), max, %	5.0	5.0
Moisture Content, max, %	3.0	3.0
Loss on ignition, max, %	6.0*	6.0

\* The use of class F fly ash containing up to 12% loss of ignition may be approved by the user if acceptable performance results are available



bituminous coals, while type C fly ash is generated by combustion of lignite and sub-bituminous coals. In the current investigation, special attention was given to class F fly ash, because this type of fly ash is mainly generated in large quantities by most of the electrical power plants in Maryland (about 600,000 tons of high carbon content class F fly ash are being produced each year). Almost all of these fly ashes are disposed on lagoons and landfills as they cannot be reused efficiently in construction applications. Concrete industry is the largest consumer of fly ashes, however, high carbon content (LOI > 6%) ashes are typically avoided due to interferences with the air entrapment agents.

Class F fly ashes are glassy fine-grained particulates with typical particle sizes ranging between 0.1 and 1  $\mu\text{m}$  (Sajwan et al. 2006). Several types of spherical grain forms have been discovered to possibly exist in its texture: cenospheres (hollow spherical shells), plerospheres (hollow spheres incorporating smaller spheres), spheres with internal or external crystals, spheres with vesicles, and also solid spheres (Fisher and Natusch 1979, Dudas and Waren 1987). The pozzolanic character of class F fly ashes is revealed by their ability to form cementitious complexes in the presence of moisture (Manz 1999). Color is one relevant qualitative indicator in terms of estimating the lime content and/or organic content of the fly ash. Cockrell et al. (1970) concluded in their study that lighter color points toward the presence of high lime and low carbon contents, whereas darker colors imply high organic content for organics. Surface area of the fly ash is another valuable indice of the adsorption capacity of fly ashes, since adsorption process is a surface-related phenomenon (Sarkar and Acharya 2006). Smith et al. (1997) concluded in their study that the primary adsorption sites for organics are located on the surface of the

carbon present in the fly ash. As the major source of surface area in the fly ash is represented by its carbon content (Hurt et al. 1997), it can be concluded that higher unburned carbon content (loss on ignition, LOI %) in the fly ash generally results in larger surface area that is accessible for adsorption of organics. It has been observed that the carbon in the fly ash has a much greater surface area that is suggested by the external geometry of the fly ash particle, and that is due to the internal porosity of the carbon particles. The surface area of the type F fly ash carbon typically ranges from 30 to 70 m<sup>2</sup>/g, which is considerably larger than the surface area of the inorganic components of the fly ash (about 0.8 m<sup>2</sup>/g) (Külaots et al. 1998).

The use of adsorption phenomenon for purification of waters contaminated with organic compounds is quite a popular treatment technique, and as it can be observed from the drawn conclusions of the studies mentioned above, all the beneficial engineering properties revealed there designate the high carbon content fly ash to be a good candidate as a sorbent for organics, and subsequently to be used as an alternative clean-up treatment for remediation of groundwater polluted with organic contaminants. However, some concerns have been expressed regarding the use of fly ash in such applications related to the concerns vis-à-vis undesirable release of toxic constituents (e.g., As, Cr, Se, Cd, Cu, Pb) from fly ash into the environment. Several researchers performed leaching studies to investigate the mechanisms and the potential levels of heavy metals release from different waste (solid) materials simulating the expected environmental conditions. These studies are summarized in the sections below.

### **2.3. LEACHING MECHANISM AND FACTORS INFLUENCING LEACHING OF METALS**

The most important parameters that control the leaching of metals from solids surfaces are: pH, solubility of metals, redox, solid-to-liquid ratio, presence and speciation of organic ligands, characteristics of the background electrolyte (ionic strength, pH), characteristics of solid phase (specific surface area of the solid particles, total metal concentration in solid phase, point of zero charge), cation exchange capacity, speciation, contact time between the solid and the leachant, and flow rate of the leachant. However, the influence of each parameter may be more pronounced in one material than in another, and from one leachant to another (van der Sloot 1996).

When leaching solution seeps into the solid material, the micropores of the particles are saturated and the soluble metal species within the solid matrix are immobilized. As result, the chemical potential is increased and releases of the heavy metals into the solution occur. The concentration gradient is the driving force which determines the abundant migration of metal species within the matrix in the surrounding solution until an equilibrium is established between the solid and liquid phase. Once the equilibrium is reached, the exchange of species between the solid and the leaching solution still continues but at a constant rate to keep the system in balance (Ogunro and Inyang 2003). Then, the so called, first flush phenomenon happens when a large concentration of metals is being washed off from the fly ash while the initial percolation of the metal-free leachant through the porous media (Bowders et al. 1990, Goswami and Mahanta 2007). Creek (1991) showed that most of the traced metals in fly ash showed “early leaching behavior” indicating that the largest part of metal concentrations were

leached out in the initial pore volumes of flow. This behavior may be explained by the findings of other researchers who suggested that most of the metal species are easily displaced and dissolved into the solution due to the fact that these species are located on the exterior of the spherical glass-like particles (DiGioia et al. 1986) and that they are just loosely bound on the surface of the fly ash (Chu et al. 1978, Santhanam et al. 1979) and are chemically more active (Theis et al. 1977). The findings of the same studies showed that the high concentration of adsorbed metal species exposed to the leaching solution, and so the higher potential for leaching (release into the solution) is related to relatively large surface area of fly ashes.

At the same time, the distribution of the active surface species has a significant input on leaching behavior of metals, and this is closely related to the point of zero charge factor ( $\text{pH}_{\text{zpc}}$ ) (i.e., the pH at which the positively charged surface species are in perfect balance with the negatively charged surface species, so the net surface charge of the solid surface is zero). This factor delineates the availability of negatively or positively charged surface species for complexation with the positively charged cations or negatively charged anions. Allen et al. (1993) concluded that metals sorption onto solid surfaces is affected by any change in the surfaces potential as this is reflected into a change in the electrostatic attraction repulsion forces between the charged surface sites and the cations and anions present in the system. Ricou et al. (1999) found that a raise in pH above  $\text{pH}_{\text{zpc}}$  of the solid material will determine an increase in availability of the negatively charged surface sites which will favor adsorption of metals (cations) on the surface of the solid material.

As it is well documented in the literature, pH is one of the key parameters controlling the adsorption/release of the metals and metalloids (van der Sloot et al. 1998) onto/from solid surfaces. At acidic pH anion sorption is generally favorable due to availability of positively charged surface species, while at alkaline pH, cation sorption becomes important due to availability of deprotonated (negatively charged) surface species for complexation. In other words, leachability of metals is inversely proportional to the pH of the leaching solution, while the anions show reverse behavior relative to pH (Hoek and Comans 1996). However, the presence of dissolved ligands (especially organic) species will significantly influence leaching of the metals. The formation of soluble metal-ligand complexes increases the aqueous dissolved metal concentrations and diminishes sorption of metals onto the solid surface.

Changes in redox conditions which are closely linked to changes in pH, play a significant role in the leaching behavior of metals. Since the metals can occur in oxidized or reduced soluble form, a change in the redox conditions may lead to their transformation into harmless or more toxic forms (van der Sloot 1996). In Figures 2.2 and 2.3 is shown the dependence of metal species distribution as a function of pH and redox conditions. Ionic strength is another factor that has an impact on metals leaching, mainly due to its influence on the solid surface potential (Dankwarth and Gerth 2002). A raise in ionic strength of the leaching solution decreases the surface potential and enhances adsorption of anion species. Another factor that influences the leaching behavior of the metals is the flow rate of the eluant in the system

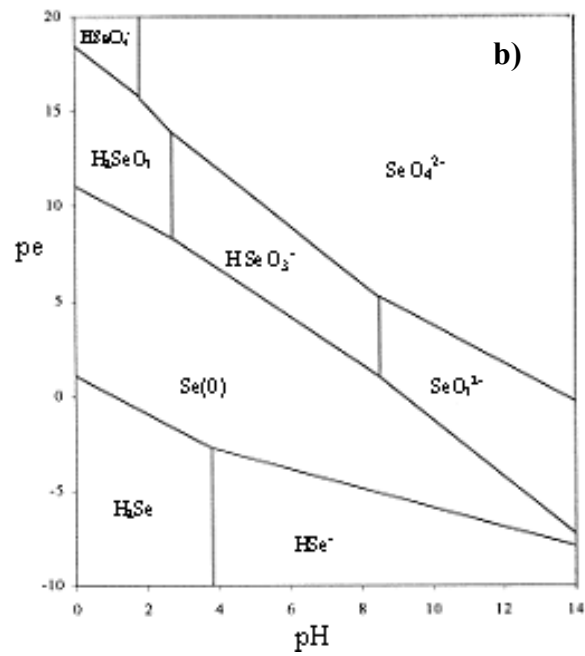
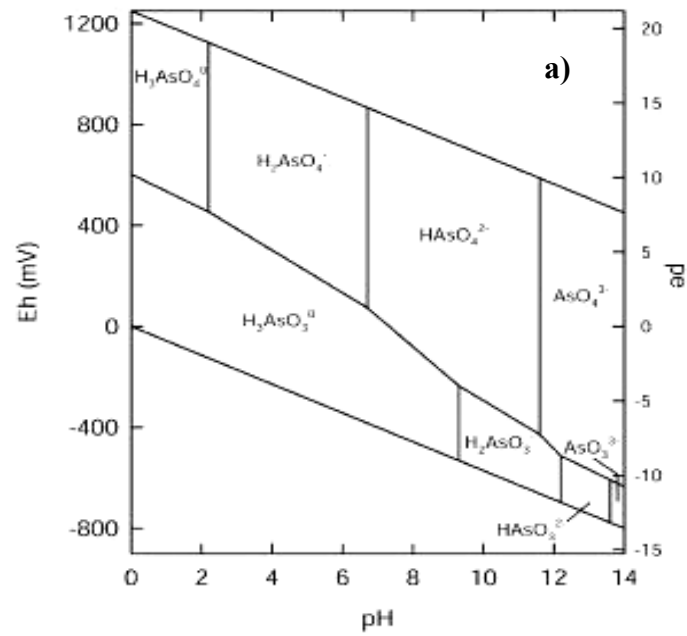


Figure 2. 2. pe-pH diagrams for aqueous (a) arsenic and (b) selenium species (adopted from Frankenberger 2002 and 1998, respectively)

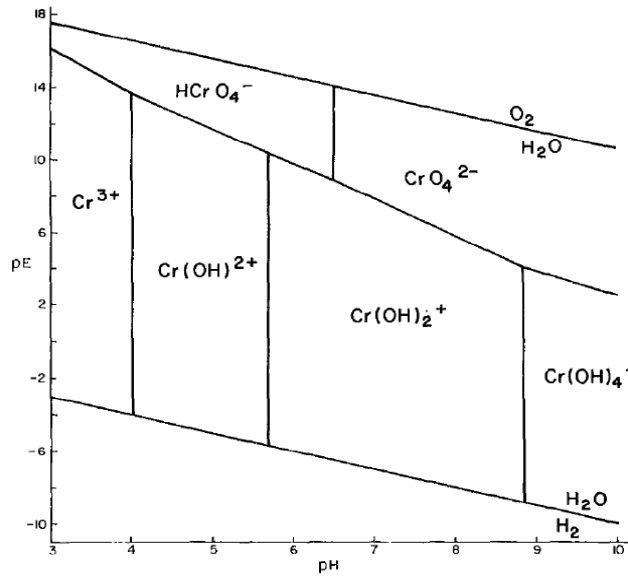


Figure 2. 3. pE-pH relationship for dissolved aqueous Cr species. (from Baes and Mesmer 1976)

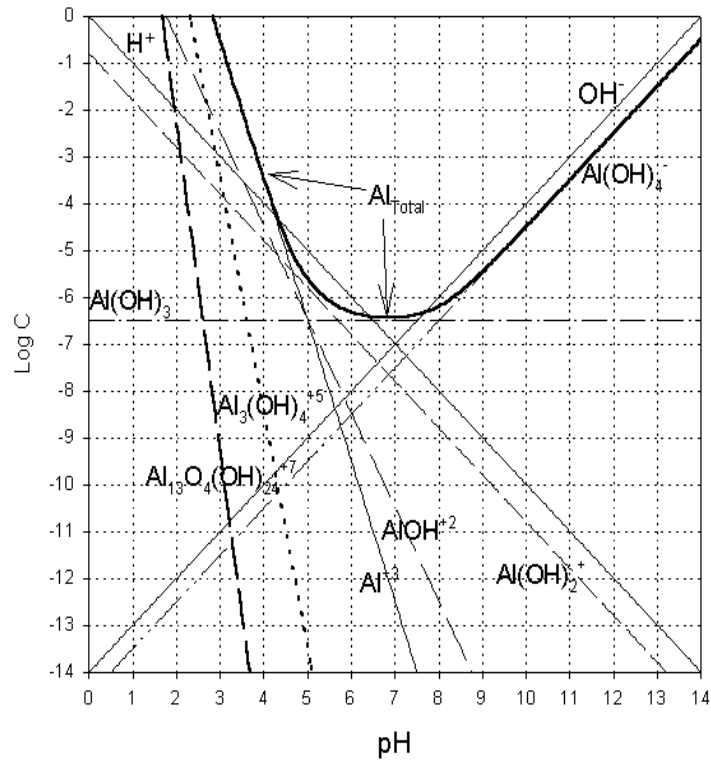


Figure 2. 4. Aluminum solubility vs pH (from Sposito 1996)

(Alesii et al. 1980, Creek 1992). Alesii et al. (1980) reported that lower flow rates will determine “a greater attenuation of the metal ions in solution”. Closely related to this parameter is the contact time between the solid surface and the leachant solution, which will directly influence the leaching of metals behavior. Total metal concentrations available on the solid surface and the solubility property of each metal are also effective on the overall leaching behavior. Di Toro et al. (1986) concluded that as the total concentration of metals increases the partition coefficient diminishes. As indicated by Jang et al. (1998) this increase in total metals also increases the dissolved metal concentrations in the aqueous phase and decreases the adsorbed metal concentration onto the solid surface.

#### **2.4. LABORATORY LEACHING STUDIES**

A large variety of laboratory bench-scale experiments simulating various conditions were designed by several researchers to address the release of toxic metals from waste materials (Theis et al. 1982, Creek and Shackelford 1992, Edil et al. 1992, Biliski and Alva 1995, Chichester and Landsberger 1996, Ghosh and Subbarao 1998, Kanungo and Mohapatra 2000, Chang et al. 2001, Lee and Benson 2002, Ogunro and Inyang 2003, Geeta Kandpal et al. 2005, Sauer et al. 2005, Bin-Shafique et al. 2006). Methods like: Toxicity Characteristic Leaching Procedure (TCLP), Extraction Procedure (EP), Water Leach Tests following ASTM 3987-85, or modified versions of it, as well as column leaching tests, have been conducted by many investigators to evaluate the possible leachable contaminants from particulate waste materials and their potential environmental impacts.



#### **2.4.1. Batch Water Leach Tests (WLT)**

Batch tests are considered to represent the “worst case” scenario with regard to leaching of metals from waste solid materials, providing a rapid approximate estimation about the extent of metals leaching. Chang et al. (2001) have performed a comparison study to evaluate the performance of three standard leaching procedures: TCLP, EP and ASTM. Several researchers have chosen to use the ASTM Water Leach Test procedure in their leaching studies as it simulates the environmental conditions in the field. This is due to the fact that the pH buffering capacity is controlled by the environmental factors such as solid material used, carbonate system, and alkalinity and not by addition of acidic solution which will alter the natural conditions, and implicitly the leaching behavior of the metals and metalloids as in the case of TCLP and EP tests. However, it should be noted that the WLT procedure does not fully simulate the actual site leaching conditions.

Lee and Benson (2002) performed ASTM water leach tests to determine the potential release of heavy metals from twelve foundry sands for their use as reactive media in permeable reactive barrier (PRB) applications. The leachates were analyzed for antimony (Sb), arsenic (As), barium (Ba), beryllium (Be), cadmium (Cd), chromium (Cr), copper (Cu), iron (Fe), lead (Pb), manganese (Mn), mercury (Hg), nickel (Ni), selenium (Se), thallium (Ti), and zinc (Zn).

Sauer et al. (2005), and Bin-Shafique et al. (2006) have also conducted water leach tests on class C fly ashes, and fly ash-soil mixtures for their possible use in highway construction applications. The effluents were analyzed for cadmium (Cd), selenium (Se), chromium (Cr), and silver (Ag). The concentrations for the fly ashes were in the range of 0.7-3.6 ppb ( $\mu\text{g/L}$ ) for cadmium, 59-123 ppb ( $\mu\text{g/L}$ ) for total chromium,

18-82 ppb ( $\mu\text{g/L}$ ) for selenium, and 2.2-6.2 ppb ( $\mu\text{g/L}$ ) for Ag. The EPA MCL and secondary drinking water standard limits were slightly exceeded for selenium and chromium. Bin-Shafique et al. (2006) described two types of leaching behavior for fly ash and on fly ash-soil mixtures based on WLTs data. The concentrations of Cd and Ag released in the aqueous phase were insensitive to the fly ash content, and only a slight inconsistent decrease or increase was observed with increasing fly ash content in the fly ash-soil mixtures. In case of Cr and Se (anionic species), a non-linear increase in metal concentrations released was detected with increasing fly ash content of the mixture. They explained this phenomenon by the increase of pH coupled with higher fly ash content, which enhances dissolution of anions.

WLTs on four Indian fly ashes using synthetic rainwater (pH = 5.6) as leaching solution were carried out by Praharaj et al. (2002) to better understand the potential mobility of inorganic contaminants from fly ash in a disposal pond. Different liquid-to-solid ratios (4, 8, 12, 16) were employed in this study, and concentrations of Al, Ca, K, Mg, Na, P, S, Si, As, Ba, Fe, Mn, Mo, Ti, V, Pb, Zn, Co, Cr, Cu, Ni and Cd were measured in the resulted leachate. Their reported results indicate that most of the metals (As, Ca, Mg, Mn, Na, Zn) demonstrated maximum leaching at small liquid-to-solid ratios (4 and 8) followed by a decrease in leaching concentrations at higher liquid-to-solid ratios. This is in contradiction with what Long (2003) found that “higher L/S ratios resulted in higher concentrations and fractions of metals removed”. Several metals did not leach at all or they leached in insignificant concentrations: Cd, Cr, Co, and Ni. Of concern showed to be As, Fe, Mn and Mo which leached at concentrations way above drinking water standard limits recommended by U.S. EPA and World Health

Organization. They also investigated the changes in specific surface area of the fly ash particles before and after leaching and found that the fly ash particles exhibit a decrease in surface area and an increase in surface roughness post-leaching, which was attributed to the removal of the active surface sites and soluble finest particles.

A series of batch leaching tests were conducted by Fytianos and Tsaniklidi (1998) to determine the leachability potential of Pb, Cd, Cr, Cu, Zn, Ca and Mn from fly ashes originated from Greece. They used the cascade leaching test in which a sequential leaching procedure is being applied to the same fly ash sample by refreshing the leaching agent several times. Liquid-to-solid ratios of 5 to 100 have been used in this study. The leaching reagent was distilled water acidified to pH 4 with HNO<sub>3</sub>. The mixture was allowed to equilibrate for 23 hours after which the supernatant was subtracted, filtrated, and analyzed for metal concentrations, and the fly ash remained was leached again with fresh acidified solution at a liquid-to-solid ratio of 40. Then, this procedure was repeated five times in total with liquid-to-solid ratios from 5 to 100. They observed a decrease in pH with the increase of liquid-to-solid ratio which was attributed to “depletion of materials controlling this parameter”, in other words as the L/S ratio increased the buffering capacity of the fly ash decreased. They also investigated the pH effect on the leaching behavior by using leaching solutions with different pHs (4 and 8). The results indicated that leaching increased as the pH dropped from 8 to 4, which was explained by the increased intensity of attack on the ash mineral phases at acidic pH (Roy and Griffin 1984).

Kanugo and Mohapatra (2000) performed WLTs on fly ashes from two Indian power plants in order to asses and evaluate the release of various metal contaminants (Na,

K, Ca, Mg, Ba, Zn, Cd, Pb, Cr, Mn, Co, Ni, Cu, As, Se, Fe, Al, and Si) at three different pH values 3, 5.5, and 8. In their study, mixtures of 25:1 liquid-to-solid ratios were prepared with fly ash and deionized water (pH adjusted with a base or an acid as needed), and allowed to equilibrate for up to 30 days with 3-4 minutes of agitation 5 times daily. The leachate resulted was analyzed for concentration of metals mentioned above. Their results indicated a considerable decrease in metal concentrations with increase of pH from 3 to 8. They also explained the increased leaching at low pH by the increased “attack of aluminosilicate matrix at an acidic pH”.

Leaching of metal behavior in batch WLTs was also investigated by Theis et al. (1982) for eleven fly ashes by equilibrating a mixture of fly ash and leaching solution at a 1:5 solid-to-liquid ratio for 24 hours on a shaker table, followed by filtration and analysis for trace metals (As, Cd, Cr, Cu, Pb, Ni, and Zn). The pH of the leachant was varied (3, 6 and 9). A pattern of decreasing concentration of metals leached with increasing pH was predicted again like in the previous studies. The release of arsenic exhibited different trend with a sharp increase to 40% of the total concentrations at pH 12.

Although batch WLTs proved to provide a reasonable indicator regarding the behavior of metals in short-term leaching, most researchers chose to perform flow-through column tests which were concluded to offer a more realistic insight into the release of metals from fly ash behavior provided that the test conditions more closely mimic the real environmental conditions.

#### 2.4.2. Column leaching tests

Bin-Shafique et al. (2006) set up column experiments with soil-fly ash mixtures operated in an up-flow mode using 0.1 M LiBr solution equilibrated with the atmosphere as percolating eluant (influent pH = 6). The pH of the effluent leachate ranged between 7.1 and 9.6 among all soil-fly ash mixtures. The seepage velocities were in the order of  $10^{-5}$  cm/s, and Peclet number varied between 4.9 and 18.4 inferring that mass transport in the columns was both advection and diffusion dominated as is actually proved by the elution curves which were well described with the analytical solution for advective-dispersive transport described by van Genuchten (1981). The pattern of the elution curves indicates that the release of metals from the mixture specimen into the leaching solution decreases with increase of flow pore volumes. They also compared the results from batch WLTs with the column leach tests, and found that scaling factors of 50 for Ag and Cd, 10 for Cr and Se can be applied to WLTs results to estimate the initial peak concentrations in column experiments. The metal concentrations in the initial effluent samples from the column packed with soil-fly ash mixtures ranged between 4 and 42.1 ppb for Cd, 60.1 and 487.2 ppb for Cr, 10.8 and 289.1 ppb for Se, and 5.1 and 72 ppb for Ag.

Creek (1991) used column tests to evaluate the impact of flow rate on leaching behavior of metals from soil-fly ash (class F) mixtures. The test results suggested that higher release of metals occurred during experiments with lower flow rates indicating “flow-rate dependent leaching trends”, and this was explained by the possible time-dependency of dissolution processes. This is contradiction with what Long (2003) found that higher flow rates generally caused more mass leaching. Long (2003) acknowledged the importance of adopting the appropriate field conditions with regard to flow rate or

hydraulic gradient in the laboratory experiments if attempting to use their outcome in prediction of real site conditions. Eight of the thirteen metals investigated exhibited “early leaching behavior” meaning that the highest metal concentrations leached out in the initial pore volumes of flow. Mitchell (1976) suspected that the “early leaching behavior” can be explained by an increase in the predisposition (tendency) to be solvated due to charge density of cation metals (i.e., Al, Cu).

Chichester and Landsberger (1996) conducted column experiments to investigate the leaching dynamics of metal contaminants from fly ash. Deionized water with a pH of 5.7 was used in their experiments as percolating leaching influent solution. A constant-water head was provided with a hydraulic gradient of 4. Consistent with the findings of Bin-Shafique et al (2006), the metals concentrations released decreased sharply at higher pore volumes of flow.

Ogunro and Inyang (2003) attempted to relate the batch and column leaching test results using a mathematical modeling framework to help predict metal transport from waste materials used in geotechnical construction. The tests were conducted with mixtures of bottom ash and asphalt concrete. The columns were operated in up-flow mode using acidified distilled water (pH = 4.5) at a flow rate of 6 mL/min. For comparison purposes, the column experiments were continued until a liquid-to-solid ratio equal to that of batch tests (i.e., 10) was reached (after about 200 h). Leaching of aluminum and copper was monitored in all samples from the column and batch tests. Similar to the findings of previous researchers, the results indicated that high wash-out and detachment of metals by percolating solution occurs at the initial stages of the column test. They explained the phenomenon by the increase in the chemical potential

which initiates the leaching of metals from within the solid matrix into the surrounding solution until the concentration difference between the leachant and the solid material was reduced and an equilibrium stage was reached. Considering the high Peclet numbers (>5) exhibited from the column tests, the release and transport of metal contaminants from column specimens was suspected to be advection-dominated.

Evaluation of metals release was also investigated by Edil et al. (1992) in column experiments packed with 50% fly ash + 50% sand mixture compacted with two different hydraulic conductivities. As leachant, a mixture of several salts was added to deionized water to attain a certain ionic strength. Al, As, Cr, Se, Si, and Sr concentrations were measured in all column samples collected. They found that the elution curve patterns of most metals release imply a first-flush behavior, with some exception for Cr in the column cases with lower hydraulic conductivities.

All these works generated some knowledge to help in understanding process of the mechanisms of heavy metals release from solid wastes and factors that influence it.

## **2.5. LEACHING MECHANISM AND FACTORS INFLUENCING DESORPTION OF ORGANICS**

The fly ashes with high levels of carbon contents have been identified as good candidates for sorption of organics from groundwater contaminated with organic compounds, therefore, the potential (suitability) for their re-utilization as barrier material in remediation and treatment technologies has been investigated by Demirkan et al. (2007). However, little is known about the undesirable released of the organic contaminants once absorbed from such barriers, and about their fate and transport from

barrier layer, therefore, an additional objective of this study is to investigate the potential release of organic contaminants from fly ash-amended PRBs.

Among the factors observed to influence adsorption/desorption of organics from solid phase, the following are mentioned to have the most impact: properties of the solid sorbent (organic matter content, dissolved organic carbon content, surface area (pore size) of the solid particles, adsorption capacity), properties of the organic compound (solubility, hydrophobicity, partition coefficient), contact time between leaching solution and sorbent (failure to attain equilibrium between the two phases may lead to hysteresis), aging (contact time between organic contaminant and solid sorbent), biotic or abiotic degradation, pore water velocity of the leachant, and concentration of organic contaminant (Farrell and Reinhard 1994, Kan et al., 1994, Cornelissen et al. 1998, Keijzer et al. 2002, Gunasekara and Xing 2003).

The results of many studies investigating adsorption/desorption of organics from various solid sorbents (sediments, sands, activated carbon) imply occurrence of hysteresis phenomenon, meaning that the sorption and desorption of organics are irreversible which is suggested by the fact that the sorption and desorption isotherms are not identical. Hysteresis of sorption/desorption processes have been recognized by several researchers: however, the exact causes for hysteresis are not well understood, and further investigation is required to elucidate the mechanism of slower release of organic pollutants from solid sorbents as comparing to their sorption.

In order to explain the mechanism of desorption of organics from solid sorbents, the assumption that desorption is diffusion controlled has been considered (Farrell and Reinhard 1994, Cornelissen et al. 1998, Keijzer et al. 2002). In order to predict the



contaminant release from solid sorbents the equilibrium behavior should be well understood in order to identify the appropriate concentration gradient for initiation of diffusion driving force (Schaefer et al. 2000). Generally, retarded desorption of organic compounds from sorbent matrix was found to mainly be due to their diffusion and sequestration in voids of the organic matter, and/or due to diffusion and entrapment in the mineral phase micro-pores (Cornelissen et al. 1998). This accentuates the important role of organic matter in adsorption/desorption behavior of organic contaminants (Kan and Anjaneyulu 2005).

Kan et al. (1994), Adamson and Gast (1997) and Kommalapati et al. (2002) hypothesized that some structural alteration of the sorbent matrix and specifically the organic matter component of the matrix, experience such changes that voids undergo physical rearrangement after adsorption of organic molecules may happen. These molecules may occlude the adsorbed organic molecules in the organic matter, disfavoring their release and causing desorptional retardation. They also suggested that these structural changes may be caused by the changes in pH, ionic strength, and coagulation processes.

Because of the higher adsorption energies due to the interaction potential of the opposing walls, the organic molecules are preferentially absorbed in the micropores of the sorbent matrix, being subject to stronger bonding as the pore size approaches the size of the absorbed molecule. In a nutshell, due to sorbent microporosity, three effects that contribute to reduce desorption rates may be observed, such as: increased steric hindrance, increased sorption energies, and increased surface area to volume ratios. In other words, the pore diffusion controls the slow desorption, therefore, smaller pore size

leads to higher sorption energy, more restricted diffusion, and a slow release of organic contaminants due to unfavorable energetic conditions. For this reason, these high-energy sorption sites are also called slow sites (Farrell and Reinhard 1994).

The initial adsorbate concentration is recognized to have a significant effect on the desorption rates as well (Pignatello 1990, Farrell and Reinhard 1994, Gunasekara and Xing 2003). Investigations performed by the mentioned researchers on this hypothesis revealed that the amount of slowly released adsorbate increases with its decreasing concentration. This is explained by the increased high-energy sites to adsorbate molecule ratios, resulting in higher energy of bonding and reduced desorption. In the opposite case, the ratios are lower at high concentrations of organic solute, due to the limited amount of high-energy sites available for bonding. These sites immediately get saturated with now abundantly available organic molecules, and so a large part of the adsorbate molecules become loosely bound with low energy binding sites, being easily desorbed when percolating solution moves within the solid matrix. Brusseau et al. (1991), Liu and Amy (1993) and Grathwohl et al. (1993), studied the impact of the flow rate of the leaching solution on the desorption of organics behavior and they concluded that election of the flow rates can influence the shape of the elution breakthrough curves, and can determine the occurrence of extended tailings. The non-equilibrium desorption phenomenon of due to heterogeneities affecting the transport of organic compounds due to presence of regions of mobile water carried by the input flow-through and immobile water bordering solid particles was observed by Brusseau and Rao (1989), van Genuchten and Wagenet (1989), and Keijzer et al. (2002).

Biotic and abiotic degradation of the organic solutes in the contaminated solid matrix was proposed as another explanation for the hysteresis (Miller and Pedit, 1992; Hermosin et al., 1987). Several researchers showed that degradation of naphthalene occurs in contaminated soils under reducing, anaerobic conditions (Coates et al. 1996, Lagenhoff et al. 1996, Meckenstock et al. 2000).

Presence of dissolved organic carbon (DOC) species in the leaching system will boost complexation with organic pollutants enhancing their solubility and increasing the amounts released into the percolating leachant (Abdul et al. 1990, Dunnivant et al. 1992, and Maxin and Kögel-Knabner 1995)

## **2.6. LABORATORY DESORPTION TESTS**

Previous efforts have concentrated on investigation of adsorption/desorption of organics behavior in soil, sediments, soil organic matter, activated carbon, harbor sludges, sands, silica gel and other solids (Pignatello 1990, Pavlostathis and Mathavan 1992, Kan et al. 1994, Farrell and Reinhard 1994, Cornelissen et al. 1998, Schaefer et al. 2000, Keijzer et al. 2002, Kommalapati et al. 2002, Gunasekara and Xing 2003, Khan and Anjaneyulu 2005, Sarkar and Acharya 2006) and limited information exists about the desorption behavior of organics from fly ashes. Existing studies on organics desorption usually deal with two different types of laboratory tests: batch desorption and column desorption tests.

### 2.6.1. Batch desorption of organics tests

Sarkar and Acharya (2006) studied the re-use of fly ash in remediation of groundwater contaminated with phenolic compounds. They performed batch adsorption tests by spiking the fly ash with phenolic compound solutions of different concentrations to evaluate the adsorption capacity of the fly ash, after which they also carried out leaching experiments to evaluate the release of the organics from fly ash. Their results indicated that no desorption of phenolic compounds occurs, and fly ash could be a viable option and cost-effective alternative for treatment of groundwater with phenol-like contaminants.

Sequential decant-refill batch steps were employed by several researchers to evaluate the desorption behavior of various organic compound from different solid matrixes (Kan et al. 1994, Kommalapati et al. 2002, Gunasekara and Xing 2003, Khan and Anjaneyulu 2005). Gunasekara and Xing (2003) investigated sorption/desorption of naphthalene by soil organic matter using sequential desorption technique, by first saturating soil samples with naphthalene solutions of different concentrations followed by desorption step that consist of sequential replacement of the background solution with fresh leachant and analysis of desorbed concentrations after each step. The general desorption isotherm patterns indicated an increase in desorption with increase in naphthalene concentrations, most probably due to a decrease in high-energy sites to absorbate molecules ratios with increasing solute concentrations. This was manifested by the limited amount of high-energy sites available for bonding relative to abundantly available naphthalene molecules, which immediately get saturated, and so a large part of the naphthalene molecules were loosely bound with low energy binding sites, and were

easily released when leaching solution came in contact with the solid matrix. The potential for microbial degradation was eliminated by addition of  $\text{HgCl}_2$  as biocide.

Similar procedure was followed by Kan et al. (1994) who conducted adsorption/desorption experiments to determine the factors that influence the release of naphthalene from soils and sediments. Up to 20 desorption steps were necessary for naphthalene concentrations to drop below detection limits. Only 11-37% of the adsorbed naphthalene was released at the end of desorption experiments and in all cases over 50% of the adsorbed naphthalene did not desorb. The patterns of desorption curves imply the occurrence of hysteresis, indicated by resistance to desorption of significant fractions of naphthalene which is believed to suffer hindered diffusion from the micropores of organic matter. The hypothesis of structural alteration of the sorbent matrix, by which the organic matter voids undergo physical rearrangement after adsorption step occluding the adsorbed naphthalene molecules in the organic matter, is also considered as an explanation for irreversible sorption of naphthalene.

Desorption hysteresis of four volatile organic compounds (1,2-dichloroethane, 1,1,2-trichloroethane, 1,4-dichlorobenzene, and hexachlorobutadiene) was evaluated by Kommalapati et al. (2002) in sequential decant-refill batch experiments similarly as described in the studies above. Sodium azide was added to the leaching solution to avoid biodegradation of organic contaminants under investigation. Desorption curves exhibited a first rapid desorption stage (during the first few desorption steps) suggested by relatively high aqueous concentrations, followed by a slow desorption stage, suggested by the reduced water concentrations. Their findings were consistent with the ones mentioned in the above investigations identifying the presence of hysteresis, explained by

matrix configuration changes involving physical rearrangement of organic matter voids occluding the adsorbed molecules determining retarded desorption.

### **2.6.2. Column leaching of organics tests**

Column leaching tests are recommended if intended to evaluate the desorption behavior of organic contaminants from solid sorbents under more realistic conditions, providing a better insight regarding the release and mobility of potential toxic compounds into the environment. The tests may also provide data sets that can be integrated in mathematical modeling to predict the fate and transport of contaminants. Several researchers investigated desorption of various organic compounds from different solid matrixes including sand, harbor sludges, soils; however, limited information exists about column leaching of organics from fly ashes.

Keijzer et al. (2002) used column experiments to evaluate the desorption behavior of PAHs in harbor sludges from Netherland. A mixture of sand and harbor sludge was used for packing the column specimens. They used 0.01 M NaCl as leaching solution, maintaining a constant hydraulic head of 1. To avoid microbial activity, column experiments were performed at 4 °C, under dark and anaerobic conditions. The results exhibited exponential decrease of organic aqueous concentration with time. The partition coefficients that they attained from column experiments were higher than those obtained from batch experiments. Diffusion-controlled desorption was observed in all column experiments.

Culver et al. (1997) conducted column experiments to help them in modeling of desorption of organic contaminants from long term contaminated soils. Column

specimens consisted from field contaminated soil. Deionized organic-free water was the percolating solution introduced in the column by a peristaltic pump with a constant flow rate. The elution curves exhibited asymmetrical breakthrough curves with long tailings. They used the distributed kinetic model to describe their data, and it showed to provide a good fit to the elution curves obtained experimentally. However, their best fit parameters resulted from the batch experiments were not useful in providing reasonable predictions for the column tests, and neither the other way around. This may be attributed to the considerably distinctive experimental conditions (contact time, agitation, solid-to-liquid ratios, etc).

## CHAPTER 3

### MATERIALS AND METHODS

#### 3.1. MATERIALS

##### 3.1.1. Solid materials

Fly ashes originating from six different power plants around Maryland were investigated in this study. Powder activated carbon (PAC) and sand were employed as reference materials in all the laboratory experiments performed in this research study.

##### 3.1.1.1. Fly ashes

###### *3.1.1.1.a. Sources of fly ashes*

The fly ash samples used in the current research study were provided by six different power plants around Maryland: Brandon Shores (BS), Chalk Point (CP), Dickerson, Morgantown (MT), Potomac River (PR) and Paul Smith (PS). The locations of the power plants are shown in Figure 3.1. Small batches (several kilograms) of fly ash were obtained from each power plant. One of the power plants, Dickerson, provided us with two different fly ashes with different LOI values, and for the purposes of this study they were named after the subsection of the power plant where they originated from: Dickerson Precipitator (DP) and Dickerson Baghouse (DBh).

These six sites were selected for the high carbon content (i.e., high loss on ignition) type of fly ash that they produce. As is demonstrated in this study, the HCC plays a significant role in the sorption and desorption of organics.



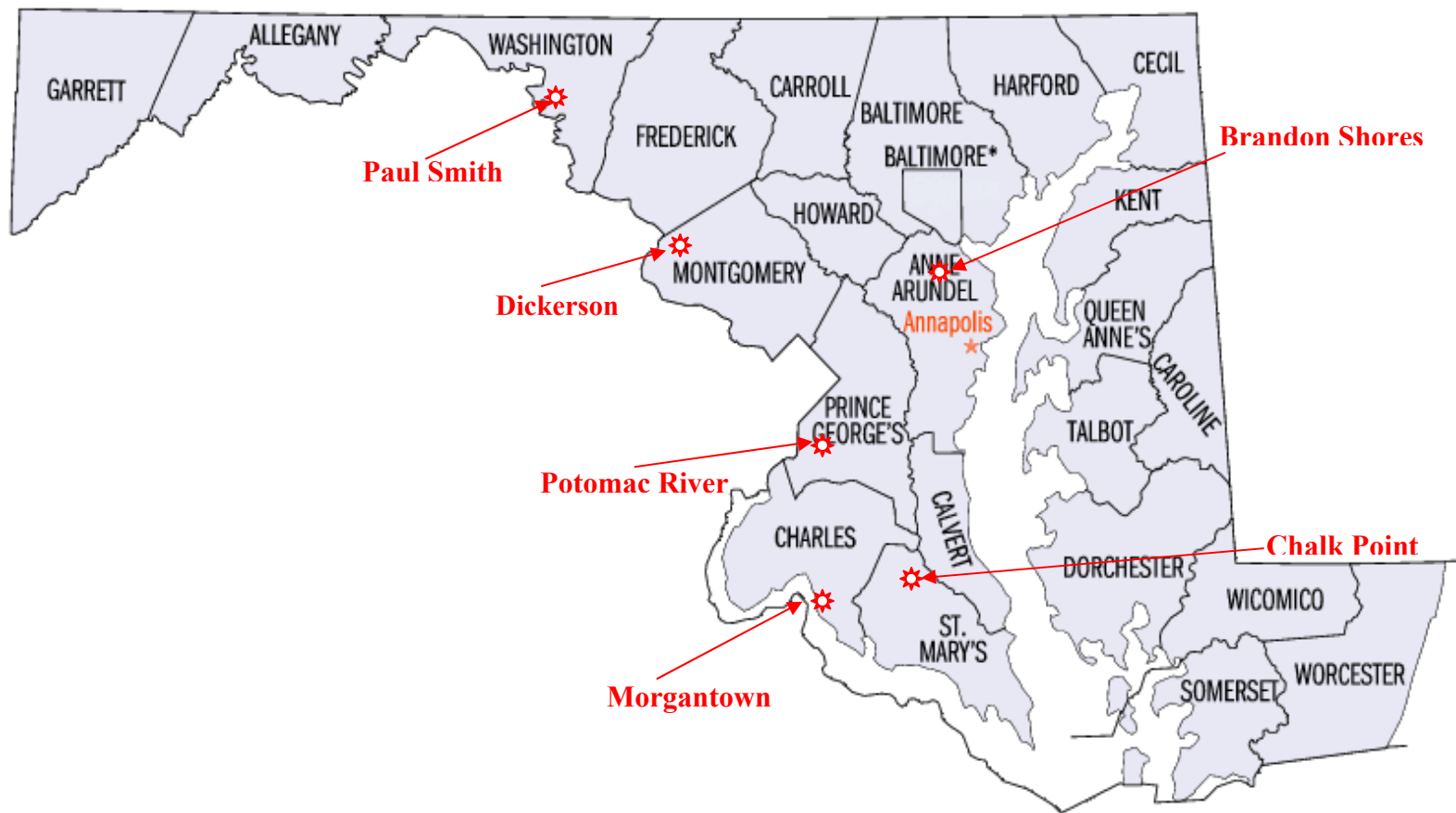


Figure 3. 1. Locations of power plants from which samples of fly ash were obtained

### ***3.1.1.1.b. Chemistry and physical properties of fly ashes***

Several laboratory analyses have been employed, in the larger project of which this work is a part, in order to determine the chemical composition, index properties, and physical characteristics of these materials. These analyses included: X-ray diffraction analysis, loss on ignition, particle size distribution, Atterberg limits, and specific gravity.

X-ray diffraction analysis was performed by a specialized laboratory to determine the chemical composition of the fly ashes. All seven fly ashes were scanned and analyzed for the minerals expected to be present in the fly ash in significant amounts. From the resulting X-ray diffraction pattern that was obtained, the chemical composition of each fly ash was defined and is presented in Table 3.1. According to ASTM C 610, the fly ashes investigated in this study can be classified as Class F fly ashes. For example, all seven fly ashes have a very low lime (CaO) concentration, in the range of 0.73 to 7.82 %, which is typical for Class F fly ashes. The chemical composition of all seven fly ashes is dominated by siliceous and aluminous minerals. Among the major silicate minerals commonly found in fly ash, quartz (SiO<sub>2</sub>) was identified in very high concentrations (up to 50.8%). The presence of aluminous minerals was in the form of aluminum oxide (Al<sub>2</sub>O<sub>3</sub>) minerals (ranging from 23.06 to 27.26 % in the seven fly ashes).

Loss on ignition is the chemical composition parameter with most significance for our study, being one of the factors that most impacts the capacity of the fly ash for sorption of organics. Four of the fly ashes have been determined to have a very high

**Table 3. 1. Major minerals and their concentrations determined by X-ray diffraction analysis rapport.**  
 (All concentrations are in percentage values.)

<b>Compound (% by weight)</b>	<b>SiO<sub>2</sub></b>	<b>Al<sub>2</sub>O<sub>3</sub></b>	<b>Fe<sub>2</sub>O<sub>3</sub></b>	<b>CaO</b>	<b>MgO</b>	<b>Na<sub>2</sub>O</b>	<b>K<sub>2</sub>O</b>	<b>Cr<sub>2</sub>O<sub>3</sub></b>	<b>TiO<sub>2</sub></b>	<b>MnO</b>	<b>P<sub>2</sub>O<sub>5</sub></b>	<b>SrO</b>	<b>BaO</b>	<b>LOI</b>
<b>Fly ash</b>														
<b>Brandon Shores</b>	45.13	23.06	3.16	7.82	0.83	0.25	1.68	0.02	1.42	0.01	0.09	0.06	0.06	13.4
<b>Chalk Point</b>	50.16	23.09	14.51	2.67	1.27	0.56	2.25	0.02	1.21	0.04	0.32	0.11	0.14	3.2
<b>Dickerson Baghouse</b>	37.73	27.26	11.53	3.77	0.53	0.25	1.02	0.04	1.5	0.01	1.33	0.24	0.1	14.9
<b>Dickerson Precipitator</b>	34.91	24.42	12.59	3.18	0.52	0.26	1.05	0.03	1.29	0.01	1.02	0.21	0.11	20.5
<b>Morgantown</b>	49.15	25.48	13.74	2.48	0.87	0.58	1.86	0.03	1.37	0.02	0.58	0.13	0.08	3.1
<b>Potomac River</b>	52.47	24.9	6	1.47	1.28	0.79	2.85	0.02	1.29	0.03	0.23	0.15	0.17	8.3
<b>Paul Smith</b>	50.8	26.88	5.51	0.73	0.57	0.21	2.19	0.02	1.48	0.01	0.17	0.03	0.05	10.7

loss on ignition value: Dickerson Precipitator with 20.5% LOI, Dickerson Baghouse with 14.9% LOI, Brandon Shores with 13.4% LOI, and Paul Smith with 10.7% LOI. Another set of studies were performed to determine the physical properties of the fly ashes. The particle size distribution was determined for each fly ash by mechanical sieving and hydrometer analyses following ASTM D 422 standard procedure (Figure 3.2). The non-plastic character of the fly ashes was proven by the attempts made to measure the Atterberg limit. The specific gravity of each fly ash was determined as well and the results are presented in Table 3.2. The pH of the seven Maryland high carbon content fly ashes was determined using EPA method SW-846 Method 9045, described in Section 3.5.1 and the results are presented in Table 3.3.

**Table 3. 2. Specific gravity of the seven fly ashes**

<b>Fly ash</b>	<b>Specific gravity, G<sub>s</sub></b>
Brandon Shores (BS)	2.17
Chalk Point (CP)	2.43
Dickerson Baghouse (DB)	2.35
Dickerson Precipitator (DP)	2.37
Morgantown (MT)	2.45
Potomac River (PR)	2.35
Paul Smith (PS)	2.2

**Table 3. 3. pH of the seven fly ashes**

<b>Fly ash</b>	<b>pH</b>
Brandon Shores	9.16
Dickerson Bag-house	9.44
Dickerson Precipitator	9.6
Morgantown	6.65
Paul Smith	7.55
Potomac River	8.52
Chalk Point	8.81

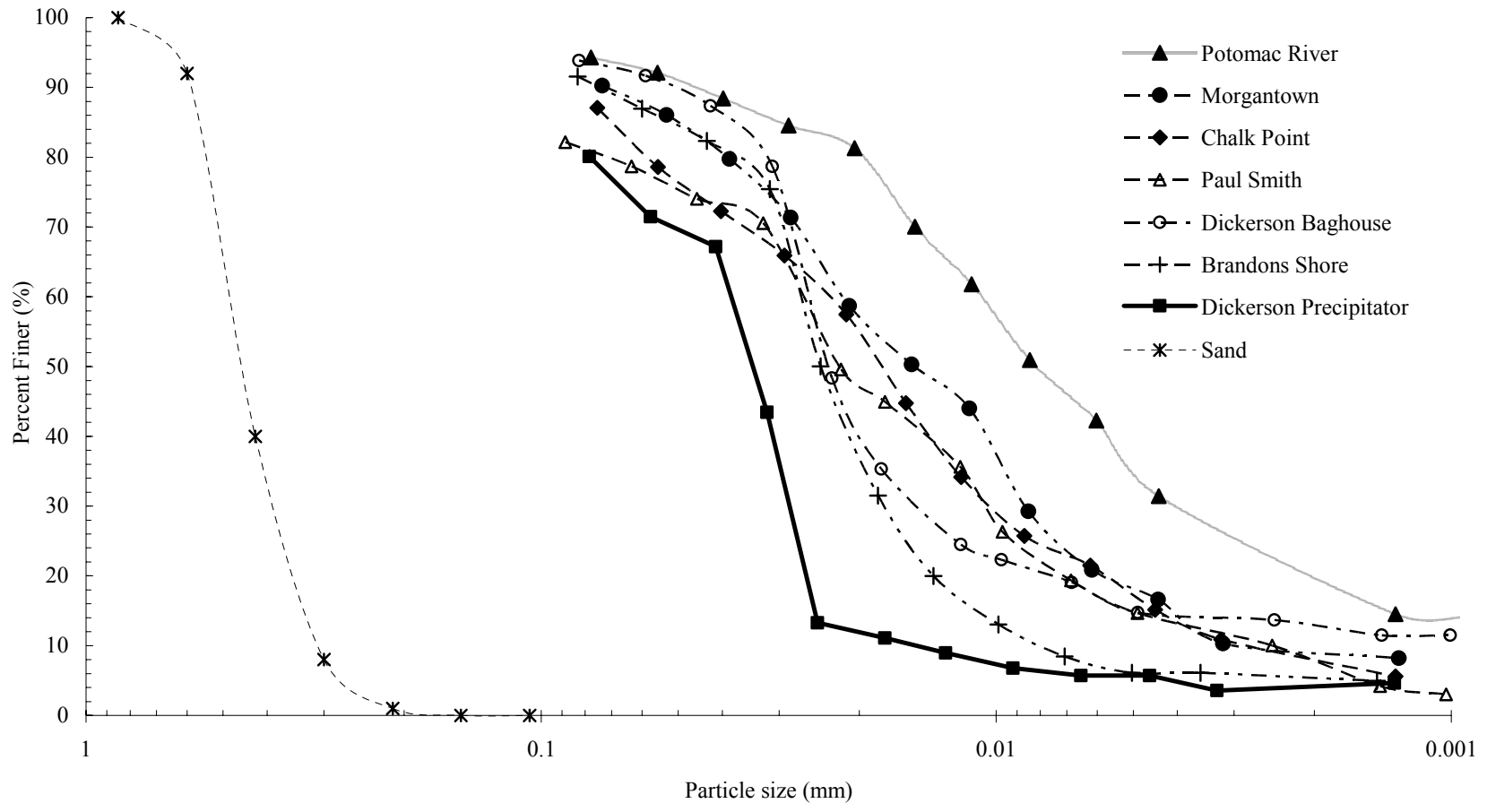


Figure 3. 2. Grain size distribution of the seven fly ashes and sand used in this study

### **3.1.1.2. Sand**

To create the porous media for the column reactor experiments described below, mixtures of fly ash (40% by weight) with sand (60% by weight) were prepared. Unground silica, from Berkeley Springs plant (West Virginia) was the sand used in preparation of the fly ash-sand mixtures. The grain size distribution of the sand as provided by the manufacturer is presented in Figure 3.2. Subangular, has been determined to be the predominant shape of the sand grains. The specific gravity, pH and hardness of the sand are 2.65, 6.5 and 7 mohs, respectively. The chemical composition of the sand materials reported by the manufacturer is summarized in Table 3.3. As expected, quartz is the predominant mineral present (99.7%).

### **3.1.1.3. Powder Activated Carbon (PAC):**

The Powder Activated Carbon (PAC) HYDRODARCO B from Norit Americas Incorporation was employed as a reference material in the sorption and desorption of organic contaminant studies. This PAC is generated by steam activation of lignite coal under strictly controlled conditions and is reported to have a very good adsorption capacity for organics. The grain size distribution of the powder activated carbon particles as provided by the manufacturer is presented in Table 3.4.

**Table 3. 4. Chemical composition of the sand used in the study**  
(from material datasheet; Berkely Spring plant, West Virginia)

<b>Compound</b>	<b>% (by weight)</b>
SiO <sub>2</sub> (Silicon Dioxide)	99.7
Fe <sub>2</sub> O <sub>3</sub> (Iron Oxide)	0.022
Al <sub>2</sub> O <sub>3</sub> (Aluminum Oxide)	0.07
TiO <sub>2</sub> (Titanium Oxide)	0.02
CaO (Calcium Oxide)	0.01
MgO (Magnesium Oxide)	<0.01
Na <sub>2</sub> O (Sodium Oxide)	<0.01
K <sub>2</sub> O (Potassium Oxide)	0.01
LOI (Loss on Ignition)	0.2

**Table 3. 5. Grain size distribution of PAC particles**  
(from material datasheet; Norit Americas Corporation)

<b>Finer than</b>	<b>%</b>
150 µm (#100 sieve)	99
75 µm (#200 sieve)	95
45 µm (#325 sieve)	90



### **3.1.2. Aqueous phase**

Solutions used in all the experiments were prepared using deionized water, generated by the Hydro Service reverse osmosis ion exchange system (modell2PRO-20).

#### **3.1.2.1. Synthetic groundwater recipe**

The chemical composition of the artificial groundwater used for all column and batch experiments in the current study is presented in Table 3.5. The constituents can be separated in three categories: macronutrients (including  $\text{FeSO}_4 \cdot 7\text{H}_2\text{O}$ ,  $\text{MgSO}_4 \cdot 7\text{H}_2\text{O}$ ,  $\text{NH}_4\text{Cl}$ ,  $\text{NaH}_2\text{PO}_4$ ,  $\text{KCl}$ ), micronutrients (including  $\text{MnCl}_2$ ,  $\text{Na}_2\text{SeO}_3$ ,  $\text{H}_3\text{BO}_3$ ,  $\text{Na}_2\text{MoO}_4 \cdot 2\text{H}_2\text{O}$ ,  $\text{CoCl}_2 \cdot 6\text{H}_2\text{O}$ ,  $\text{NiSO}_4 \cdot 6\text{H}_2\text{O}$ ,  $\text{CaSO}_4 \cdot 5\text{H}_2\text{O}$  and  $\text{ZnSO}_4 \cdot 7\text{H}_2\text{O}$ ), and a buffer solution (PIPES). This is the same dilute mineral salt nutrient solution recipe as used by Murphy et al. (1997) except for the addition of potassium chloride ( $\text{KCl}$ ) as an essential macronutrient for bacterial growth. Two stock solutions were prepared by dissolving 100 times the concentration of each macro- and micro-nutrient mineral, respectively, in two 1L flasks filled with deionized groundwater. A buffer stock solution was prepared by dissolving 25 times (151.2 g) the PIPES concentration (Sigma Aldrich, 99%) in a 2L flask about 75% filled with deionized water. The pH was adjusted to 6.8-6.9 by adding about 175mL of 4N  $\text{NaOH}$ , and the volume was then adjusted to 2L with deionized water. For preparation of 1L artificial groundwater solution, 10 mL of the macro-nutrient stock solution, 10 mL of the micro-nutrient stock solution, and 40 mL of the buffer stock solution were mixed together and diluted to 1L with deionized water. The pH of the solution freshly prepared was recorded each time. To avoid any bacterial contamination, the groundwater solution was autoclaved for 20 minutes at 121°C and 21 psi.

**Table 3. 6. Mineral composition of the groundwater (from Murphy et al. 1997)**

<b>Macro nutrient compounds</b>	<b>Concentration, mg/L</b>
Ferrous sulfate heptahydrate, $\text{FeSO}_4 \cdot 7\text{H}_2\text{O}$	0.1
Magnesium sulfate heptahydrate, $\text{MgSO}_4 \cdot 7\text{H}_2\text{O}$	2
Ammonium chloride, $\text{NH}_4\text{Cl}$	3
Sodium phosphate dibasic, $\text{Na}_2\text{HPO}_4$	0.6
<i>Potassium chloride, KCl</i>	<i>0.6</i>
<b>Trace element compounds</b>	<b>Concentration, <math>\mu\text{g/L}</math></b>
Manganese chloride, $\text{MnCl}_2$	5
Sodium selenite, $\text{Na}_2\text{SeO}_3$	5
Boric acid, $\text{H}_3\text{BO}_3$	5
Sodium Molybdate Dihydrate, $\text{Na}_2\text{MoO}_4 \cdot 2\text{H}_2\text{O}$	5
Cobalt Chloride Hexahydrate, $\text{CoCl}_2 \cdot 6\text{H}_2\text{O}$	5
Nickel Sulfate Hexahydrate, $\text{NiSO}_4 \cdot 6\text{H}_2\text{O}$	5
Calcium Sulfate Pentahydrate, $\text{CaSO}_4 \cdot 5\text{H}_2\text{O}$	5
Zinc Sulfate Heptahydrate, $\text{ZnSO}_4 \cdot 7\text{H}_2\text{O}$	5
<b>Buffer Solution Concentration</b>	<b>mM</b>
PIPES, $\text{C}_8\text{H}_{18}\text{N}_2\text{O}_6\text{S}_2$	10

## **3.2. REACTOR SYSTEMS**

### **3.2.1. Batch test experimental set up**

The experiments performed in this research to examine the release of metal and organic contaminants from fly ash were performed in either batch or column reactor systems. In all cases, the fly ash materials to be tested were sieved through a number 10 sieve and mixed homogeneously prior to use. All batch tests for the leaching of metals were performed in acid washed 50 mL plastic centrifuge tubes with plastic screw caps (VWR). For the batch desorption tests conducted on organic contaminants, the reactors were 60 mL glass centrifuge tubes capped with Teflon faced silicon septa caps (Cole Parmer). In both cases, the tubes containing the mixture to be analyzed were mixed on a tumbler rotator.

### **3.2.2. Column tests and experimental set up**

All column experiments were performed in Chromaflex glass columns (Kimble-Kontes, part # 420830-3020). PTFE bed supports with 20  $\mu\text{m}$  pores were placed at both top and bottom ends, through which the eluant diffused into the column providing a uniform continuous flow. A few of the columns were equipped with three sampling ports (at 7, 15, and 23 cm height) along the glass walls. Leak-free seals at the column ends were provided by screw caps which also held flangeless fittings. The columns were operated in an up-flow mode, with flow provided by a peristaltic pump on the influent line. The influent line consisted of PTFE tubing connecting an aspirator bottle filled with the feed solution to the fitting on the bottom

of the column. On the effluent end of the column, PTFE tubing made the connection between the column and the effluent collection bottle.

All column specimens were packed with three different layers of porous media (Figure 3.3). The bottom 8-cm layer was packed with sand, the next 19-cm layer was packed with a mixture that consists of 40% fly ash and 60% sand, and the last 3 cm were packed with another layer of 100% sand. The bottom sand layer was intended to provide a uniform flow across the column, and to prevent the very small fly ash particles from migrating downward due to gravitational forces and clogging the influent tubing. The 8 cm height of this layer was chosen such that it would reach slightly beyond the level of the first sampling port, in those columns with sampling ports, providing the possibility for monitoring the influent solution from inside the column. The top sand layer was designed to prevent the small and light fly ash particles from migrating upward with the water flow and clogging the effluent tubing. The remaining 19 cm height for the middle fly ash/sand mixture layer provided a reasonable geometrical symmetry between the two sampling ports in the fly ash-sand mixture. In Figure 3.4 is shown a sketch of column experiments set up. In this study, a simple dry packing procedure was applied for adding the porous media to the column. First, the materials used for packing were screened through a 2-mm sieve to remove bulky fragments that could cause anomalous packing. Known quantities of screened and well-mixed sand and fly ash-sand mixture were prepared before proceeding. Then, the material was added to the column using a funnel with a narrow, 30 cm long brass cylinder, which had a holding capacity that was just enough to form a 0.5 cm thick layer.

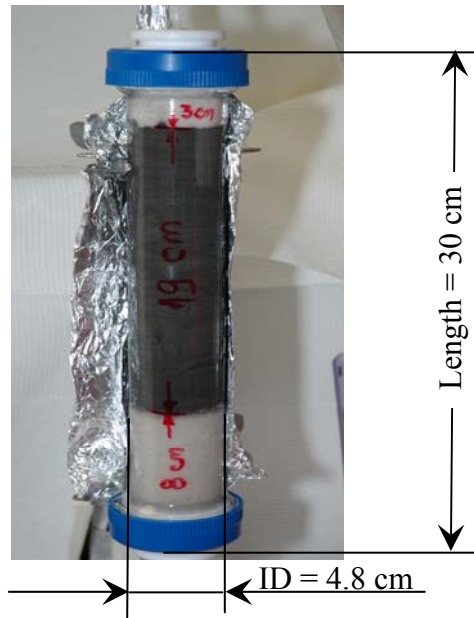


Figure 3. 3. Image of a packed column with the three porous media layers

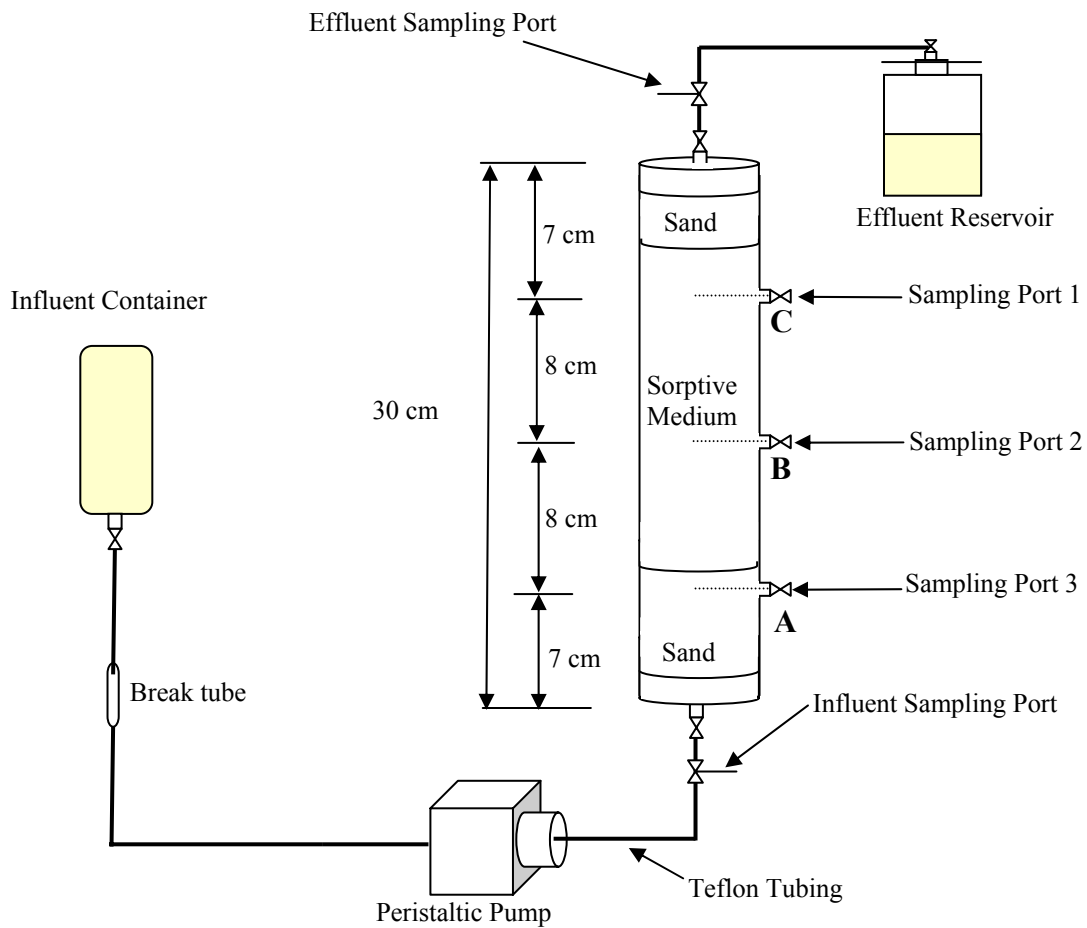


Figure 3. 4. Schematic of the column experiment set up (Demirkan, 2008)

The methodology consisted of gradually adding small 0.5 cm deep batches of material to prevent the segregation and the preferential deposition of larger grained particles. For each addition, the funnel was introduced into the column with the bottom tip resting on the last layer formed, after which the funnel was filled to capacity with dry material which was then slowly, and uniformly released into the column until the funnel was completely emptied. Each addition was followed by gentle compaction with a controlled number of tamps (3 to 4 tamps) using a heavy flat metal pestle with a round head of 4.6 cm diameter. The compressing plane of the pestle was leveled so that the pressure input over the freshly deposited layer was equal on the whole surface. This packing sequence was repeated until the column was filled to the top, with the three types of layers described above. The uniformity of packing was checked after each 5 cm layer of material deposited. After each 5 cm layer was deposited, the weight of the material remaining was measured and, by subtraction from the known initial mass, the packed amount of material was determined and the bulk density of each 5 cm layer was calculated. The results showed a reasonable uniformity along the column. Once the column was filled, it was connected with the influent and the effluent assemblies described above. At that point, the metal leaching or organic contaminant sorption/desorption experiments were performed as described in Sections 3.3.2 and 3.4.2, respectively. These tests were then followed by tracer tests and permeability tests on each column, which are described in the following paragraphs.

Conservative bromide tracer tests were carried out on each of the column specimens prepared for the metal leaching and sorption/desorption of organics

experiments. Bromide was chosen as tracer chemical for this study because it is absent from the artificial groundwater recipe used in this work, and it is non-reactive, and is easily quantified. The influent tracer (NaBr) concentration (1000 mg/L) dissolved in the artificial groundwater solution was selected such that it did not change the density of the aqueous solution. This solution was injected up-flow in the column system through a Teflon tubing set up using a peristaltic pump at a 50-60 mL/h flow rate (same flow rate as used in desorption of organics and leaching of inorganics experiments). This solution was injected as a step input into the column at time zero. Extensive sampling was then performed every 15-20 minutes from the effluent port over the entire test period to monitor for the tracer breakthrough. In the case of experiments performed in columns with sampling ports along the column, sampling was also performed from the ports. At least 2.5 mL of sample was collected each time. The measurement of the tracer concentration in the collected samples was performed within 24 hours as described in Section 3.5.1. Once the tracer breakthrough had occurred, a tracer washout experiment was performed by following the same procedure as described above, except that the feed solution was a step input of bromide-free artificial groundwater solution.

Constant head hydraulic conductivity tests were performed on all column specimens, after the input/washout tracer tests were completed. Several fundamental test conditions are required for the success of the test: a laminar continuous flow with no changes in the volume of the specimen during the test, a completely saturated specimen, and steady state flow conditions without changes in hydraulic gradient. Measures were taken to ensure that these conditions were satisfied before starting the

test. Two transparent glass cylinders attached on a board with a metric scale were used as manometer tubes for measuring the water heads. The two manometer tubes were connected through a series of fittings and tubing to the inlet and the outlet, respectively, of the column reactor. A constant flow of artificial groundwater was injected into the column and continued until a stable head condition, with no significant change in water manometer levels, was reached. Next, at different time intervals, measurements of the flow rate ( $Q$ ), and head loss ( $\Delta h$ ) (the difference in level in the manometers) were recorded, and coefficient of hydraulic conductivity ( $k$ ) for each specimen was calculated as follows:

$$k = \frac{Q \times \Delta L}{A \times \Delta h} \quad (3.1)$$

where  $Q$  is flow rate,  $L$  is specimen height,  $A$  is cross-sectional area of the specimen;  $\Delta h$  is head loss.

Finally, the homogeneity and isotropic character of the column specimens were visually inspected at the end of the permeability test. To accomplish this, the specimen was drained and carefully removed from the column and then cautiously broken across the transversal area. Subsequently, the column and was examined for evidence of segregation of fine particles. Reasonably uniform homogenous specimens were attained using the dry packing methodology described above (see Figure 3.5).





**Figure 3. 5. Transversal section through the mixture layer of column specimens**

### **3.3. METAL LEACH TESTS**

#### **3.3.1. Batch–Water Leach Test (WLT)**

Batch-Water Leaching Tests (WLTs) were conducted on the seven Maryland fly ashes alone or mixed at different percentage ratios with sand by using a slightly modified version of the standard method ASTM D 3987-85. This standard method has been adopted by many researchers who have performed similar studies (e.g., Lee and Benson 2002, Sauer et al. 2005, Bin-Shafique et al. 2006). The standard method was followed with two modifications. One, the batch reactor system was downsized from a 2 L mixture of leachant/solid to a 50 mL mixture of leachant/solid, to fit the equipment available in the laboratory. Two, the leaching solution was modified. The liquid-to-solid ratio was maintained constant in the case of all materials. Specifically, the standard leaching solution is deionized water; however, the leaching solution used in this work was either the artificial groundwater solution described above, or deionized water with a fixed ionic strength (IS=0.02M) solution, which was intended to simulate the ionic strength of groundwater.

Before starting the procedure, the materials (fly ashes, sand) to be tested were sieved and mixed homogeneously by hand. Subsequently, 2.4 g of the fly ash, or fly ash-sand mixture was added to a 50 mL plastic centrifuge tube followed by 48 mL leachant (i.e., the artificial groundwater solution or deionized water with fixed ionic strength (IS = 0.02M)). This mixture corresponds to a L:S ratio of 20:1 (ml/g). Next, the mixture was agitated continuously on a tumbler rotator at a rate of 29 rpm for 18 hours at room temperature (18-25°C) for equilibration. After equilibration, separation

of the aqueous phase from the solid phase was accomplished by centrifugation of the 50 mL batch reactor tubes at 3000 rpm, 20 °C for 15-20 minutes using a Beckman GPR centrifuge.

The aqueous samples were analyzed for dissolved aluminum, arsenic, chromium and selenium. These metals were selected for analysis because the Toxicity Characteristic Leaching Procedure (TCLP) tests results provided by several of the power plants suggested that they will leach in concentrations that will probably impose serious concerns related to the impact on the environment and human health. To determine the dissolved metal concentrations, the suspended solids were removed by filtration of the supernatant through a 0.2 µm pore size, 25 mm diameter membrane disk filters (Pall Corporation) fitted in a 25 mm Easy Pressure syringe filter holder (Pall Corporation) by using a 60 mL luer-lock plastic syringe. After filtering, the filtrated sample was transferred into an acid-washed plastic centrifuge tube for further analysis. The pH of the aqueous phase was monitored immediately using a pH/Ion meter. It is recommended to analyze the samples for metal concentrations as soon as possible, especially for µg/L concentration levels. However, if it was necessary to preserve the sample for later analysis, after the pH was recorded, the filtrate was acidified to pH <2 using 1.5 mL of concentrated trace metal-grade HNO<sub>3</sub> (Fischer Scientific) per liter of sample. The acidified samples were then stored in a refrigerator at +4 °C to prevent any change in volume due to evaporation. Metal concentrations of interest were determined in the filtered and acidified supernatant by atomic absorption spectrophotometry as described in Section 3.5.2.

### **3.3.2. Column leach tests**

Column metal leach experiments were performed on all seven fly ashes employed in this research. The column specimens were packed as described in Section 3.2.2. Sterilized artificial groundwater solution (prepared as described in Section 3.1.2.1.) was used as the eluant for all leaching experiments. The solution was injected into the column in an up-flow mode at a 50-60 mL/h flow rate, to simulate the natural real field conditions. The leaching of the target metals (aluminum, arsenic, chromium, selenium) was monitored in the samples collected from the effluent port of the column. During the first 48 hours of testing, frequent sampling (every 3-4 hours) was necessary in order to catch the breakthrough curve describing the leaching of each metal studied. After 48 h, the sampling frequency was decreased to twice a day for few days, and once a day as the temporal change in the metals concentration became less significant. After collection, the samples were filtered through a 0.2  $\mu\text{m}$  pore size membrane filters using a plastic syringe, as described above. The filtrate was transferred into an acid-washed plastic centrifuge tube, and preserved and/or analyzed as described above for the batch metal leaching test.

### **3.4. ORGANIC CONTAMINANTS DESORPTION TESTS**

A series of sorption/desorption tests were conducted on three selected fly ashes to study their possible use in a permeable sorptive barrier application. Two different types of tests were conducted: small-scale batch tests and column tests. All tests were conducted using two organic contaminants that represent the PAHs and BETEX groups in petroleum residues (i.e., naphthalene and o-xylene, respectively).

### **3.4.1. Sequential desorption of organics – Batch test**

Sequential desorption of organics was the batch procedure used in this study because it has been concluded that this method is the most representative and more closely simulates the real field conditions in which PRBs are going to be applied. Three fly ashes were selected so as to cover the whole range of carbon content for all power plants: Dickerson Precipitator (LOI = 20%), Paul Smith (LOI = 10%), and Morgantown (LOI = 3%). Stock solutions of the organic contaminants (10 ppm naphthalene, and 40 ppm o-xylene) were prepared by addition to sterilized artificial groundwater (as described above). Due to the relatively low solubility, naphthalene was first prepared as a high concentration stock in methanol before addition to the artificial groundwater solution, while ensuring that the relative volume of added methanol stock did not exceed 0.1% by volume.

The sorption step was performed following ASTM D-5285 method. According to this standard method, the test should be conducted with a solid-to-liquid ration that gives 20-80% sorption. Therefore, a series of preliminary batch kinetic tests were first conducted to study and to identify the optimum solid-to-liquid ratio and equilibration times for all investigated fly ashes. Based on these tests it was determined that a 1:120 solid to liquid ratio was most appropriate for the sorption stage.

For the sorption step the materials (fly ashes) to be tested were first sieved and mixed homogeneously. Next, the 1:120 (g/mL) solid-to-liquid ratio mixture (fly ash + solution) was prepared in a 60-mL glass centrifuge tube batch reactors, capped with

Teflon faced silicon septa. Headspace was eliminated by filling the tubes to the top to exclude possibility of volatilization. Then, the tubes were set up on the tumbler rotator and covered with aluminum foil to avoid photodegradation of the organics and agitated at a rate of 29 rpm for 48 hours at room temperature (18-25 °C) to ensure equilibration. After equilibration, the aqueous phase was separated from the solid phase by centrifugation at 3000 rpm, 20 °C for 15-20 minutes using a Beckman GPR centrifuge.

To determine the sorption efficiency, the concentration of the organic compound remaining in the supernatant after the sorption step was determined. For this, a sample of the supernatant was taken and all the suspended solids were removed by filtration of the supernatant through a series of 0.2-0.45 µm pore size PTFE membrane filters (Pall Corporation) using a 2.5 mL luer-lock glass syringe. The filtered sample was subsequently transferred to 8 mL amber vials capped with an open top screw thread with PTFE-faced rubber septa. Next, this supernatant was analyzed spectrophotometrically for the concentration of the target compounds as described in Section 3.5.4. Analysis was always conducted within 24 hours from the sample removal. The amount of organic compound sorbed was determined as the difference between the initial and final concentrations measured in the supernatant, and expressed as milligrams of organic compound per gram of sorbent (i.e., mg/g).

Following the sorption test, a series of batch desorption tests were conducted using a sequential desorption procedure as described by Kan et al. (1994). For the desorption tests, the remainder of the supernatant from the sorption experiment was carefully removed (avoiding loss of the sorbent) using a 4-in stainless steel syringe

needle fitted in a 60 mL luer-lock plastic syringe. Next, fresh sterilized artificial groundwater solution was added to the sorbent residue in the glass centrifuge tube. The mixture was placed again on the tumbler rotator, covered with aluminum foil and agitated at a rate of 29 rpm at room temperature for 2h the first 5 steps, and then for 24 hours for the rest of the steps until the concentration measured in supernatant dropped below the detection limit. At the end of each desorption time interval, the contents of the centrifuge tube was then centrifuged. As described above, a part of the supernatant was removed, filtered to remove any solid phase particles remaining in suspension, and the concentration of the organic compound desorbed was determined spectrophotometrically. A mass balance on the sorbed-desorbed organics was performed by subtracting the amount desorbed in each desorption step from the amount sorbed determined at the end of the sorption step as described above.

For a more accurate mass balance calculation, the contaminant still present in the solid phase (sorbent) after removal of the supernatant and before addition of the fresh artificial groundwater solution was determined gravimetrically. The target compound present was subtracted from the final desorbed mass determined as described above. This allows for a precise mass balance determination of the desorbed compound.

Finally, another concern in the desorption experiments was the loss of sorbent with and during supernatant decanting (removal). Therefore, to confirm the magnitude of this potential experimental error, the dry weights of the sorbent were determined before and after the sorption and desorption experiments. No significant change in the sorbent dry weights was observed, with the mass loss in all cases  $\Delta \leq 5$ -10 mg (1-2% by weight).

### **3.4.2. Column for desorption of organics test**

The column specimens for the organic contaminant desorption experiments were packed as described in Section 3.2.2. Three fly ashes were selected for these experiments as representative, to cover the whole range of LOI: Dickerson Precipitator with 20.5% LOI, Paul Smith with 10.7% LOI, and Morgantown with 3.1% LOI. For a more complete understanding of the sorption and desorption of the organic contaminants, columns with three sampling ports along the walls were used for these experiments, providing the possibility for monitoring the process of sorption/desorption of organics inside the column at different levels. Separate column tests were conducted for each organic contaminant, i.e., 10 ppm naphthalene and 40 ppm o-xylene were used as the test concentrations. Initially, the columns were saturated with artificial groundwater and then fed with a step input of the artificial groundwater plus organic contaminant solution. Then the sorption process was monitored by periodic sampling from the three ports and from the effluent port, followed by spectrometric analysis for the organic concentration. A syringe pump was used for sample extraction from the ports. Measures were taken such as the extraction rate did not significantly impact the flow uniformity along the column. Specifically, extraction flowrates of 6-8 mL/h were adopted, and extractions were performed from no more than two ports simultaneously. The frequency of sampling was different for each column, depending on how fast the changes in effluent concentrations of organics occurred. Columns packed with fly ash with a high LOI percentage (e.g., Dickerson Precipitator – 20.5% LOI) did not necessitate very frequent sampling, with once a day sampling being sufficient. Columns packed with



fly ash having medium values of LOI % (Paul Smith with 10.7% LOI) required more frequent sampling, at every 6-9 hours. Columns packed with low LOI fly ash (Morgantown with 3.1 % LOI) necessitated the most extensive sampling, with sampling every hour, and the tests completed within 2 days. These experiments (performed by Demirkan, 2008) continued until the effluent sample reached saturation.

When the column effluent reached saturation, the desorption experiment was initiated, which was performed by the author. To start the experiment, the columns were fed with the sterilized groundwater solution without the organic contaminant. The desorption of organics evolution was monitored by periodic sampling from the three ports and from the effluent port, followed by spectrometric analysis for the organics concentration. The tests were considered completed when the concentration of the organic contaminants in the effluent samples reached undetectable levels.

### **3.5. ANALYTICAL METHODS**

#### **3.5.1. pH determination**

The pH determination of the seven Maryland fly ashes subject of study in this project was performed using SW-846 Method 9045 - for soil samples. The materials to be tested were first screened through a No. 10 sieve. A solution with a 1:1 solid to liquid ratio was prepared by weighing 20 g of sieved fly ash, transferring it into a 50 mL beaker, and then adding of 20 mL of deionized water. The resulting suspension was mixed thoroughly using a spatula for 1 minute at 10 minute intervals for ½ hour time period after which the suspension was allowed to equilibrate undisturbed for one

hour. During this time the calibration of the pH meter was performed by using three calibration standard buffer solutions of pH 4, 7 and 10. After the one hour equilibration time, the pH was measured by immersing the pH electrode tip into the mixture and recording the reading on the meter display. While immersing the electrode, the stirring of the sample is recommended to avoid the possible interferences due to sedimentation potential and suspension effect. The pH electrode was rinsed with deionized water and blotted dry with a Kim wipe before analyzing a new sample. At the time of pH measurement the samples were all at room temperature (15-25<sup>0</sup>C). Two replicates were analyzed for each fly ash and the mean values reported.

The pH of the water samples collected from the column tests and batch tests was also determined using same pH meter as above. Method ASTM D1293-99 Standard Test Method for pH of Water was used. Two replicates were measured for each sample and the mean values reported

### **3.5.2. Bromide analysis in tracer test samples**

At least 2.5 mL of sample were collected for analysis of the bromide tracer. The measurement of the tracer concentration in the collected samples from the column tests was performed within 24 hours. Between collection and analysis, the samples were stored at +4 <sup>0</sup>C in a refrigerator to avoid any change in volume. The samples were allowed then to reach the room temperature before conducting the measurements using a Bromide ion electrode (Cole Parmer). A slope-check and calibration was performed prior to the measurements. Four to five standard

concentrations (e.g., 0.1, 1, 10, 50, 100 ppm) were used to construct the calibration curve. A 5 M NaNO<sub>3</sub> solution was used as an Ionic Strength Adjuster (ISA) for all standard solutions and samples. The calibration curve was created by plotting the millivolt readings for each standard against the corresponding known standard concentrations used, and then performing a standard linear regression used to determine the tracer concentration in the unknown samples.

### **3.5.3. Determination of metal concentrations by Atomic Absorption**

#### **Spectrophotometry**

The metal concentrations of interest were determined in the filtered and acidified supernatant by atomic absorption spectrometry (AAS). A Perkin Elmer Model 5100 ZL with a graphite furnace module was used for atomic absorption spectrometric analysis of all samples for chromium (method EPA 218.2), selenium (method EPA 272.2) and aluminum (method EPA 202.1) concentrations. Perkin Elmer hollow cathode lamps were used with wavelengths corresponding to the metals analyzed: 309.3 nm for aluminum, 196 nm for selenium, and 357.9 nm for chromium. After the samples were filtered and acidified they were ready for analysis. 1mL aliquots of sample were poured into small cups which were next placed on the sampler device of the instrument. When the concentration of the samples exceeded the range of the linear calibration curve, the samples were diluted as appropriate to attain concentrations within a linear calibration range.

Certified atomic absorption stock solutions were used for preparation of the standard solutions destined for construction of calibration curves for each metal.

Arsenic reference standard stock solution of 10 ppm concentration was procured from VWR International. Aluminum, chromium and selenium reference standard stock solutions of 1000 ppm concentration were purchased from Ricca Chemical Company. In order to avoid inconsistent interferences during atomic absorption spectrometry analysis, the calibration standards were prepared within the same matrix (in the same background solution) as the unknown aqueous samples to be analyzed. Specifically, the artificial groundwater solution was employed as the background solution for standards and samples. Four different standard concentrations were used for each metal for the calibration of the instrument to cover a range of metal concentrations present in the samples. All standards were prepared by serial dilution from the 1000 ppm certified atomic absorption stock solutions. Calibration curves were constructed at a correlation coefficient of 0.99, after and before each series of 10-15 samples were measured. The results reported by the spectrometer were the average value of the two replicate measurements performed on the same sample. The detection limit for graphite furnace module was determined to be 2 ppb for Cr, Se, and Al.

For determination of total soluble arsenic species concentration by Hydride Generation Atomic Absorption Spectrometry (EPA method 206.3), a Perkin Elmer model 5000 Atomic Absorption Spectrometer supplied with a MHS -10 Mercury Hydride System was used. The HGAAS procedure involves insertion of sodium borohydride solution as reducing agent into an etanche reaction vessel with the sample, producing a violent reaction with the release of volatile hydride. Because this procedure only allows measurement of  $As^{3+}$  species, a pre-reduction step must be introduced for reduction of pentavalent arsenic species to trivalent arsenic species,

allowing quantification of total arsenic in solution. Therefore, prior to the addition of the reducing agent, the aqueous sample was subjected to a pretreatment such that the metal under investigation will be found in the desired ionic form in solution. Accordingly, prior to starting the analysis, a fresh 10% potassium iodide solution, and 3% sodium borohydride ( $\text{NaBH}_4$ ) in 1% sodium hydroxide solution was prepared. The reductant solution ( $\text{NaBH}_4$ ) was filtered through a 0.45  $\mu\text{m}$  filter to eliminate impurities. The analyzing apparatus was configured in conformity with the suggestions from the Operator's Guide. The operating parameters and chemicals used are summarized in Table 3.6. Standard solutions ranging from 1 to 50 ppb were prepared from 10 ppm Arsenic certified atomic absorption stock solution (VWR) in the same matrix (i.e., in the same artificial groundwater background solution) as the unknown aqueous samples to be analyzed, to avoid inconsistent interferences. 2 mL aliquots of samples, standards and blank solutions were used for analysis. If a concentration outside the linear range of the calibration curve was expected, the samples were diluted as appropriate prior to analysis to keep the measured absorbance value in the linear range. 2 mL aliquots of samples, standards solution, and blank solution, were transferred in a plastic centrifuge tube, and 0.6 mL of 32% hydrochloric acid (HCl) solution and 0.2 mL of potassium iodide (KI) solution were added. The mixture was next covered and vortexed few seconds for homogenization and was allowed to react for 60 minutes at room temperature prior to analysis. The quartz cell was set up on the 10 cm, one slot burner head, and adjusted such that a minimum absorbance value was recorded. The spectrometer was auto-zeroed at the

**Table 3. 7. Operating parameters and chemicals for arsenic determination on the HGAAS**

Element – source	Arsenic – Perkin Elmer Hollow Cathode Lamp (HCL)
Wavelength	193.7 nm
Slit setting	0.7 nm
Flame	Air/Acetylene
Reductant	3% NaBH <sub>4</sub> in 1% NaOH
Purge (carrier) gas	N <sub>2</sub> or Ar
Absorption cell	Quartz cell, 165 mm long, 12 mm diameter
Pretreatment solutions	10% KI , 32% HCl (metal trade grade)

maximum absorbance value recorded by analyzing the blank. For calibration of the equipment, the pretreated aliquots of standard were transferred into the reaction vessel which was next reattached to the hydride generator module. When the absorbance reading on the digital display reached the minimum value again, the reducing solution was injected into the reaction vessel, and the injection was ceased immediately after the maximum absorbance value was recorded from the digital display. When the reductant solution is dispensed into the reaction vessel, a violent reduction reaction takes place with the pretreated aqueous sample with liberation of hydrogen reducing the metal ions to volatile hydride. This volatile hydride is further transported by the flow of the inert carrier gas (Ar) through a hose to the quartz cell, where it is decomposed and the absorption value recorded. Each standard was analyzed five times and the average values were used to construct the calibration curve of absorbance versus concentration. A calibration was performed before and after each set of 10-15 samples. The best fit regression line was calculated and used to interpret the unknown samples absorbance values in terms of arsenic concentrations.

All samples were analyzed using the same *modus operandi*. Between two samples the reaction vessel was rinsed several times with 0.18M hydrochloric acid in order to get rid of any borohydride traces. The concentration of arsenic present in the aqueous samples was determined and quantified by direct comparison to the standard calibration curve constructed as described above.

#### **3.5.4. Organics determination by fluorescence analysis**

All analyses of the organic contaminants (naphthalene and o-xylene) were performed by fluorescence spectroscopy, using a Shimadzu 5301 Fluoro-Spectro-Photometer. The excitation and emission wavelengths used for naphthalene and o-xylene were 273 nm and 336 nm and 267 nm and 289 nm, respectively. Standard solutions with concentrations of 0.4 ppm, 0.8 ppm, 1.6 ppm, 4 ppm, 8 ppm, and 16 ppm in deionized water were prepared for construction of the calibration curve for naphthalene. The naphthalene solutions were prepared using a concentrated naphthalene solution in methanol stock as described above. Standard solutions with concentrations of 5ppm, 10 pmm, 20 ppm, 40 ppm, 80 ppm in deionized water were prepared for construction of calibration curve for o-xylene. The method detection limits of the instrument were determined to be 0.0165 ppm for naphthalene, and 1.273 ppm for o-xylene.

The batch and the column samples were all analyzed by fluorescence spectroscopy. The samples extracted from the sampling ports and from the effluent were poured into the 3.5 mL Quartz cell (Shimadzu) which was covered with the PTFE cap and positioned in the specially constructed compartment inside the instrument, and the sample was exposed to the fluorescent light emitted by the lamp. The concentrations measured were recorded by the computer attached to the instrument.

#### **3.6. MATHEMATICAL MODELS**

Mathematical models are important tools for evaluating and predicting leaching of contaminants under different environmental conditions. The transport of



contaminants during leaching from a porous media in plug flow system is described by the advective-dispersive-reactive equation (ADRE) (Brusseau, 1996). Two analytical solutions to the ADRE were used in this study to model the laboratory column leach data presented in Chapter 5: the solution to the ADRE assuming local equilibrium sorption, and a solution to the ADRE with rate-limited desorption. The ADRE, with the assumption of local equilibrium, can be written for one-dimensional uniform flow as (Brusseau, 1996):

$$R_d \cdot \frac{\partial C}{\partial t} = D \cdot \frac{\partial^2 C}{\partial x^2} - v \cdot \frac{\partial C}{\partial x} \quad (3.2)$$

where  $R_d$  is retardation factor,  $C$  is pore fluid solute concentration within the porous media (mg/L),  $t$  is time (h),  $D$  is dispersion coefficient (including both dispersion and diffusion) ( $\text{cm}^2/\text{h}$ ),  $x$  is distance (cm), and  $v$  is seepage velocity (cm/h). Equation (3.1) defines the one-dimensional transport of a contaminant species through a piston flow system and assumes the presence of advective movement of the contaminant via percolating eluant flow under a constant hydraulic gradient, dispersive transport by longitudinal spreading of the contaminant, and retardation by surface-related equilibrium sorption phenomenon. Under these conditions  $R_d$  is defined as follows:

$$R_d = 1 + \left( \frac{\rho_b \cdot K_d}{n} \right) \quad (3.3)$$

van Genuchten (1981), and van Genuchten and Alves (1982), derived an analytical solution to this version of the ADRE that would describe the leaching of contaminants species initially at a uniform equilibrium concentration in the pore phase of the solid, in which case the elution curves are represented by the

complement of the traditional solute breakthrough elution patterns from conventional column experiments:

$$\frac{C(L, T')}{C_o} = 1 - \frac{1}{2} \cdot \left\{ \operatorname{erfc}\left(\frac{R_d - T'}{2 \cdot (T' \cdot R_d / P_L)^{1/2}}\right) + \exp(P_L) \cdot \operatorname{erfc}\left(\frac{R_d + T'}{2 \cdot (T' \cdot R_d / P_L)^{1/2}}\right) \right\} \quad (3.4)$$

where  $C$  is effluent concentration (at distance  $x = L$  after  $T'$  pore volumes of flow have leached) (mg/L), and  $C_o$  is initial pore fluid concentration (mg/L).  $T'$  and  $P_L$  are the pore volumes of flow leached, and Peclet number, respectively, and can be calculated using the following equations:

$$T' = \frac{v \cdot t}{L} \quad (3.5)$$

$$P_L = \frac{v \cdot L}{D} \quad (3.6)$$

The initial and boundary conditions, respectively, for this analytical solution are given by van Genuchten (1981) and van Genuchten and Alves (1982) as follows:

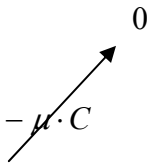
$$C(x, 0) = C_i \quad (3.7)$$

$$\left( v \cdot C - D \frac{\partial C}{\partial x} \right) \Big|_{x=0} = \begin{cases} v \cdot C_{in}; & 0 < t \leq t_0 \\ 0; & t > t_0 \end{cases} \quad (3.8)$$

The first boundary condition defined in Equation (3.8) corresponds to an input influent concentration of contaminant ( $C_{in}$ ) into the system between  $t = 0$  and  $t = t_0$ .

The second boundary condition at  $t > t_0$  defined by equation (3.9) refers to the subsequent period when the column specimen is flushed with clean water.

The model proposed by Fry et al. (1993) is an analytical solution to the ADRE with the assumption of non-equilibrium, or rate-limited desorption. The solution additionally includes a first-order decay coefficient to model the decay of solute in the aqueous phase. However, the decay component of the equation was neglected in the current study due to the fact that the column specimens were sterilized by gamma irradiation during specimen preparation phase and the entire testing periods were relatively short. Leaching is modeled herein as a one-site phenomenon using a linear, first-order relationship in which the rate of desorption is proportional to a first-order rate coefficient and the concentration gradient between the liquid and solid phase. The resulting governing equations for this model, with one-dimensional, steady-state flow occurs through the column system, are for the aqueous phase:

$$\frac{\partial C}{\partial t} + \frac{\rho_b}{n} \cdot \frac{\partial S}{\partial t} = D \cdot \frac{\partial^2 C}{\partial x^2} - v \cdot \frac{\partial C}{\partial x} - \mu \cdot C \quad (3.10)$$


and for the solid phase:

$$\frac{\partial S}{\partial t} = \alpha \cdot (K_d \cdot C - S) \quad (3.11)$$

where  $C$  is aqueous concentration of the contaminant (mg/L),  $S$  is sorbed concentration onto the solids (mg/kg),  $t$  is time (h),  $\rho_b$  is bulk density in the column specimen,  $n$  is porosity of column specimen,  $x$  is distance (cm),  $D$  is dispersion coefficient (cm<sup>2</sup>/h),  $v$  is pore water velocity (cm/h),  $\mu$  is first-order decay coefficient (1/h),  $\alpha$  is first order desorption rate coefficient (1/h), and  $K_d$  is equilibrium partition coefficient (L/kg).

Solution of Equations (3.10) and (3.11), requires selection of the initial and boundary conditions. The assumptions of the model are: 1) the column specimen is initially contaminated and contaminant concentrations (aqueous and sorbed) are uniformly distributed, 2) there is no contaminant flux at the inlet of the column and no dispersive flux of contaminant is present at the column outlet, 3) the sorbed amount on the solid surface ( $S_0$ ) can only decrease by mass transfer and advection or dispersion into the aqueous phase, and 4)  $S_0$  and the aqueous concentration ( $C_0$ ) are initially in linear equilibrium and are related with a partition coefficient ( $K_d$ ). These initial conditions are expressed by the following relationships:

$$C(x,0) = C_0; \quad 0 \leq x \leq L \quad (3.12)$$

$$S(x,0) = S_0; \quad 0 \leq x \leq L \quad (3.13)$$

$$S_0 = K_d \cdot C_0 \quad (3.14)$$

where  $C_0$  is initial aqueous concentration at time  $t = 0$  (mg/L),  $S_0$  is initial sorbed concentration onto the solid surface at time  $t = 0$  (mg/kg), and  $L$  is length of the column (cm).

In this study,  $S_0$  was determined from the leachable amount of metal calculated using the mass balance of the total metal released during column leaching test divided by the amount of solid in the column specimen:

$$S_0 = \frac{\sum_{i=1}^n \{Q \cdot (t_i - t_{i-1}) \cdot (\frac{C_i + C_{i-1}}{2})\}}{M_{solid}} \quad (3.15)$$

where,  $Q$  is the influent flow-rate used in column experiment (L/h),  $t_i$  and  $t_{i-1}$  are the times of sampling (h),  $C_i$  and  $C_{i-1}$  are concentrations measured at times  $t_i$  and  $t_{i-1}$ , respectively (mg/L or  $\mu\text{g/L}$ ) ( $t_i - t_{i-1}$ ) represents the elapsed time between two

measurements (h);  $M_{solid}$  is amount of total solids present in the column specimen (kg),  $n$  is total number of samples collected from the column effluent, and  $i$  denotes the number of samples collected.

With respect to the boundary conditions, at the inlet of the column ( $x = 0$ ), the contaminant flux is zero at all times while at the exit end of the column ( $x = L$ ) there is no dispersive flux of contaminant. These conditions are expressed mathematically as follows:

$$-D \cdot \frac{\partial C}{\partial x}(0, t) + v \cdot C(0, t) = 0; \quad t \geq 0 \quad (3.16)$$

$$\frac{\partial C}{\partial x}(L, t) = 0; \quad t \geq 0 \quad (3.17)$$

To simplify solution of the governing equations, Fry et al. (1993) non-dimensionalized the equations developed above by defining the following dimensionless parameters:

$$\begin{aligned} C^* &= C / C_0 & S^* &= S / S_0 \\ \gamma^* &= \rho_b \cdot K_d / n & \alpha^* &= \alpha \cdot L / v \\ x^* &= x / L & t^* &= t \cdot v / L \\ D^* &= D / v \cdot L = 1 / P_L \end{aligned} \quad (3.18)$$

where  $P_L$  is column Peclet number, and  $t^*$  is number of pore volumes of flow. As a result, the rate of change in concentration, in either liquid or solid phase, is determined by the two dimensionless terms: the dimensionless first-order desorption rate coefficient ( $\alpha^*$ ), and the dimensionless partition coefficient ( $\gamma^*$ ).

Substituting the dimensionless parameters into Equations (3.10) and (3.11), the following relationships are obtained:

$$\frac{\partial C^*}{\partial t^*} + \gamma^* \cdot \frac{\partial S^*}{\partial t^*} = D^* \cdot \frac{\partial^2 C^*}{\partial x^{*2}} - v \cdot \frac{\partial C^*}{\partial x^*} \quad (3.19)$$

$$\frac{\partial S^*}{\partial t^*} = \alpha^* \cdot (C^* - S^*) \quad (3.20)$$

Similarly, the initial conditions can be redefined as follows:

$$C^*(x^*, 0) = 1; \quad 0 \leq x^* \leq L \quad (3.21)$$

$$S^*(x^*, 0) = 1; \quad 0 \leq x^* \leq L \quad (3.22)$$

along with the redefined boundary conditions:

$$-D^* \cdot \frac{\partial C^*}{\partial x^*}(0, t^*) + C^*(0, t^*) = 0; \quad t^* \geq 0 \quad (3.23)$$

$$\frac{\partial C^*}{\partial x^*}(1, t^*) = 0; \quad t^* \geq 0 \quad (3.24)$$

Fry et al. (1993) analytically solved the new dimensionless form of Equations (3.19) and (3.20) using an eigenfunction integral equations method by combining them into a single equation. This single equation is a linear partial differential equation which can be solved in parts, and at the end the solution to each part are computed together to form the full final solution. A detailed step by step presentation of the calculations performed toward reaching the final solution is given in the original paper (Fry et al.1993). The solution into its final form, and the solutions of

the partial terms are given in Equations (3.25) and Equations (3.26) through (3.33), respectively.

$$C^*(x^*, t^*) = \sum_{j=1}^{\infty} a \cdot X \cdot (x^*) \cdot T_j \cdot (t^*) + \sum_{j=1}^{\infty} X \cdot (x^*) \cdot \phi_j \cdot (t^*) \quad (3.25)$$

where  $a = 1/\sigma \cdot \lambda$ .  $\sigma$  and  $\lambda$  are defined along with other parameters below:

$$\sigma = \frac{1}{4} \cdot \left[ 2 + \frac{1}{2 \cdot \xi^2 \cdot D^{*2}} + \frac{1}{\xi} \cdot \left( 1 - \frac{1}{4 \cdot \xi^2 \cdot D^{*2}} \right) \cdot \sin(2 \cdot \xi) - \frac{1}{\xi^2 \cdot D^*} \cdot \cos(2 \cdot \xi) + \frac{1}{\xi^2 \cdot D^*} \right] \quad (3.26)$$

$$\lambda = D^* \cdot \xi^2 + \frac{1}{4 \cdot D^*} \quad (3.27)$$

$$\tan \xi - \frac{4 \cdot D \cdot \xi}{4 \cdot D^2 \cdot \xi^2 - 1} = 0 \quad (3.28)$$

$$\xi = \frac{(4 \cdot D^* \cdot \lambda - 1)^{1/2}}{2 \cdot D^*} \quad (3.29)$$

$$X = \exp\left(\frac{x^*}{2 \cdot D^*}\right) \cdot \left[ \frac{1}{2 \cdot D^* \cdot \xi} \cdot \sin(\xi \cdot x^*) + \cos(\xi \cdot x^*) \right] \quad (3.30)$$

$$T_j = \frac{1}{2 \cdot D^* \cdot \xi} \cdot \exp\left(\frac{\alpha^* + \alpha^* \cdot \gamma^* + \lambda}{2} \cdot t^*\right) \cdot \left\{ \cosh(\omega \cdot t^*) + \frac{\alpha^* - \alpha^* \cdot \gamma^* - \lambda}{2 \cdot \omega} \cdot \sinh(\omega \cdot t^*) \right\} \quad (3.31)$$

$$\omega^2 = \frac{(\alpha^* + \alpha^* \cdot \gamma^* + \lambda)^2 - 4 \cdot \alpha^* \cdot \lambda}{4} \quad (3.32)$$

$$\phi_j = \frac{\alpha^* \cdot \gamma^* \cdot a}{\omega} \cdot \exp\left(-\frac{\alpha^* + \alpha^* \cdot \gamma^* + \lambda}{2} \cdot t^*\right) \cdot \sinh(\omega \cdot t^*) \quad (3.33)$$

## CHAPTER 4

### EVALUATION OF TRANSPORT PARAMETERS IN COLUMN TESTS

Permeable reactive barriers are placed in front of a plume, and the contaminants are immobilized and/or transformed into less harmful compounds as the plume flows through the barrier wall under field gradients. Therefore, one desirable characteristic of the selected reactive medium is to provide no constraints to the groundwater flow, i.e., high it should have hydraulic conductivity. In other words, “a PRB is a barrier to contaminants, but not to groundwater flow” (Powell and Puls 1997, Powell and Powell 1998). In addition, an evaluation of solute transport parameters (e.g., hydrodynamic dispersion, porosity) is crucial in predicting the fate and transport of contaminants in subsurface environments.

To determine the transport and flow parameters in this study, laboratory tracer experiments and constant-head hydraulic conductivity tests were conducted on all column specimens. The column specimens were prepared following the procedures described in Section 3.2.2. For the tracer tests, a solution of artificial groundwater spiked with ( $C_0$ ) 1000 ppm sodium bromide (NaBr) (a non-reactive tracer) was supplied to the influent end of the column as a step input at a constant flow rate, using a peristaltic pump. A flow rate  $Q$  of 40 to 60 mL/h was selected to simulate typical velocities ( $3 \times 10^{-3}$  to  $2 \times 10^2$  m/d) expected in field conditions (Gelhar et al. 1992). Subsequently, tracer concentrations were periodically monitored at the sampling ports (where available) located along the central axis of the column, and at the effluent port



until a steady-state concentration profile was achieved throughout the column. Once the tracer breakthrough had occurred, a tracer washout experiment was performed by following the same procedure with the same flowrates, except that the feed solution was a step input of bromide-free artificial groundwater solution. The washout tests were conducted to confirm the results of the step-input experiments. Subsequently, the breakthrough and washout curves for all the packed specimens were constructed by plotting the tracer concentration ratios ( $C/C_0$ ) against the time of sampling. A total of 14 column experiments were performed. Of those experiments, 10 were conducted in columns equipped with 2-3 sampling ports along the central axis, allowing rigorous monitoring of tracer migration along the column, while the remaining four were performed in columns with sampling performed only at the effluent end.

Estimation of solute transport parameters in the columns was performed by fitting a theoretical, one-dimensional continuous source transport model called TRAFIT3D (Schicke 1996) to the experimental data (see Appendix 1 for details). This approach allowed quantification of the solute transport parameters by using a non-linear least squares parameter optimization method. Several input parameters were necessary to perform the nonlinear regression: the length of the column, the cross-sectional area of the column, and the flow rate used in the column experiments. In addition, initial estimates for the seepage velocity ( $v_x$ ) and the dispersion coefficient ( $D_H$ ), were required, as well as the experimental tracer breakthrough concentrations as a function of time. The program determines the best fit values for the seepage velocity, and hydrodynamic dispersion coefficient by using a modified version of Levenberg-Marquardt method, which minimizes the sum of squared

residuals between the experimental and modeled concentrations. The porosity ( $n$ ), is calculated from the best fit velocity ( $n = \text{flow} / (\text{cross-sectional area} \times \text{seepage velocity})$ ). Output files for the tracer and washout test model fits are provided in Appendix 1.

In order to use the program TRAFIT3D for the washout data, it was necessary to invert the data, i.e., the data were modeled backwards in time. To accomplish this, the final concentration of the tracer curve was set as the initial concentration for the washout curve, and a “mirror” image of the washout curves was created resulting in a breakthrough-like curve. When, the “mirrored” washout modeled results were flipped back and the input/washout experimental data and modeled results were plotted versus time, bell shaped curves were observed. Examples of laboratory and model tracer breakthrough and washout curves for the columns packed with a mixture of 40% Potomac River (PR) fly ash and 60% sand, and 40% Dickerson Precipitator (DP) fly ash and 60% sand, respectively, are shown in Figures 4.1 and 4.2, respectively. The curves are based on data collected from the effluent port of the PR column, and from the four sampling ports of the DP column. The tracer breakthrough-washout curves for all columns are given in Appendix 1. The breakthrough-washout data typically exhibit symmetric bell shaped curves similar to the observations made by Padilla et al. (1999). In order to verify this symmetry, the tracer and the inverted washout curves of selected columns were plotted on same graph. Figures 4.3 and 4.4 provide these comparisons for a column with one port (effluent) and another one with multiple ports, respectively. The tracer and washout curves are highly comparable in all cases. The discrepancies are attributed to operational errors, fluctuations in flow rates, and measurement errors.

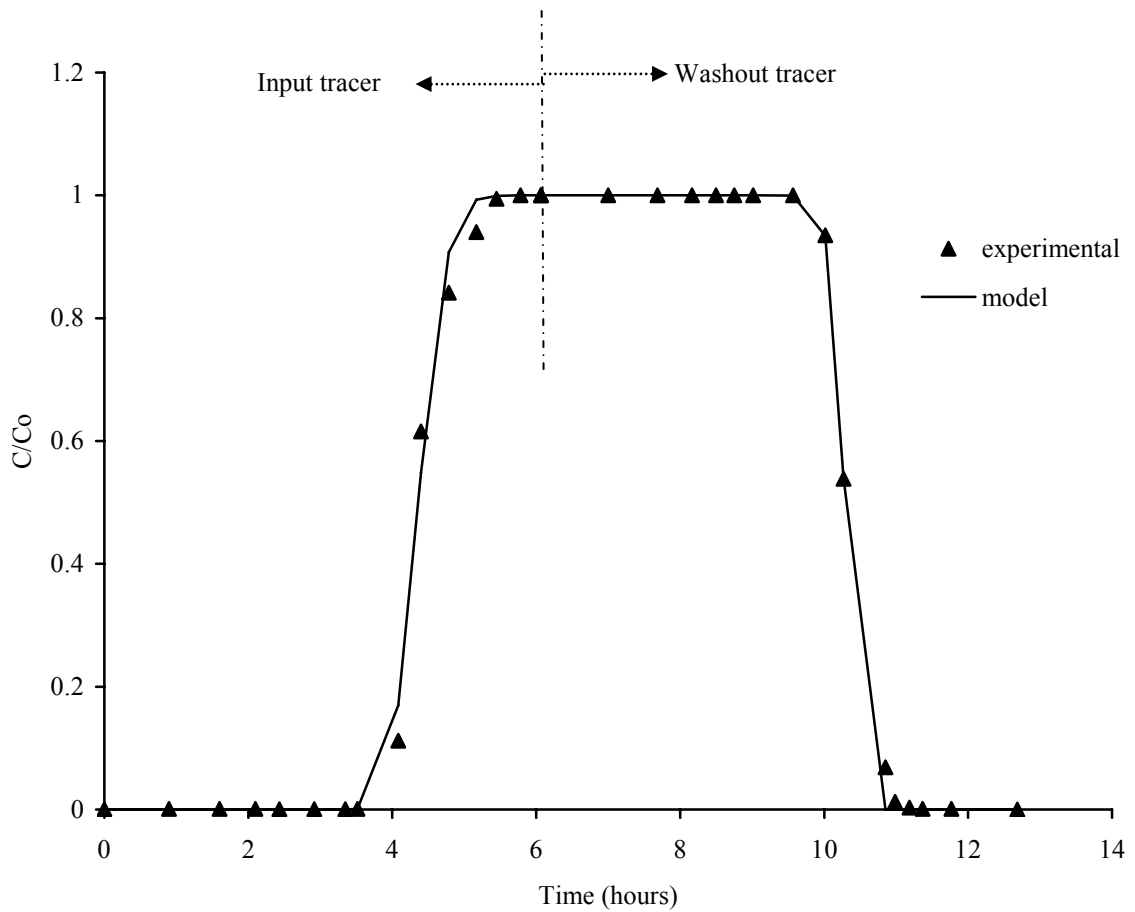


**Figure 4. 1. Observed and modeled bromide tracer breakthrough and washout curves for the 40% Potomac River fly ash/60% sand column. The sampling was conducted at the effluent port only. Each experimental data point represents a single measurement.**

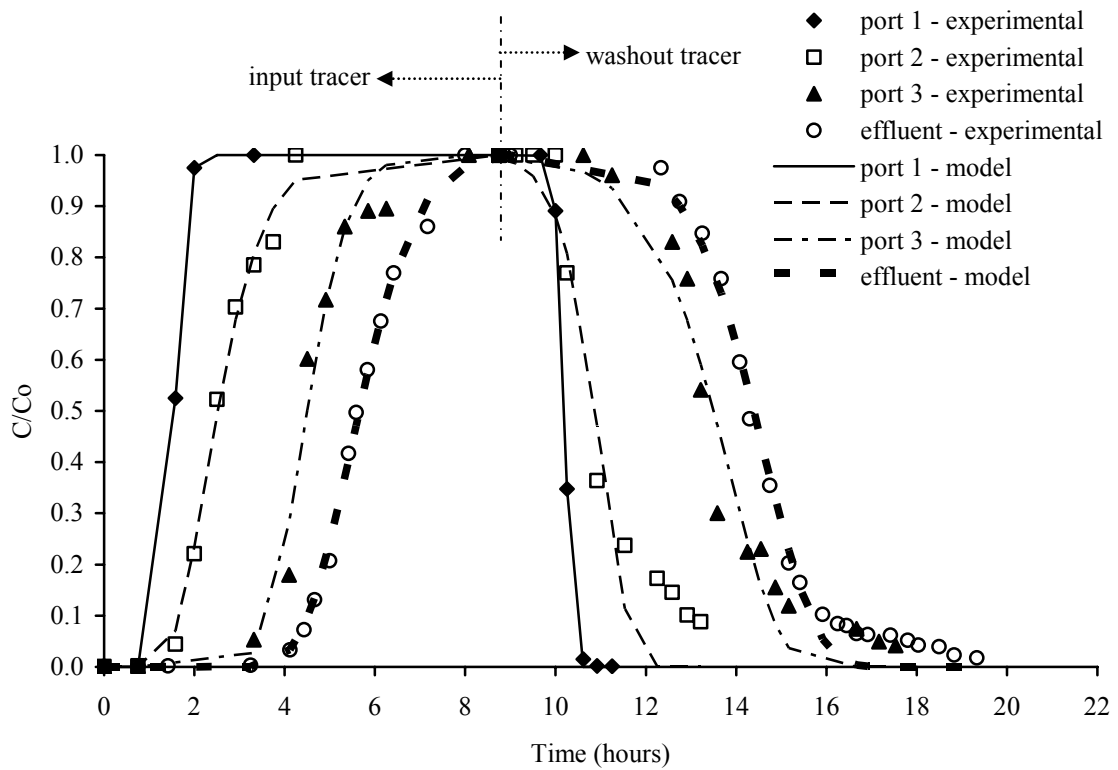


**Figure 4. 2. Observed and modeled bromide tracer breakthrough and washout curves for the 40% Dickerson Precipitator fly ash/60% sand column. The sampling was conducted at the three ports along the column as well as at the effluent port. Each experimental data point represents a single measurement.**

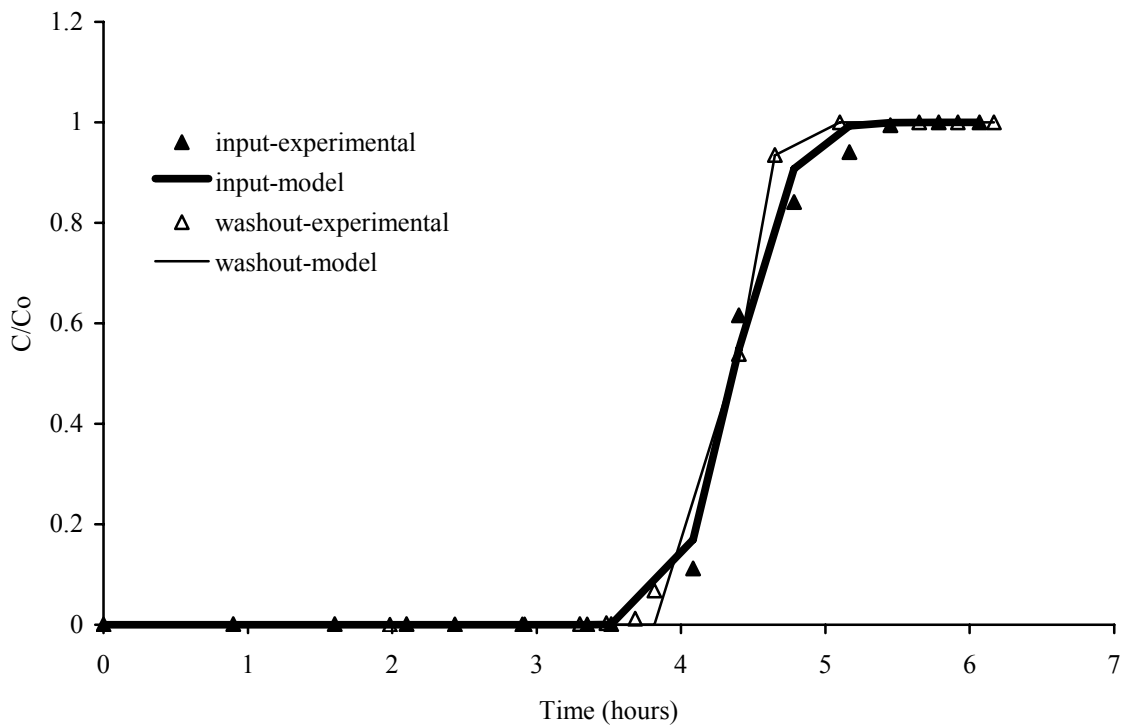


**Figure 4. 3. The bromide tracer input and inverted washout curves for the 40% Potomac River fly ash/60% sand mixture column. Each experimental data point represents a single measurement.**

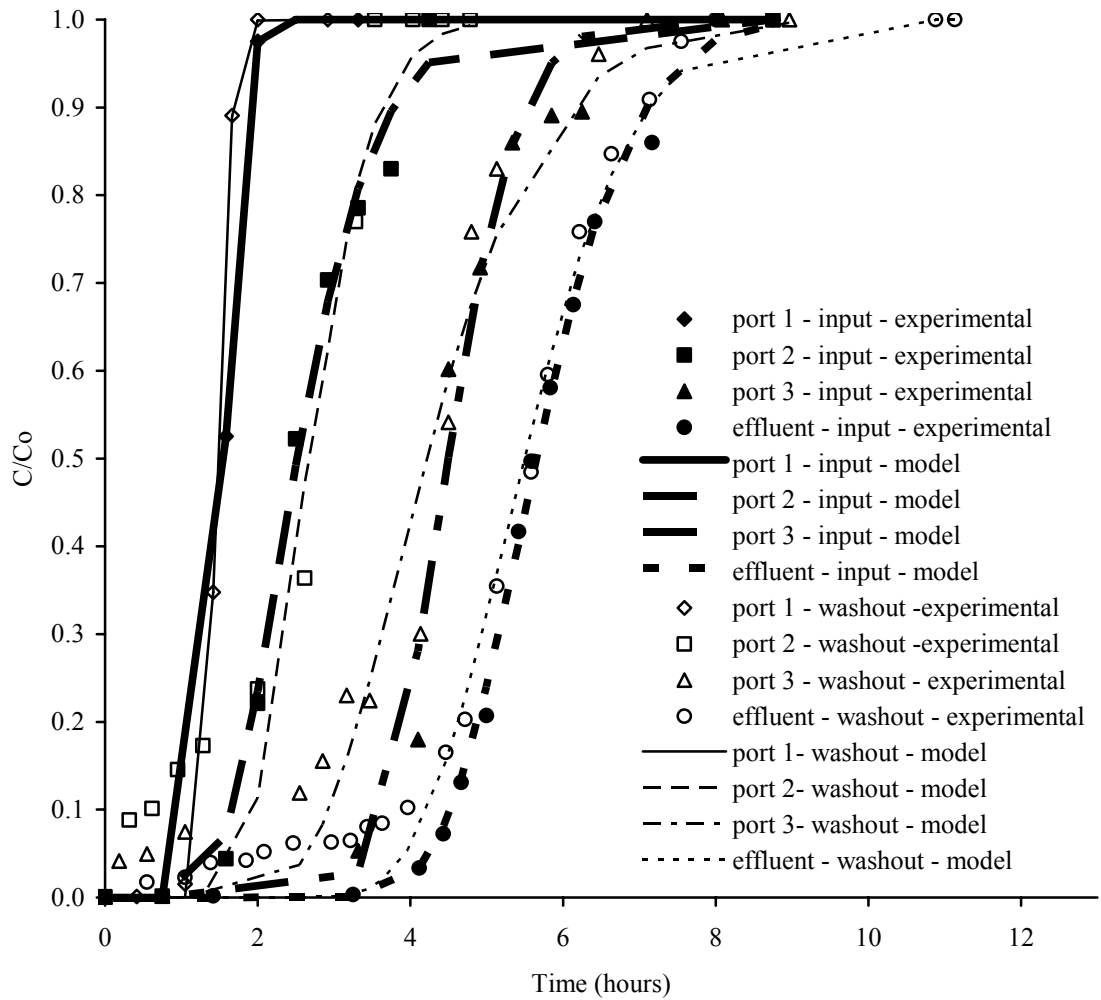


**Figure 4. 4. The bromide tracer input and inverted washout curves for the 40% Dickerson Precipitator fly ash/60% sand mixture column. Each experimental data point represents a single measurement.**

Based on these observations, the transport parameters were determined using the input (tracer) curves only. The resulting best fit parameters ( $v_x$ ,  $D_H$ ) are summarized in Table 4.1. Porosity values were calculated by the program using the best-fit seepage velocities and the input flow rates, as described above. The calculated porosities ranged between 0.53 and 0.45 for the bottom sand layer, and between 0.33 and 0.43 for the fly ash–sand mixture layer. The values agree reasonably well with the porosities of 0.32 -0.46 and 0.31-0.53 reported by Creek (1991) and Bin-Shafique et al. (2006), respectively, for similar sands and sand-fly ash mixtures.

In addition to the porosity, two other parameters were calculated from the experimental data: the longitudinal dispersivity ( $\alpha$ ), and the Peclet number ( $P_L$ ). Because the best fit seepage velocities are in a range between  $1.1 \times 10^{-3}$  cm/s and  $2.3 \times 10^{-3}$  cm/s, it was assumed that the mechanical dispersion was dominant over molecular diffusion. Therefore, the longitudinal dispersivities ( $\alpha$ ) for all column specimens were calculated using the following relationship (Robbins 1989):

$$\alpha = \left( \frac{D_H}{v_x} \right) \quad (4.1)$$

where  $D_H$  is dispersion coefficient ( $m^2/s$ ), and  $v_x$  is seepage velocity (cm/s). It was confirmed that ignoring molecular diffusion in the calculation of longitudinal dispersivities introduced an error of <5%. The column Peclet number was calculated from the best fit parameters by using the following relationship:

$$P_L = (v_x \cdot L) / D_H \quad (4.2)$$

where,  $L$  is the length of the column, which was equal to 30 cm for the columns used in the current study. These calculated values are summarized in table 4.1 as well

**Table 4. 1. Flow and transport related properties of specimens used in column experiments**

Column mixtures (contaminant)	port	$v_x$ (cm/s)	$n$	$D_H$ (m <sup>2</sup> /s)	$Q$ (ml/h)	$\alpha$ (cm)	$P_L$
2% PAC + 98% Sand (o-Xylene)	1	$1.5 \times 10^{-3}$	0.53	$2.9 \times 10^{-8}$	52	0.19	420
	2	$1.5 \times 10^{-3}$	0.42	$8.7 \times 10^{-9}$		0.06	
	3	$1.5 \times 10^{-3}$	0.41	$5.7 \times 10^{-9}$		0.04	
	Effluent	$1.4 \times 10^{-3}$	0.30	$1.9 \times 10^{-8}$		0.13	
2% PAC + 98% Sand (Naphthalene)	1	$1.1 \times 10^{-3}$	0.45	$7.8 \times 10^{-9}$	52.2	0.07	118
	2	$1.8 \times 10^{-3}$	0.36	$5.2 \times 10^{-7}$		0.89	
	3	$1.5 \times 10^{-3}$	0.43	$2.7 \times 10^{-7}$		0.77	
	Effluent	$1.3 \times 10^{-3}$	0.38	$1.1 \times 10^{-7}$		0.83	
40% Morgantown + 60% Sand (o-Xylene)	1	$1.6 \times 10^{-3}$	0.51	$1.1 \times 10^{-8}$	52.9	0.07	392
	2	$1.9 \times 10^{-3}$	0.35	$1.2 \times 10^{-8}$		0.07	
	3	$2 \times 10^{-3}$	0.33	$2.1 \times 10^{-8}$		0.11	
	Effluent	$1.8 \times 10^{-3}$	0.28	$1.3 \times 10^{-8}$		0.08	
40% Motganton + 60% Sand (Naphthalene)	2	$1.9 \times 10^{-3}$	0.32	$1.1 \times 10^{-7}$	40	0.58	56.2
	3	$1.3 \times 10^{-3}$	0.36	$6.3 \times 10^{-8}$		0.49	
40% Dickerson Precipitator + 60% Sand (Naphthalene)	1	$1.2 \times 10^{-3}$	0.41	$6.6 \times 10^{-9}$	49	0.05	191
	2	$1.6 \times 10^{-3}$	0.38	$1.2 \times 10^{-7}$		0.78	
	3	$1.4 \times 10^{-3}$	0.43	$4.1 \times 10^{-8}$		0.29	
	Effluent	$1.5 \times 10^{-3}$	0.31	$6.6 \times 10^{-8}$		0.46	
40% Dickerson Precipitator + 60% Sand (o-Xylene)	2	$1.6 \times 10^{-3}$	0.40	$1.2 \times 10^{-7}$	52.2	0.77	142
	3	$1.4 \times 10^{-3}$	0.43	$2.1 \times 10^{-8}$		0.15	
	Effluent	$1.5 \times 10^{-3}$	0.33	$2.5 \times 10^{-8}$		0.17	
40% Paul Smith + 60% Sand (Naphthalene)	1	$1.6 \times 10^{-3}$	0.51	$2.6 \times 10^{-8}$	56	0.17	376
	2	$1.8 \times 10^{-3}$	0.40	$7.5 \times 10^{-8}$		0.43	
	3	$2 \times 10^{-3}$	0.35	$8.4 \times 10^{-9}$		0.04	
	Effluent	$2 \times 10^{-3}$	0.27	$1.4 \times 10^{-8}$		0.06	
40% Paul Smith + 60% Sand (o-Xylene)	2	$1.9 \times 10^{-3}$	0.34	$3 \times 10^{-8}$	51.9	0.16	183
	3	$1.6 \times 10^{-3}$	0.40	$4.4 \times 10^{-8}$		0.27	
	Effluent	$1.8 \times 10^{-3}$	0.27	$22 \times 10^{-8}$		0.12	
40% Paul Smith + 60% Sand	1	$1.5 \times 10^{-3}$	0.41	$9 \times 10^{-9}$	54	0.06	345
	2	$1.5 \times 10^{-3}$	0.41	$7.5 \times 10^{-9}$		0.05	
	3	$1.7 \times 10^{-3}$	0.41	$3.6 \times 10^{-8}$		0.22	
	Effluent	$1.5 \times 10^{-3}$	0.36	$3.1 \times 10^{-8}$		0.21	
100% Sand (Naphthalene)	2	$1.7 \times 10^{-3}$	0.54	$2.4 \times 10^{-8}$	59.9	0.14	415
	3	$1.7 \times 10^{-3}$	0.53	$8.3 \times 10^{-9}$		0.05	
40% Brandon Shores + 60% Sand	Effluent	$2 \times 10^{-3}$	0.41	$1.8 \times 10^{-8}$	52.8	0.09	340
40% Potomac River + 60% Sand	Effluent	$1.9 \times 10^{-3}$	0.44	$1.4 \times 10^{-8}$	54	0.07	416
40% Chalk Point + 60% Sand	Effluent	$2.3 \times 10^{-3}$	0.36	$3.3 \times 10^{-8}$	54	0.14	208
40% Dickerson Baghouse + 60% Sand	Effluent	$2 \times 10^{-3}$	0.41	$4.4 \times 10^{-8}$	53	0.22	135

**Note:**  $v_x$  represents the best fit seepage velocities provided by the trafit 3d program,  $n$  represents the best fit porosity  $D_H$  is the best fit dispersion coefficient,  $Q$  is the flowrate used in column experiments,  $P_L$  is the Peclet number calculated as average between the ports,  $\alpha$  is the longitudinal dispersivity calculated with equation (4.1).



The low dispersion coefficients ( $D_H$ ) and the correspondingly large Peclet numbers (if  $P_L > 5$ ) suggest that the solute transport is mainly advection-dominated (Shackelford 1994). This was also evidenced by a sharp increase in the initial portion of the tracer curves and very little spreading in the washout curves. The hydrodynamic dispersion coefficients range from  $5.7 \times 10^{-9}$  to  $5.2 \times 10^{-7}$  m<sup>2</sup>/sec, comparable with the ones reported by Bin Shafique et al. (2006) in similar column studies. The calculated Peclet numbers, on the other hand, are one to two orders of magnitude higher than the ones determined by Bin Shafique et al. (2006), due probably to the larger column and/or smaller dispersivities in the column experiments.

Table 4.2 provides a summary of the constant head hydraulic conductivity test results. The measured hydraulic conductivity for the sand alone was  $4.5 \times 10^{-2}$  cm/sec, while the hydraulic conductivities ranged from  $4.8 \times 10^{-5}$  cm/sec to  $1.9 \times 10^{-4}$  cm/sec for the fly ash-sand mixtures. These results for the fly ash sand mixtures are comparable with the ones reported by Creek (1991) (range,  $1.4 \times 10^{-4}$  cm/sec to  $1.0 \times 10^{-7}$  cm/sec) for similar mixtures. The measured hydraulic conductivities are at least one order of magnitude higher than values previously reported for pure fly ash (Long 2003) ( $K_{\text{mean}} \sim 7 \times 10^{-6}$  cm/sec), and at least two orders of magnitude higher than the ones reported by Bin Shafique et al. (2006) for clay-fly ash mixtures ( $K_{\text{mean}} \sim 10^{-7}$  cm/sec). Although, the measured hydraulic conductivities for the fly ash-sand mixtures in this study are in the lower range of typical silty sands (Coduto 1999), they and are not expected to impede the flow through a PRB under field conditions.

**Table 4. 2. Constant – head hydraulic conductivity test results**

<b>Column study</b>	<b><math>\Delta h</math> (cm)</b>	<b>K (cm/sec)</b>
100% SAND (Naphthalene)	0.28	$4.5 \times 10^{-2}$
2% PAC + 98% Sand (o-Xylene)	6.4	$9.7 \times 10^{-3}$
2% PAC + 98% Sand (Naphthalene)	31.26	$1.3 \times 10^{-3}$
40% Morgantown + 60% Sand (o-Xylene)	47.37	$4.8E \times 10^{-5}$
40%Morgantown + 60% Sand (Naphthalene)	15.05	$1.1 \times 10^{-4}$
40%Dickerson Precipitator + 60% Sand (Naphthalene)	18.06	$1.6 \times 10^{-4}$
40%Dickerson Precipitator + 60% Sand (o-Xylene)	20.52	$1.6 \times 10^{-4}$
40%Paul Smith + 60% Sand (Naphthalene)	28.54	$9.5 \times 10^{-5}$
40%Paul Smith + 60% Sand (o-Xylene)	12.84	$1.6 \times 10^{-4}$
40%Dickerson Baghouse + 60% Sand	17.8	$1.7 \times 10^{-4}$
40%Brandon Shores + 60% Sand	19.3	$1.9 \times 10^{-4}$
40%Potomac River + 60% Sand	21.1	$1.1 \times 10^{-4}$
40%Chalk Point + 60% Sand	19.8	$1.5 \times 10^{-4}$
40%Paul Smith + 60% Sand	23.2	$1.7 \times 10^{-4}$

## CHAPTER 5

### METAL CONTAMINANTS - RESULTS AND DISCUSSIONS

#### 5.1. BATCH WATER LEACHING TESTS

Batch water leach tests (WLTs) were conducted on seven fly ashes and several sand-fly ash mixtures in order to evaluate the leaching potential of the target four metals (aluminum, arsenic, chromium, and selenium). Two different leaching solutions were used to investigate the effect of the eluant on the leaching behavior of the metals: a deionized water with ionic strength fixed (IS = 0.02M using CaCl<sub>2</sub>), and a dilute mineral salt nutrient solution recipe described by Murphy et al. (1997). Details on leaching solutions are given in Section 3.1.2.1. A series of five batch WLTs were conducted for each fly ash employing four different sand-fly ash mixtures and fly ash alone, and were repeated for each of the two leaching solutions. Duplicate tests were conducted on each mixture with a given leaching solution. The results are presented in Table 5.1, and the average aqueous concentrations (along with the standard deviations indicated by error bars) of the four metals are plotted against fly ash content in Figures 5.1 through 5.8.

As expected, for all seven fly ashes, aqueous concentrations increased as the fly ash content increased. In other words, the metal concentrations from the sand-fly ash mixtures tend to be lower than those from fly ash alone. The metal concentrations generally varied linearly with fly ash content (Table 5.1). In few cases R<sup>2</sup> values were relatively low (R<sup>2</sup><0.9), suggesting that an estimation based on a simple dilution

**Table 5. 1. Aqueous concentrations of metals from WLTs with fly ash alone and sand-fly ash mixtures**

Fly ash	Sand + Fly ash Mixture	pH <sup>DI</sup>	Metal concentrations								pH <sup>GW</sup>
			Aluminum (mg/L)		Arsenic (µg/L)		Chromium(µg/L)		Selenium(µg/L)		
			C <sub>aq</sub> <sup>DI</sup>	C <sub>aq</sub> <sup>GW</sup>	C <sub>aq</sub> <sup>DI</sup>	C <sub>aq</sub> <sup>GW</sup>	C <sub>aq</sub> <sup>DI</sup>	C <sub>aq</sub> <sup>GW</sup>	C <sub>aq</sub> <sup>DI</sup>	C <sub>aq</sub> <sup>GW</sup>	
Paul Smith	100% FA	8.6	0.93	0.25	335.4	238.4	12	11.3	227.5	216.8	7.42
	20% sand+80%FA	8.44	0.86	0.15	311.3	212.8	7.4	9.4	203.2	103.5	7.38
	30% sand+70%FA	8.46	0.90	0.13	279.3	202.2	6.4	9.3	188.8	83.3	7.31
	50% sand+50%FA	8.32	0.66	0.07	246.4	184.4	6	7	168.7	79.5	7.3
	60% sand+40%FA	8.16	0.72	0.04	214.2	161.3	5.4	6.6	173	47.4	7.28
Dickerson	100% FA	10.83	15.52	2.85	355.7	348.8	24.3	38.5	357.2	339	8.51
	20% sand+80%FA	10.67	13.9	2.16	334.9	328.7	15.9	33.6	335.3	227.4	8.42
	30% sand+70%FA	10.63	12.46	1.66	295	308	14.1	32.9	313.4	210	8.36
	50% sand+50%FA	10.5	9.73	1.21	194	246	13.8	22.7	258	156.9	8.26
	60% sand+40%FA	10.41	8.37	1.07	245.5	226.3	9.7	18.6	289.3	142	8
Morgantown	100% FA	8.42	16.30	2.39	319.8	379.1	59.4	93.6	88.5	46.5	7.31
	20% sand+80%FA	8.31	14.31	1.68	290.2	348.4	40.1	88.4	81.7	43.5	7.21
	30% sand+70%FA	8.3	13.16	1.17	275.3	324.3	34.9	80.9	56.9	41.2	7.24
	50% sand+50%FA	8.2	10	0.86	229.1	287.3	26.8	54.5	35.8	36.9	7.2
	60% sand+40%FA	8.1	8.38	0.34	207	256.5	27	47.1	35.3	33.3	7.2
Potomac River	100% FA	8.77	0.51	0.13	134	345.7	21.9	35.2	9	22	7.64
	20% sand+80%FA	8.8	0.45	0.10	132.7	332.7	16.9	32.3	8.1	16.5	7.54
	30% sand+70%FA	8.48	0.44	0.08	129.2	314.9	13.4	27.2	7.7	14.7	7.51
	50% sand+50%FA	8.28	0.37	0.06	127.5	302.9	12.1	18.7	7.6	14.6	7.4
	60% sand+40%FA	8.2	0.35	0.04	123.6	287.6	8.9	15.1	5.5	13.2	7.22
Dickerson	100% FA	10.41	17.55	3.99	386.3	192.1	25.4	56.8	191.1	113.2	8.32
	20% sand+80%FA	10.14	15.73	2.61	363.3	171.9	19.1	51.3	170.8	91.3	8.13
	30% sand+70%FA	9.92	15.35	1.84	292.1	162.8	17.8	48.1	158.1	84.7	7.99
	50% sand+50%FA	9.91	10.06	1.24	299.8	155.1	13.6	36.2	144	69.7	7.89
	60% sand+40%FA	9.72	9.31	1.04	256.1	140.2	13.8	29.9	143	56.1	7.72
Chalk Point	100% FA	8.22	8.92	1.94	181.4	165.2	49.0	68.4	17.8	15.3	7.35
	20% sand+80%FA	8.05	7.81	1.41	173	141.8	37.2	65.3	14.3	14.4	7.25
	30% sand+70%FA	7.97	7.3	0.78	166.5	134.7	32.3	54.8	12.3	13.5	7.26
	50% sand+50%FA	7.67	6.42	0.24	154.2	136	30.4	39.6	11.8	13.4	7.2
	60% sand+40%FA	7.6	5.49	0.21	145.4	116.5	24.1	31.6	10.4	13.2	7
Brandon Shores	100% FA	8.93	2.55	0.23	201.2	160.6	22.5	24.3	16	9	7.82
	20% sand+80%FA	8.63	2.34	0.19	167.1	149	16.2	21.8	13.8	8.1	7.77
	30% sand+70%FA	8.54	2.13	0.09	162.9	130.1	13.5	19.5	12.8	7.1	7.52
	50% sand+50%FA	8.44	1.76	0.09	151.6	124.3	17.4	14.1	8	5.5	7.5
	60% sand+40%FA	8.28	1.50	0.08	142.5	97.7	9	11	6.2	4.1	7.43
Sand	100% Sand	-	0.08	0.05	22.6	23.9	2.7	3.2	2.6	0.8	

**Note:** pH<sup>DI</sup>, pH<sup>GW</sup> = pH measured in WLTs with deionized water (with ionic strength fixed, IS=0.02M), and groundwater, respectively; C<sub>aq</sub><sup>DI</sup>, C<sub>aq</sub><sup>GW</sup> = aqueous concentrations measured in WLTs with deionized water (with ionic strength fixed, IS=0.02M), and groundwater, respectively. These are the average of duplicate tests.

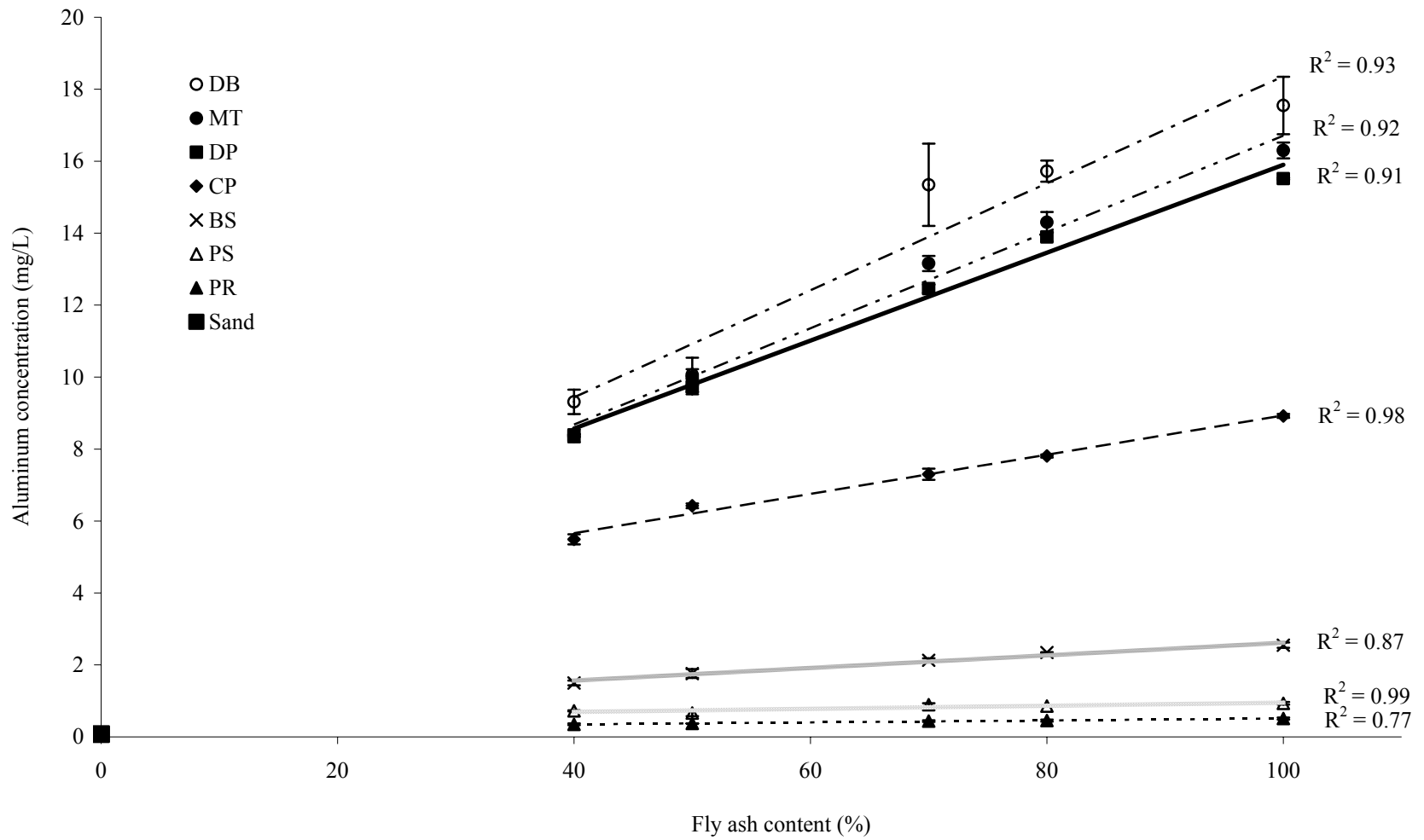


Figure 5. 1. Aluminum aqueous concentrations in WLTs conducted with deionized water with ionic strength fixed (IS=0.02M) on different sand-fly ash mixtures. Symbols represent the average values of two experimental replicates, error bars represent the standard deviation, and lines represent the linear best fit to the data.

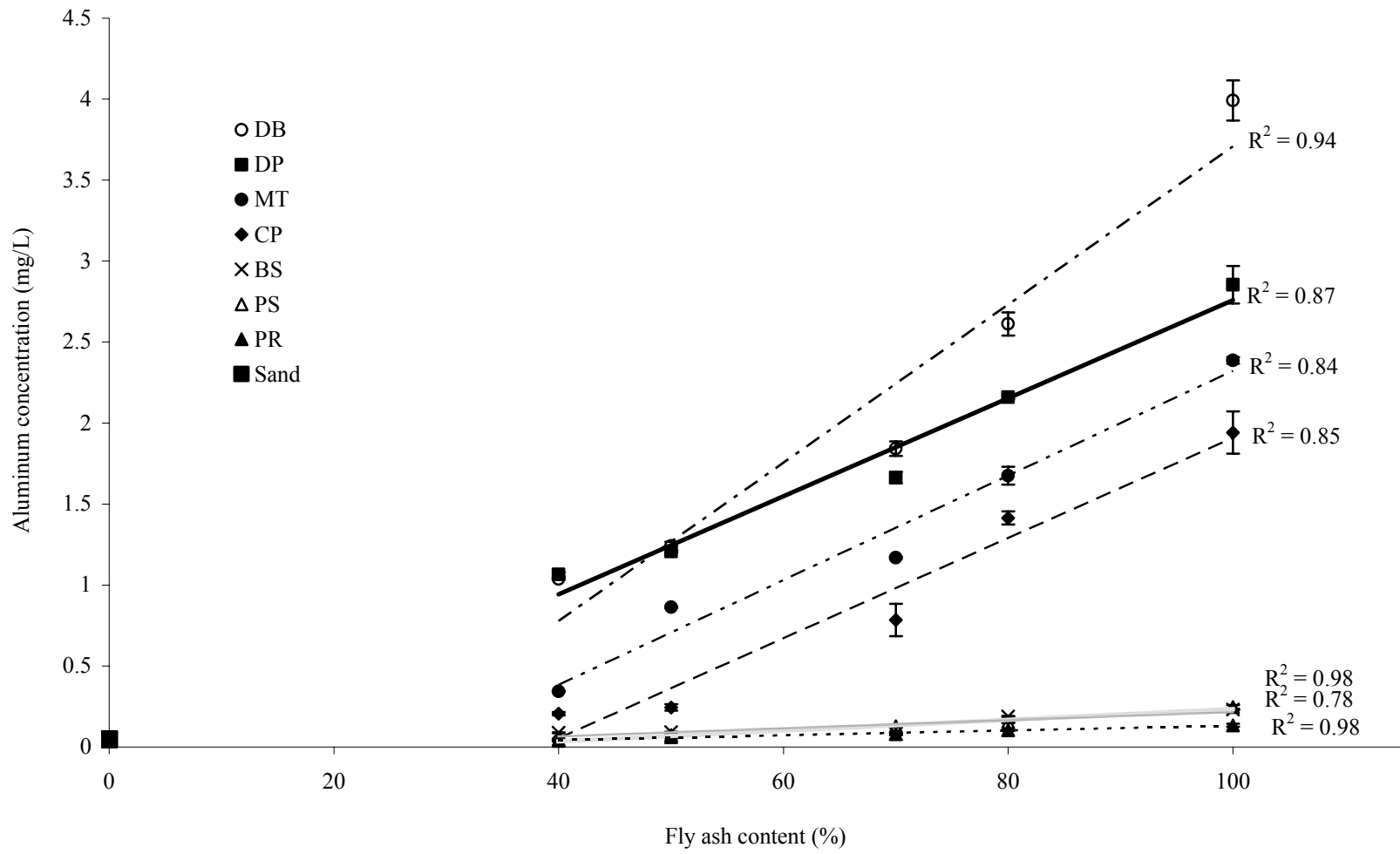


Figure 5. 2. Aluminum aqueous concentrations in WLTs conducted with artificial groundwater solution on different sand-fly ash mixtures. Symbols represent the average values of two experimental replicates, error bars represent the standard deviation, and lines represent the linear best fit to the data. .

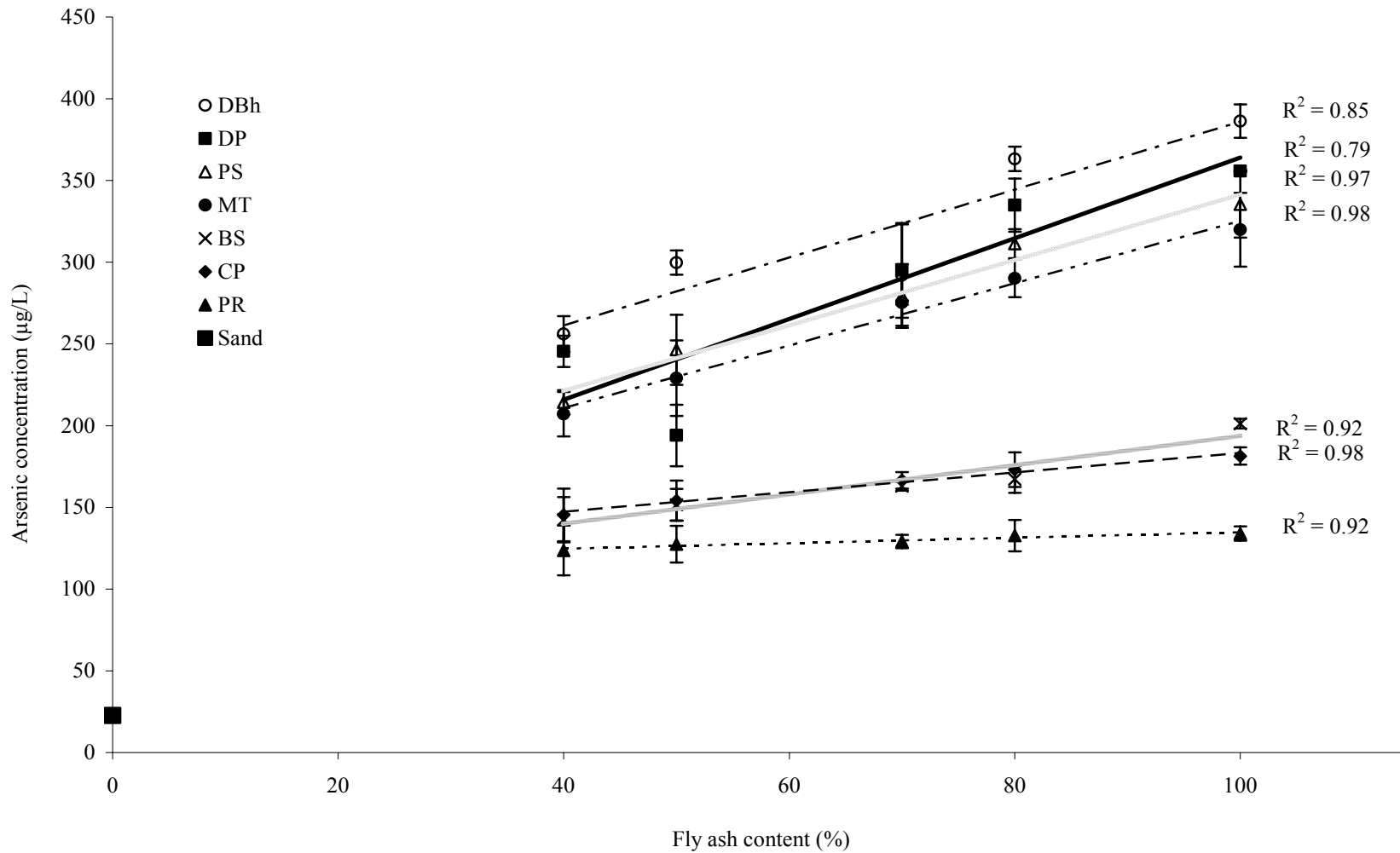


Figure 5. 3. Arsenic aqueous concentrations in WLTs conducted with deionized water with ionic strength fixed (IS=0.02M) on different sand-fly ash mixtures. Symbols represent the average values of two experimental replicates, error bars represent the standard deviation, and lines represent the linear best fit to the data.

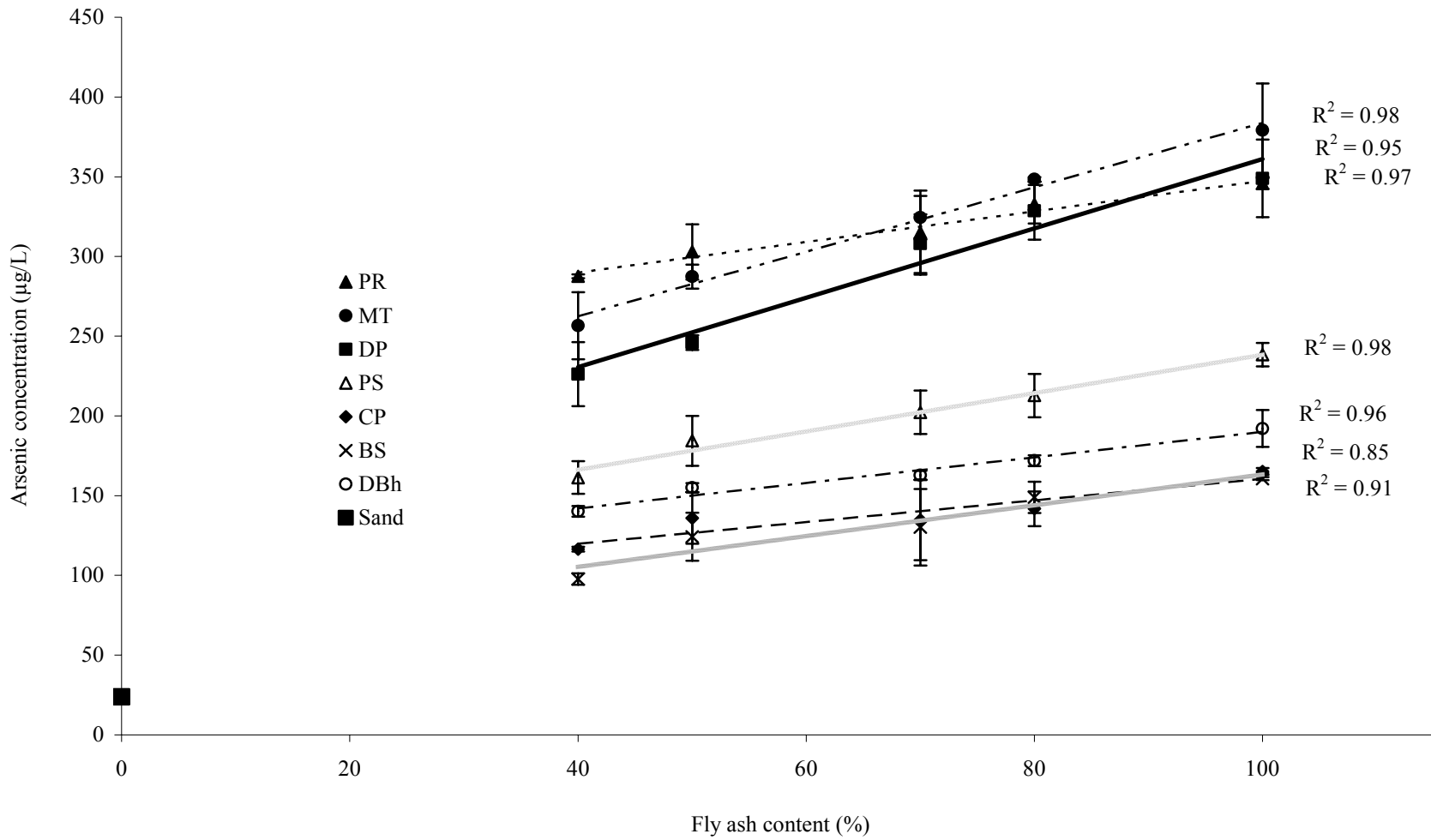


Figure 5. 4. Arsenic aqueous concentrations in WLTs conducted with artificial groundwater solution on different sand-fly ash mixtures. Symbols represent the average values of two experimental replicates, error bars represent the standard deviation, and lines represent the linear best fit to the data.



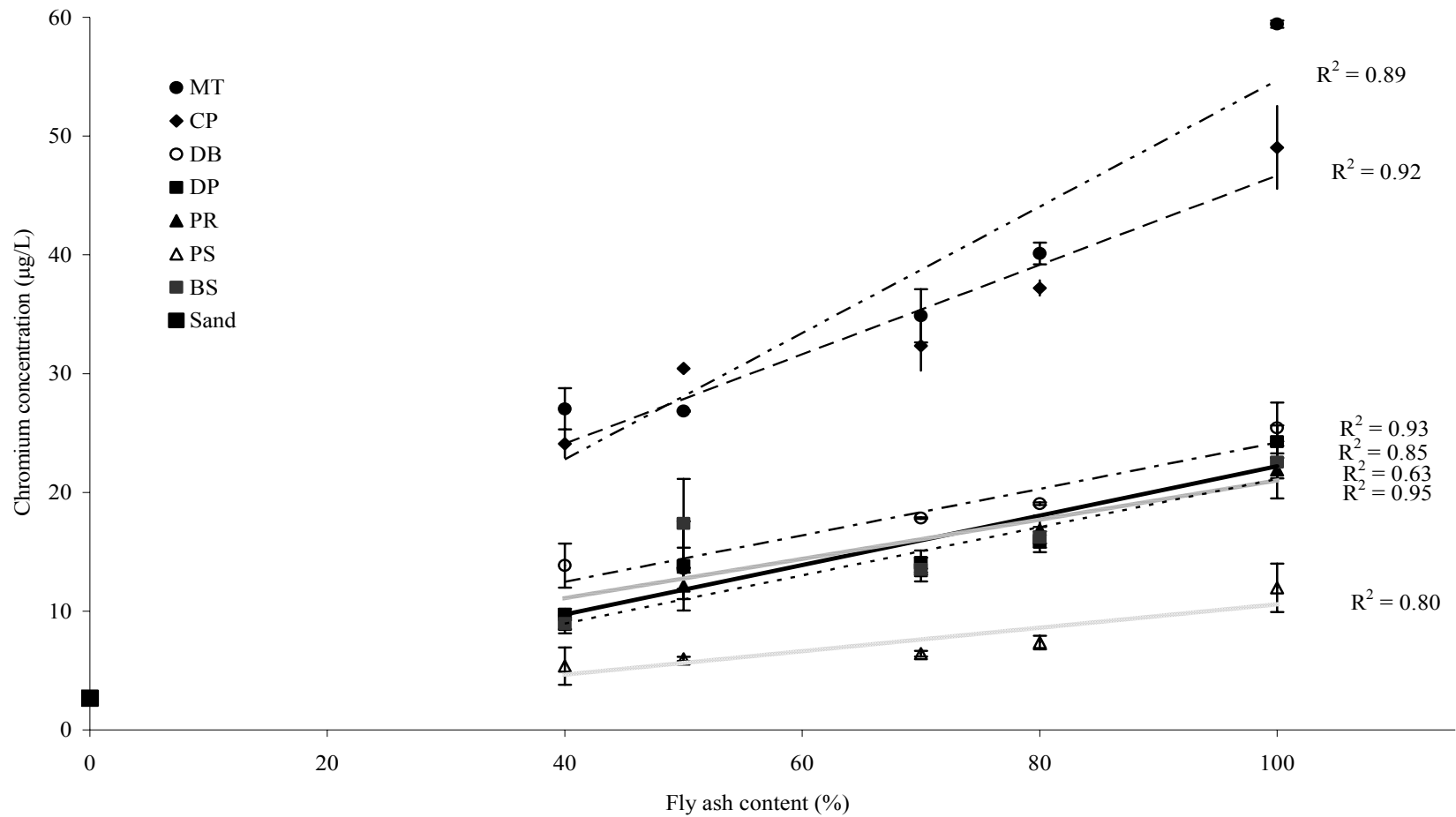


Figure 5. 5. Chromium aqueous concentrations in WLTs conducted with deionized water with ionic strength fixed (IS=0.02M) on different sand-fly ash mixtures. Symbols represent the average values of two experimental replicates, error bars represent the standard deviation, and lines represent the linear best fit to the data.

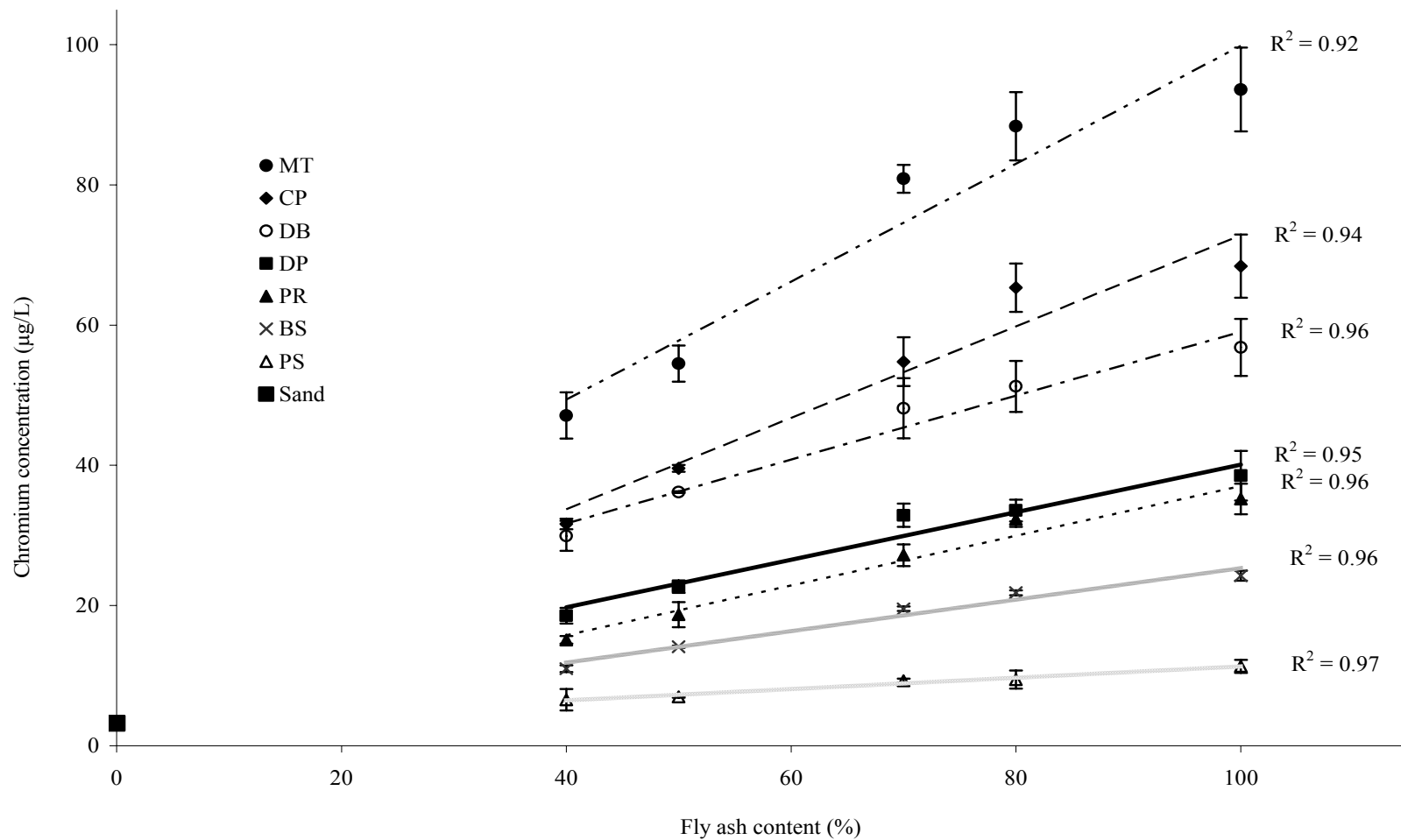


Figure 5. 6. Chromium aqueous concentrations in WLTs conducted with artificial groundwater solution on different sand-fly ash mixtures. Symbols represent the average values of two experimental replicates, error bars represent the standard deviation, and lines represent the linear best fit to the

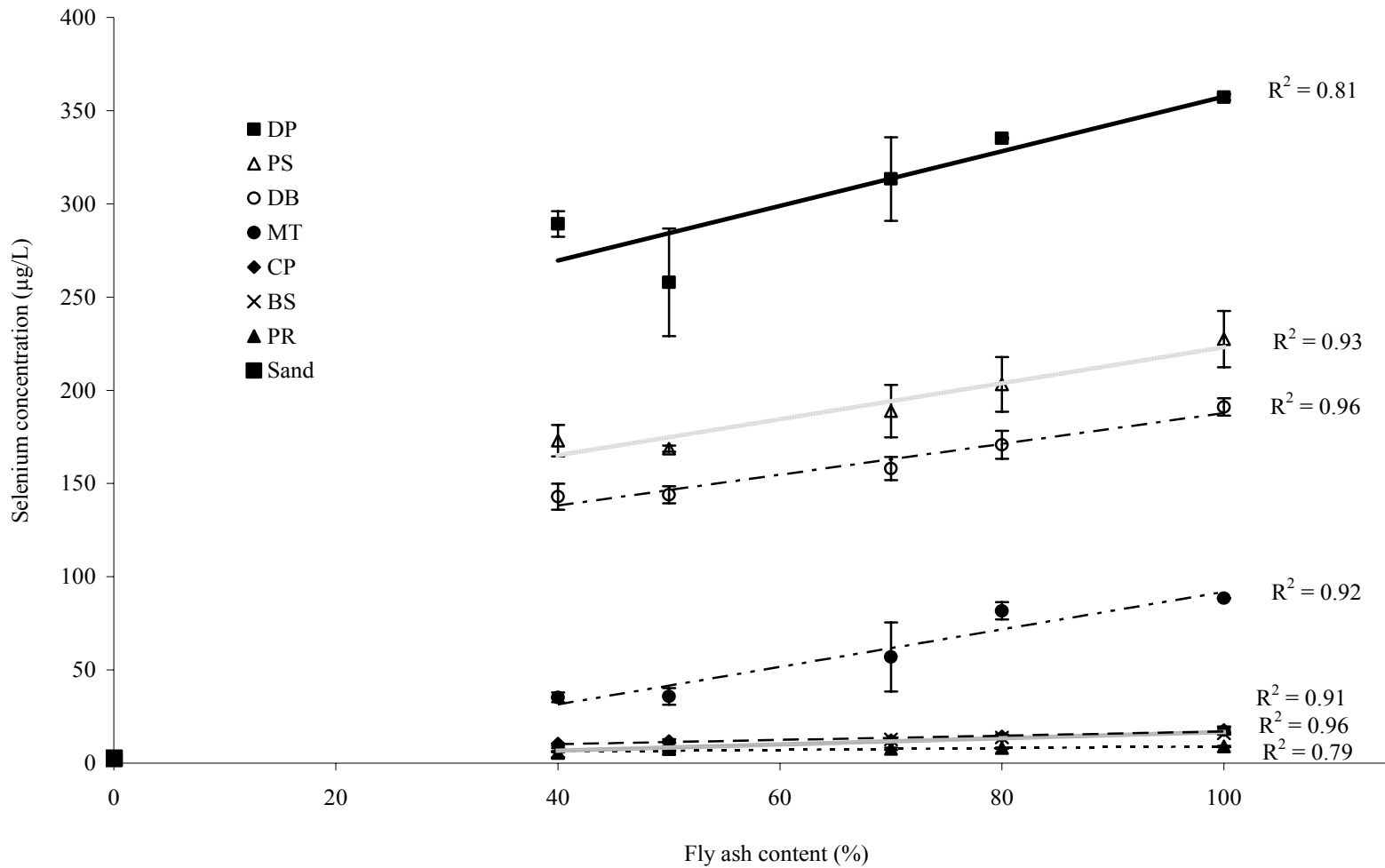


Figure 5. 7. Selenium aqueous concentrations in WLTs conducted with deionized water with ionic strength fixed (IS=0.02M) on different sand-fly ash mixtures. Symbols represent the average values of two replicates, error bars represent the standard deviation, and lines represent the linear best fit to the data.

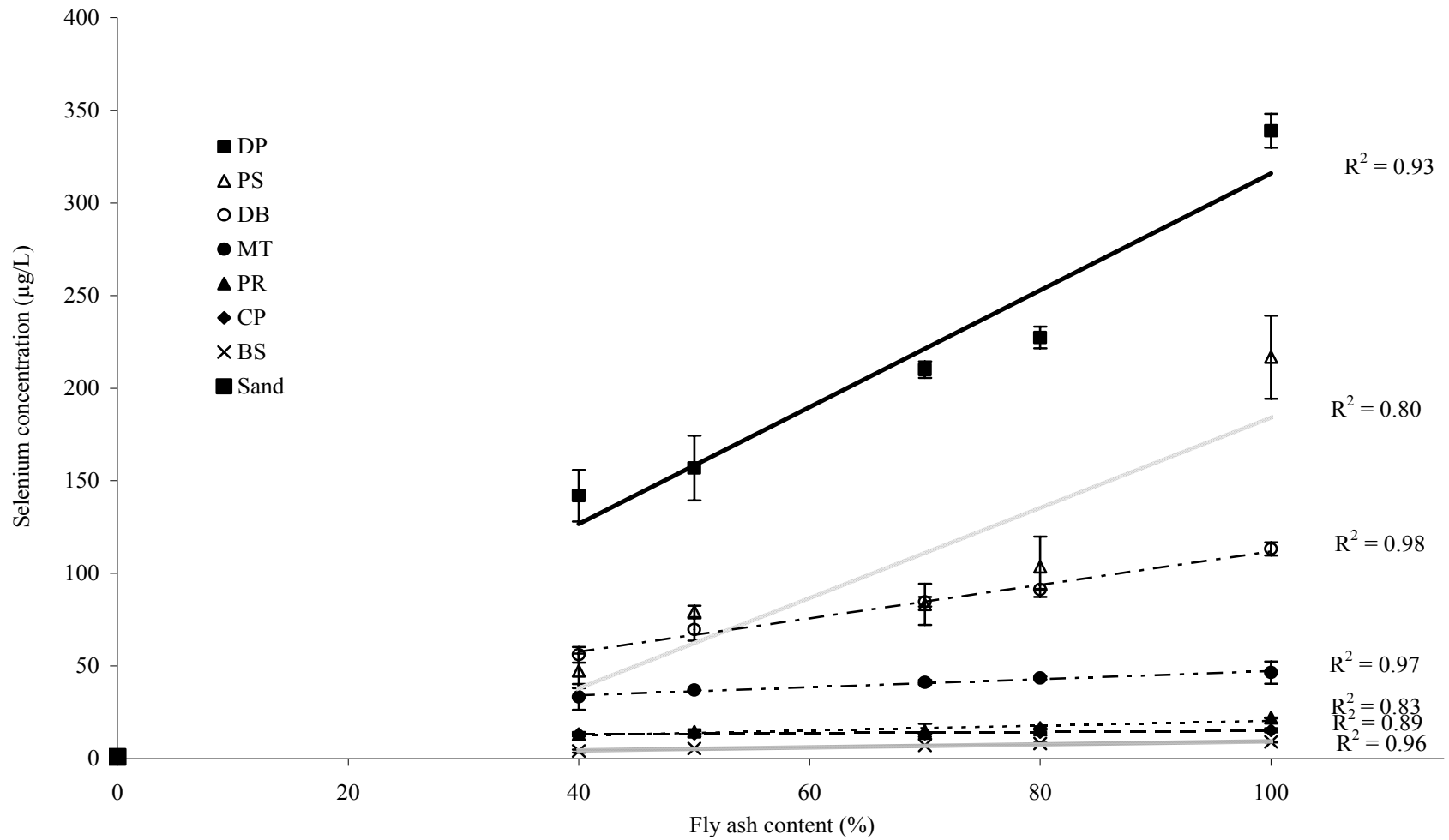


Figure 5. 8. Selenium aqueous concentrations in WLTs conducted with artificial groundwater solution on different sand-fly ash mixtures. Symbols represent the average values of two replicates measured experimental data, error bars represent the standard deviation, and lines represent the linear best fit to the data.

calculation may not be appropriate in these cases. The non-linear leaching behavior could be explained by the variation in pH imposed by the change in fly ash content. The relatively higher pH obtained with deionized water suggest that the pH was completely buffered by the fly ash mineral components, while in case of artificial groundwater the buffering action of the fly ash components was probably attenuated by the presence of the PIPES buffer. Similar trends were observed by McBride et al. (1994), Bin Shafique et al. (2006), and Genç-Fuhrman et al. (2007). They suggested that the pH increases are attributed to the buffering reactions which are mainly caused by the exchangeable base cations, decomposition or dissolution of the minerals present in the fly ash, and the processes enhanced during agitation motion.

pH is one of the key factors controlling the adsorption/leaching of metal cations and anions onto/from solid particle surfaces (van der Sloot et al.1998, Yin et al. 2002, Hammer et al. 2003). Distribution of the surface species and availability of the metal anionic and cationic species are highly dependent on the pH, and thereby several possible leaching mechanisms may interact in a complex manner to determine the observed trends. The increase in leaching metalloid concentrations with increasing fly ash content can be attributed to the increase of available anionic species as a result of increasing fly ash amount (as source of metals), and to the small increases in pH (see Table 5.1) that ultimately enhances solubilization of anionic species. Another reason for increase in solubilization can be the unavailability of positively charged surface species for complexation at basic pH conditions. Hoek and Comans (1996) also concluded that the leaching potential of metalloids species (anionic species like:  $\text{SeO}_4^{2-}$  and  $\text{SeO}_3^{2-}$ ) increases with increasing pH due to

unavailability of positively charged surface species for complexation.

To better understand the effect of the eluant on the leaching behavior the test data with the groundwater solution are plotted against the data with the deionized water solution in Figures 5.10 through 5.13. The aluminum concentrations (Figure 5.11) in the WLTs conducted with deionized water are about ten fold higher than the ones from WLTs conducted with artificial groundwater. Considering the higher pH conditions for the tests conducted with deionized water as compared to the tests conducted with groundwater, the main cause for this phenomenon is assumed to be the increase in the solubility of aluminum with increasing pH (above pH 6.5), as can also be noticed in Figure 5.9. Another possible explanation could be the addition of  $\text{CaCl}_2$  to the deionized water solution to adjust the ionic strength.  $\text{Ca}^{2+}$  cations present in the solution may have reduced the surface negativity of the fly ash particles, and caused the displacement of  $\text{Al}^{3+}$  from the surface into the aqueous phase by electrostatic effects (Kinraide 1998). Praharaj et al. (2002) and Long (2003) investigated the changes in specific surface area of the fly ash particles before and after leaching and found a decrease in surface area of fly ash and an increase in surface roughness post-leaching, which were attributed to the removal of the active surface sites and soluble species loosely attached on the surface. In comparison, from the results in Figures 5.12 and 5.13, the concentrations of the chromium and selenium in the WLTs conducted with deionized water are about 2 and 0.5 times, respectively, the concentrations from WLTs conducted with artificial groundwater. In comparison, it is difficult to draw any conclusions when the two test results for arsenic were correlated (Figure 5.11), given the scatter in the data.

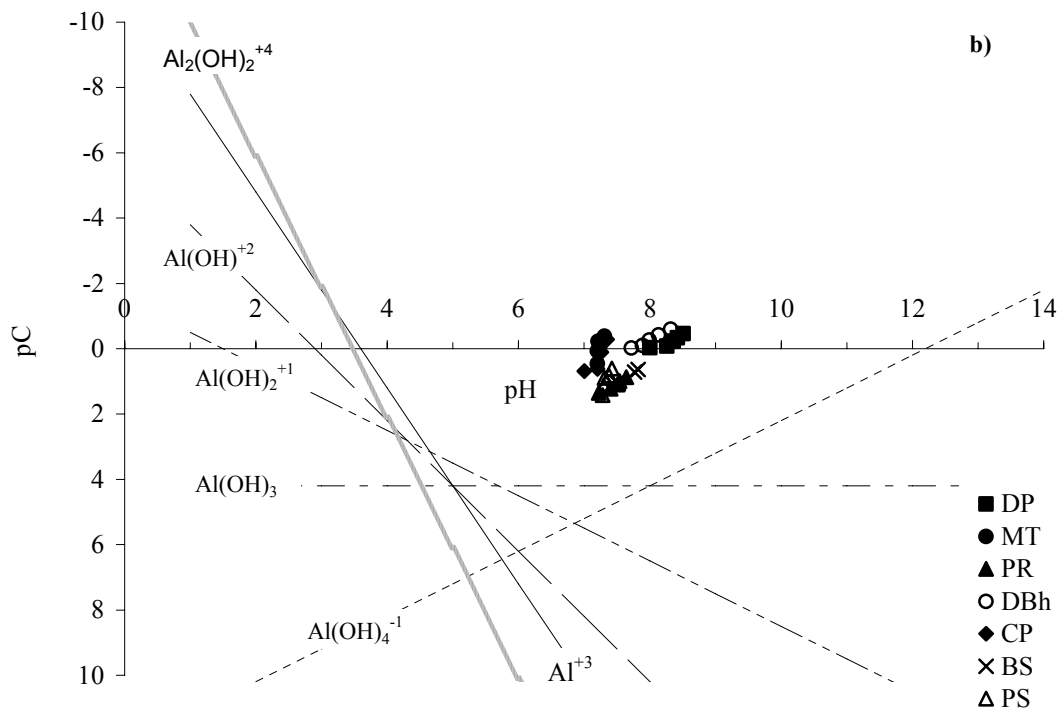
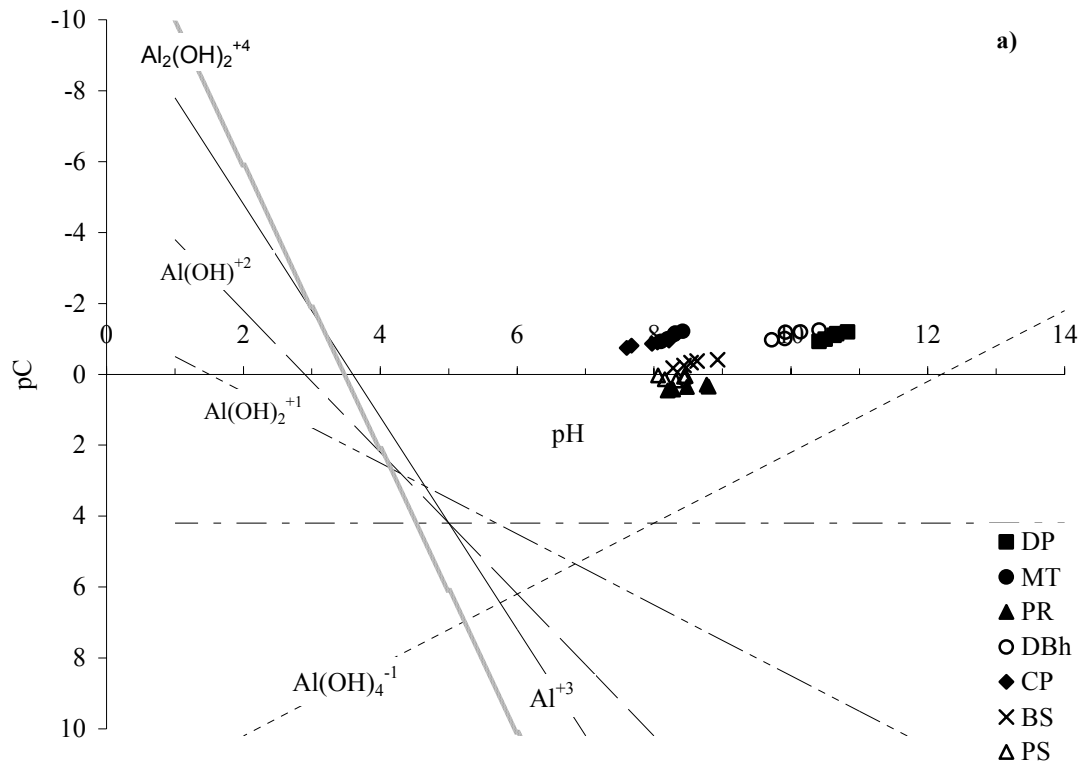
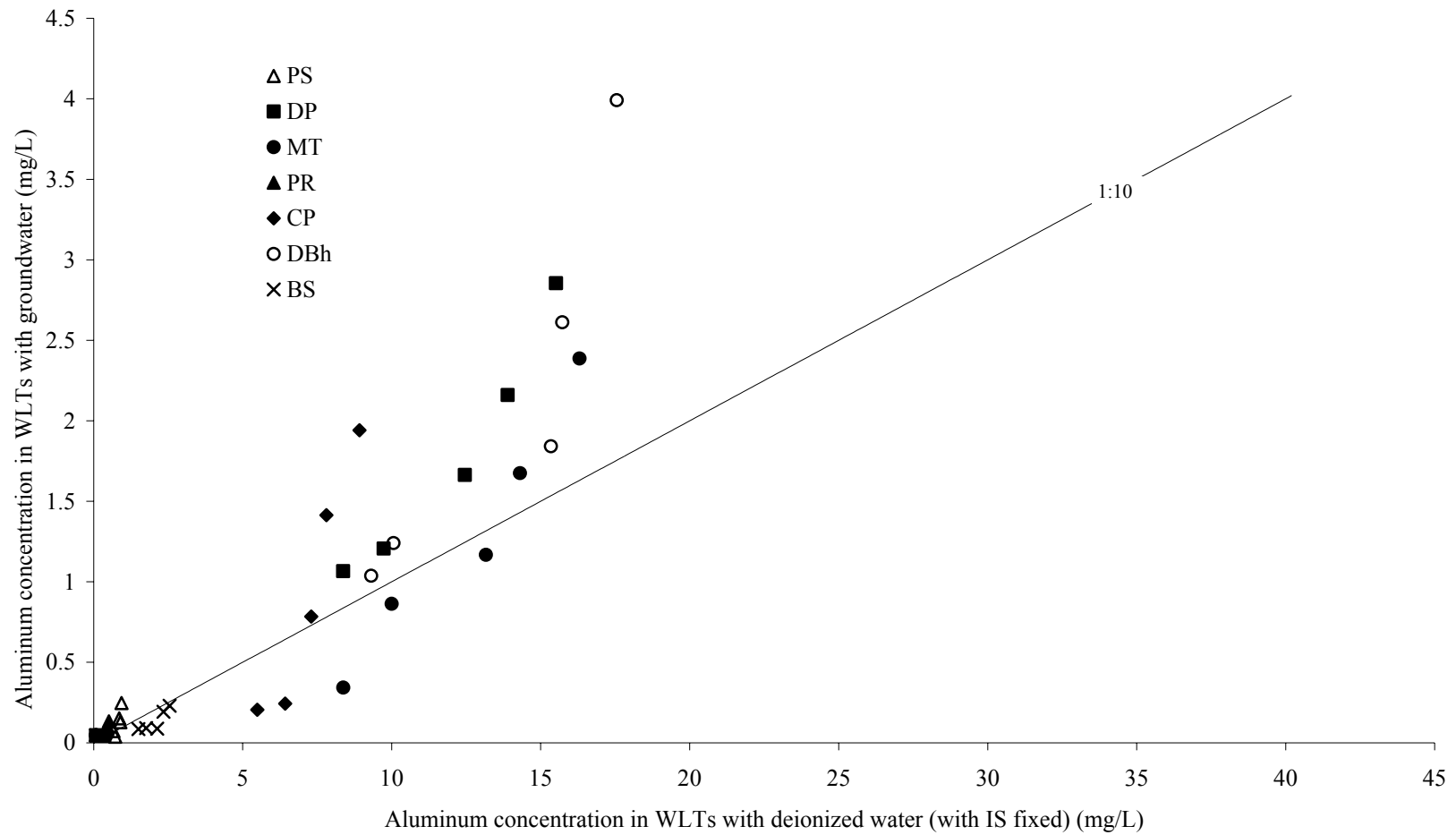


Figure 5. 9. pC – pH diagram for aluminum from WLTs with a) deionized water and b) groundwater





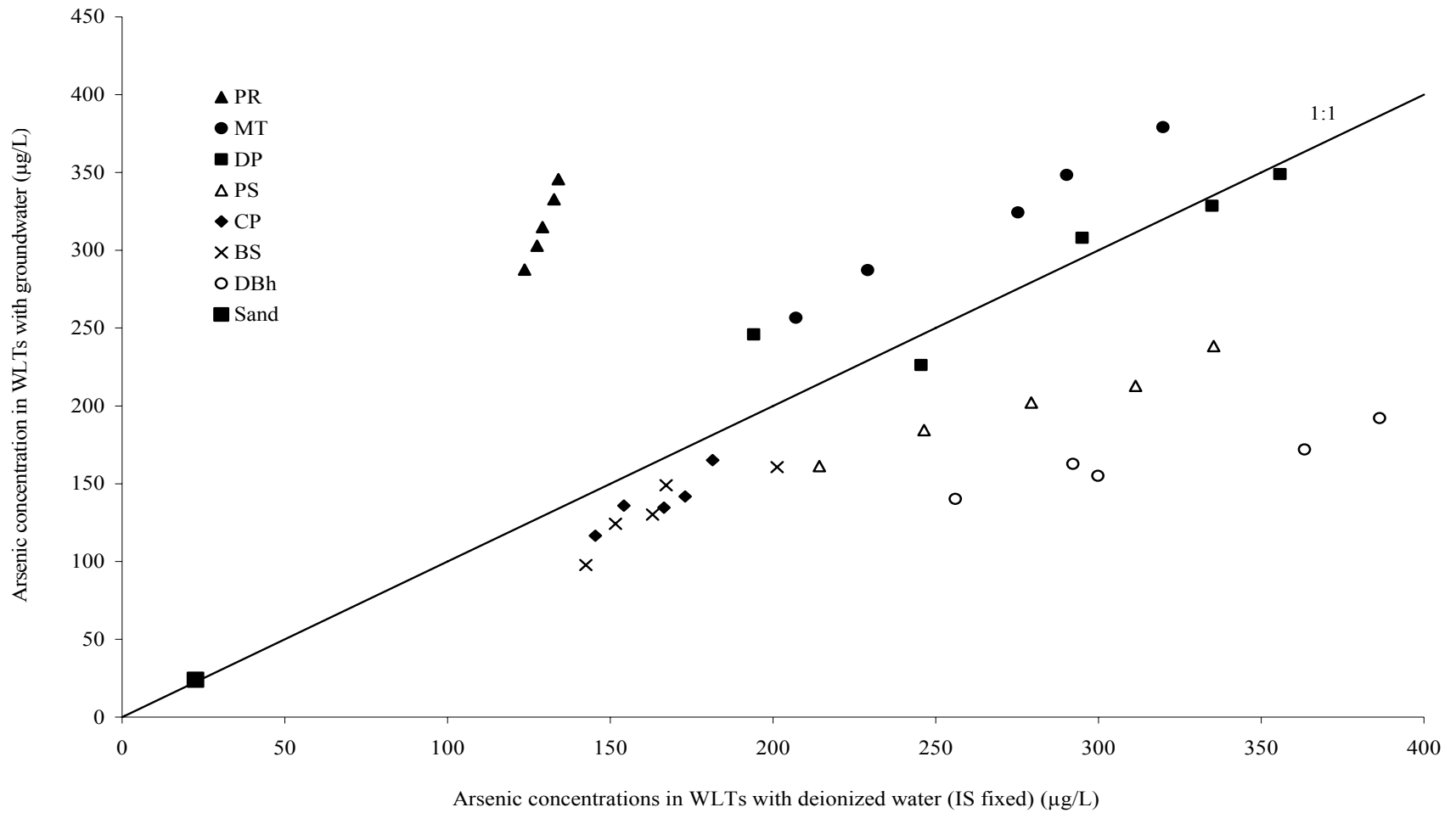


Figure 5. 11. Relationship between the WLTs conducted with groundwater and with deionized water for arsenic. Symbols represent the average of duplicate experiments.

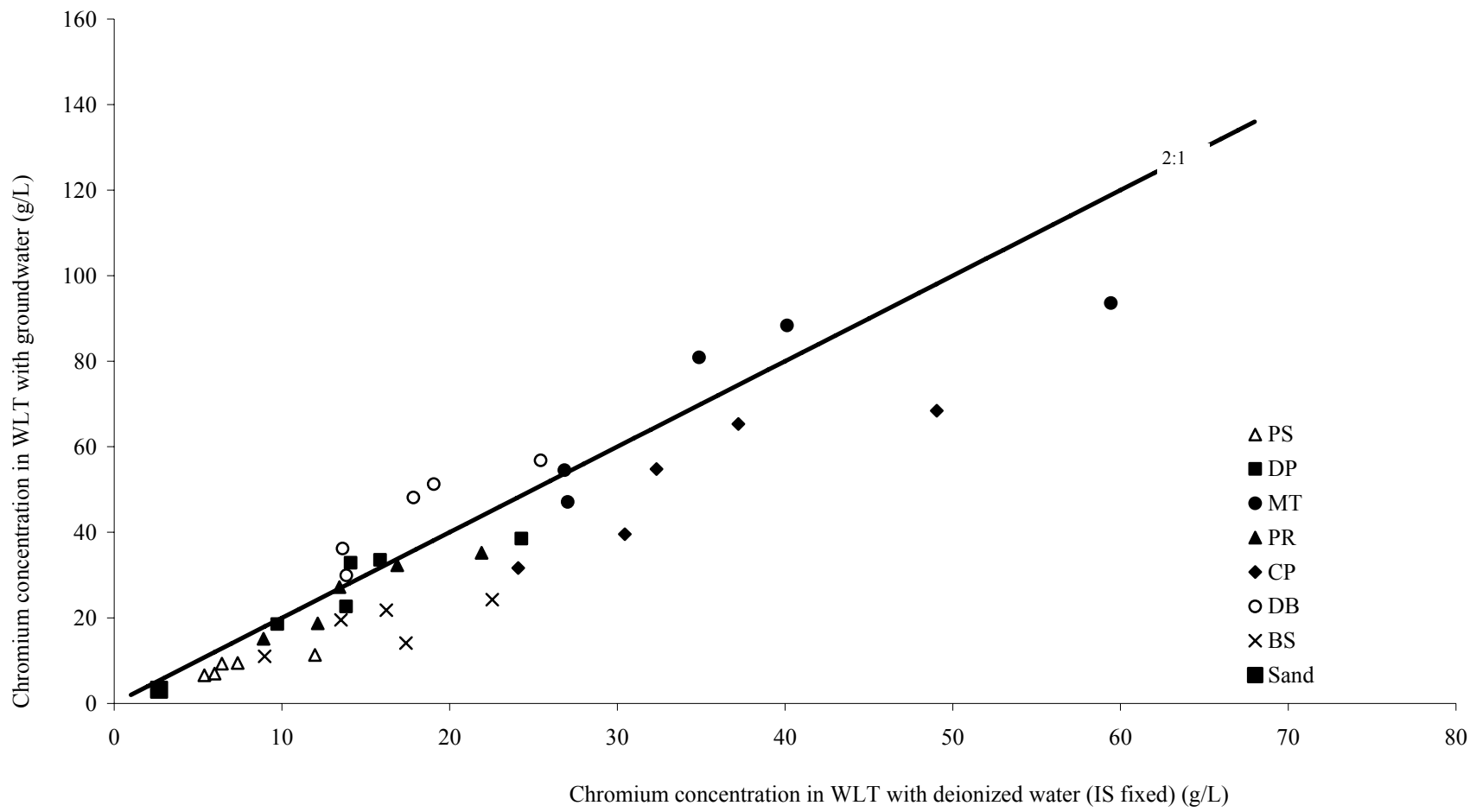


Figure 5. 12. Relationship between the WLTs conducted with groundwater and with deionized water for chromium. Symbols represent the average of duplicate experiments.

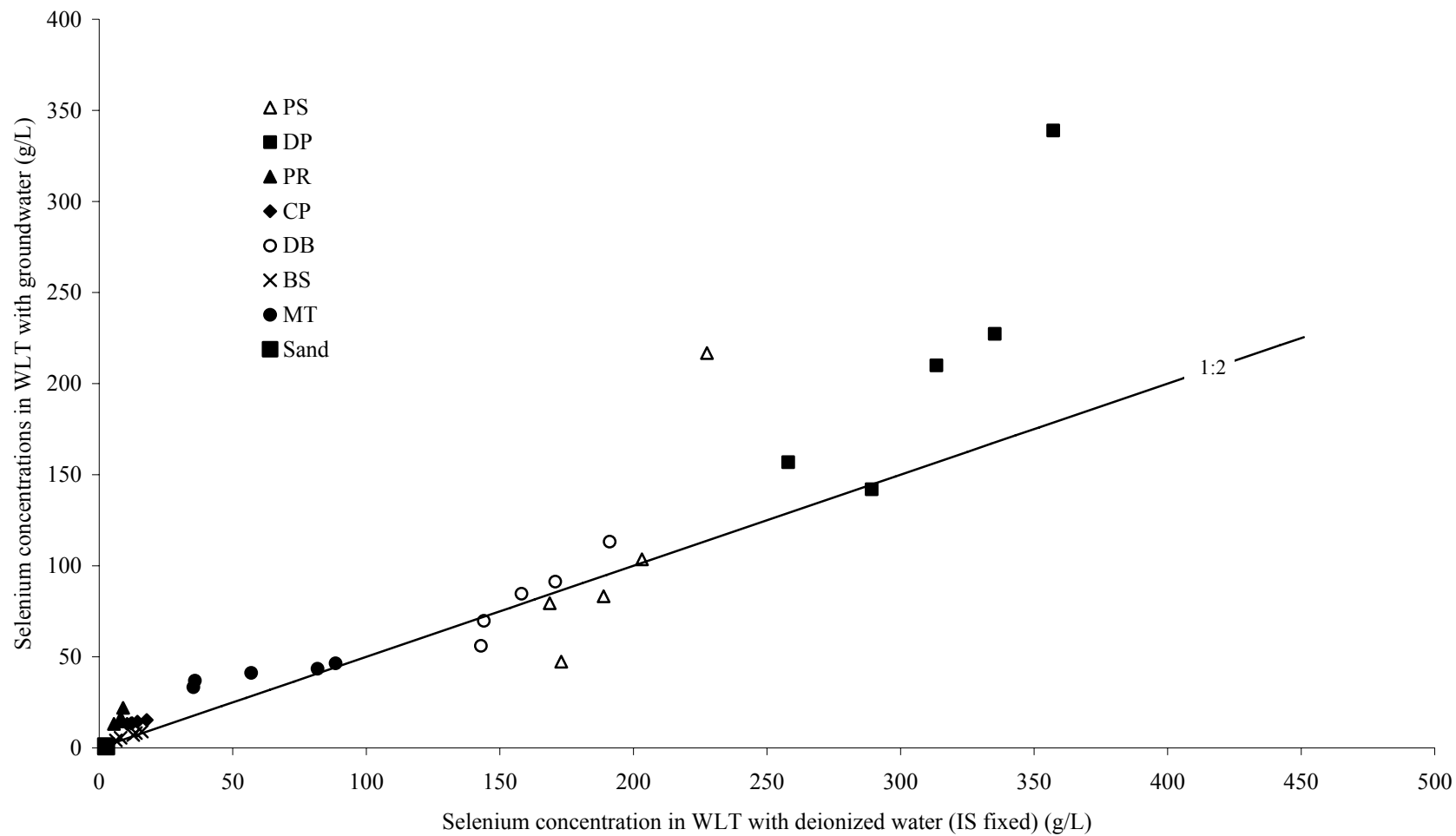


Figure 5. 13. Relationship between the WLTs conducted with groundwater and with deionized water for selenium. Symbols represent the average of duplicate experiments.

## **5.2. COLUMN LEACHING TESTS RESULTS**

Column leaching tests (CLTs) were conducted on mixtures of all seven Maryland fly ashes with sand to provide more realistic estimates of the leaching behavior and transport parameters for the four metals of concern (aluminum, arsenic, chromium, selenium).

### **5.2.1. pH measurements**

pH was monitored at the effluent port of each column experiment. The pH of the leachates are plotted against the pore volumes of flow (PVF) in Figure 5.14. pH stays fairly constant and is slightly basic for the initial pore volumes of flow suggesting that the pH was buffered by the fly ash inside the column. As mentioned before, the elevated values for the pH may be due to the buffering reactions initiated by the dissolution and/or decomposition of the minerals components of the fly ash (McBride et al. 1994 and Genç-Fuhrman et al. 2007). Figure 5.14 shows that pH initially remains constant for several pore volumes of flow, then decreases at the later stages, and eventually drops to a level comparable to the pH of artificial groundwater solution (i.e, pH = 6.8). Similar trends were observed by Qiao et al (2005) in a study on use of fly ash in waste stabilization/solidification systems. Fytianos and Tsaniklidi (1998) attributed the observed decrease in pH with increasing liquid-to-solid ratios (progressing pore volumes of flow) to the “depletion of materials controlling this parameter”. Therefore, it is believed that the buffering capacities of the Maryland fly ashes tested in this study diminish and the pH in the system is ultimately governed by the PIPES buffer present in the groundwater recipe as more pore volumes of flow pass through the column and more fly ash mineral components are washed out

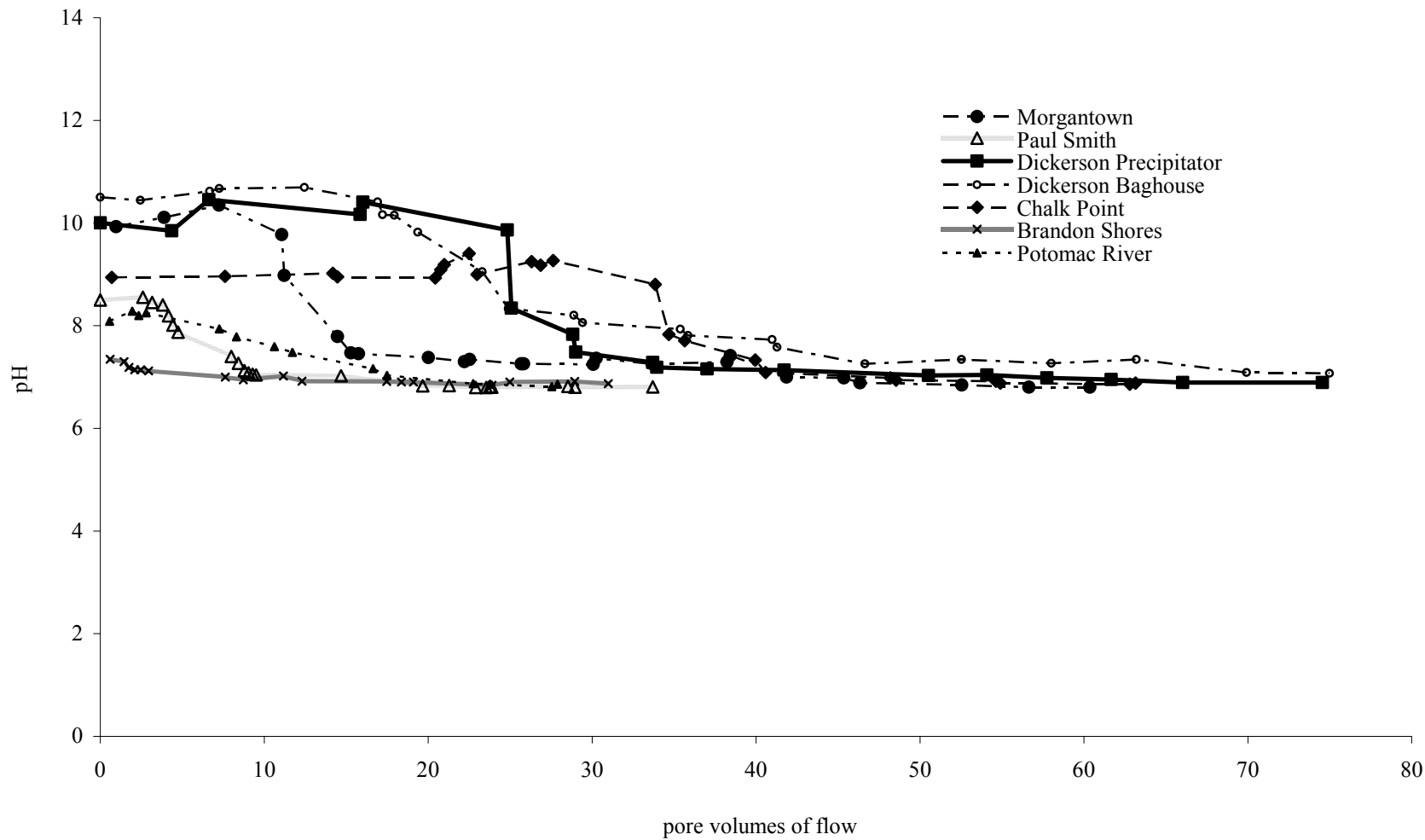


Figure 5. 14. pH in the CLTs. Average values of two measurements are plotted against the pore volumes of flow.

from the column system. The pH of the columns reached a steady state typically within 15-35 pore volumes of flow. The pH of Dickerson Baghouse, Dickerson Precipitator and Chalk Point columns fluctuated and reached to a steady state after 30-35 PVF. Brandon Shores fly ash showed the least buffering capacity indicated by the almost flat pH versus PVF curve, rapidly approaching the PIPES buffered groundwater pH level. It is difficult to relate the shapes of the pH elution curves to one single factor, but rather the curves are influenced by a series of factors, including flow rate, mineral composition of the fly ash, and percolating eluant solution.

Considering the observed pH range in the columns (pH= 6.8-10.5) and the trends provided in Figures 2.2 through 2.4, As, Se and Cr are likely to be available in their anionic species in the environment. In this pH range, the dominating As species are  $\text{HAsO}_4^{2-}$  and  $\text{AsO}_4^{3-}$ , the Cr species is  $\text{CrO}_4^{2-}$ , and the Se species are  $\text{SeO}_4^{2-}$  and  $\text{SeO}_3^{2-}$ , so it is expected that these species will be present in the collected samples. Alkaline conditions in the environment are believed to be responsible for this speciation. At acidic pHs, where generally positively charged surface species are available, sorption of anionic metal species is commonly favorable, while at alkaline pHs sorption of cationic metals species becomes important due to availability of deprotonated (negatively charged) surface species for complexation. In other words, leachability of metals is inversely proportional to the pH, while the metalloids show reverse leaching behavior relative to pH (Hoek and Comans 1996).

### **5.2.2. van Genuchten (1981) and Fry et al. (1993) models**

Two different analytical solutions described in Section 3.6 were used to model the metals data from column leaching tests. The equilibrium model proposed by van

Genuchten (1981) is based on mass transport due to advection, dispersion and retardation via equilibrium sorption. In comparison, the model developed by Fry et al. (1993) is a non-equilibrium model and assumes rate-limited desorption, which is modeled with a linear first-order rate equation in which the rate of desorption is proportional to the first-order rate coefficient ( $\alpha$ ), and the metal concentration gradient between the liquid (C) and solid (S) phases as shown in Equation (3.11). The best fits of the two models to the chromium data from two mixtures are presented in Figure 5.15. The elution curves for chromium do not agree well with the analytical model described by Shackelford and Glade (1997), but are well-described by the analytical solution proposed by Fry et al. (1993). This suggests that there exists a physical non-equilibrium caused by the rate-limited diffusive mass transfer and/or a chemical non-equilibrium caused by the rate-limited sorption/desorption reactions between the species in the liquid and the solid phases. Therefore, based on this preliminary investigation, the van Genuchten (1981) solution was eliminated for future modeling activities and the Fry et al. (1993) analytical solution was applied to all column data. To confirm the appropriateness of the Fry et al. (1993) model, graphs of  $\log(C/C_0)$  versus time were constructed using the column leach tests data and a linear pattern was observed, indicating that the use of a first-order model equation for explaining the leaching of metals behavior in the column specimens was adequate (Geeta Kandpal et al.2005). In addition, a pattern suggesting first order kinetics can be observed from the elution curves presented in Figure 5.15 and Figs. 5.16-5.19. It should be noted that only mass transfer from the solid phase to the liquid phase along

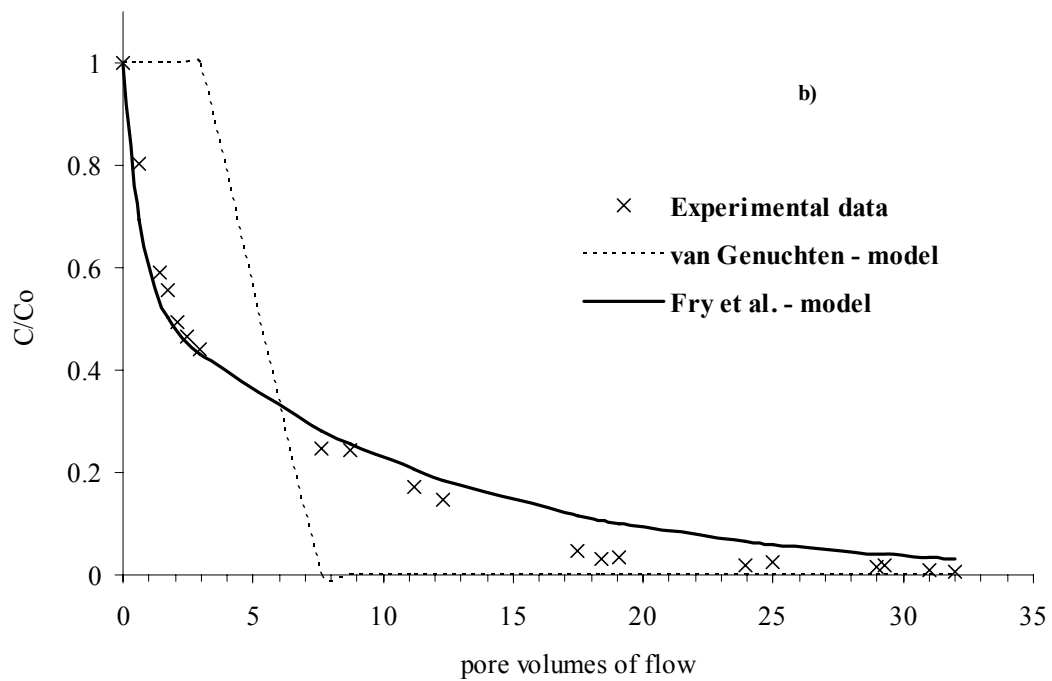
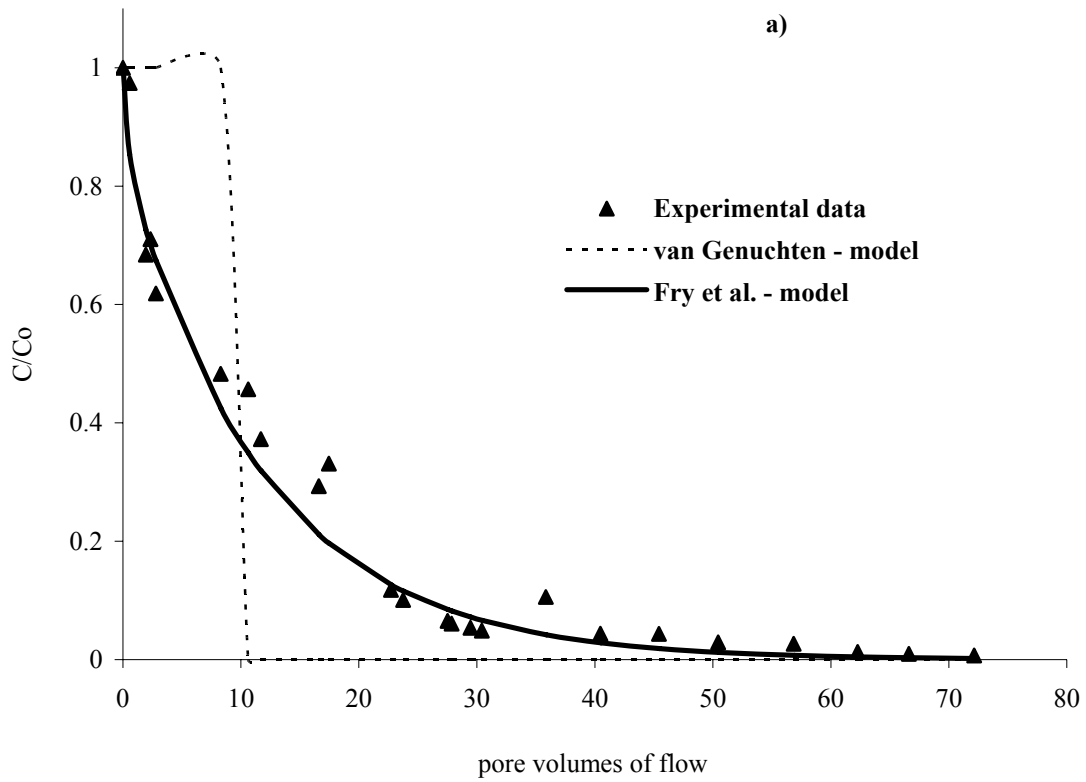


Figure 5. 15. Predictions of the two analytical solutions for a) 40% Potomac River / 60% Sand and b) 40% Brandon Shores / 60% Sand column data Symbols represent the measured single point experimental data, and lines represent the best fit model results from the analytical solutions above mentioned.



with advection and dispersion in the aqueous phase were considered in this study, and degradation of the metals in the aqueous or solid phase were deemed insignificant. As discussed in Chapter 3, the Fry et al. (1993) analytical solution assumes that: 1) the column specimen is initially contaminated with metals and the concentrations are uniformly distributed, and 2) the sorbed amount on the solid surface ( $S_0$ ) and the aqueous concentrations ( $C_0$ ) are initially in linear equilibrium and can be defined with a partition coefficient ( $K_d$ ) as given in Equation (3.14). The metal concentration measured in the very first effluent collected from the column (after about one pore volume of flow has passed through the column) was assumed to be the initial aqueous concentration ( $C_0$ ) in equilibrium with sorbed concentration of the metal ( $S_0$ ). All subsequent measured concentrations were normalized relative to this initial concentration and plotted against the pore volumes of flow leached to obtain the leaching elution curves. As the partitioning coefficient,  $K_d$ , reflects only the partitioning involved in linear, reversible and instantaneous sorption/desorption processes, the initially sorbed concentration of the metal ( $S_0$ ) was determined from the leachable amount calculated using the mass balance of the total metal released during column leaching test divided by the amount of solid in the column specimen (Equation 3.14). The first order desorption rate were estimated to provide the best fit of the model to all column data.

#### **5.2.2.1. Metal Concentrations**

Table 5.2 presents the modeling parameters (first-order desorption rate, partition coefficient and retardation factors) for all column tests. The elution curves presented

in Figures 5.16 through 5.19 suggest that there is a large initial leaching of the metals followed by near constant concentrations after about 30 PVF. The initial leaching is due to release of these metals from the water soluble fraction as well as from the sites with low adsorption energies (Kandpal et al. 2005). Another reason for the release of the metalloids (As, Cr, and Se anionic species) during the initial 15-35 PVFs may be the predominantly alkaline pH environment, which is expected to enhance the solubilization of the anionic species due to unavailability of positively charged surface species for complexation. However, as the pH decreases and eventually approaches to a value comparable to the pH of the PIPES buffered groundwater (neutral-slightly acidic), slower desorption of metalloids species occur, suggested by the flattening of the elution curves above 30-35 PVF. This may be related to the pH sensitive changes in speciation of the surface sites (more and more positively charged surface sites become available for complexation) and implicitly changes in net surface charge (McBride, 1994). Chichester and Landsberg (1996) and Bin Shafique et al. (2006) observed similar leaching elution curves in column testing of soil-fly ash mixtures.

The data in Table 5.3 suggest that initial leached amount is related to the amount of soluble metal in the fly ash. For instance, Al is present in the fly ashes in large amounts (Table 3.1) and the highest initial concentrations in CLTs are measured for this metal. Furthermore, relatively faster leaching of aluminum was also observed in all CLTs (Figure 5.16). This is mainly explained by the basic pH conditions for the initial pore PVFs which enhance the Al solubilization (above pH 6.5). Edil et al. (1992) reported similar behavior for metals with high concentrations, a sharp decrease

**Table 5. 2. Metals leaching parameters from CLTs**

Column specimen	Aluminum			Arsenic			Chromium			Selenium		
	Kd (L/Kg)	R	$\alpha$ (1/h)	Kd (L/Kg)	R	$\alpha$ (1/h)	Kd (L/Kg)	R	$\alpha$ (1/h)	Kd (L/Kg)	R	A (1/h)
40%Morgantown + 60% Sand (Naphthalene)	0.30	3.2	0.054	1.33	10.8	0.036	0.64	5.7	0.002	1.02	8.5	0.035
40%Dickerson Precipitator + 60% Sand (Naphthalene)	0.60	4	0.112	1.09	6.4	0.028	1.46	8	0.023	1.23	7.1	0.028
40%Paul Smith + 60% Sand (Naphthalene)	0.45	3.1	0.001	1.75	9.2	0.045	1.07	6	0.003	2.86	14.4	0.019
40%Dickerson Baghouse + 60% Sand	1.10	5.4	0.033	3.50	14.9	0.039	2.28	10	0.017	3.44	14.7	0.022
40%Brandon Shores + 60% Sand	1.33	6.3	0.023	-	-	-	1.17	5.7	0.033	1.56	8.3	0.038
40%Potomac River + 60% Sand	1.67	8	0.036	-	-	-	1.51	7.3	0.042	1.60	8.5	0.042
40%Chalk Point + 60% Sand	0.77	4.4	0.064	1.73	8.8	0.160	1.24	6.6	0.046	3.03	14.6	0.022

**Note:**  $K_d$  is the partition coefficient between the fly ash and aqueous phase,  $\alpha$  is the first order desorption rate,  $R$  is the retardation factor based on  $K_d$ .

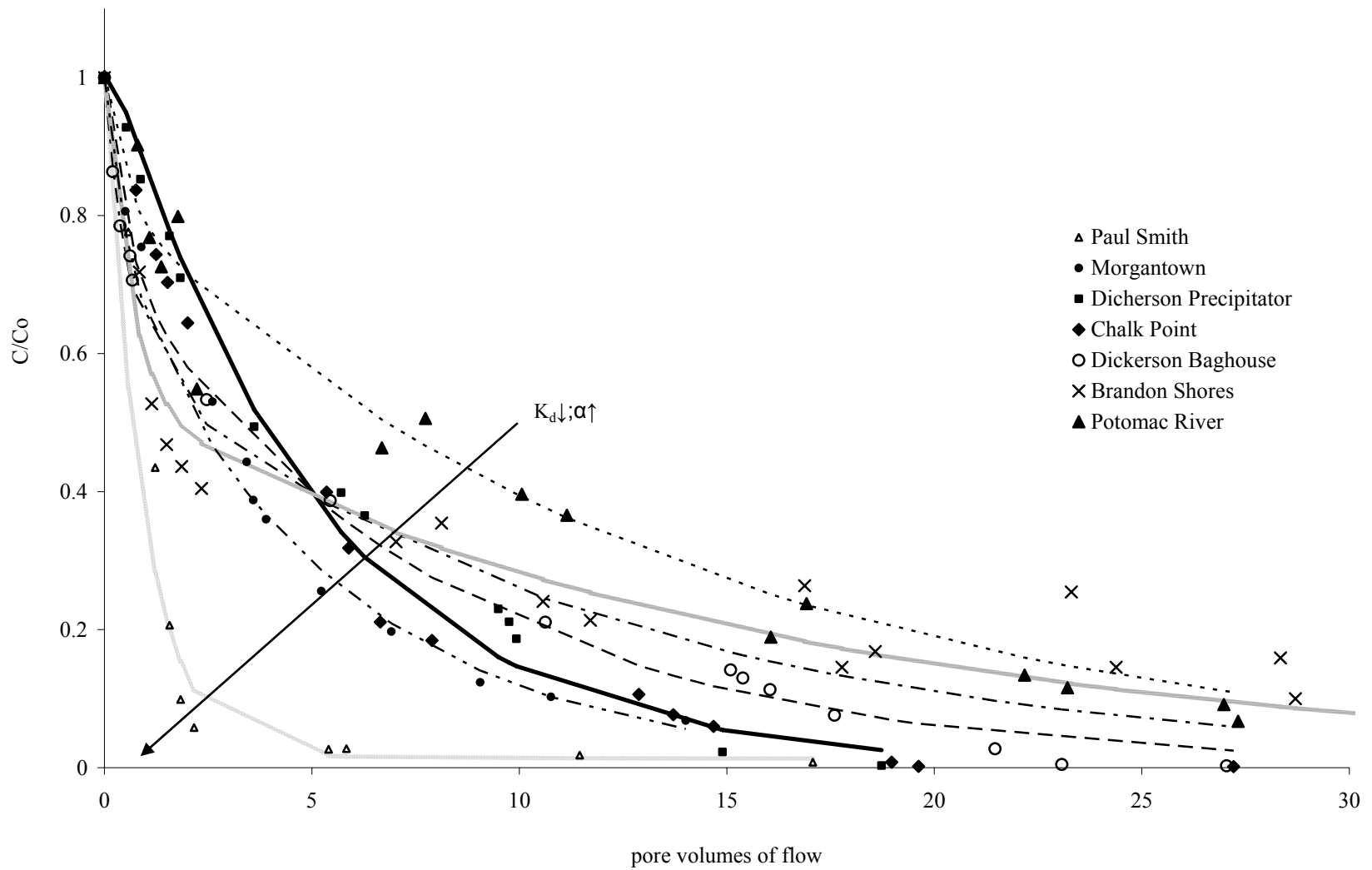


Figure 5. 16. Elution curves for aluminum from CLTs. Symbols represent the single point measured experimental data, and lines represent the best fit model results from the analytical solutions proposed by Fry et al. (1993).

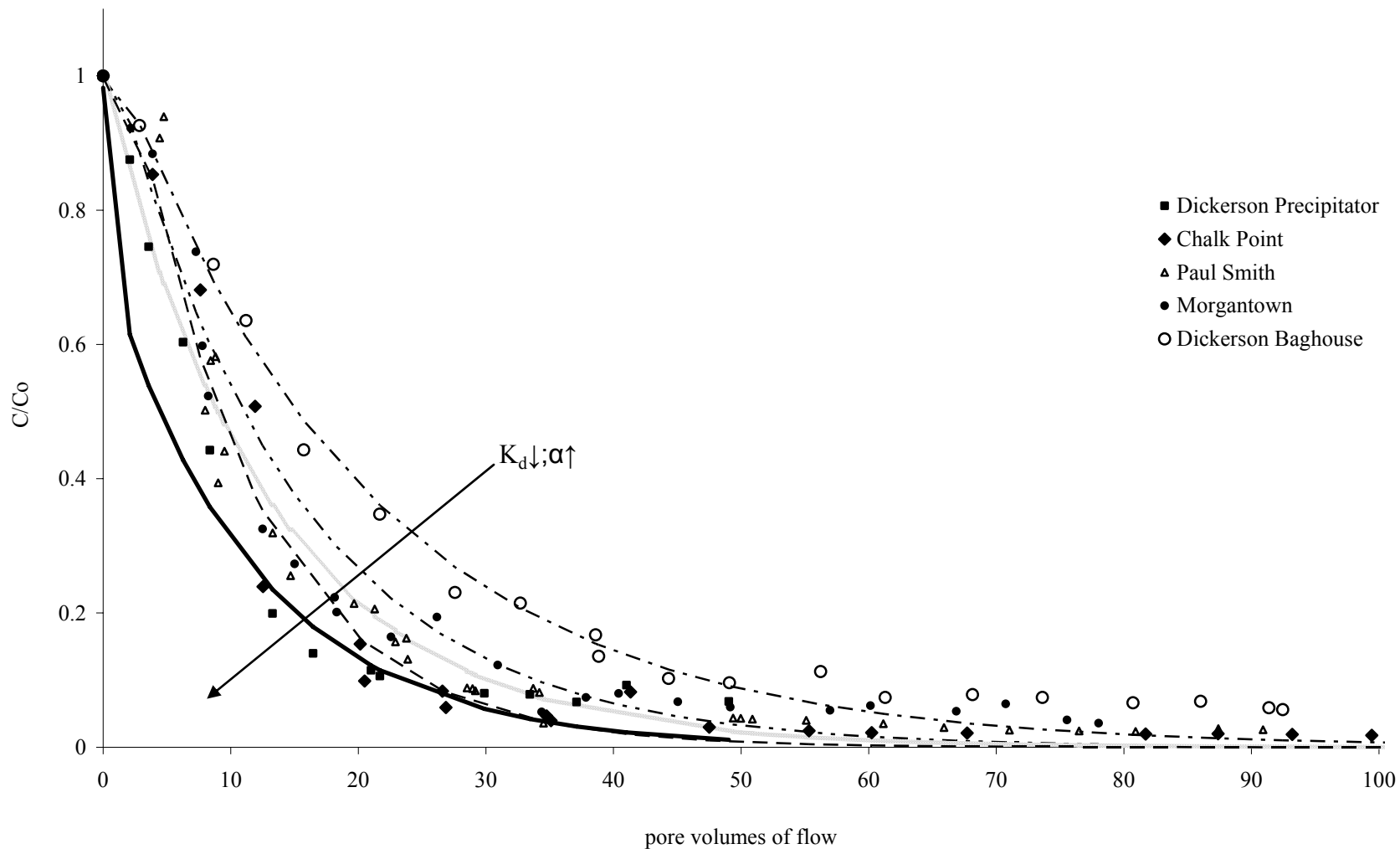


Figure 5.17. Elution curves for arsenic from CLTs. Symbols represent the single point measured experimental data, and lines represent the best fit model results from the analytical solutions proposed by Fry et al. (1993).

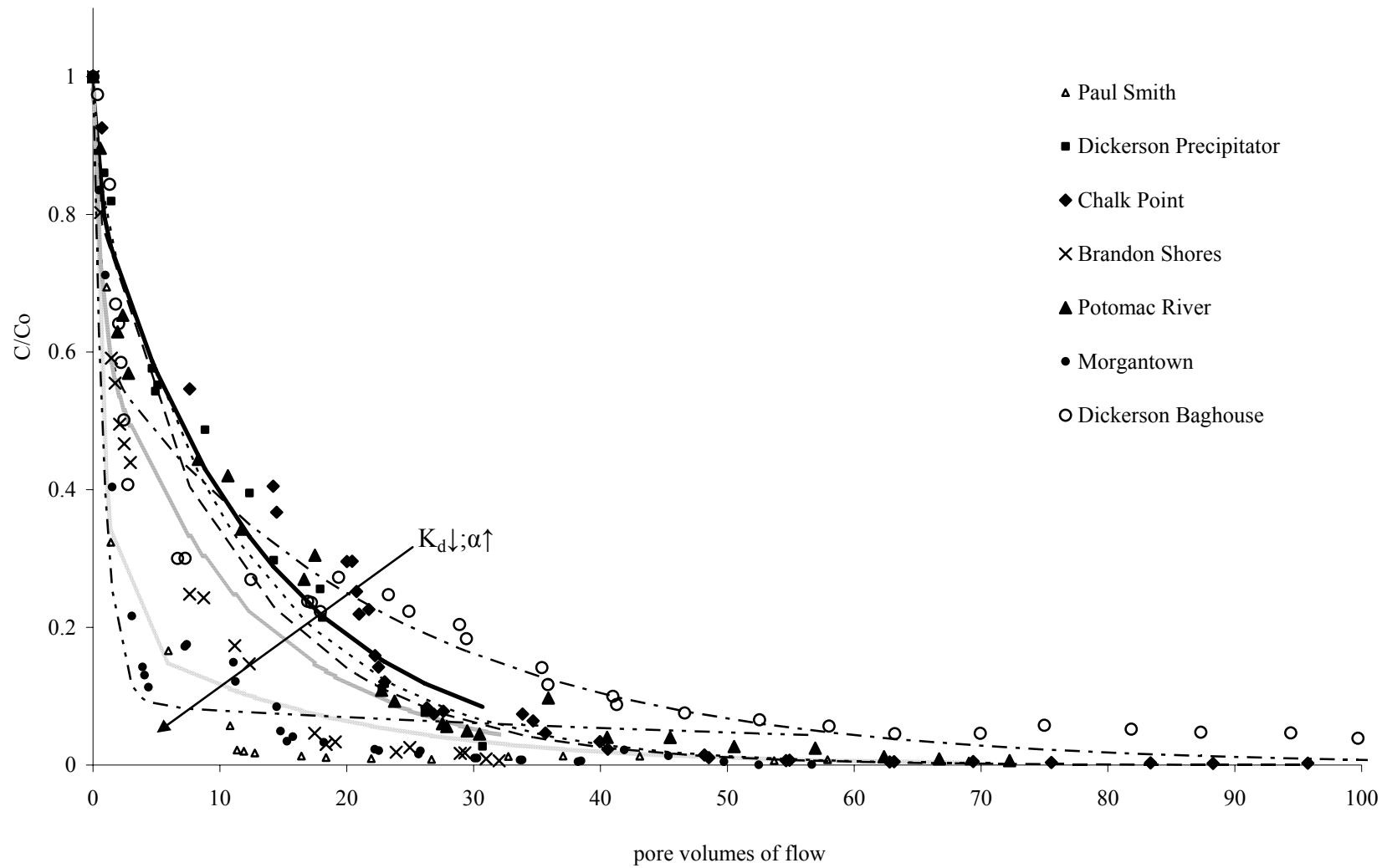


Figure 5. 18. Elution curves for chromium from CLTs. Symbols represent the single point measured experimental data, and lines represent the best fit model results from the analytical solutions proposed by Fry et al. (1993).

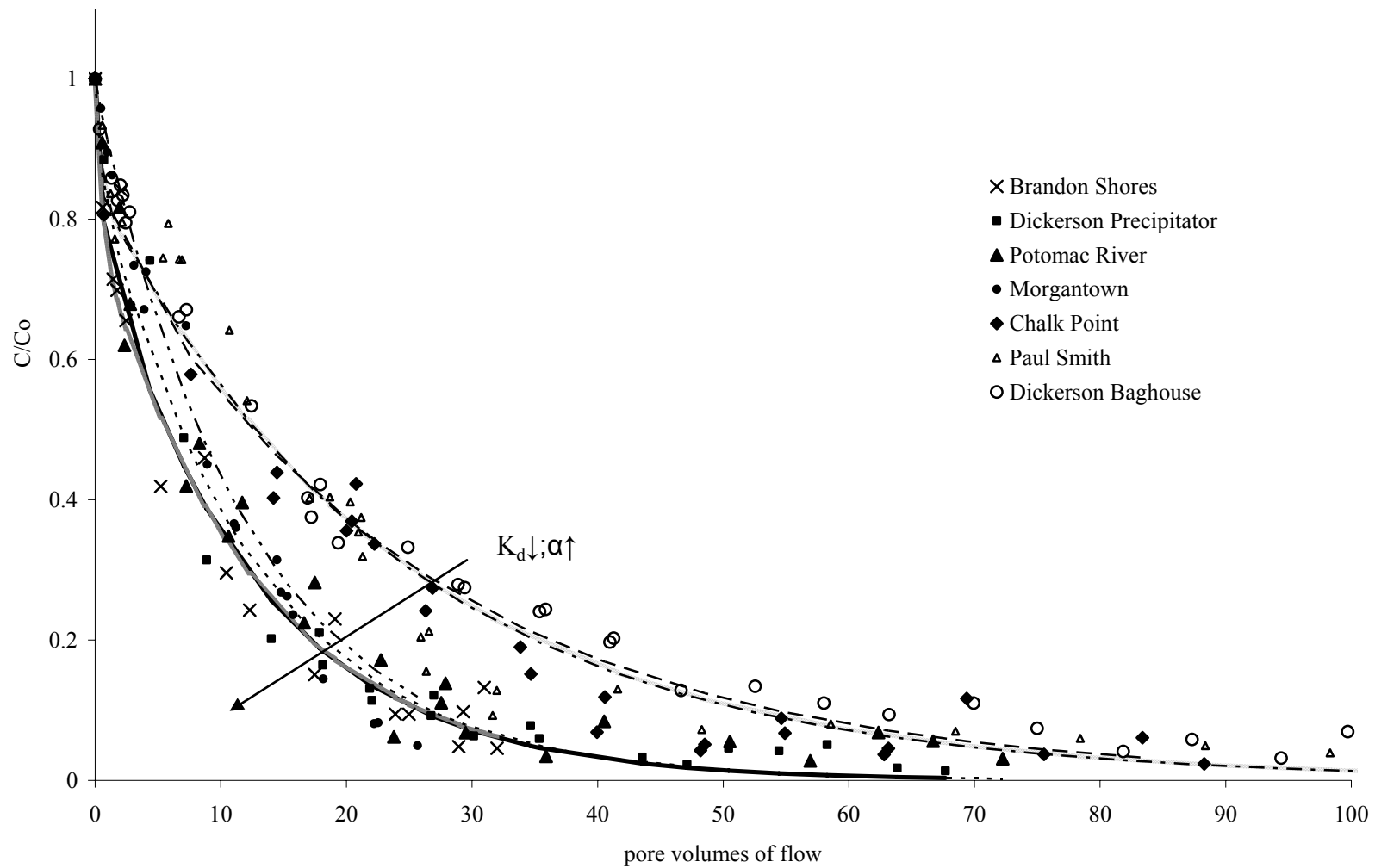


Figure 5. 19.Elution curves for selenium from CLTs. Symbols represent the single point measured experimental data, and lines represent the best fit model results from the analytical solutions proposed by Fry et al. (1993).

**Table 5. 3. Peak initial metal concentrations from column leaching tests**

Column specimen	Initial pH	Metal concentrations			
		Aluminum Co (mg/L)	Arsenic Co (mg/L)	Chromium Co (mg/L)	Selenium Co (mg/L)
40%Paul Smith + 60% Sand (Naphthalene)	8.5	1.3	1.77	0.099	0.19
%Dickerson Precipitator + 60% Sand (Naphthale	10	48.9	3.21	0.097	0.26
40%Morgantown + 60% Sand (Naphthalene)	9.9	29.9	2.55	0.599	0.09
40%Potomac River + 60% Sand	8.1	0.2	-	0.046	0.07
40%Dickerson Baghouse + 60% Sand	10.5	53.9	2.35	0.180	0.17
40%Chalk Point + 60% Sand	9	19.6	2.65	0.370	0.06
40%Brandon Shores + 60% Sand	7.4	0.2	-	0.011	0.02

**Note:** Co = initial peak effluent aqueous concentration in column leaching tests (CLTs)



at early pore volumes of flow (a pattern referred to as “first - flush” leaching) followed by a decrease in leaching. Ogunro and Inyang (2003) explained that the wash-out and detachment of metals by percolating solution occurs at the initial stages of the column test. They explained the reason for this phenomenon as the increase in the chemical potential which initiated the leaching of metals from the solid matrix into the surrounding solution until the concentration difference between the leachant and the solid material was reduced and a steady state was reached. The release and transport of metal contaminants from their columns were reported to be advection-dominated due to high Peclet numbers ( $P_L > 5$ ). The high Peclet numbers observed in the current study (Table 4.1) also suggest that advection is dominant over dispersion and so it was assumed to be the dominant mechanism during leaching of the four metals from the columns. This also suggests that advection was also dominant compared to the rate of desorption, consistent with the rate limited desorption which as observed determines first order kinetics behavior.

The leaching elution curves for all four metals agree reasonably well with the predictions of the analytical solution proposed by Fry et al. (1993). The leaching of the four metals from the seven fly ash-amended CLTs exhibit similar patterns, differing by partition coefficient ( $K_d$ ) and first-order rate coefficient. The data presented in Table 5.2 and Figures 5.16 to 5.19 show that metal leaching (removal) rate increased with increasing first-order desorption rate ( $\alpha$ ) and decreasing partition coefficient ( $K_d$ ) (Fry et al.1993). The partition coefficients for Al ranged between 0.3 and 1.67 L/kg, and the retardation factors ranged between 3.1 and 8. The  $K_d$  and R ranges were 1.02-3.44 L/kg and 7.1-14.7, respectively, for Se. The partition

coefficients stayed in a range of 1.1 to 3.5 L/kg and 0.64 to 2.28 L/kg for As and Cr, respectively, while the retardation factors for the same two metals varied between 6.4 and 14.9 and 5.7 and 10. Similar ranges for As and Cr were also reported by Bin Shafique et al. (2006).

### **5.3. RELATIONSHIP BETWEEN WLTs AND CLTs RESULTS**

It is well-known that a more quantitative analysis of metal leaching from fly ash-soil mixtures can be made in column tests, as column set-ups more closely define the “field behavior” of these materials as compared to batch-scale tests. However, batch tests are easier to perform. Therefore, attempts were made to compare the results of the two tests with an aim to help the practicing engineers to roughly predict the “field behavior” from simple batch leaching tests. However, several issues have to be considered before studying this relationship. First of all, testing conditions that include liquid-to-solid (L:S) ratios, duration of leaching, dynamicity, and redox environment are different for these two systems. For instance, the L:S ratio did not change during the batch experiments; however, the column experiments were conducted under continuous percolation of eluant, i.e., constant increase in L:S ratio (Ogunro and Inyang, 2003). A second issue is the difference in duration of the tests. In the “short term” batch experiments, smaller equilibration times were allowed for leaching, while in “long term” column leaching experiments leachate was collected and analyzed for extended times. Third, compared to the “smooth” fluid movement inside the column set-up, the agitation motion in the batch procedure was more aggressive, and probably enhanced the surface contact between the leaching solution

and the solid particulates. This may have resulted in faster leaching rates of the metals and equilibrium between the liquid and the solid phase was reached within a shorter period of time. The pH conditions may have also been influenced by this agitation. The increased dissolution of mineral components of the tested metals may enhance variations in pH and ultimately affect their leaching behavior. As the speciation of As, Cr, and Se is highly dependent on the redox conditions, the differences between the redox environments in the batch and column experiments are likely to contribute to the disparity in the tests results (Sauer et al. 2005), but cannot be quantified with the available data.

Since a direct comparison between the two tests is not available, two different approaches have been undertaken. First, the initial peak effluent metal concentrations from the CLTs ( $C_0$ ) have been compared to the concentrations leached during batch WLTs ( $C_{aq}$ ) (Figure 5.20). Generally, the initial effluent concentrations in CLTs were higher than the  $C_{aq}$ s measured in WLTs. Differences in L:S ratios between the two leaching tests (a ratio of 20:1 in WLTs versus 0.15:1 in CLTs at the initial PVFs ) may be responsible for the observed phenomenon. The graphs also show that  $C_0$  for Al is 1 to 100 times higher than  $C_{aq}$ . Similarly,  $C_0$  for As, Cr, and Se is 10 to 30, 1 to 20, and 1 to 6 times higher than  $C_{aq}$ , respectively. Bin Shafique et al (2006) made a

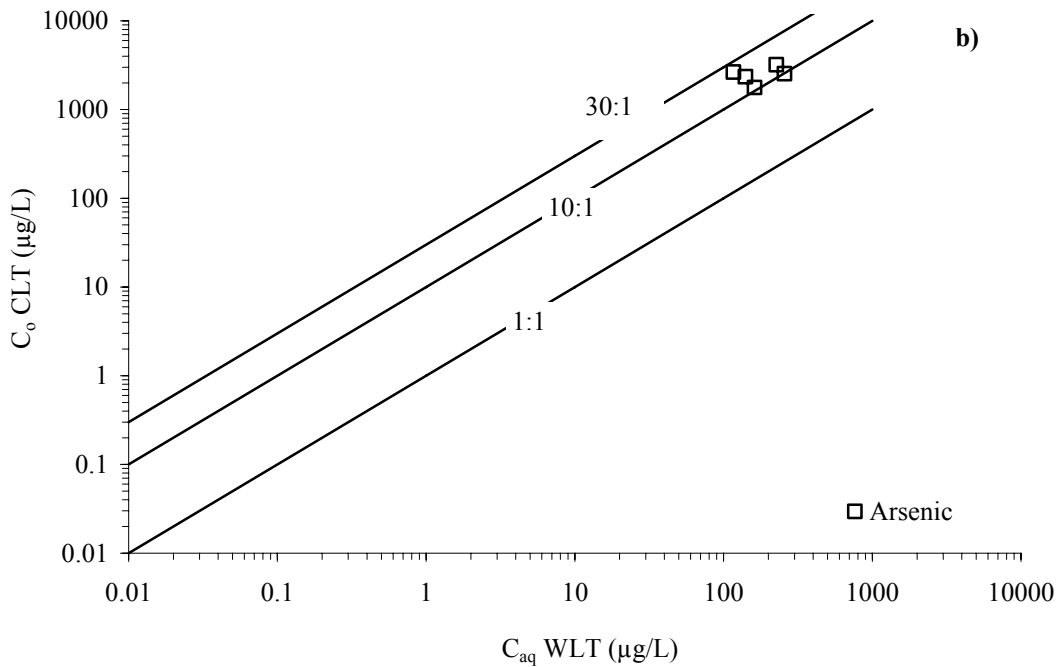
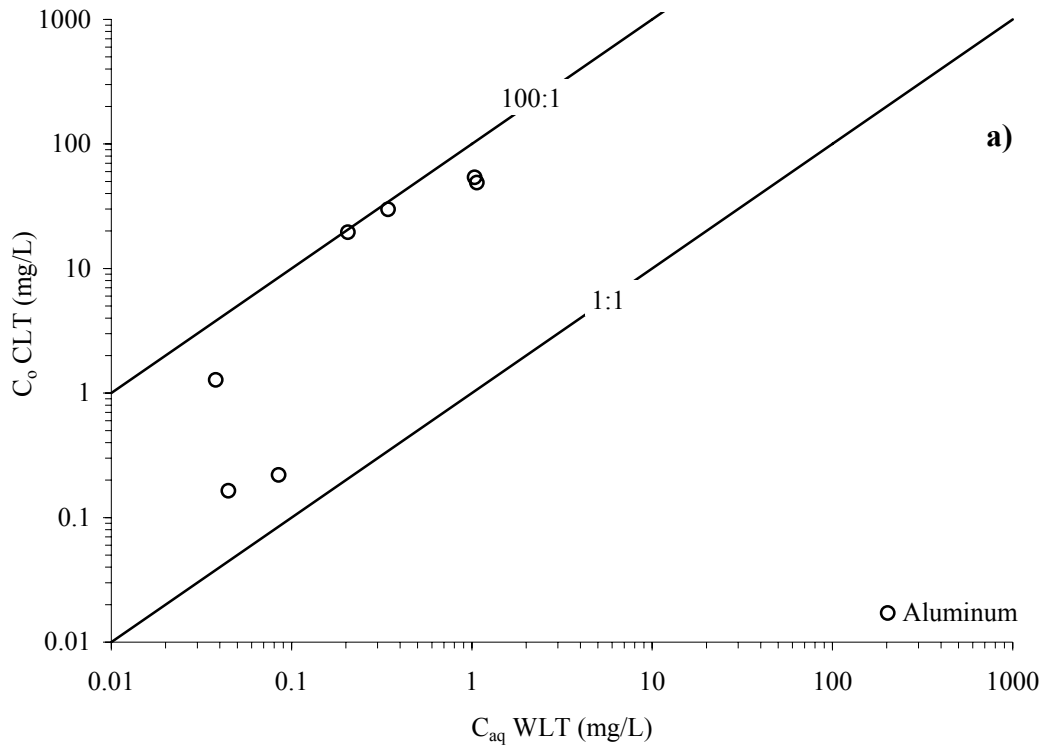


**Figure 5. 20. Comparison of the peak initial effluent concentrations from CLTs and aqueous concentrations from WLTs for 60% sand + 40% fly ash mixtures: (a) Al, (b)As, (c) Cr, and (d) Se.**

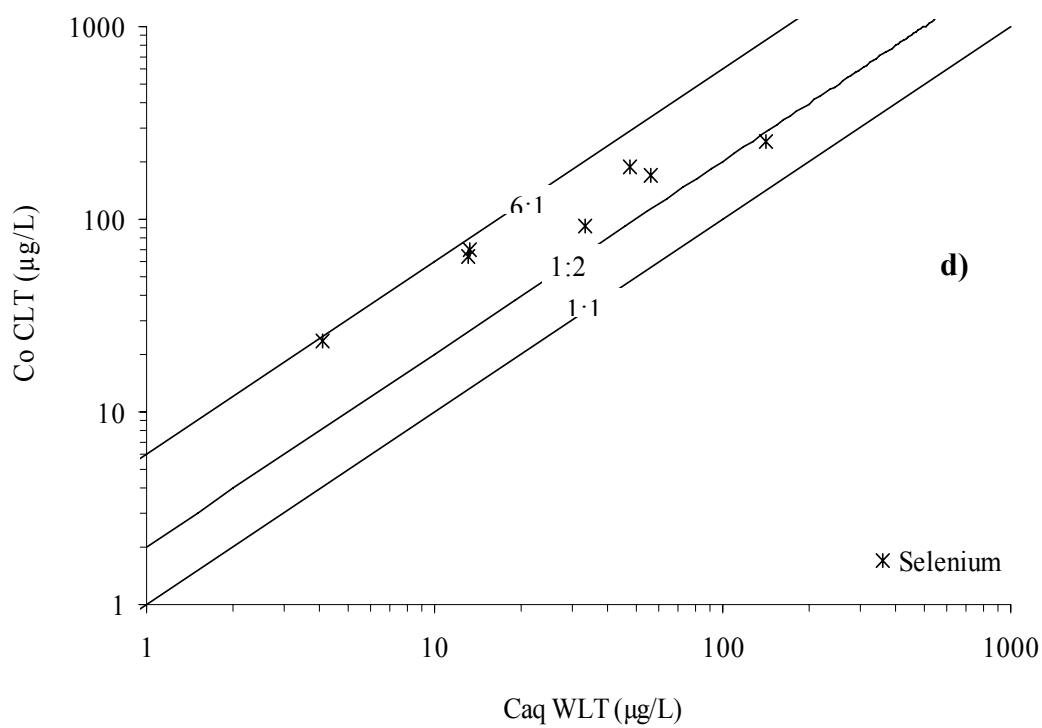
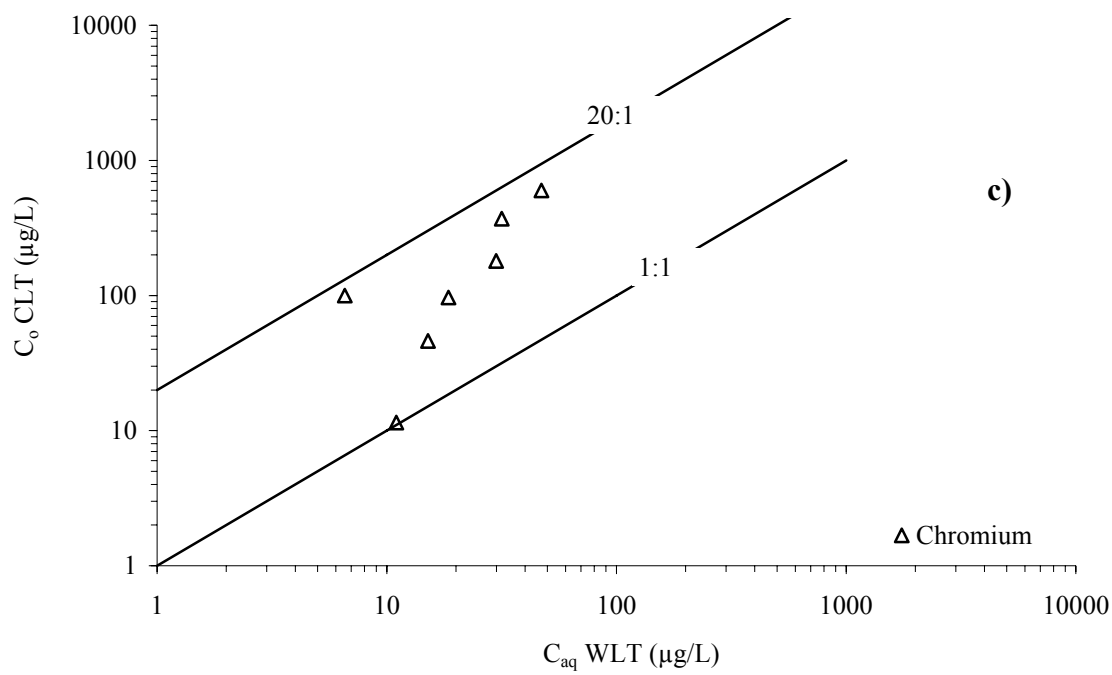


Figure 5.20. (Continued) Comparison of the peak initial effluent concentrations from CLTs and aqueous concentrations from WLTs for 60% sand + 40% fly ash mixtures: (a) Al, (b) As, (c) Cr, and (d) Se.

similar comparison and concluded that the initial effluent concentrations of chromium and selenium from column tests can be conservatively estimated by applying a scaling factor of 10 to the water leach tests.

A second approach used to compare the batch and column test data involved up-scaling the WLTs results to the column experimental set-up in order to predict the leachable amount in CLTs. This was done by performing mass balance calculations to predict the leachable amount of metals from the materials (sand and fly ash) packed in the column using the measured metal concentrations in batch leaching tests. The column design used in this study (described in Section 3.2.2.) involved a 8-cm bottom and a 3-cm top layer of sand separated by a middle 19-cm layer of 60% sand + 40% fly ash mixture. The sand WLT data were up-scaled to the amount of sand present in the two layers in the column, and the leachable amounts of metals were predicted. Similarly, the results from the WLTs performed on 60% sand+40% fly ash mixtures were used to predict the leachable amount from the middle sand-fly ash mixture layer in the column. The calculations were performed using the following relationship:

$$\text{Predicted leachable amount} = \left[ \left( \frac{C_{aq}^{sand} \cdot V_w}{M_{sand\ WLT}} \right) \cdot M_{sand\ CLT} \right] + \left[ \left( \frac{C_{aq}^{mix} \cdot V_w}{M_{mix\ WLT}} \right) \cdot M_{mix\ CLT} \right] \quad (5.1)$$

where,  $C_{aq}^{sand}$  is the measured metal concentration in the batch WLTs performed on sand alone (mg/L or  $\mu\text{g/L}$ ),  $V_w$  is the volume of solution in the WLTs (L),  $M_{sand\ WLT}$  is the amount of sand used in WLTs (g),  $M_{sand\ CLT}$  is the mass of sand present in the two pure

sand layers in the column (g),  $C_{aq}^{mix}$  is the measured metal concentration in the WLTs performed on 60% sand + 40% fly ash mixtures (mg/L or  $\mu\text{g/L}$ ),  $M_{mix\ WLT}$  is the mass of mixture (60% sand + 40% fly ash) used in WLTs (g), and  $M_{mix\ CLT}$  is the mass of mixture (60% sand + 40% fly ash) present in the middle mixture layer in the column (g).

The actual leached amounts of metals in column experiments were determined through mass balance calculations that involved concentrations of metals measured at different time intervals:

$$\text{Mass balance on actual leached amount} = \sum_{i=1}^n Q \cdot (t_i - t_{i-1}) \cdot \left( \frac{C_{i-1} + C_i}{2} \right) \quad (5.2.)$$

where,  $Q$  is the influent flow-rate used in column experiment (L/h),  $t_i$  and  $t_{i-1}$  are the times of sampling (h),  $C_i$  and  $C_{i-1}$  are concentrations measured at times  $t_i$  and  $t_{i-1}$ , respectively (mg/L or  $\mu\text{g/L}$ ), and  $i$  denotes the number of samples collected.

The actual leached amounts determined by mass balance calculations (Equation 5.2.) are plotted against the predicted leachable amounts determined using the WLTs data (Equation 5.1) in Figure 5.21. The trends suggest that the leachable amounts were underpredicted 6 and 5 times for aluminum and arsenic, respectively. The predictions are relatively better for chromium and selenium even though scatter in the data is evident (Figures 5.21c and 5.21d).

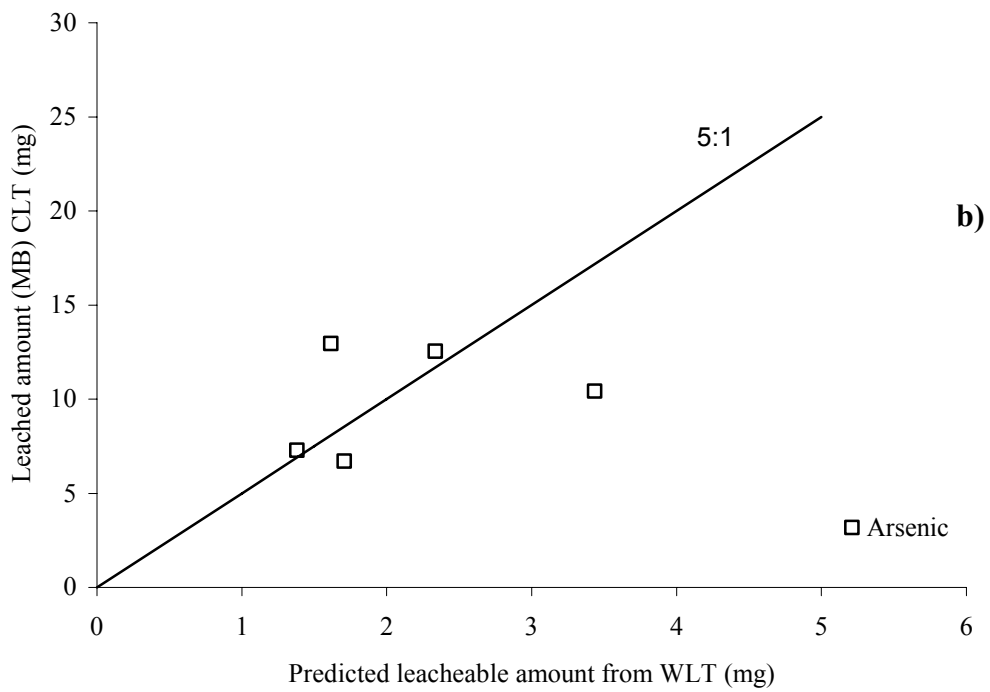
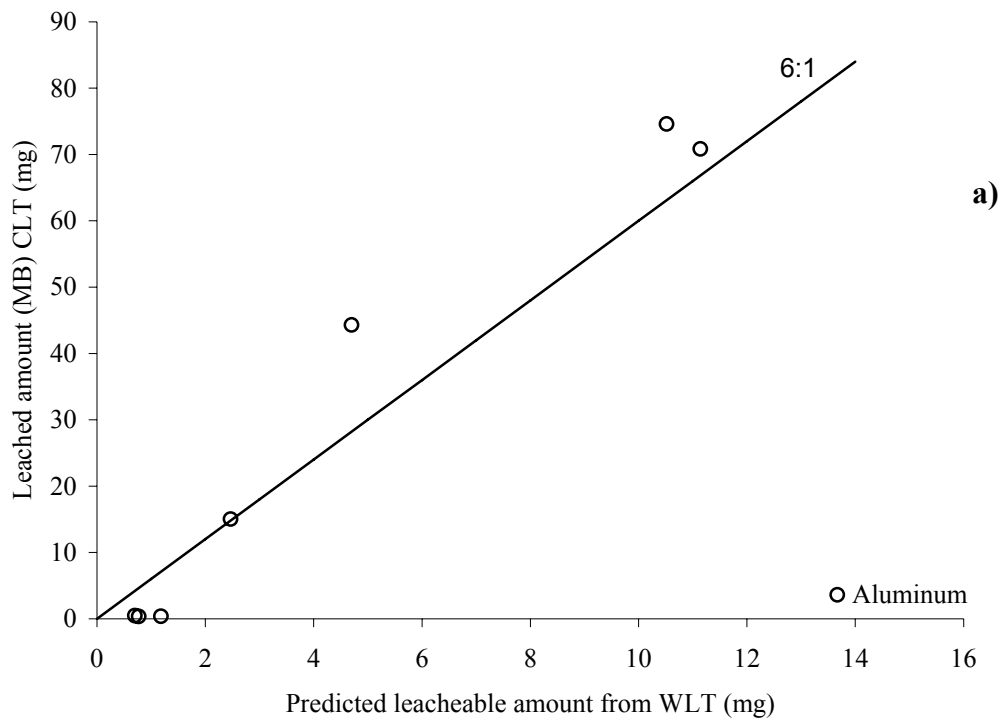


Figure 5. 21. Comparison of the actual leached amounts from CLTs to the predicted ones from WLTs for 60% sand + 40% fly ash mixtures: (a) Al, (b)As, (c) Cr, and (d) Se.



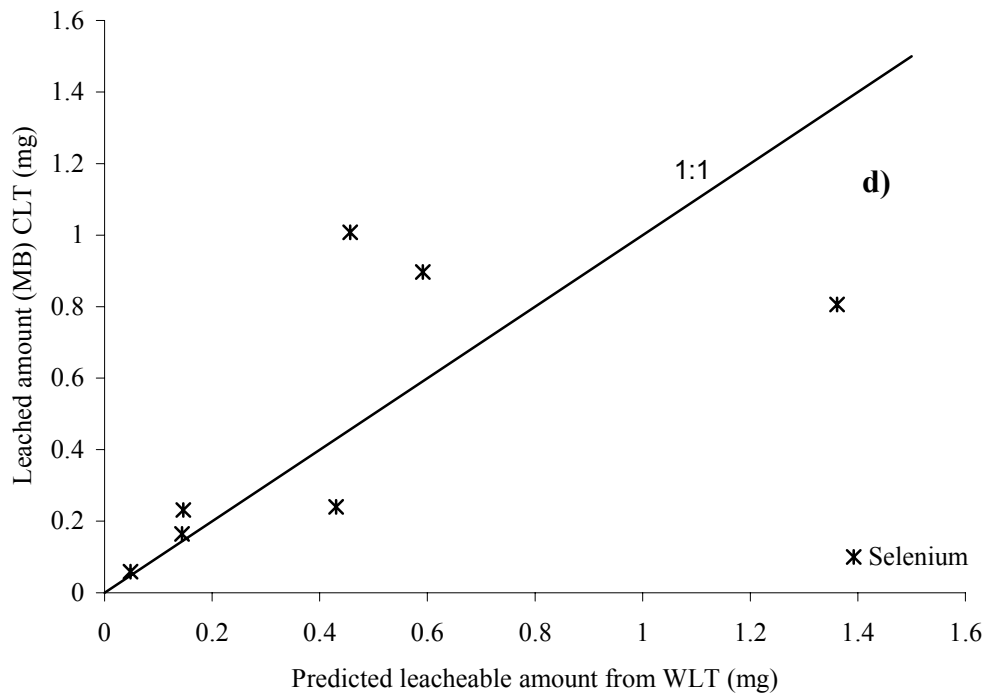
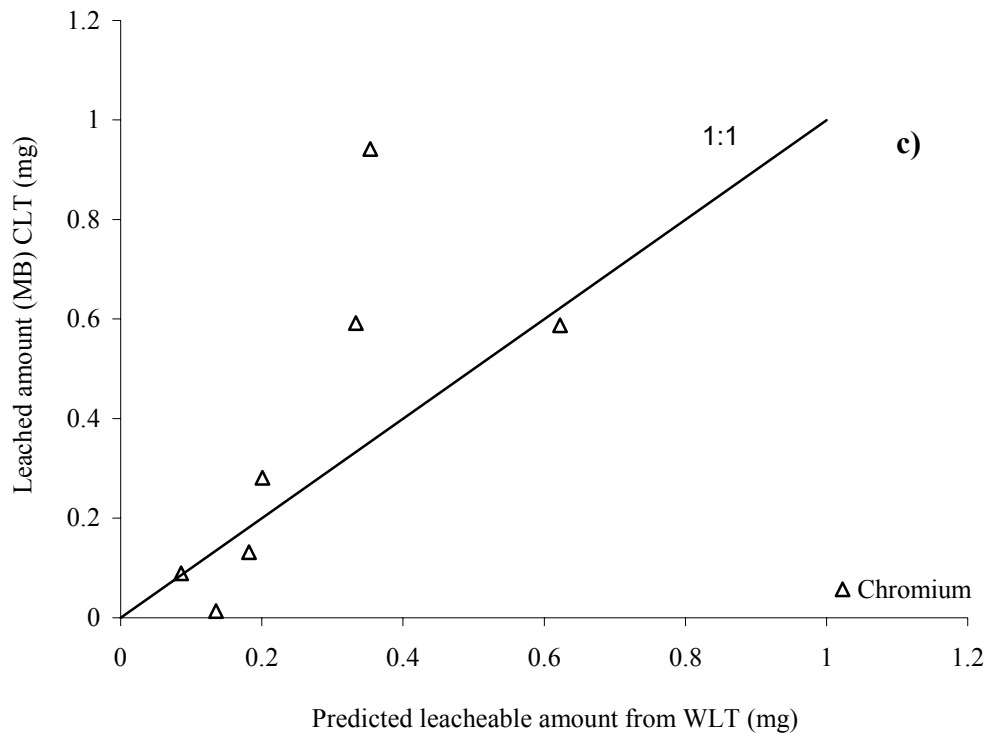


Figure 5. 21. (Continued) Comparison of the actual leached amounts from CLTs to the predicted ones from WLTs for 60% sand + 40% fly ash mixtures: (a) Al, (b)As, (c) Cr, and (d) Se.

In table 5.4 is presented a comparison of column peak initial concentrations and water leaching tests concentrations (from tests performed with sand-fly ash comparable to the column experiments) against the EPA maximum contaminant levels (MCL) admitted for drinking water and the water quality limits (WQLs) for fresh water recommended for protection of aquatic life and human health. As it can be noticed, generally, the MCL and WQLs limits have been overpassed by most of the column peak concentrations for all metals investigated (except for chromium, which in most cases did not surpassed the WQL). This may impose serious issues if the fly ashes will be considered for earthwork applications if no measures are being taken to impede the migration of the heavy metals from the fly ash into the environment.

**Table 5. 4. Comparison of the peak CLTs concentrations and corresponding aqueous WLTs concentration against the EPA MCL\* and WQL\*\*\***

<b>Column Leaching Tests (CLTs)</b>												
<b>Fly ash-sand mixture</b>	<b>Aluminum***</b>			<b>Arsenic</b>			<b>Chromium</b>			<b>Selenium</b>		
	<b>C (mg/L)</b>	<b>Exceeding MCL*? (0.05-0.2 mg/L)</b>	<b>Exceeding WQL**? (0.75 mg/L)</b>	<b>C (mg/L)</b>	<b>Exceeding MCL*? (0.01 mg/L)</b>	<b>Exceeding WQL**? (0.34 mg/L)</b>	<b>C (µg/L)</b>	<b>Exceeding MCL*? (100 µg/L)</b>	<b>Exceeding WQL**? (570 µg/L)</b>	<b>C (µg/L)</b>	<b>Exceeding MCL*? (50 µg/L)</b>	<b>Exceeding WQL**? (5 µg/L)</b>
40%Dickerson Precipitator + 60% Sand (Naphthalene)	48.9	yes	yes	3.21	yes	yes	96.7	no	no	255.5	yes	yes
40%Morgantown + 60% Sand (Naphthalene)	29.9	yes	yes	2.55	yes	yes	599.6	yes	yes	91.7	yes	yes
40%Paul Smith + 60% Sand (Naphthalene)	1.3	yes	yes	1.77	yes	yes	99.8	no	no	185.3	yes	yes
40%Dickerson Baghouse + 60% Sand	53.9	yes	yes	2.35	yes	yes	180.4	yes	no	169.5	yes	yes
40%Brandon Shores + 60% Sand	0.16	no	no	-	yes	yes	11.46	no	no	23.4	no	yes
40%Potomac River + 60% Sand	0.22	yes	no	-	yes	yes	46.09	no	no	69.8	yes	yes
40%Chalk Point + 60% Sand	19.6	yes	yes	2.65	yes	yes	370.3	yes	no	63.8	yes	yes
<b>Batch Water Leaching Tests (WLTs)</b>												
40%Dickerson Precipitator + 60% Sand	1.07	yes	yes	0.226	yes	no	18.6	no	no	142	yes	yes
40%Morgantown + 60% Sand	0.34	yes	no	0.256	yes	no	47.1	no	no	33.3	no	yes
40%Paul Smith + 60% Sand	0.04	no	no	0.161	yes	no	6.6	no	no	47.7	no	yes
40%Dickerson Baghouse + 60% Sand	1.04	yes	yes	0.14	yes	no	29.9	no	no	56.1	yes	yes
40%Brandon Shores + 60% Sand	0.08	no	no	0.098	yes	no	11	no	no	4.1	no	no
40%Potomac River + 60% Sand	0.04	no	no	0.287	yes	no	15.1	no	no	13.2	no	yes
40%Chalk Point + 60% Sand	0.21	yes	no	0.116	yes	no	31.6	no	no	13	no	yes

**Note:** \* MCL represents the maximum level contaminant concentrations that EPA allows in drinking water;  
 \*\*WQL represents the recommended water quality criteria for the protection of aquatic life and human health in fresh water;  
 \*\*\* For aluminum, because is not considered a priority pollutant the values are the secondary standards

## **CHAPTER 6**

### **ORGANIC CONTAMINANTS - RESULTS AND DISCUSSIONS**

A series of batch and column adsorption/desorption tests were conducted on fly ash and sand to evaluate their interaction with petroleum hydrocarbons in a reactive barrier application. The tests were conducted on three of the selected fly ashes, which were chosen so as to cover the whole range of carbon contents: Dickerson Precipitator (20.5%LOI), Paul Smith (10.7%LOI), and Morgantown (3.1%LOI) fly ashes. Additionally, powdered activated carbon (PAC) and silica sand were employed in the testing program as reference materials.

#### **6.1. BATCH TESTS – RESULTS AND DISCUSSIONS**

##### **6.1.1. Batch adsorption tests**

A summary of the batch adsorption test conditions and results is presented in Table 6.1. Five replicate tests were conducted on each sorbate-sorbent combination and averages of the test results were reported. The standard deviation is also reported with the results. Of the fly ashes, the highest adsorption capacity for naphthalene and o-xylene was observed for the Dickerson Precipitator fly ash, followed by Paul Smith, and Morgantown fly ashes. In comparison, sand was shown to have a very low

**Table 6. 1. Summary of results from batch adsorption experiments**

Adsorbent	Carbon content LOI (%)	Adsorption time (h)	Naphthalene					O-xylene				
			$C_{initial}$ (mg/L)	Equilibrium				$C_{initial}$ (mg/L)	Equilibrium			
				$C_{aqueous}$ (mg/L)	$q_{adsorbed}$ (mg/kg)	SD (±)	% adsorbed		$C_{aqueous}$ (mg/L)	$q_{adsorbed}$ (mg/kg)	SD (±)	% adsorbed
Sand	0.2	48	10.2	9.52	67.98	1.43	5.5	40.1	37.2	349	4.11	7.05
Morgantown	3.1	48	10.2	8.01	256.4	3.3	20.5	40.1	30.8	1095.3	9.8	23.4
Paul Smith	10.7	48	10.2	4.38	696.9	6.98	56.5	40.1	27.9	1416.2	13.1	30.5
Dickerson Precipitator	20.5	48	10.2	1.26	1084.6	5.9	87.5	40.1	21.7	2275	4.67	46.1
PAC	99	48	10.2	0.5	49786.7	11.9	96.2	40.1	22	106882	18.45	45.1

**Note:**  $C_{initial}$  is the initial concentration of solute used for sorption experiments,  $C_{aqueous}$  is the concentration of solute left in the aqueous phase after sorption step (is the average of five replicates),  $q_{adsorbed}$  is the mass of solute adsorbed on the solid phase at the end of the adsorption step, and % *adsorbed* is the percentage of solute adsorbed at the end of the adsorption step.

sorption capacity for the two organics tested (68 mg naphthalene and 349 mg o-xylene sorbed per kg of sand). PAC demonstrated greater sorption capacity for naphthalene and o-xylene among the five adsorbents tested in this study, with 49.8g naphthalene/kg PAC and 106.9 g o-xylene/ kg PAC adsorbed following adsorption step.

To mechanistically explain these results, it is useful to examine the factors that influence the adsorption/desorption of organics to/from a solid phase, and a detailed understanding of the adsorption phenomena is necessary. Among the various factors, the following five are considered to be the most important ones: (i) properties of the solid sorbent (e.g., surface area of the solid particles, organic carbon content), (ii) properties of the organic compound (e.g., solubility, hydrophobicity, partition coefficient), (iii) contact time between the leaching solution and sorbent, (iv) pore water velocity of the leachant, and (v) concentration of the organic contaminant (Farrell and Reinhard 1994, Kan et al. 1994, Okuda et al. 1996, Pennel et al. 1996, Cornelissen et al. 1998, Keijzer et al. 2002, Gunasekara and Xing 2003). Of these factors, the two that were varied in this study were the properties related to the adsorbent and the organic contaminant.

With respect to the properties of the solid sorbent, Smith et al. (1997) concluded from their study that the primary adsorption sites for organics are located on the surface of the carbon present in the fly ash. A higher unburned carbon content (i.e., loss on ignition, LOI %) in fly ash generally results in a larger surface area that is accessible for adsorption of organics, as the major source of surface area in fly ash is represented by its carbon content (Hurt et al. 1997). For example, it has been

observed that the carbon in the fly ash has a much greater surface area than the external geometry of the fly ash particle due to internal porosity of the carbon particles (Külaots et al. 1998). This is consistent with the conceptual model of Pignatello and Xing (1996) who suggest that the high surface area of a sorbent is related to the porous texture of its carbonaceous constituents. In order to reach all sorption sites, the sorbate molecule has to traverse the percolating solution, diffuse into the matrix of the sorbing material, enter the easily accessible mesopores, and further to infiltrate into harder to penetrate micropores. A schematic conceptualization of these processes is presented in Figure 6.1.

The data presented in Figure 6.2 and Table 6.2 show that Dickerson Precipitator fly ash has the highest fines content, the highest LOI value, and as a result provides the greatest surface area available for sorption, followed by the Paul Smith and Morgantown ashes. These results are consistent with the trend in organic contaminant adsorption capacity (Dickerson Precipitator > Paul Smith > Morgantown), and thus, support the findings of the existing research studies. More extensive adsorption isotherms studies for the fly ashes tested with naphthalene and o-xylene were performed by Melih Demirkan (2008) and further confirm these trends (see Figure 6.3). The best fits to these experimental data were achieved by Freundlich and Langmuir sorption models and the parameters determined from these two isotherm models are summarized in Table 6.3. Again, the trend in these data is the same: sorption to the Dickerson Precipitator fly ash is greater than that to the Paul Smith, and in turn Morgantown fly ashes.

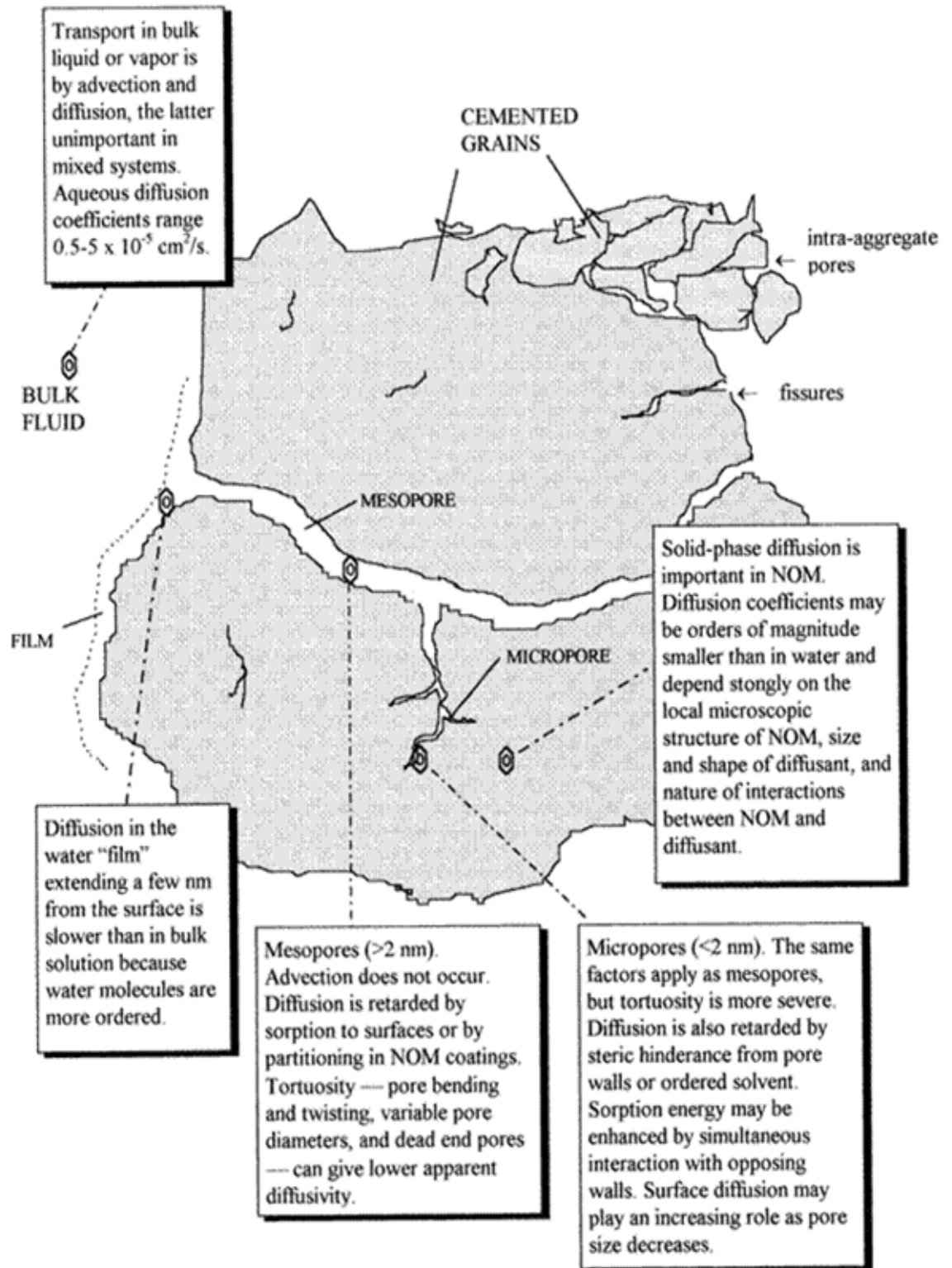


Figure 6. 1. Schematic of possible pathways for sorption of an organic molecule onto the organic matrices of a sorbing material. (Pignatello and Xing 1996)



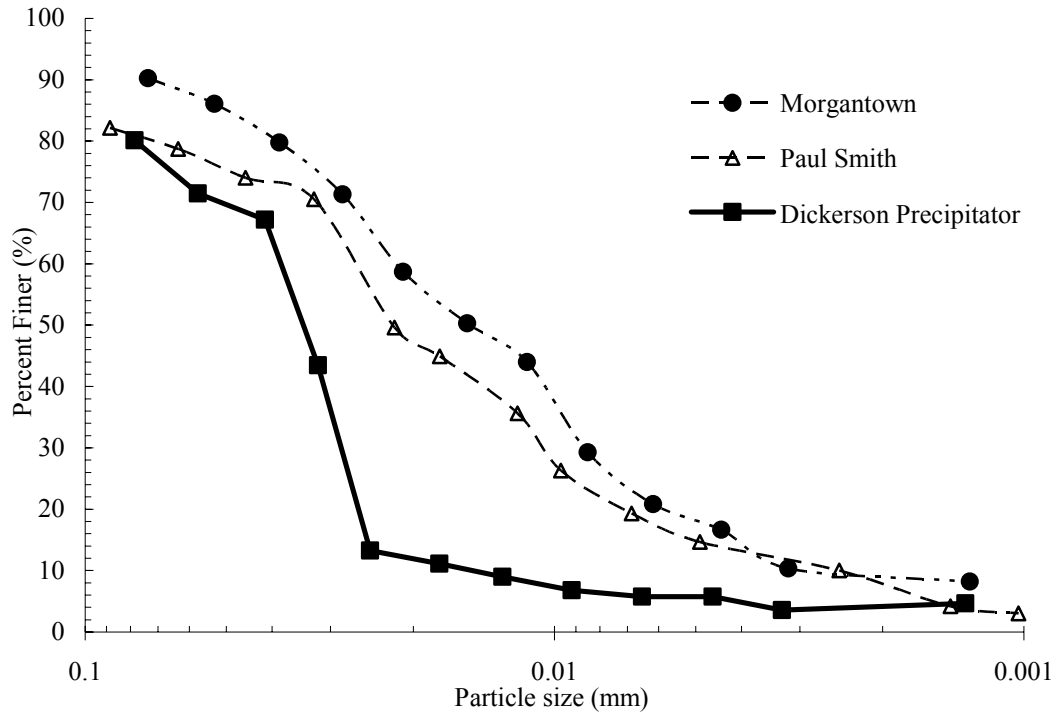


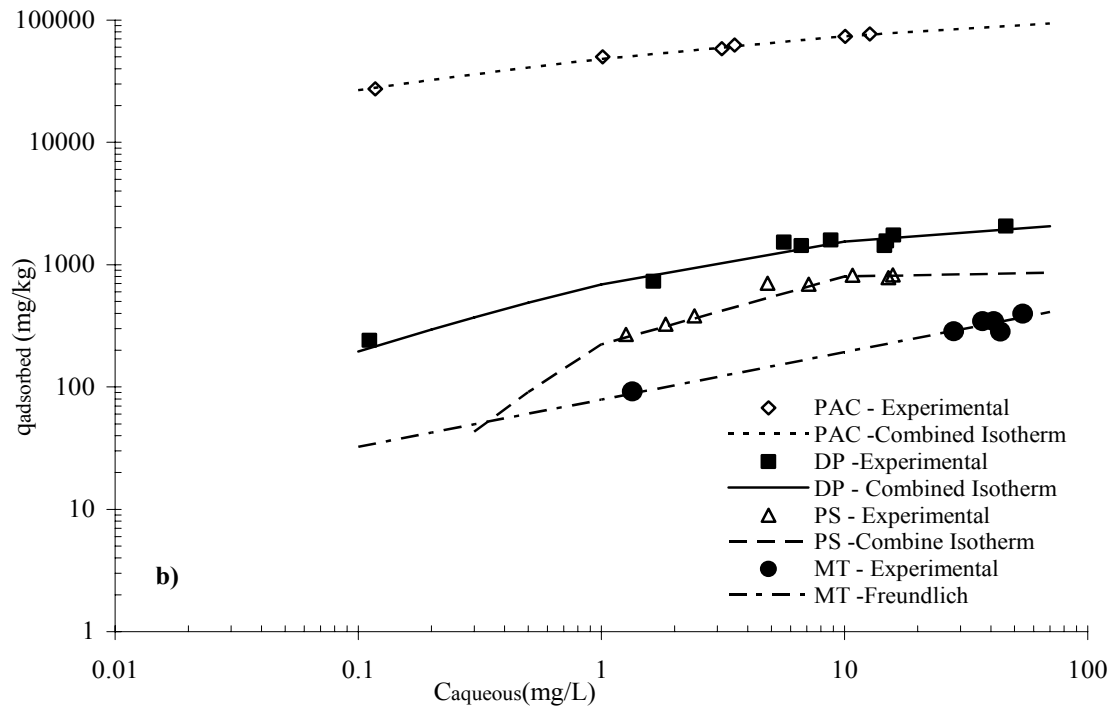
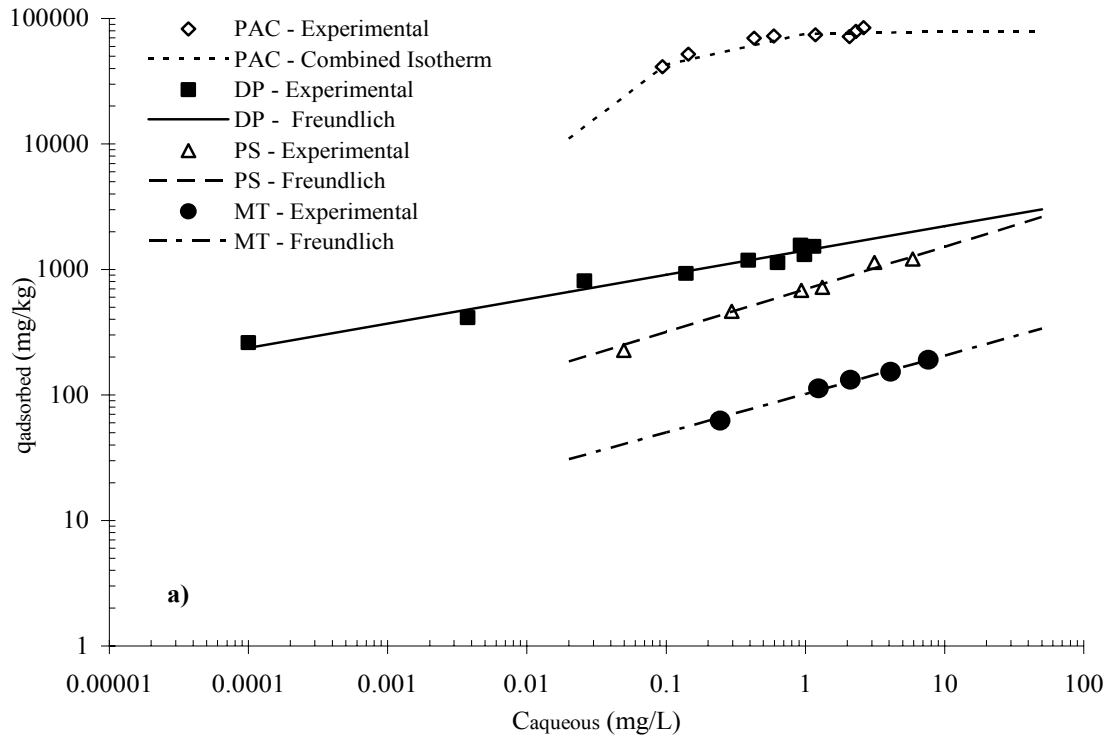
Figure 6. 2. Grain size distribution for Dickerson Precipitator, Paul Smith and Morgantown fly ash

Table 6. 2. Correlation between carbon content and specific surface area of fly ash

Fly Ash	SSA <sup>a</sup> (m <sup>2</sup> /g)	LOI% <sup>b</sup>
Dickerson Precipitator	11.08	20.5
Paul Smith	5.15	10.7
Morgantown	1.36	3.1

<sup>a</sup> Specific Surface Area of the solid fly ash particles

<sup>b</sup> Loss On Ignition



**Figure 6. 3. Adsorption isotherms with best fit models after a) naphthalene and b) o-xylene adsorption experiments with Dickerson Precipitator, Paul Smith and Morgantown fly ash. Demirkan (2008)**

**Table 6. 3. Adsorption isotherms parameters from batch adsorption tests (Demirkan et al. 2008)**

Fly ash	Naphthalene		O-xylene	
Morgantown	$K_F$ (L/kg) <sup>a</sup>	102	$K_F$ (L/kg) <sup>a</sup>	46.4
	$n^a$	0.306	$n^a$	0.528
Paul Smith	$K_F$ (L/kg) <sup>a</sup>	697	$Q_{max}$ (mg/kg) <sup>b</sup>	876
	$n^a$	0.339	$K_L$ (L/kg) <sup>b</sup>	0.644
Dickerson Precipitator	$K_F$ (L/kg) <sup>a</sup>	1506	$Q_{max}$ (mg/kg) <sup>b</sup>	1983
	$n^a$	0.207	$K_L$ (L/kg) <sup>b</sup>	0.396

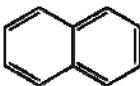
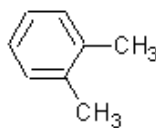
<sup>a</sup> Freundlich Isotherm: ( $q_i = K_F [C_f]^n$ )  $K_F$  = Freundlich equilibrium isotherm constant (L/kg),  
 $n$  = dimensionless empirical,  $C_f$  = final concentration of naphthalene (mg/L).

<sup>b</sup> Langmuir Isotherm: ( $q_i = (Q_{max} K_L C_f) / (1 + K_L C_f)$ )  $K_L$  = Langmuir isotherm coefficient (L/kg)  
 $Q_{max}$  = sorption capacity of particular solid (mg/kg).

The properties of the organic compound will also affect the sorption/desorption behavior. Kodadoust et al. (2005) studied the physicochemical properties of seven organic compounds for their effect on sorption onto sediments, and indicated that the partition coefficient,  $K_d$ , for their tested compounds correlated well with the molecular weight, total molecular surface area, molar volume, and boiling point of the compound. The strongest positive correlations were obtained for molecular weight, molar volume, and total surface area. Indeed, it is well known that the degree hydrophobicity of a non-polar organic compound increases with increasing size, volume and mass of the compound, and the driving force for sorption is the repelling expulsion from water and the van der Waals interactions with the solid surface. A distribution ratio,  $K_d$ , can be calculated by taking the ratio of the contaminant total equilibrium concentrations in the sorbed and aqueous phases. Based on the data in Table. 6.1, this ratio was always larger for naphthalene than for o-xylene. This is consistent with the physicochemical properties of naphthalene and o-xylene listed in Table 6.4. Specifically, the molecular weight and molar volume of naphthalene are greater due to its relatively larger size. Correspondingly, the aqueous solubility  $C_{\text{naphthalene}}^{\text{aq.sat}} < C_{\text{o-xylene}}^{\text{aq.sat}}$ , and octanol-water partition coefficient  $\text{Log } K_{\text{ow naphthalene}} > \text{Log } K_{\text{ow o-xylene}}$  also suggest that naphthalene is more hydrophobic than o-xylene.

Consistent with the observations of Kodadoust et al. (2005), the higher boiling point for naphthalene than for o-xylene (218 °C versus 144.5 °C) indicates that greater activation energies will be required for sorption of naphthalene than for o-xylene.

**Table 6. 4. Physicochemical properties of naphthalene and o-xylene**

Properties	Naphthalene	O-xylene
Molecular formula	C <sub>10</sub> H <sub>8</sub>	C <sub>8</sub> H <sub>10</sub>
Molecular weight (MW)	128.19	106.16
Chemical structure		
Solubility in water at 25 <sup>0</sup> C (mg/L) (C <sup>aq.sat</sup> )	31.7	178
Partitioning coefficients	Log K <sub>ow</sub>	3.35
	Log K <sub>oc</sub>	2.97
Henry's law constant (atm·m <sup>3</sup> /mol)	4.6x10 <sup>-4</sup>	5.18x10 <sup>-3</sup>
Vapor pressure at 25 <sup>0</sup> C (mm Hg)	0.087	6.61
Density at 20 <sup>0</sup> C (g/cm <sup>3</sup> )	1.145	0.88
Molar volume (cm <sup>3</sup> /mol)	148	121.2
Specific gravity	1.14	0.87
Melting point <sup>0</sup> C	80.5	-25.2
Boiling point <sup>0</sup> C	218	144.5

**Note:** The physicochemical properties presented in this table were summarized from: Agency for Toxic Substances and Diseases Registry (ATSDR)–Toxicological profile website (<http://www.atsdr.cdc.gov/toxprofiles/tp71-c4.pdf>), and Sangster Research Laboratories under auspice of the Canadian National Committee for CODATA sponsored by Canada Institute for Scientific and Technical Information CISTI website (<http://logkow.cisti.nrc.ca/logkow>)

### 6.1.2. Batch sequential desorption tests

Upon completion of the batch adsorption tests, the final equilibrium concentrations in the aqueous solution were measured, and the specimens were then subjected to a sequential desorption procedure, as described in Section 3.4.1., by applying successive decant/refill steps. A series of ten sequential desorption tests were performed for studying the sorption/desorption behavior of naphthalene and o-xylene onto the five adsorbents described above. About 95% of the supernatant was refreshed with background solution in each step. Five replicate tests were conducted on each sorbate-sorbent combination and averages of the test results were reported. A liquid-to-solid (L:S) ratio of 120:1 was used in all tests, except the tests with PAC, which were performed at a ratio of 600:1.

The results of the batch desorption experiments are summarized in Table 6.5. The amount of solute adsorbed and then desorbed (in each step, and total) and the percentage of solute desorbed from the successive desorption steps were determined by using the following equations developed by Kan et al. (1994):

$$q_{adsorbed} = (C_{initial} - C_{aqueous}) * \frac{V_{water}}{M_{solid}} \quad (6.1)$$

$$\Delta q_{desorbed}^i = [C_i - C_{i+1} * (1 - r)] * \frac{V_{water}}{M_{solid}} \quad (6.2)$$

$$q_{desorbed} = \sum_{i=1}^n \Delta q_{desorbed}^i \quad (6.3)$$

$$\% \text{ solute desorbed} = \frac{\sum_{i=1}^n \Delta q_{desorbed}^i}{q_{adsorbed}} * 100\% \quad (6.4)$$

where  $q_{adsorbed}$  is the mass of solute adsorbed on the solid phase at the end of the adsorption step (mg/kg);  $C_{initial}$  is the initial concentration of solute used for sorption experiments (mg/L);  $C_{aqueous}$  is the concentration of solute left in the aqueous phase after sorption step (mg/L);  $\Delta q^i_{desorbed}$  is the change in the solid phase concentration (mg/kg) during the  $i^{th}$  desorption step;  $C_i$  and  $C_{i-1}$  are the aqueous concentrations (mg/L) at the end of  $i^{th}$  and  $(i+1)^{th}$  desorption steps, respectively;  $r$  is the fraction of supernatant refreshed in each desorption step ( $\sim 0.95$ );  $V_{water}$  is the volume of solution (L);  $M_{solid}$  is the mass of the solid used in each batch reactor (kg);  $n$  is the number of desorption steps.

The solid phase concentration of the solute is plotted against the desorption steps for the three fly ashes in Figure 6.4 and the data evaluated in Table 6.5. Based on the data in Table 6.5 the Dickerson Precipitator fly ash may irreversibly adsorb some of naphthalene, or at least convert it into a slowly reversible fraction, with only 55% of the sorbed naphthalene released after 21 desorption steps, while the Paul Smith and Morgantown fly ashes released almost all of the naphthalene after several desorption steps (96% and 95 % desorption after 19 and 13 steps, respectively). All of the solute was released from the sand after 3 desorption steps, indicating that the sand has no capacity to irreversibly adsorb organics. Similar trends were observed for o-xylene. Of the three fly ashes, Dickerson Precipitator demonstrated highest capacity to “irreversibly” adsorb o-xylene with about 64% of the adsorbed amount being released in about 12 sequential desorption steps (711.6 mg o-xylene/Kg fly ash remained adsorbed), followed by Paul Smith fly ash, with 430.8 mg o-xylene/ Kg fly ash remaining adsorbed after 11 sequential desorption steps, and at last Morgantown

fly ash, with about 411.2 mg o-xylene/ kg fly ash remaining adsorbed after 9 desorption steps. As was expected, PAC revealed the highest capacity to strongly adsorb both organics, converting them into irreversibly adsorbed or at least slowly desorbable, with only 29% of the sorbed naphthalene being released after 21 desorption steps, and 66% of the sorbed o-xylene being released after about 12 sequential desorption steps.



**Table 6. 5. Summary of results from batch sequential desorption experiments**

<b>Naphthalene</b>										
<b>Adsorbent</b>	<b>L:S<sup>a</sup></b>	<b>% LOI</b>	<b>C<sub>input</sub><sup>b</sup> (mg/L)</b>	<b>T<sup>c</sup> (h)</b>	<b>q<sub>adsorbed</sub><sup>d</sup> (mg/kg)</b>	<b>SD (±)</b>	<b># steps<sup>e</sup></b>	<b>q<sub>desorbed</sub><sup>f</sup> (mg/kg)</b>	<b>SD (±)</b>	<b>% desorbed</b>
Sand	120:1	0.2	10.2	48	68	1.43	3	67.9	0.97	100
Morgantown	120:1	3.1	10.2	48	256.4	3.3	13	231.7	2.31	95
Paul Smith	120:1	10.7	10.2	48	696.9	6.98	19	663.8	11.7	96
Dickerson Precipitator	120:1	20.5	10.2	48	1084.6	5.9	21	653.1	6.32	55
PAC	600:1	99	10.2	48	49786.7	11.9	21	14318	4.21	29
<b>O-xylene</b>										
<b>Adsorbent</b>	<b>L:S<sup>a</sup></b>	<b>% LOI</b>	<b>C<sub>input</sub><sup>b</sup> (mg/L)</b>	<b>T<sup>c</sup> (h)</b>	<b>q<sub>adsorbed</sub><sup>d</sup> (mg/kg)</b>	<b>SD (±)</b>	<b># steps<sup>e</sup></b>	<b>q<sub>desorbed</sub><sup>f</sup> (mg/kg)</b>	<b>SD (±)</b>	<b>% desorbed</b>
Sand	120:1	0.2	40.1	48	349.04	4.11	3	349.3	3.9	100
Morgantown	120:1	3.1	40.1	48	1095.2	9.8	9	544.8	11.24	45
Paul Smith	120:1	10.7	40.1	48	1416.2	13.1	11	985.3	14.7	64
Dickerson Precipitator	120:1	20.5	40.1	48	2275	4.67	12	1563.4	12.65	64
PAC	600:1	99	40.1	48	106882	18.45	12	69849	21.31	66

<sup>a</sup> liquid-to-solid ratio used in batch experiments, <sup>b</sup> initial concentration in the adsorption batch experiments, <sup>c</sup> equilibrium time employed in sorption experiments, <sup>d,f</sup> mg of organic compound adsorbed/desorbed per g of sorbent, <sup>e</sup> number of sequential desorption steps

The cumulative percentage of the solutes desorbed plotted against each desorption step in Figure 6.5 supports these findings. Nevertheless, care must be taken in interpreting these figures based on percentages desorbed. For example, each fly ash provides different sorption capacities for each organic compound, and different initial concentration have been used for the two organic compounds in the sorption step. So, even though in terms of percentage in the case of Dickerson Precipitator a higher percentage of o-xylene is released than naphthalene for a given number of desorption steps, in terms of  $q_{\text{remained adsorbed}}$  at the end of desorption test we can see that more organic contaminants remains adsorbed per unit mass of solid with increasing of the carbon content of the fly ash. The desorption isotherms are plotted for the two organic contaminants in Figure 6.6 following the approach undertaken by Sato and Comerford (2006) in a study on desorption of phosphorus from contaminated soils. Freundlich and Langmuir isotherm models are used to describe the naphthalene and o-xylene desorption from Maryland fly ashes. The parameters for desorption isotherms are given in Table 6.7. A comparison of Figures 6.3 and 6.6 as well as Tables 6.5 and 6.6 indicates that the adsorption and desorption curves and parameters are highly different, i.e., there is hysteretic behavior.

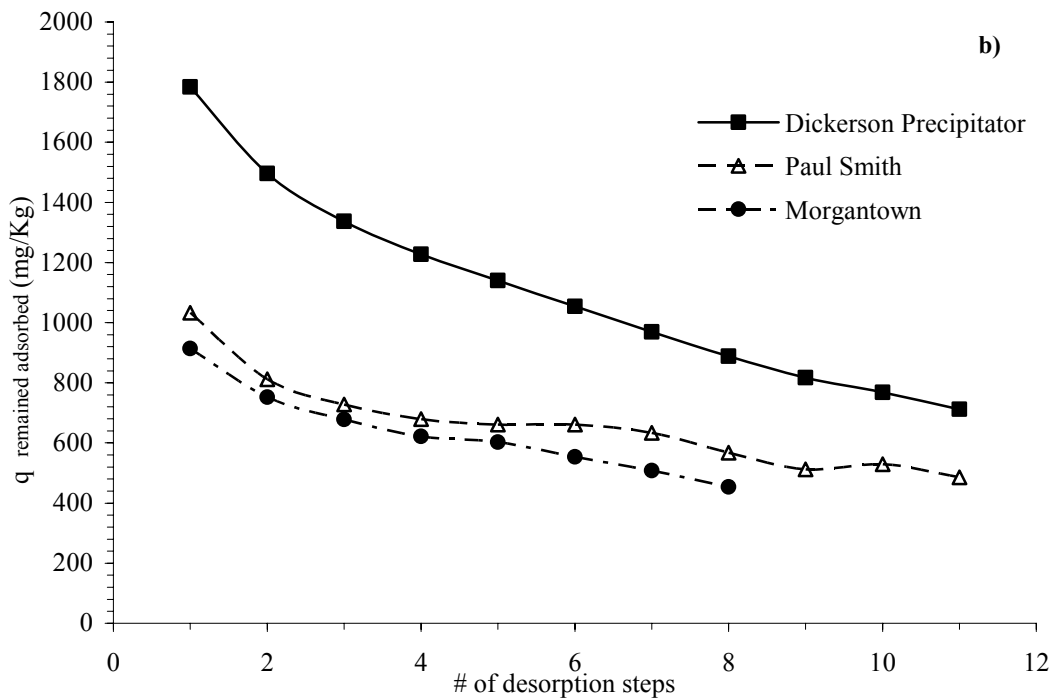
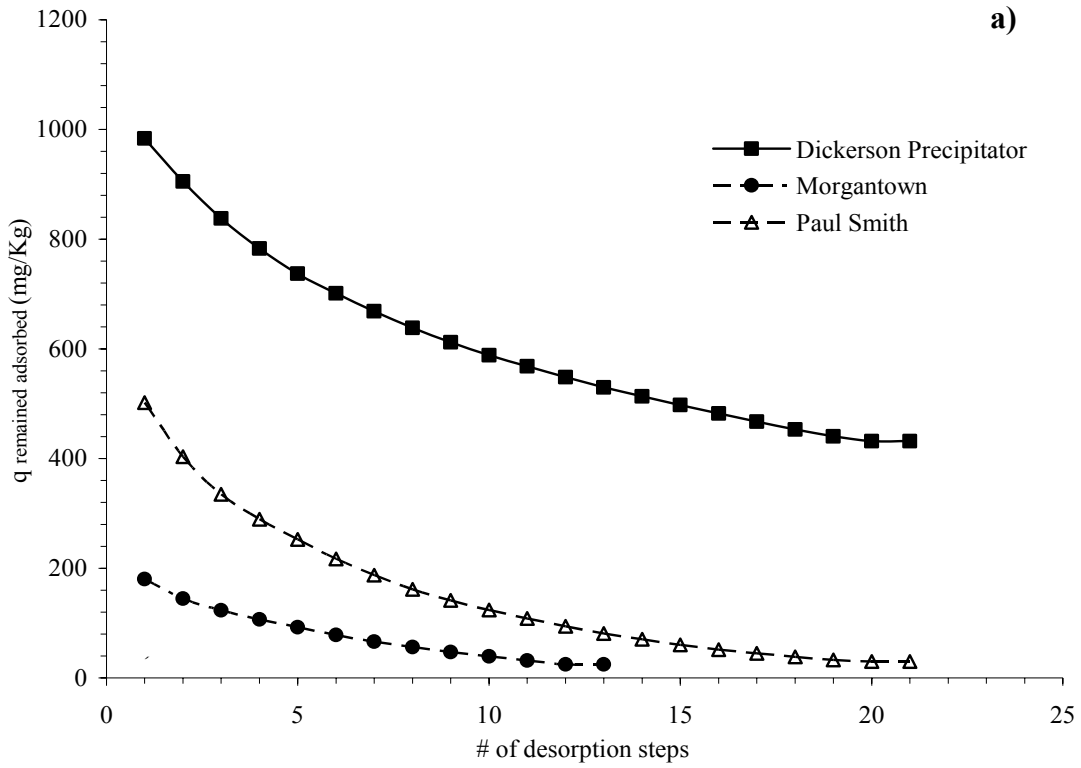
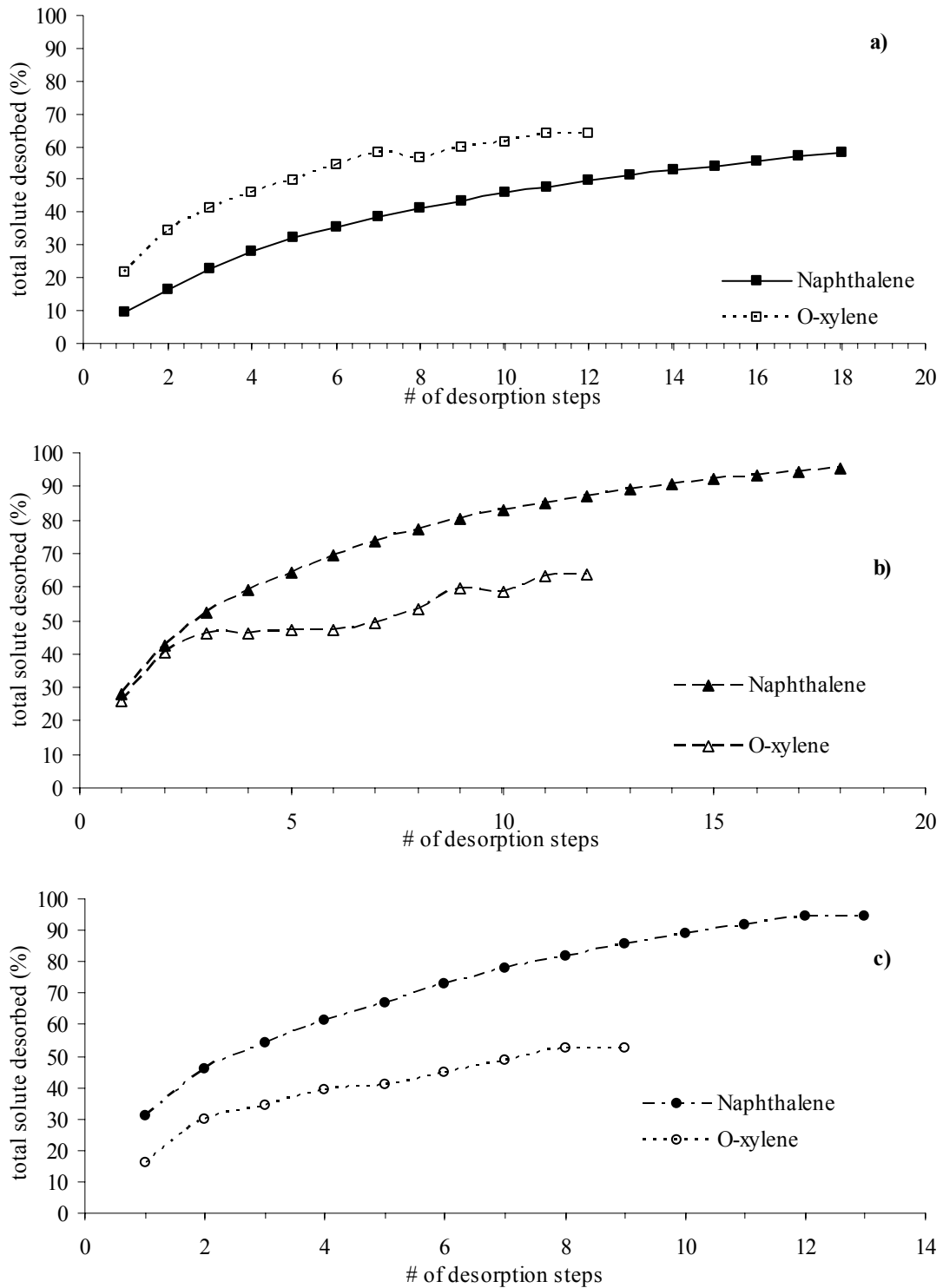
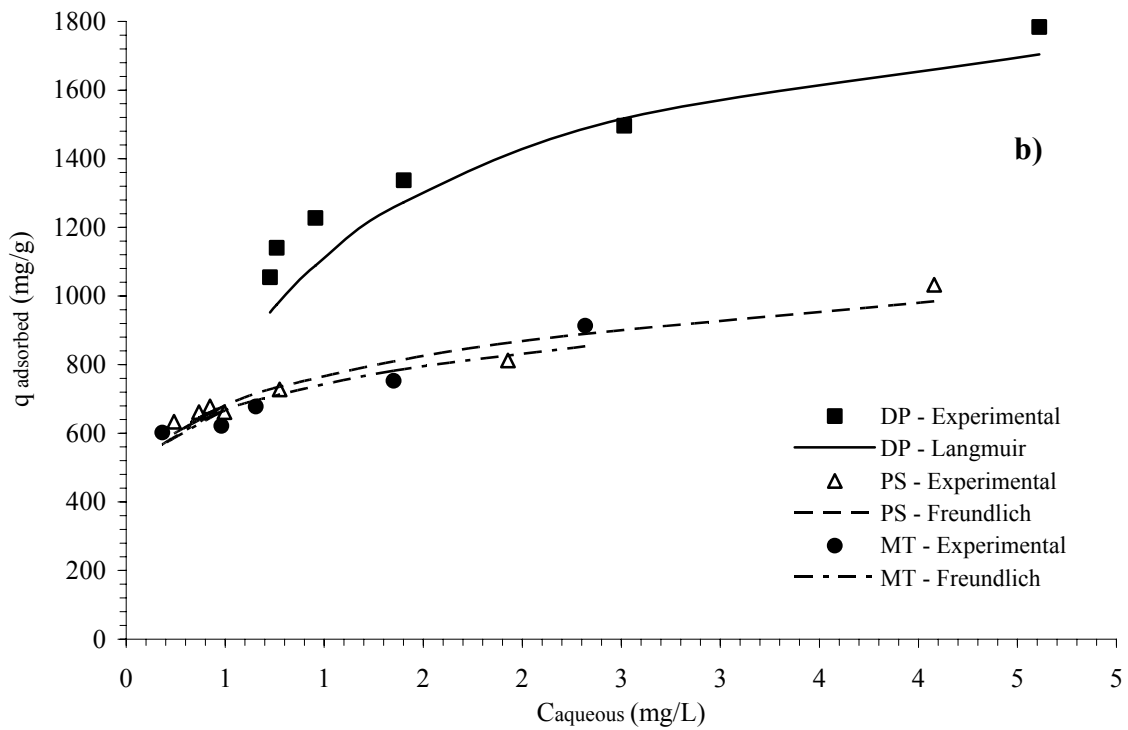
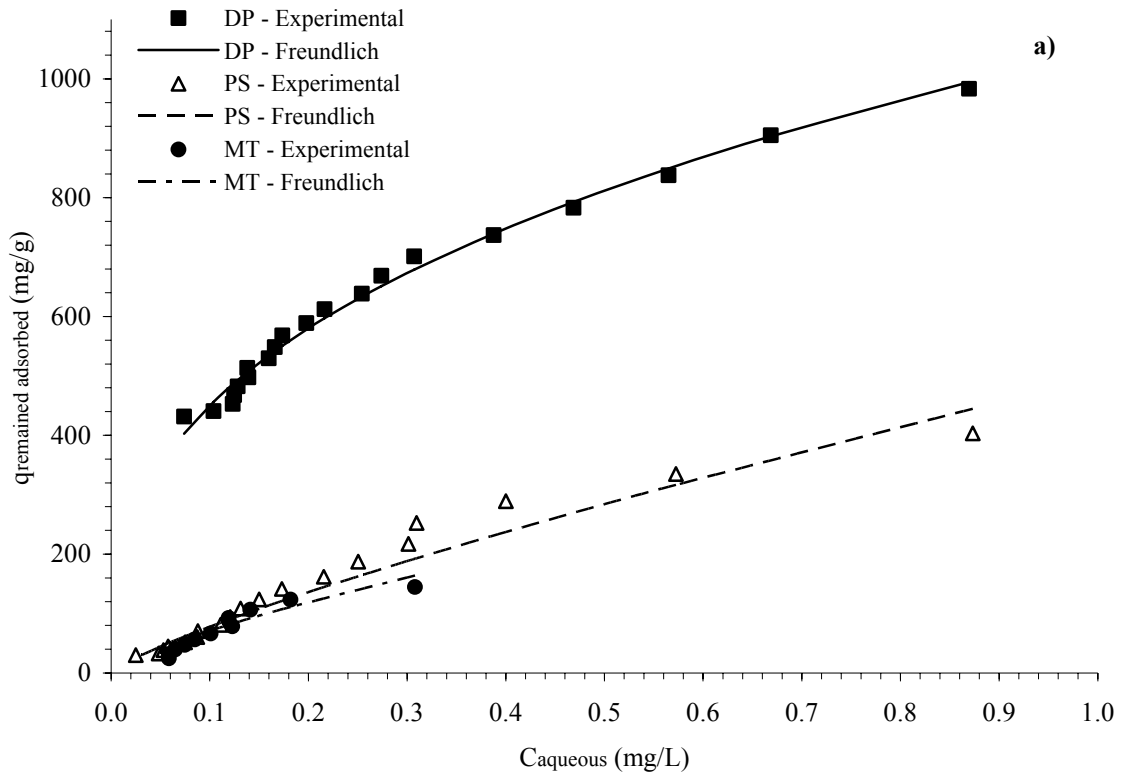


Figure 6. 4. Change in solid phase concentration of a) naphthalene and b) o-xylene after each desorption step. Each data point represents the average value of the five replicates.



**Figure 6. 5. Total solute desorbed from successive desorption steps from a) Dickerson Precipitator; b) Paul Smith; c) Morgantown fly ashes. Each data point represents the average value of the five replicates.**



**Figure 6. 6. Desorption isotherms with best fit models after a) naphthalene and b) o-xylene sequential desorption experiments with Dickerson Precipitator, Paul Smith and Morgantown fly ash.**

**Table 6. 6. Desorption isotherm parameters from batch sequential desorption tests**

Fly ash	Naphthalene		<i>O</i> -xylene	
Morgantown	$K_F$ (L/kg) <sup>a</sup>	92.5	$K_F$ (L/kg) <sup>a</sup>	17.58
	$n^a$	0.74	$n^a$	0.89
Paul Smith	$K_F$ (L/kg) <sup>a</sup>	496	$K_F$ (L/kg) <sup>a</sup>	770
	$n^a$	0.803	$n^a$	0.176
Dickerson Precipitator	$K_F$ (L/kg) <sup>a</sup>	1047 0	$K_L$ (L/kg) <sup>a</sup>	1.25
	$n^a$	0.367	$Q_{max}$ (mg/kg) <sup>b</sup>	2000

<sup>a</sup> Freundlich Isotherm: ( $q_i = K_F [C_f]^n$ )  $K_F$  = Freundlich equilibrium isotherm constant (L/kg),  
 $n$  = dimensionless empirical,  $C_f$  = final concentration of naphthalene (mg/L).

<sup>b</sup> Langmuir Isotherm: ( $q_i = (Q_{max} K_L C_f) / (1 + K_L C_f)$ )  $K_L$  = Langmuir isotherm coefficient (L/kg)  
 $Q_{max}$  = sorption capacity of particular solid (mg/kg).

Several conceptual explanations have been proposed in literature for the occurrence of hysteretic behavior of organic pollutants with respect to sorption and desorption, such as observed in this study. Kan et al. (1998) proposed existence of double compartment in which sorption/desorption processes take place: one “labile desorption compartment” from which the organic molecule can be easily released, and one “entrapped and irreversible compartment” in which the adsorbed molecules are hindered by the sorbent organic matrices due to some distortions, alterations and rearrangements that take place in the organic structure of the adsorbent. They have concluded that desorption process occur in a molecular environment which is dissimilar to the environment in which the adsorption process occurs. During the sorption equilibrium period, the pressure exerted by solute molecules during their penetration into the micropores could cause the expansion of the pores beyond their elasticity limits (an irreversible deformation of the pores), and some pore openings which were accessible in the sorption process may become blocked during desorption. This will leave some solute molecules sequestered inside the pores, and make them resistant to desorption (Cheng et al. 2004).

Irreversible pore deformation and physicochemical rearrangement in sorbent matrices upon adsorption have been also proposed by Yang and Xing (2007). In the process summarized in Figure 6.7, Yang and Xing (2007) proposed that small particles (aggregates) may undergo some rearrangements to create new interstitial spaces available for adsorption, and close some opened ones that entrap the sorbed molecules and prevent them from desorption. Rathousky and Zukal (2000) suggested that the infiltration pressure of sorbate molecules can produce the expanding and/or

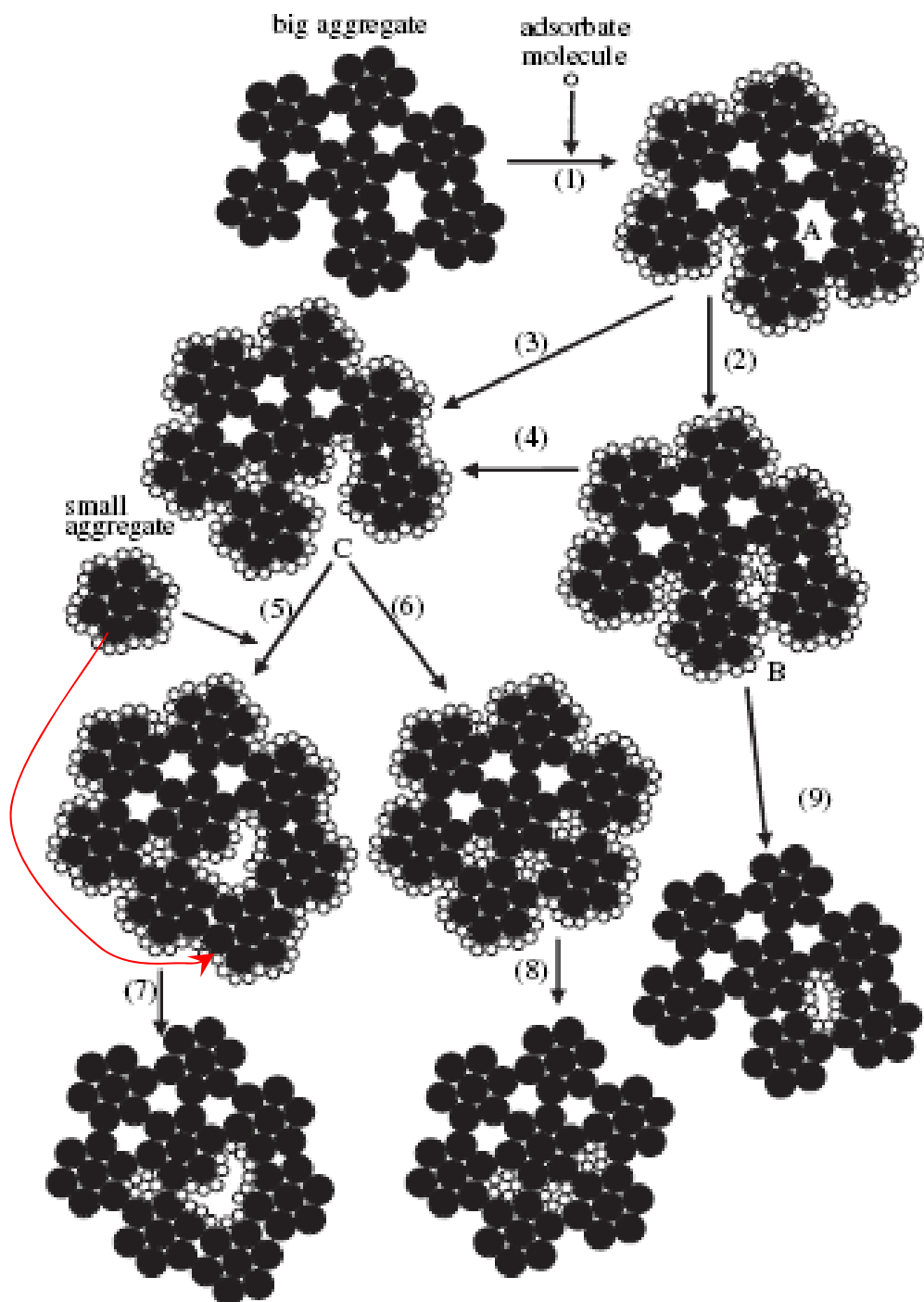


Figure 6. 7. Adsorption - desorption scheme of organic compounds on solid sorbents. (1) adsorption, (2) penetration into space A, (3) rearrangement leading to opening of space A, (4) deformation at site B leading to opening of space A, (5) rearrangement at site C by combining with another small aggregate, (6), (7), (8), and (9) desorption and entrapment of organic molecules in the closed interstitial spaces. (Yang and Xing, 2007)



opening of some of the isolated interstitial voids between small particles and make them available for sorption. In the desorption step, the molecules loosely adsorbed on the surface will desorb primarily in the percolating solution, followed by the sorbed molecules in the opened pores. This process will leave the sequestered molecules sorbed into the pores that are closed due to structural rearrangements. This last fraction is, therefore, irreversibly sorbed and this results in hysteresis.

In another study Kan et al. (2000) proposed that several organic compounds may form complexes with the organic colloids, and that the adsorbate molecule can then be masked by the complex and may not desorb. They introduced a constrictivity factor to explain the limited diffusion of the irreversibly sequestered sorbate fraction. The factor is related to a decrease in the pore size due to adsorption of the molecule, and the decrease causes a multipoint interaction between the molecule and pore walls and restricts the diffusion of the molecule into the desorbing solution.

## **6.2. COLUMN ADSORPTION/DESORPTION TESTS**

Batch tests are considered to represent the “worst case” scenario, and provide a rapid, approximate estimation of the extent of desorption of organic contaminants. However, the sequential desorption batch procedure does not fully simulate the actual site leaching conditions, such as would occur with fly ash-amended permeable reactive barriers. Therefore, flow-through column tests are generally conducted to offer a more realistic insight into the field behavior, provided that the test conditions more closely mimic the real environmental conditions. Accordingly, column adsorption/desorption tests were conducted with the two organic compounds and

three fly ashes, following the procedures described in Sections 3.2.2 and 3.4.2. PAC, and silica sand were also employed as reference materials in testing.

Prior to running desorption experiments, adsorption tests were conducted on all the column specimens until the saturation stage was reached (experiments performed by M Demirkan, 2008). Saturation was defined as being achieved when the influent and effluent concentrations were equal. Subsequently, the desorption experiments were run, during which samples were extracted from the effluent ports of all columns, as well as from the ports along the height of selected columns (Figure 3.4). The experimental conditions for the column tests are summarized in Tables 4.1 and 4.2. A total of 9 column desorption tests were conducted to provide insight into the desorption process and allow for estimation of the reversibly sorbed fraction of organic compounds to selected fly ashes. The column sorption/desorption test results are summarized in Table 6.7 and described more in detail in the following subsections.

### **6.2.1. Column Adsorption Test Results**

The results of the adsorption tests conducted on the two reference materials were as expected. The silica sand exhibited very little adsorption, while the PAC mixed with the sand had a large sorption capacity for the organic contaminants as evidenced by the large number of pore volumes of flow to reach saturation. Of the three fly ashes employed in the experiments, the Dickerson Precipitator required the largest number of pore volumes of flow (PVFs) to reach saturation (214 PVFs for naphthalene and 43 PVFs for o-xylene), followed by Paul Smith (with 81 PVFs for naphthalene and 23

PVFs for o-xylene), and Morgantown fly ashes (with 34 PVFs for naphthalene and 6.2 PVFs for o-xylene). These findings along with the  $q_{\text{adsorbed}}$  values provided in Table 6.7 suggest that the Dickerson Precipitator fly ash has the highest adsorption capacity for both organic compounds. All of the fly ashes required a greater number of pore volumes to reach saturation with naphthalene than with o-xylene, indicating a slower adsorption rate for naphthalene.

As previously mentioned, the properties of an organic compound will affect its adsorption behavior onto a sorbent, and the physicochemical properties of naphthalene and o-xylene listed in Table 6.4 can be used to help interpret the results of the column adsorption tests. Kodadoust et al. (2005) observed longer adsorption equilibrium times for compounds with lower solubility. They also determined strong correlations between the degree of adsorption and the boiling point of organic compounds. Similarly, Pignatello and Xing (1996) reported that there are two reasons for slower adsorption of larger aromatic compounds: greater activation energy necessary for sorption, and increased mass transfer limitations due to bigger volume and mass. The molecular weight and molar volume of naphthalene are greater compared to o-xylene due to its relatively larger size and, thus, mass transfer limitations are expected to be greater, consistent with the slower rate of adsorption observed. It is speculated that o-xylene may have had easier access to reach sorption sites by penetrating deeper into the micropores of the solid matrices due to its smaller molecule size. Finally, the higher boiling point for naphthalene than o-xylene (218 °C versus 144.5 °C), which indicates that greater activation energies are required for sorption of naphthalene, and the low aqueous solubility and high octanol-

**Table 6. 7 Summary of column adsorption/desorption test results**

<b>Naphthalene</b>								
Column specimen	%	Adsorption phase			Desorption phase			
		LOI	C <sub>input</sub> <sup>b</sup> (mg/L)	PV <sup>c</sup> -sorption	q <sub>adsorbed</sub> <sup>e</sup> (mg/kg)	PV <sup>d</sup> - desorption	q <sub>desorbed</sub> <sup>f</sup> (mg/kg)	% desorbed
100% Sand	0.2	5	1.9	1.7	2.3	1.4	83	1.2
40%Motgantou + 60% Sand <sup>a</sup>	3.1	9.4	34	105.2	27	35.21	33	11
40%Paul Smith + 60% Sand	10.7	9.6	81	522.8	60	247.1	47	50
40%Dickerson Precipitator + 60% Sand	20.5	8.9	214	1410.1	273	648.5	46	117
2%PAC + 98% Sand	99	9.5	327	25920.7	204	8260.1	32	138
<b>O-Xylene</b>								
Column specimen	%	Adsorption phase			Desorption phase			
		LOI	C <sub>input</sub> <sup>b</sup> (mg/L)	PV <sup>c</sup> -sorption	q <sub>adsorbed</sub> <sup>e</sup> (mg/kg)	PV <sup>d</sup> - desorption	q <sub>desorbed</sub> <sup>f</sup> (mg/kg)	% desorbed
100% Sand	0.2	NA	NA	NA	NA	NA	NA	NA
40%Motgantou + 60% Sand	3.1	34.9	6.2	189.32	21.31	147.3	78	5
40%Paul Smith + 60% Sand	10.7	35.5	23	992.8	148.6	888.2	89	19
40%Dickerson Precipitator + 60% Sand	20.5	30.3	43	1834.3	175.1	1404.7	76	32
2%PAC + 98% Sand	99	38.9	95	29860.1	175.7	13270.1	44	59

**Note:** <sup>a</sup> sand % used for mixture in the column specimen, <sup>b</sup> average input concentration in the column experiments, <sup>d</sup> pore volumes of flow in the sorption/desorption column experiments, <sup>e, f</sup> mg of organic compound adsorbed/desorbed per g of fly ash, and <sup>g</sup> pore volume of flow at 80% of the solute is desorbed. NA: Not analyze

water partition coefficient of naphthalene are all consistent with slower adsorption of naphthalene than o-xylene.

### **6.2.2 Column Desorption Test Results**

Similar to the batch tests, adsorption/desorption hysteresis was also observed for the column tests. As seen in Table 6.7, about 33 to 47% of the naphthalene originally adsorbed onto the fly ashes was desorbed, whereas the desorbed percentage ranged from 76 to 89% for o-xylene, based on measurements conducted at the effluent port. Thus, the adsorption/desorption process was not completely reversible during the experimental periods, which is attributed to the existence of resistance to desorption and the occurrence of slowly desorbing fractions as observed by previous researchers (Di Toro et al. 1982, Karickhoff and Morris 1985, Pignatello and Xing 1996, Kan et al. 1998, Cheng et al. 2004, Yang and Xing 2007)..

Fewer or similar pore volumes of flow were necessary for removal of rapidly desorbing desorption of naphthalene than for saturation adsorption. This may be explained by the fact that the readily desorbable naphthalene molecules were adsorbed by weak van der Waals forces in larger micropores, and as soon as the reversibly adsorbed fraction was desorbed, the concentrations dropped to levels below the detection limit of the spectrophotometric method. On the other hand, more pore volumes of flow were required for desorption of readily desorbable o-xylene than for saturation adsorption. This is attributed to the smaller molecule size of o-xylene, which may allow it to more easily penetrate deeper into the micropores of the solid matrices, thereby delaying the diffusion back into the desorbing solution.

To compare the desorption of naphthalene and o-xylene for all the three fly ashes, we examined the pore volumes of flow that were required to reach the 80% desorption level. Karickhoff and Morris (1985) and Connaughton et al. (1993) suggested the use of the pore volumes at about the 80% desorption for analysis of desorption as their findings showed that desorption for the remaining 20% can be “slowly reversible”. In this work, the number of pore volumes required to reach 80% desorption was greater for naphthalene than for o-xylene for all three fly ashes. This is attributed to the larger molecule size, higher hydrophobicity and lower solubility of naphthalene compared to o-xylene and correspondingly stronger sorption to the sorbent matrix. Similar observations were made by Badr et al. (2004) in a study of naphthalene and phenanthrene adsorption/desorption onto/from soils. Their results indicated that phenanthrene strongly adsorbed onto soil particles and desorbed at lower rates due to its relatively higher hydrophobicity and larger molecule size, leading to slower desorption rates as compared to naphthalene.

Figures 6.8 through 6.11 show the elution curves for the two organics from the fly ash columns and the PAC column, and Figure 6.12 provides the elution curve for the naphthalene from the sand column. A comparison of the data indicates that the elution curves shift towards right with increasing LOI, reflecting the higher pore volumes required for complete adsorption with greater sorption. This effect is more clearly visible when the data from the effluent ports are plotted against pore volumes of flow in Figure 6.13. The rate of sorption is reflected by the slopes of the adsorption curves, which decrease with increasing LOI of the sorbent and greater sorption. As expected, the PAC exhibits very good adsorption characteristics even

though only 2% by mass of the reactive medium was composed of PAC as compared to 40% by mass fly ash in the other columns. In comparison, the sand column suggests advective-dispersive flow behavior, and very little adsorption with the slope of the adsorption curve primarily due to dispersion.

The order of appearance of the breakthrough measured at the ports follows the port locations. For instance, breakthrough was reached at relatively fewer pore volumes at port 1 as compared to the other ports. There is a noticeable difference between the curves for ports 1 and 2 and ports 2 and 3 due to presence of fly ash, and the data recorded at port 3 are very close to the ones registered by the effluent port.

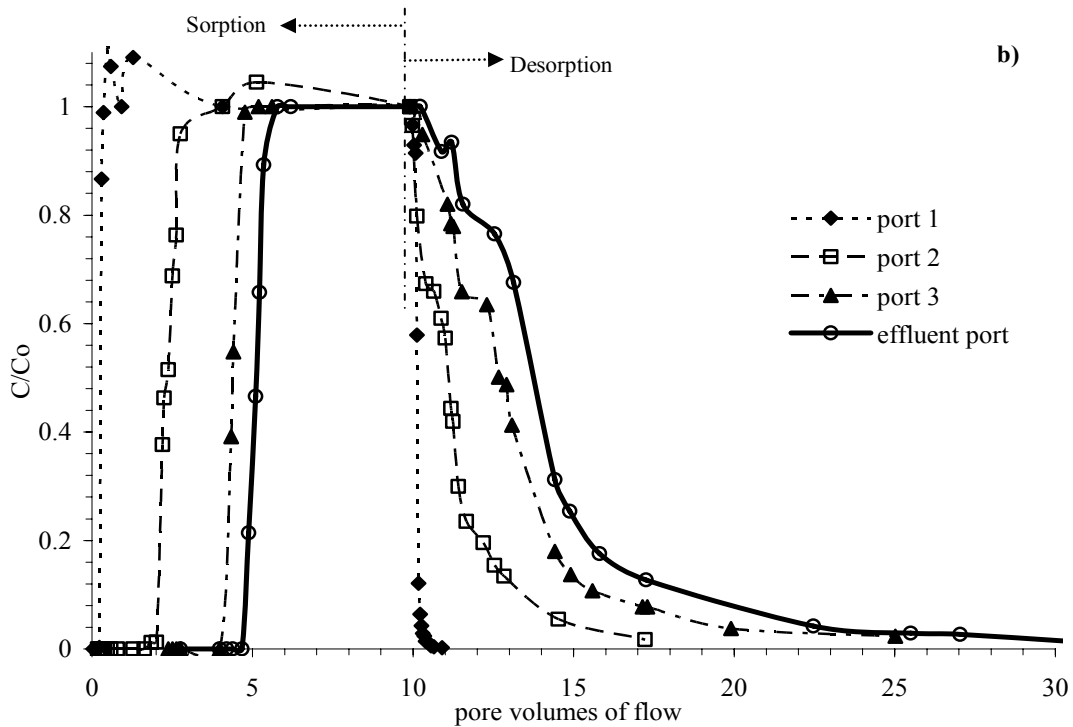
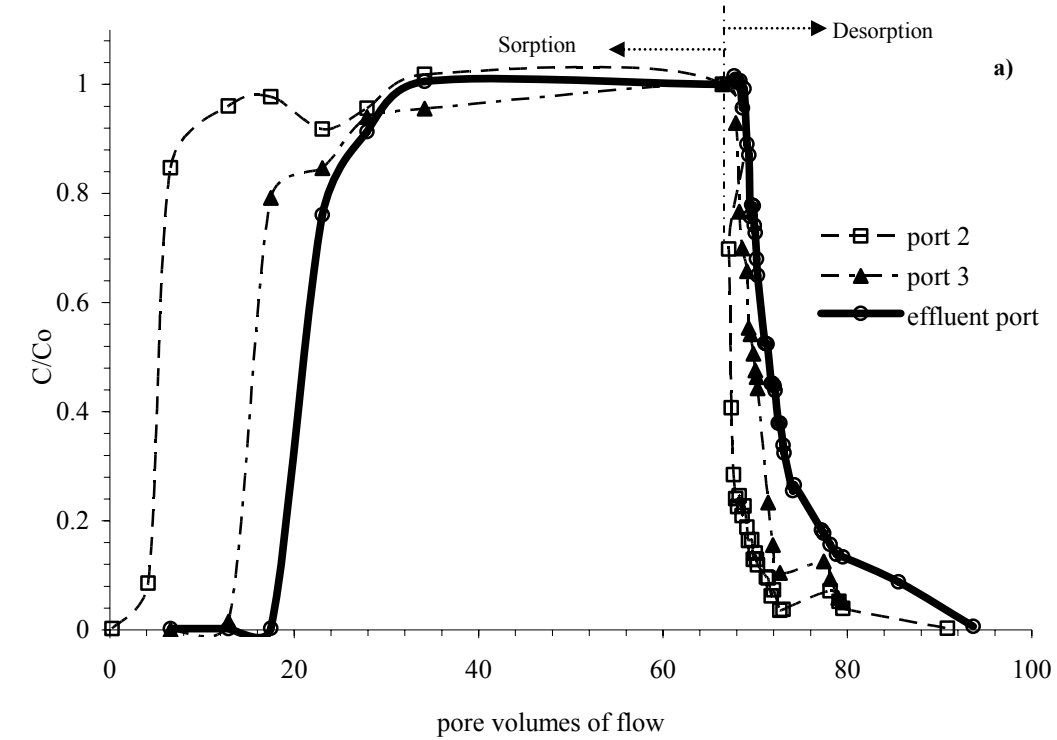


Figure 6. 8. Sorption-desorption elution curves for a) naphthalene, and b) o-xylene from the 40% Morgantown fly ash + 60% sand column. Each data point represents a single measurement.



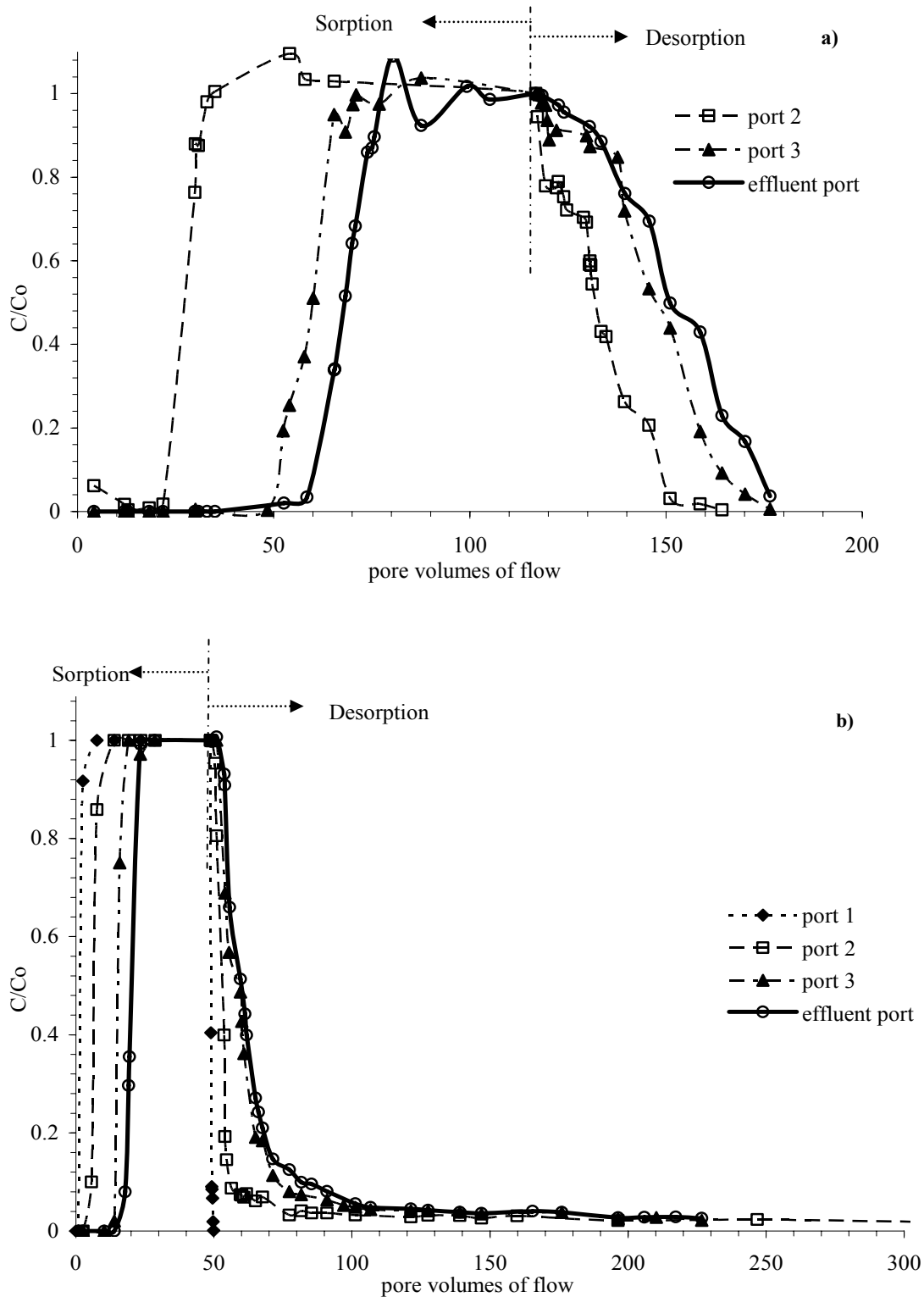


Figure 6. 9 Sorption-desorption elution curves for of a) naphthalene, and b) o-xylene from the 40% Paul Smith fly ash + 60% sand column. Each data point represents a single measurement.

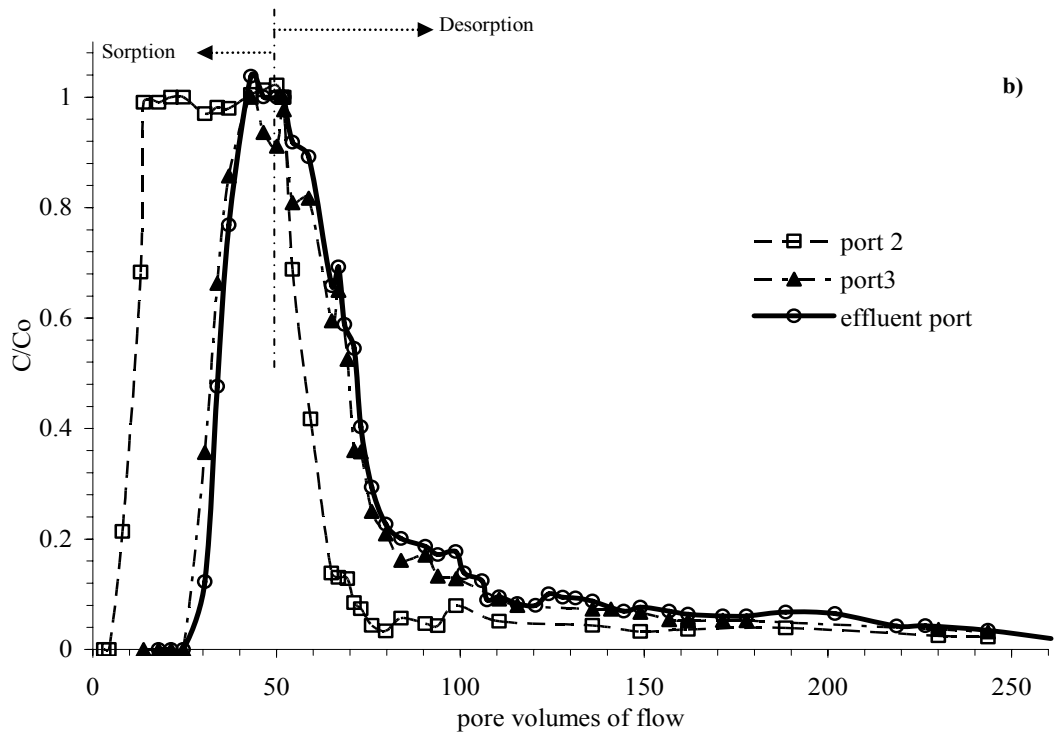
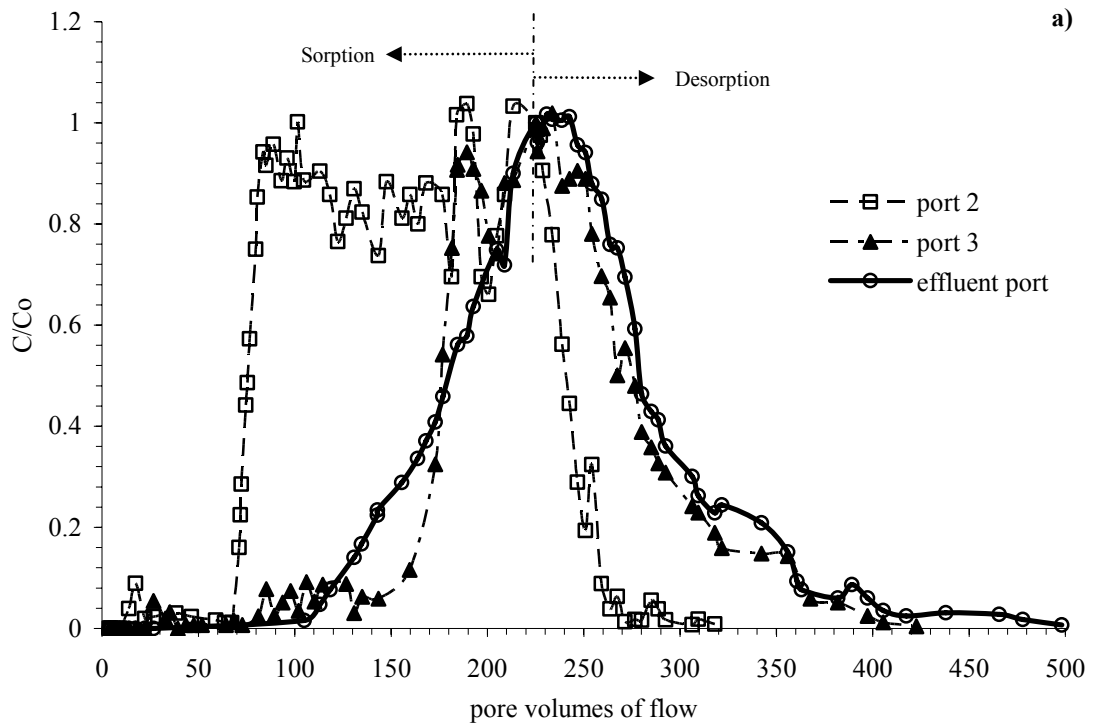


Figure 6. 10. Sorption-desorption elution curves for of a) naphthalene, and b) o-xylene from the 40% Dickerson Precipitator fly ash + 60% sand column. Each data point represents a single measurement.

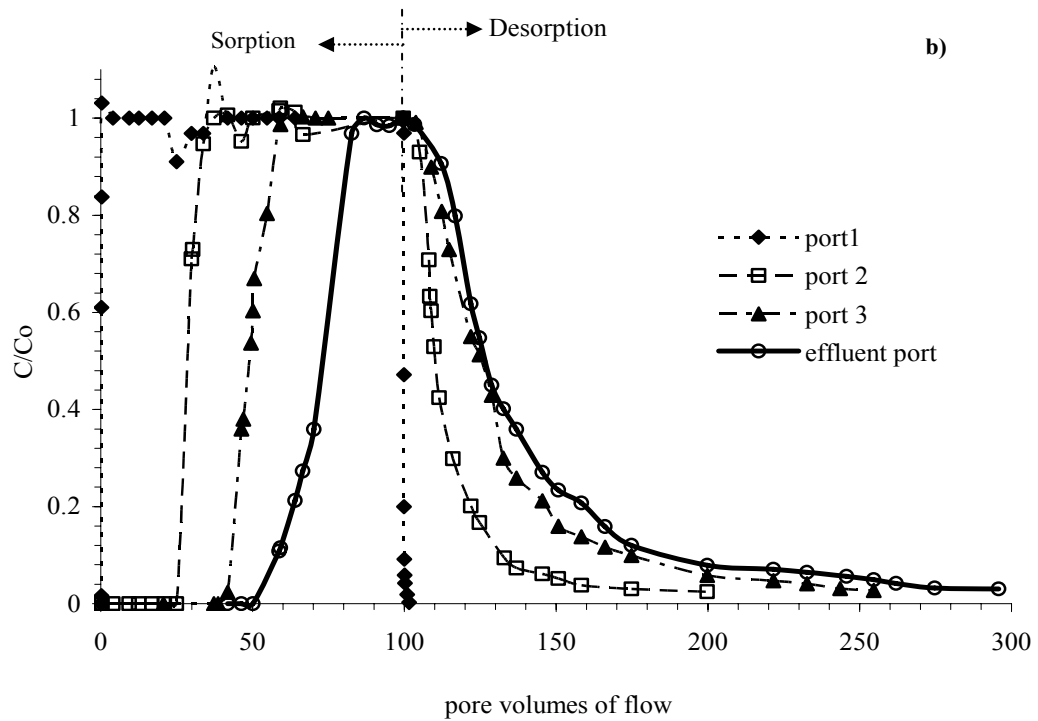
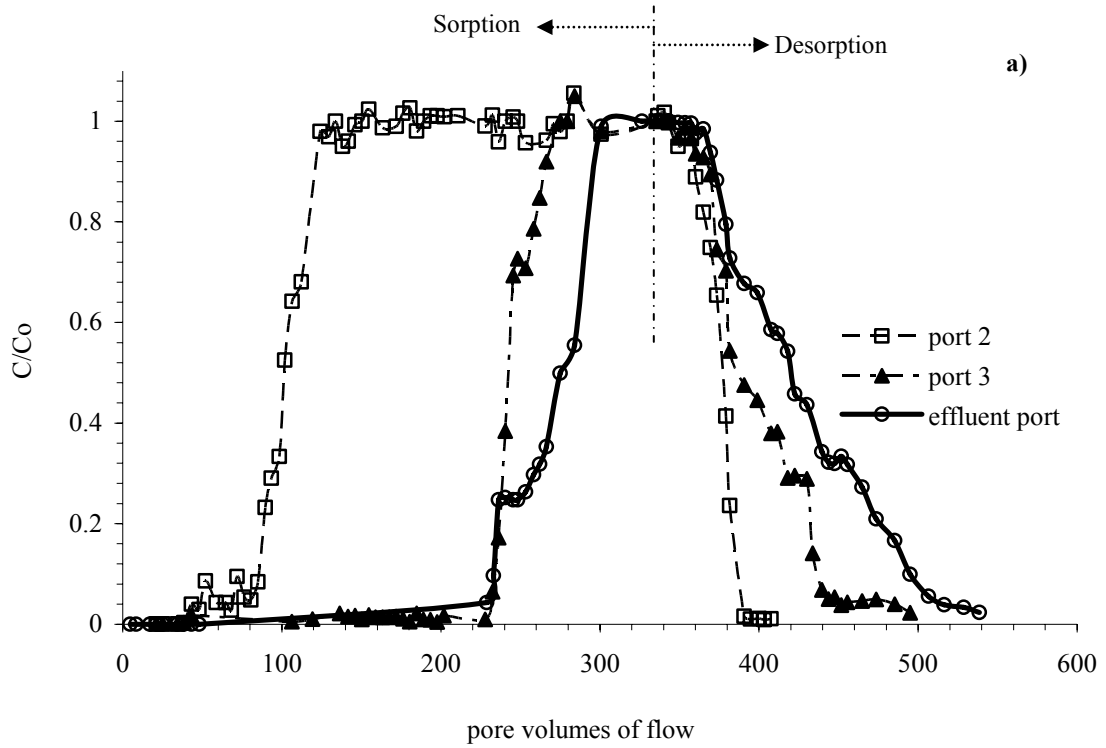


Figure 6. 11. Sorption-desorption elution curves for of a) naphthalene, and b) o-xylene from the 2% PAC fly ash + 98% sand column. Each data point represents a single measurement.

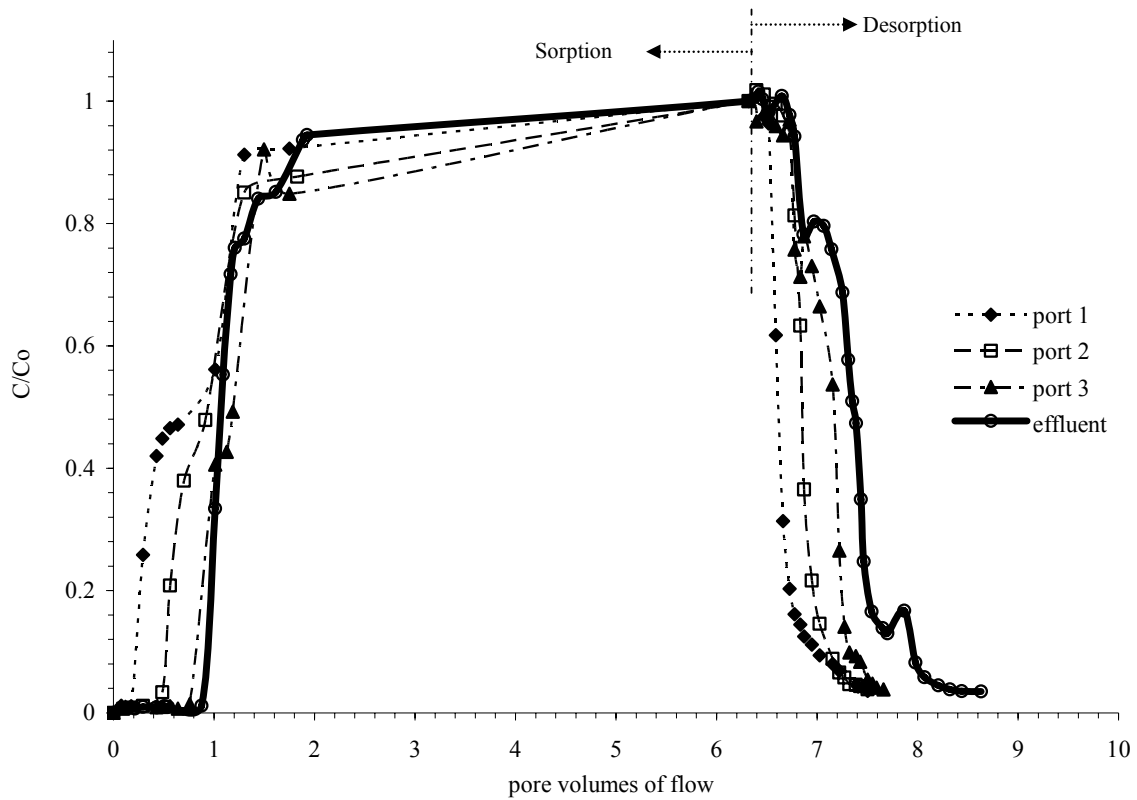


Figure 6. 12. Sorption-desorption elution curves for naphthalene from the sand column. Each data point represents a single measurement.

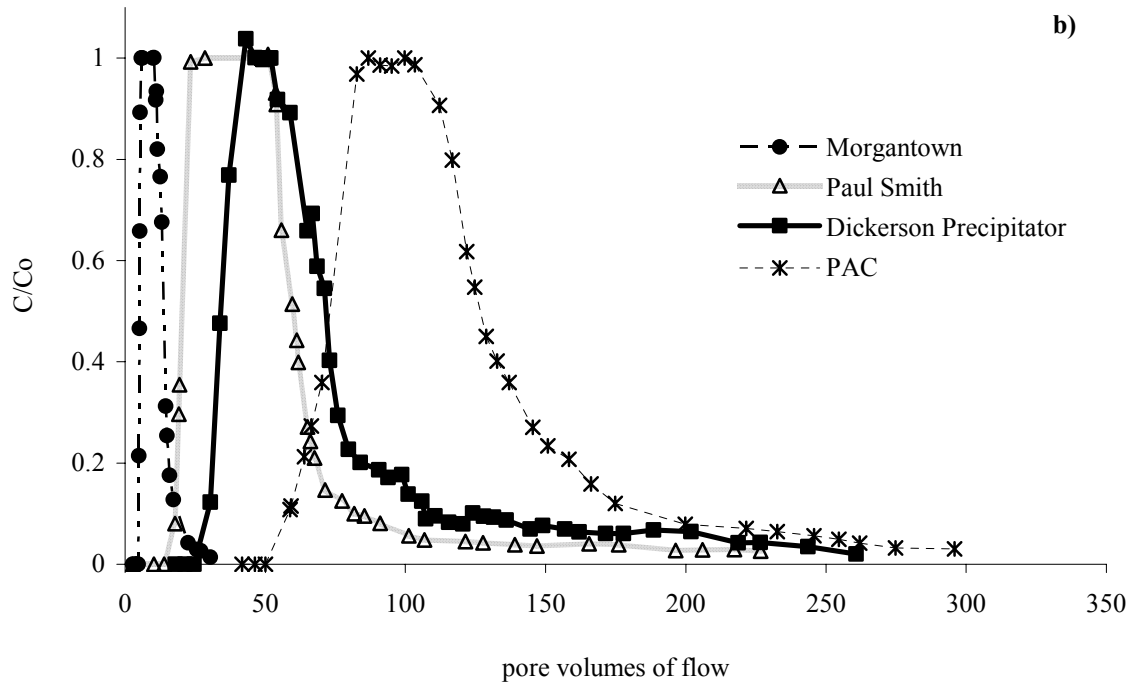
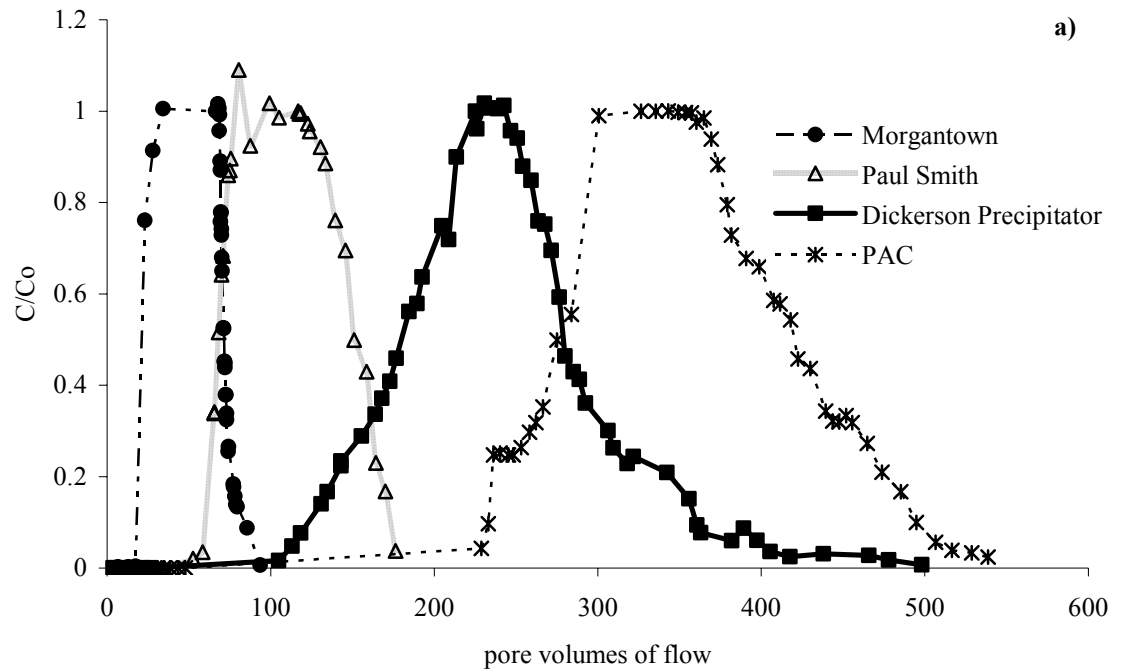


Figure 6. 13. Effluent concentrations for a) naphthalene, and b) o-xylene from the fly ash and PAC columns. Each data point represents a single measurement.

The elution curves also indicate that desorption rate is correlated with the LOI of the sorbents. This relationship was more clearly pronounced if the pore volumes at 80% desorption ( $PV_{80}$ ) are considered. As mentioned above, the use of  $PV_{80}$  can be helpful for evaluating desorption because the remaining 20% is generally “slowly reversible”. In this work, the  $PV_{80}$  values clearly increase as the LOI of the fly ash increases, indicating a slower desorption rate with increasing LOI. In addition, Karickhoff and Morris (1985), who studied the long-term desorption of hydrophobic organic compounds, reported that the final portion of the sorbed organic demonstrated a tendency to “bleed” very slowly, as evidenced by the “tailing” of the solute elution curve. Harmon and Roberts (1994) in their study of the desorption of PCE from aquifer sediment, also found that the tail ends of the desorption elution curves tended to flatten out, suggesting that about 20% of the sorbate desorbed at a much slower rate. A similar flattening of the tail end of the desorption elution curves can be observed in Figures 6.8. to 6.11. The “tailing effect” is more clearly visible for the o-xylene curves most probably due to its smaller molecule size and difficulty in its diffusion back into the desorbing solution.

The results also indicate that a much larger fraction of the organics was “irreversibly” retained, or at least very slowly desorbable, in the sorbents with higher LOI. For instance, only 0.3 mg of naphthalene were retained per gram of sand. In comparison, approximately 0.76 mg naphthalene and 0.43 mg o-xylene were retained per gram of Dickerson Precipitator fly ash (LOI = 20.5%), whereas the amounts were 0.27 mg naphthalene and 0.104 mg o-xylene, and 0.07 mg naphthalene 0.042 mg o-xylene per gram of Paul Smith (LOI=10.7%) and Morgantown fly ashes (LOI=3.1%),

respectively. Due to its high carbon content (LOI=99%), the PAC released the smallest amount of the two contaminants, and 17.7 mg naphthalene and 16.6 mg o-xylene were retained per gram of PAC.

### **6.3. COMPARISON OF RESULTS FROM BATCH AND COLUMN TESTS**

Several conclusions can be drawn by comparing the data presented in Tables 6.5 and 6.7. First, higher adsorption capacities were observed in the batch experiments, as compared to the column experiments. There may be several reasons for this observed behavior. First, the contact between the solute and sorbent surface is enhanced in case of batch experiments, due to agitation during equilibrium. This significantly increases the adsorption potential, i.e., the solute has more potential to reach all the available sorption sites on the surface of the sorbent. In the columns, on the other hand, there is very little mixing (only what occurs due to dispersion) and the fly ash particles are only in contact with the solute as the eluant solution slowly percolates through the porous media with the groundwater flow. As a result of these solute transport limitations, longer equilibrium times are required to reach saturation during the column tests.

The second important difference between the two tests is the solid-to-liquid ratio. While the sorbent is in contact with a large volume of solute solution in the batch adsorption tests, several pore volumes of flow are necessary to reach the same L:S ratios in the column experiments. Typically, lower liquid to solid ratios are associated with reduced partitioning into the solid phase (Headley, et al. 2001).

This is consistent with the findings of M. Demircan (2008) who modeled the sorption-desorption column experiments data. His results, shown in Table 6.7, indicate lower partition coefficients for both organics in the case of column experiments than the ones obtained in this work in the case of batch desorption experiments (Table 6.6).

Finally, it was observed that in the case of naphthalene all three column experiments with fly ashes allowed less desorption than was observed in the batch experiments. In other words, more naphthalene was “irreversibly” adsorbed, or at least very slowly desorbable, per gram of column specimen than in the case of batch experiments. This is reasonable, assuming that mass-transfer processes are limited in column experiments, while in the case of batch experiments mass-transfer processes are enhanced by the mixing.

Because the partition coefficient for organics is a function dependent on the organic carbon ( $f_{oc}$ ) in the adsorbing material, a common approach is to determine the correlation between  $K_d$  and  $f_{oc}$  (fraction of organic carbon) which by definition are interrelated through the following relationship:

$$K_d = K_{oc} \cdot f_{oc} \quad (6.5)$$

In Figure 6.14 are presented the obtained  $K_d - f_{oc}$  correlations for the two organic contaminants in the case of batch and column tests. It is very obvious from these graphs that the naphthalene and o-xylene adsorption/desorption on/from the fly ashes is directly correlated with the organic carbon of the fly ash as measured by loss in ignition. The partition coefficient ( $K_d$ ) increases with the increase in carbon content ( $f_{oc}$ ) of the fly ash.



**Table 6. 8. Sorption/Desorption isotherm parameters from column tests  
(M. Demirkan, 2008)**

<b>Column specimen</b>	<b><math>K_f</math></b>	<b>n</b>
40%Morgantown + 60% Sand (naphthalene)	36.5	0.3062
40%Morgantown + 60% Sand (o-xylene)	17.58	0.388
40%Paul Smith + 60% Sand (naphthalene)	190	0.339
40%Paul Smith + 60% Sand (o-xylene)	105.2	0.38
40%Dickerson Precipitator + 60% Sand (naphthalene)	670	0.194
40%Dickerson Precipitator + 60% Sand (o-xylene)	270.4	0.26
2%PAC + 98% Sand (naphthalene)	1050	0.169
2%PAC + 98% Sand (o-xylene)	445.8	0.2

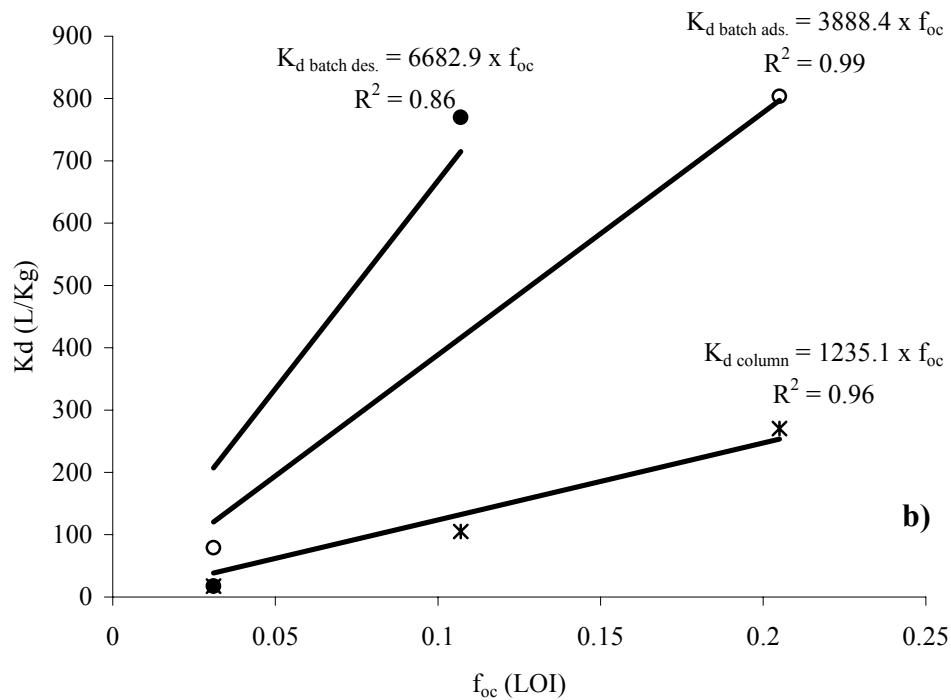
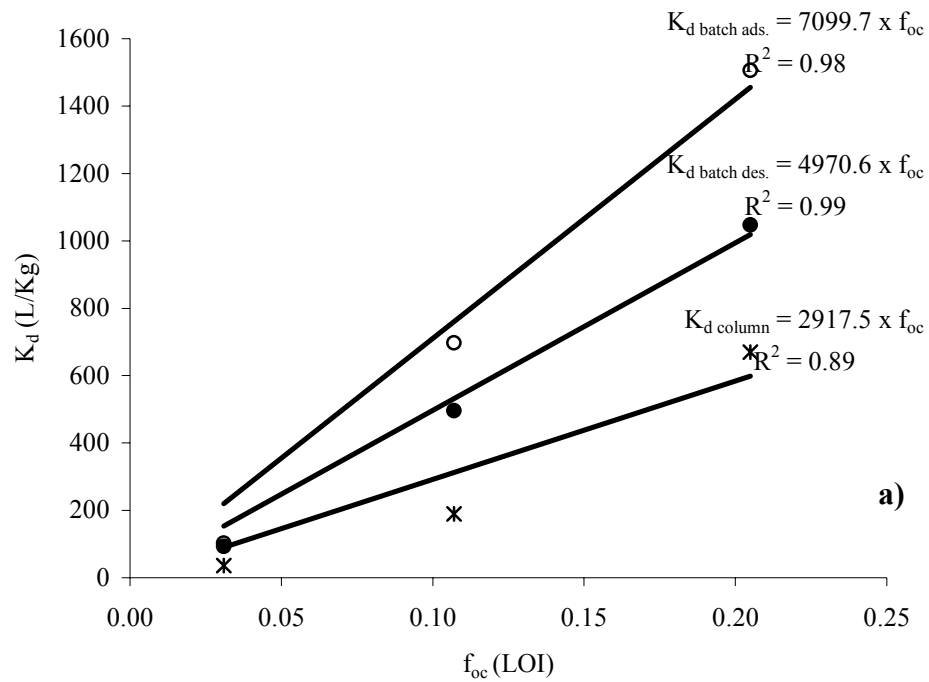


**Figure 6. 14.  $K_d - f_{oc}$  correlations in batch adsorption, desorption and column adsorption/desorption tests with a) naphthalene and b) o-xylene.**

## CHAPTER 7

### CONCLUSIONS AND RECOMMENDATIONS

#### 7.1. SUMMARY AND CONCLUSIONS

Class F fly ash is generated in large quantities in the State of Maryland and it occasionally contains a significant amount of unburned carbon (i.e., high loss on ignition). Recent data indicate that approximately 68% of this high carbon content (HCC) fly ash is placed in landfills, which consumes valuable landfill space and has the potential to impact terrestrial and aquatic resources. Due to common use of low- $\text{NO}_x$  burners in recent years, the amount of high carbon content fly ash produced by power plants in the United States is expected to increase significantly in the near future. A research project was undertaken to study the effectiveness of HCC fly ash as a reactive medium in permeable reactive barriers (PRBs). The key desirable characteristics of the reactive media in a PRB are that it should: have a long lasting and high sorption capacity for organics, maintain continuous high porosity and permeability over its lifetime, not cause adverse chemical reactions, and not act as a potential source of contaminants itself. A series of column and batch tests were performed to evaluate leaching of inorganics from the fly ash, and adsorption/desorption of two selected commonly found petroleum hydrocarbons, naphthalene and o-xylene onto/from this PRB medium. The following conclusions are derived from the study:

1. Relatively higher pH trends were obtained in the batch tests with deionized water suggesting that the pH was completely buffered by the fly ash. The

elevated (slightly basic) initial values for the pH in column experiments (due to the buffering reactions initiated by the dissolution and/or decomposition of the minerals components of the fly ash) stayed fairly constant for the initial PVFs and eventually reached to an equilibrium pH (pH~6.8) in the groundwater within 15-35 PVFs.

2. The metal concentrations increased with increasing fly ash content in the WLTs. The observed increase in concentration of anionic species can be attributed to the increase of available metal species as a result of increasing fly ash amount (as source of metals), the small increases in pH which enhances their solubilization, and to the unavailability of positively charged surface species for complexation at basic pH .
3. Aluminum concentrations in the WLTs with deionized water were about ten folds higher than with artificial groundwater mostly due to the higher pH conditions and to the increase in the solubility of aluminum with increasing pH (above pH 6.5). Relatively faster leaching of aluminum was observed in all CLTs, indicating advection and dissolution of the water soluble aluminum mineral species or loosely attached on the surface as dominant mechanisms during leaching in the columns.
4. Leaching of metals in the column experiments exhibited first order kinetics with a first-flush, followed by a decrease in slope tailing elution pattern for all fly ashes. High release of the anionic species was observed during the initial 15-35 PVFs (due to the alkaline pH, which enhances their solubilization, and due to unavailability of positively charged surface species for complexation),

and as the pH decreases approaching the pH of the buffered groundwater (nearly neutral), slower desorption of metalloids species occur, suggested by the flattening of the elution curves (due to the pH sensitive changes in speciation of the surface sites as more and more positive surface sites become available for complexation). Two parameters controlled the shape of the elution curves: first-order desorption rate

5. The naphthalene and o-xylene adsorption of the fly ashes were directly correlated with loss in ignition (unburned carbon content) of the fly ash. In the batch adsorption tests, PAC exhibited the highest adsorption capacity for naphthalene and o-xylene, followed by Dickerson Precipitator (LOI=20.5%), Paul Smith (LOI=10.7%), and Morgantown (LOI=3.1%) fly ashes. Similar sorption trends have been observed in column tests. The number of PVFs required to reach saturation were 95 with PAC, 214 PV with naphthalene and 43 PV with o-xylene for Dickerson Precipitator fly ash, 81 PV with naphthalene and 23 PV with o-xylene Paul Smith fly ash, and 34 PV with naphthalene and 6.2 PV with o-xylene for Morgantown fly ash.
6. Slower adsorption rate for naphthalene than for o-xylene have been suggested by the greater number of pore volumes of flow required to reach saturation in column tests. More PVFs were required for desorption of o-xylene than for adsorption due to the ease in deep penetration into micropores of the solid matrices, which makes more difficult and delays the diffusion back into the desorbing solution.

7. Adsorption/desorption hysteresis was obvious in both, column and batch tests. Only about 33 to 47% of the naphthalene and 76 to 89% of the o-xylene originally adsorbed onto the fly ashes in the columns was desorbed, suggesting that the adsorption/desorption process was not completely reversible during the testing periods and is attributed to the occurrence of slowly desorbing fractions of organics.

## **7.2. PRACTICAL IMPLICATIONS**

HCC fly ash, a material that is currently being landfilled in most of the country, has a good potential to be used as a reactive medium in PRBs. In addition to a promising adsorption capacity for petroleum hydrocarbons, the low cost (only transportation costs) of HCC fly ash makes it a good candidate for these remediation systems. Even though, HCC fly ashes can be viable alternatives to PACs, the presence of undesired inorganics in these coal-combustion by-products requires special attention. In a possible field application, measures must be taken during the phase after construction as the leachate at this phase is likely to include high concentration of metals. Following this first-flush period, the metal concentrations in the collected leachate are expected to be very low. Accordingly, an additional technology may be required to prevent the metal contamination of the environment. One approach could be an integrated remediation technology at the initial phase by using a pump-treat technology at the initial phase (after construction) to remove the high concentrations of the metals. Second approach could be injection of phosphate solution to groundwater. Preliminary tests conducted in this study (not documented

in the report) showed that phosphate stabilizes the metals. Existing research showed that the metals binded and are sequestered inside the phosphate mineral solid phase are very stable and have great durability and leach resistance over a wide range of environmental conditions (Zupancic et al. 2006, Chen et al. 2007).

### **7.3. RECOMMENDATIONS FOR FURTHER RESEARCH**

Future work can provide deeper understanding of the leaching mechanisms under different conditions. For instance, a comparison between the findings of the water leach and column tests was documented. Nevertheless, the comparison is “rough” and questions arise about the field representativeness of the WLTs. Currently, the Maryland Department of the Environment (MDE) requires that the fly ashes be subjected to the Toxicity Characteristic Leaching Procedure (TCLP) test to determine if the material can be used in field construction applications without causing groundwater and surface water contamination. However, the Maryland Department of Natural Resources (MD DNR) raised concerns about the use of this testing methodology, as the testing conditions are typically harsher than the ones encountered in the field, the test is not material or site specific, and it neither represents the actual leachate produced in the field nor simulates a site-specific transport condition. Furthermore, the test method is used to determine if the material is hazardous or not; however, more than 15 years of research based on TCLP and column tests clearly shows that the fly ashes are generally non-hazardous (Creek and Shackelford 1992, Kyper 1992, Chichester and Landsberger 1996, Edil 1998, Ghosh and Subbarao 1998, Qiao et al. 2006, Bin Shafique, et al. 2007) One future goal is to determine the most

appropriate leaching test for evaluating the potential environmental impacts of fly ashes when used in environmental remediation applications. To accomplish this goal, a comparison of three different leaching tests: flow-through column leaching tests, ASTM WLT, and the TCLP test can be done in the laboratory.

Another study area could be to investigate the metal adsorption capacity of HCC fly ashes for their possible use in remediation applications. Concentrations of metals in the fly ash can be varied by adding metal salts to the fly ash. The fly ash contents can also be varied similar to an approach undertaken in the current study. As pH has a clear effect of leaching of metals, the pH of the solution should be studied as well.



## **APPENDIX 1**

- FORTRAN Program “trafit3d” code
  
- TRAFIT3D program output files for tracer test
  
- Additional observed and modeled bromide tracer breakthrough and washout curves

## APPENDIX 1

### FORTRAN Program "trafit3d" code

USE numerical libraries

THIS IS A FORTRAN PROGRAM THAT CALCULATES THE SUM OF THE SQUARES OF EITHER THE ABSOLUTE OR RELATIVE RESIDUALS BETWEEN THE NORMALIZED EXPERIMENTAL CONSERVATIVE TRACER DATA AND THE NORMALIZED FLUX-AVERAGED CONCENTRATION CALCULATED USING THE CONTINUOUS POINT SOURCE MODEL AT STEADY STATE AS DESCRIBED BY ROBBINS (1989) AND THE BEST FIT HYDRODYNAMIC DISPERSION COEFFICIENT,  $D_H$ , AND AVERAGE PORE WATER VELOCITY,  $V$  (WHICH IS USED TO CALCULATE THE BEST FIT POROSITY). THE BEST FIT PARAMETERS ARE OBTAINED USING A MODIFIED LEVENBERG-MARQUARDT METHOD TO MINIMIZE THE SUMS OF THE SQUARES OF THE RESIDUALS BETWEEN OBSERVED AND CALCULATED CONCENTRATIONS. THE EXPERIMENTAL DATA ARE FROM A SAND FLOW TANK WITH A SQUARE CROSS-SECT.

THE MAIN PROGRAM CALLS FIVE SUBROUTINES:

INPUT: READS INPUT FROM A DATA FILE CALLED INDATA1D.

DUNLSF: AN IMSL SUBROUTINE THAT SOLVES A NONLINEAR LEAST SQUARES PROBLEM USING A MODIFIED LEVENBERG-MARQUARDT ALGORITHM AND A FINITE-DIFFERENCE JACOBIAN.

FCN: CALCULATES EITHER THE ABSOLUTE OR RELATIVE RESIDUAL VECTOR.

EXER: CALCULATES EXP(A) ERFC(B)

#### VARIABLES:

AREA - COLUMN CROSS SECTIONAL AREA (CM<sup>2</sup>).

BSTPOR - BEST FIT FOR POROSITY; CALCULATED FROM VELOCITY BEST FIT.

CEX(I) - NORMALIZED EXPERIMENTAL EFFLUENT CONCENTRATION AT EACH SAMPLING TIME.

CMOD(I) - CALCULATED NORMALIZED FLUX-AVERAGED EFFLUENT CONCENTRATION AT EACH SAMPLING TIME, USING OPTIMUM FIT PARAMETER VALUES.

DATPTS - NUMBER OF EXPERIMENTAL OBSERVATIONS.

VD(I) - ESTIMATED VALUES FOR AVERAGE PORE WATER VELOCITY AND HYDRODYNAMIC DISPERSION COEFFICIENT, RESPECTIVELY.

FJAC(I,J) - FINITE DIFFERENCE APPROXIMATE JACOBIAN AT SOLUTION.

FLOW - EXPERIMENTALLY DETERMINED BULK FLOW RATE (ML/HR).

FSCALE(I) - DIAGONAL SCALING MATRIX FOR FUNCTION.

LENGTH - LENGTH OF COLUMN (CM);(DISTANCE BETWEEN SAMPLING PORTS).

N - NUMBER OF PARAMETERS TO BE ESTIMATED.

PGUESS(I) - INITIAL GUESS FOR AVERAGE PORE WATER VELOCITY (CM/HR) AND HYDRODYNAMIC DISPERSION COEFFICIENT (CM<sup>2</sup>/HR) , RESPECTIVELY.

PSCALE(I) - DIAGONAL SCALING MATRIX FOR VARIABLES.

RESID(I) - ABSOLUTE OR RELATIVE RESIDUALS.

RPARAM(I) - PARAMETER VECTOR FOR OPTIMIZATION SUBROUTINE.

SUMSQ - SUM OF SQUARES OF ABSOLUTE OR RELATIVE RESIDUALS.

TIME(I) - TEST SAMPLING TIMES (HR).

```

DECLARATION OF VARIABLES
DOUBLE PRECISION TIME (70), CEX(70), CMOD(70), RESID(70), VD(2),
*RPARAM (7), FJAC(70,2), PSCALE(2), PGUESS(2), FSCALE(70)
DOUBLE PRECISION EXER, SUMSQ, LENGTH, FLOW, AREA, BSTPOR, STDDEV
INTEGER SSE, DATPTS, I, LDFJAC, IPARAM(6), N
COMMON/OBS/LENGTH, TIME, CEX, CMOD, SSE
EXTERNAL FCN, INPUT
C OPEN FILES
OPEN (5, FILE='INDAT1D', STATUS='OLD')
OPEN (6, FILE='BSTFIT1D', STATUS='UNKNOWN')
C READ INPUT VARIABLES
CALL INPUT (LENGTH, FLOW, AREA, PGUESS, SSE, DATPTS, TIME, CEX)
C INITIALIZE OPTIMIZATION SUBROUTINE ARGUMENTS
N=2
DO 90 I=1,N
PSCALE(I)=1.0
90 CONTINUE
DO 100 I=1,70
FSCALE(I)=1.0
100 CONTINUE
IPARAM(1)=0
LDFJAC=70
C CALL THE OPTIMIZATION SUBROUTINE TO SOLVE FOR THE BEST-FIT
PARAMETERS
CALL DUNLSF(FCN, DATPTS, N, PGUESS, PSCALE, FSCALE, IPARAM,
*RPARAM, VD, RESID, FJAC, LDFJAC)
C CALCULATE THE SUM OF THE SQUARES OF THE RESIDUALS
SUMSQ=0.0D0
DO 120 I=1,DATPTS
SUMSQ=SUMSQ+RESID(I)**2
120 CONTINUE
C CALCULATE THE STANDARD DEVIATION OF THE ABSOLUTE OR RELATIVE
RESIDUALS
STDDEV=DSQRT(SUMSQ/DFLOAT(DATPTS-2))
C CALCULATE THE BEST FIT POROSITY FROM THE BEST FIT AVG. PORE
WATER VELOCITY, FLOW, AND CROSS-SECTIONAL AREA
BSTPOR=FLOW/(AREA*VD(1))
C WRITE RESULTS TO OUTPUT FILE
WRITE (6, 130)
130 FORMAT (8X, 'THE BEST-FIT PARAMETERS ARE:')
WRITE (6, 140) VD(1), BSTPOR, VD(2)
140 FORMAT (10X, 'VELOCITY =', X, F6.3, 4X, 'POROSITY =', X, E12.3, 4X
*, 'DH =', X, F6.3,/)
IF(SSE.EQ.1) THEN
WRITE (6, 150)
150 FORMAT (10X, 'TIME', 8X, 'C/C"(exp)', 4X, 'C/C"(model)',
*4X, 'ABS RESIDUAL', /)
ELSE
WRITE (6, 160)
160 FORMAT (10X, 'TIME', 8X, 'C/C"(exp)', 4X, 'C/C"(model)',

```

```

*4X, 'REL RESIDUAL', /)
ENDIF
DO 200 I=1, DATPTS
WRITE (6, 190) TIME(I), CEX(I), CMOD(I), RESID(I)
190 FORMAT (8X, F6.2, 8X, F6.4, 9X, F6.4, 8X, E10.4)
200 CONTINUE
WRITE (6,*)
WRITE (6, 210) SUMSQ
210 FORMAT (18X, 'THE SUM-OF-SQUARED RESIDUALS IS: ', G10.4)
WRITE (6, 220) STDDEV
220 FORMAT (7X, 'THE STANDARD DEVIATION OF THE RESIDUALS IS: ', G10.4)
STOP
END
SUBROUTINE INPUT (LENGTH, FLOW, AREA, PGUESS, SSE, DATPTS, TIME,
CEX)
C THIS SUBROUTINE READS INPUT FROM A DATA FILE CALLED INDATA1D
C IF SSE=1, THE ABSOLUTE LEAST SQUARES (ALS) CRITERION IS USED;
C IF SSE=2, THE RELATIVE LEAST SQUARES (RLS) CRITERION IS USED.
DOUBLE PRECISION TIME(70), CEX(70), PGUESS(2)
DOUBLE PRECISION LENGTH, FLOW, AREA
INTEGER SSE, DATPTS, I
READ (5,*) LENGTH, FLOW, AREA, PGUESS(1), PGUESS(2)
write (6, *) length, flow, area, pguess(1), pguess(2)
2 FORMAT(F6.3)
READ (5,*) SSE, DATPTS
write (6, *) sse, datpts
4 FORMAT(I2)
DO 10 I=1, DATPTS
READ (5,6) TIME(I), CEX(I)
write(6,*) time(i), cex(i)
6 FORMAT(F7.4, X, F6.4)
10 CONTINUE
RETURN
END
SUBROUTINE FCN(DATPTS, N, VD, RESID)
C THIS SUBROUTINE COMPUTES THE ANALYTICAL SOLUTION TO THE
NONREACTIVE SOLUTE TRANSPORT EQUATION AT STEADY STATE (ROBBINS
1989).
THE POSITION (X), TIME (T), PORE WATER VELOCITY (VD(1)), AND THE
DISPERSION COEFFICIENT (VD(2)) ARE INPUTS. THE OUTPUT IS THE
NORMALIZED(OVER STEADY STATE) FLUX-AVERAGED CONCENTRATION
(C/C')
AT THE GIVEN POSITION AND TIME. THIS REQUIRES AN EXTERNAL FUNCTION
EXER(A,B), WHICH COMPUTES THE VALUE OF EXP(A)*ERFC(B). THE
SUBROUTINE USES THESE VALUES TO THEN CALCULATE EITHER THE
ABSOLUTE OR RELATIVE RESIDUAL VECTOR.
C DECLARE VARIABLES
DOUBLE PRECISION TIME(70), CEX(70), CMOD(70), VD(2), RESID(70),
*LENGTH
INTEGER DATPTS, N, SSE, I
COMMON/OBS/LENGTH, TIME, CEX, CMOD, SSE

```

```

C DECLARE LOCAL VARIABLES
DOUBLE PRECISION A(70), EXER
C COMPUTE THE VALUES OF THE LOCAL VARIABLES
DO 300 I=1,DATPTS
A(I)=(LENGTH-VD(1)*TIME(I))/(2.0D0*DSQRT(VD(2)*TIME(I)))
300 CONTINUE
C COMPUTE THE NORMALIZED(STEADY ST.) FLUX-AVERAGED
CONCENTRATION AT THIS REQUIRES AN EXTERNAL FUNCTION EXER(A,B)
WHICH
COMPUTES THE VALUE OF EXP(A)*ERFC(B).
DO 310 I=1,DATPTS
CMOD(I)=0.5D0*EXER(0.0D0,A(I))
310 CONTINUE
C CALCULATE EITHER THE ABSOLUTE OR RELATIVE RESIDUALS VECTOR
DO 320 I=1,DATPTS
RESID(I)=CEX(I)-CMOD(I)
IF(SSE.EQ.2) RESID(I)=RESID(I)/CEX(I)
320 CONTINUE
RETURN
END
DOUBLE PRECISION FUNCTION EXER(A,B)
C THIS SUBROUTINE IS FROM VAN GENUCHTEN AND ALVES (1982)
C PURPOSE: TO CALCULATE EXP(A)*ERFC(B)
C DECLARE DUMMY VARIABLES
DOUBLE PRECISION A, B
C DECLARE LOCAL VARIABLES
DOUBLE PRECISION C, X, T, Y
EXER=0.0D0
IF ((DABS(A).GT.170.).AND.B.LE.0.0) RETURN
IF (B.NE.0.0) GOTO 100
EXER=DEXP(A)
RETURN
100 C=A-B*B
IF ((DABS(C).GT.170.).AND.(B.GT.0.0)) RETURN
IF (C.LT.-170.) GOTO 130
X=DABS(B)
IF (X.GT.3.0) GOTO 110
T=1.0D0/(1.0D0+0.3275911D0*X)
Y=T*(0.2548296D0-T*(0.2844967D0-T*(1.421414D0-T*(1.453152D0-
*1.061405D0*T))))
GOTO 120
110 Y=0.5641896D0/(X+0.5D0/(X+1.0D0/(X+1.5D0/(X+2.0D0/(X+2.5D0/(X+
*1.0D0))))))
120 EXER=Y*DEXP(C)
130 IF (B.LT.0.0) EXER=2.0*DEXP(A)-EXER
RETURN
END

```

-----

**Potomac River - Input tracer**

**Input parameters:**

*Path length:* 30.000000000000000      *Flow rate:* 54.000000000000000      *Column surface area:* 18.095000000000000  
*Estimated seepage velocity:* 6.500000000000000      *Estimated dispersion coefficient:* 0.600000000000000

<i>Time (hours)</i>	<i>C/Co (experimental)</i>
0.000000000000000E+000	3.333740000000000E-004
0.900000000000000	1.149406000000000E-003
1.600000000000000	1.099265000000000E-003
2.100000000000000	1.051312000000000E-003
2.4333333300000	7.317180000000000E-004
2.9166666700000	6.805590000000000E-004
3.3500000000000	6.655500000000000E-004
3.5166666700000	1.201833000000000E-003
4.0833333300000	0.111791025000000
4.4000000000000	0.615661497000000
4.7833333300000	0.841274939000000
5.1666666700000	0.940513600000000
5.4500000000000	0.994440134000000
5.7833333300000	1.000000000000000
6.0666666700000	1.000000000000000

**Best fit parameters:**

**VELOCITY = 6.859      POROSITY = 0.435      DH = 0.495**

TIME	C/C'(exp)	C/C'(model)	ABS RESIDUAL
0.00	0.0003	0.0000	0.3334E-03
0.90	0.0011	0.0000	0.1149E-02
1.60	0.0011	0.0000	0.1099E-02
2.10	0.0011	0.0000	0.1051E-02
2.43	0.0007	0.0000	0.7317E-03
2.92	0.0007	0.0000	0.6806E-03
3.35	0.0007	0.0001	0.5992E-03
3.52	0.0012	0.0009	0.2853E-03
4.08	0.1118	0.1696	-.5780E-01
4.40	0.6157	0.5483	0.6737E-01
4.78	0.8413	0.9076	-.6634E-01
5.17	0.9405	0.9927	-.5214E-01
5.45	0.9944	0.9993	-.4904E-02
5.78	1.0000	1.0000	0.2292E-04
6.07	1.0000	1.0000	0.9049E-06

THE SUM-OF-SQUARED RESIDUALS IS: 0.1503E-01  
 THE STANDARD DEVIATION OF THE RESIDUALS IS: 0.3400E-01

Figure A.1. TRAFIT3D program output file for the tracer test conducted on 40% Potomac River fly ash/60% sand mixture.

**Potomac River - Washout tracer**

**Input parameters:**

Path length: 30.0000000000000  
 Flow rate: 54.0000000000000  
 Column surface area: 18.0950000000000  
 Estimated seepage velocity: 6.5000000000000  
 Estimated dispersion coefficient: 0.6000000000000  
 1 16

Time (hours)	C/Co (experimental)
1.9833333300000	1.90896000000000E-004
2.9000000000000	8.94360000000000E-004
3.3000000000000	1.27074300000000E-003
3.4833333300000	3.20629100000000E-003
3.6833333300000	1.22899410000000E-002
3.8166666700000	6.84427700000000E-002
4.4000000000000	0.538554229000000
4.6500000000000	0.935284470000000
5.1000000000000	1.0000000000000
5.6500000000000	1.0000000000000
5.9166666700000	1.0000000000000
6.1666666700000	1.0000000000000
6.5000000000000	1.0000000000000
6.9833333300000	1.0000000000000
7.6666666700000	1.0000000000000
8.6000000000000	1.0000000000000

**Best fit parameters:**

	VELOCITY = 6.839	POROSITY = 0.436	DH = 0.158
TIME	C/C'(exp)	C/C'(model)	ABS RESIDUAL
1.98	0.0002	0.0000	0.1909E-03
2.90	0.0009	0.0000	0.8944E-03
3.30	0.0013	0.0000	0.1271E-02
3.48	0.0032	0.0000	0.3206E-02
3.68	0.0123	0.0000	0.1229E-01
3.82	0.0684	0.0002	0.6824E-01
4.40	0.5386	0.5390	-.4808E-03
4.65	0.9353	0.9342	0.1073E-02
5.10	1.0000	0.9999	0.5496E-04
5.65	1.0000	1.0000	0.4186E-10
5.92	1.0000	1.0000	0.7772E-14
6.17	1.0000	1.0000	0.0000E+00
6.50	1.0000	1.0000	0.0000E+00
6.98	1.0000	1.0000	0.0000E+00
7.67	1.0000	1.0000	0.0000E+00
8.60	1.0000	1.0000	0.0000E+00

THE SUM-OF-SQUARED RESIDUALS IS: 0.4821E-02

THE STANDARD DEVIATION OF THE RESIDUALS IS: 0.1856E-01

Figure A.2. TRAFIT3D output file for the washout test conducted on 40% Potomac River fly ash/60% sand mixture.

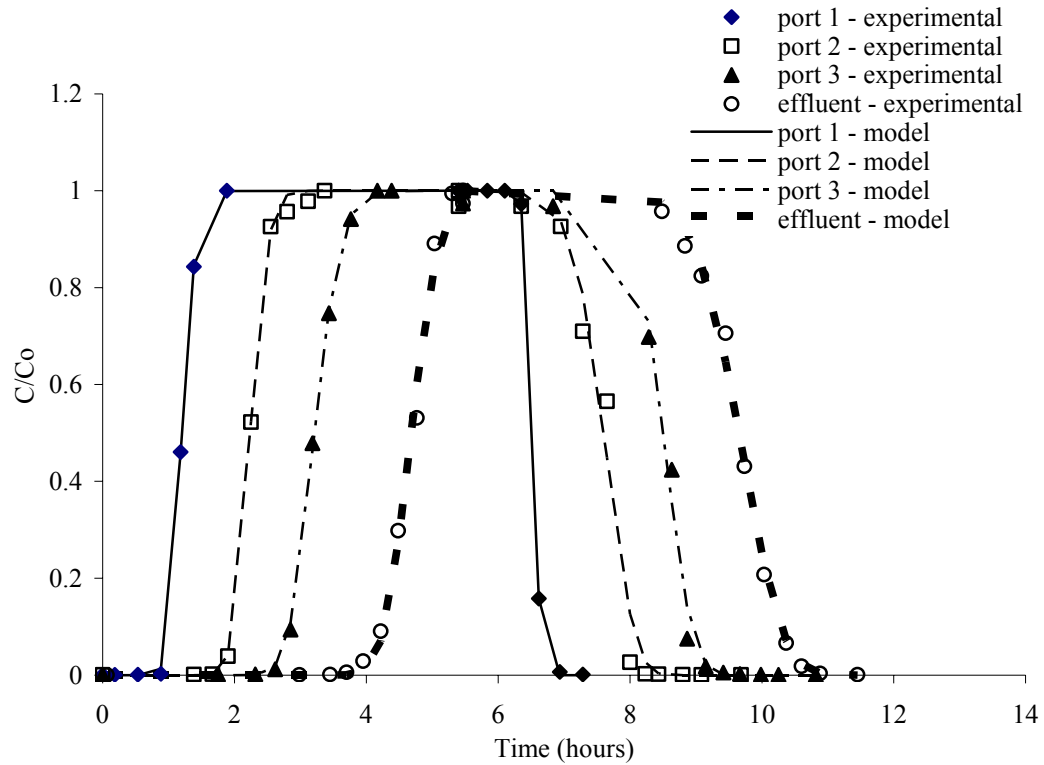


Figure A. 3. Observed and modeled bromide tracer breakthrough and washout curves for the 40% Morgantown fly ash / 60% sand column. Each experimental data point represents a single measurement.

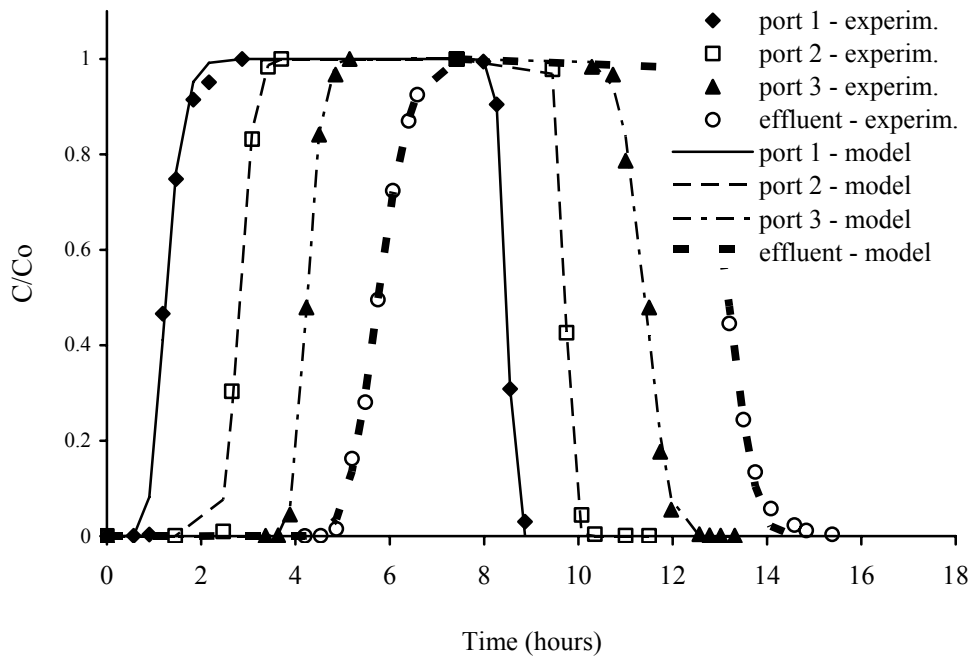


Figure A. 4. Observed and modeled bromide tracer breakthrough and washout curves for the 2% PAC / 98% sand column. Each experimental data point represents a single measurement.



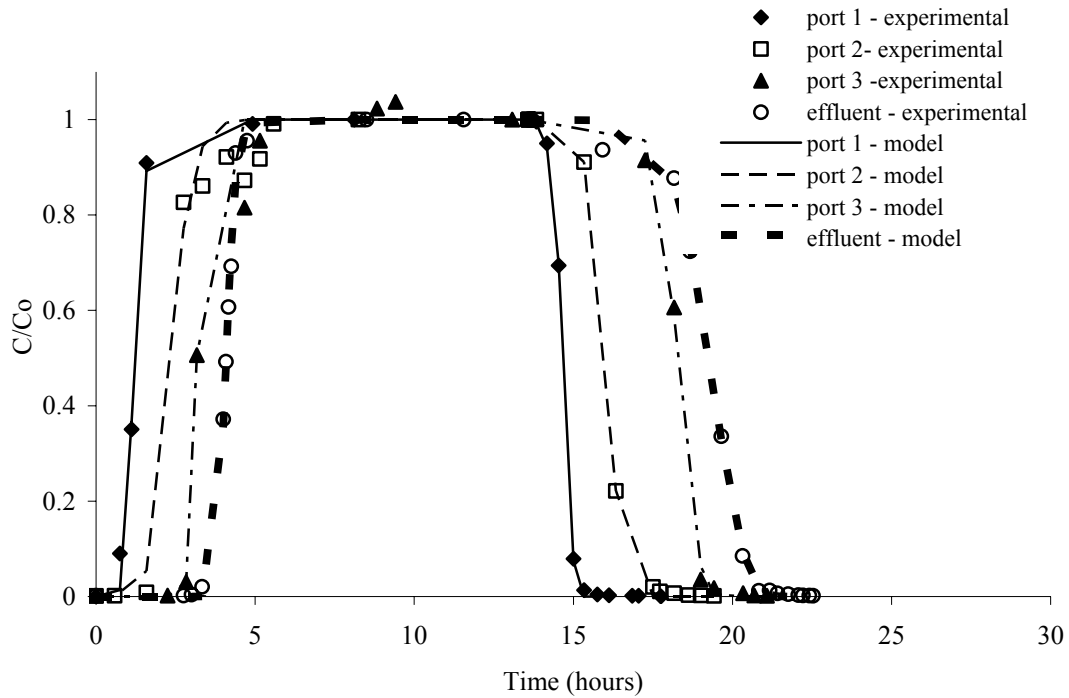


Figure A. 5. Observed and modeled bromide tracer breakthrough and washout curves for the 40% Paul Smith fly ash / 60% sand column. Each experimental data point represents a single measurement.

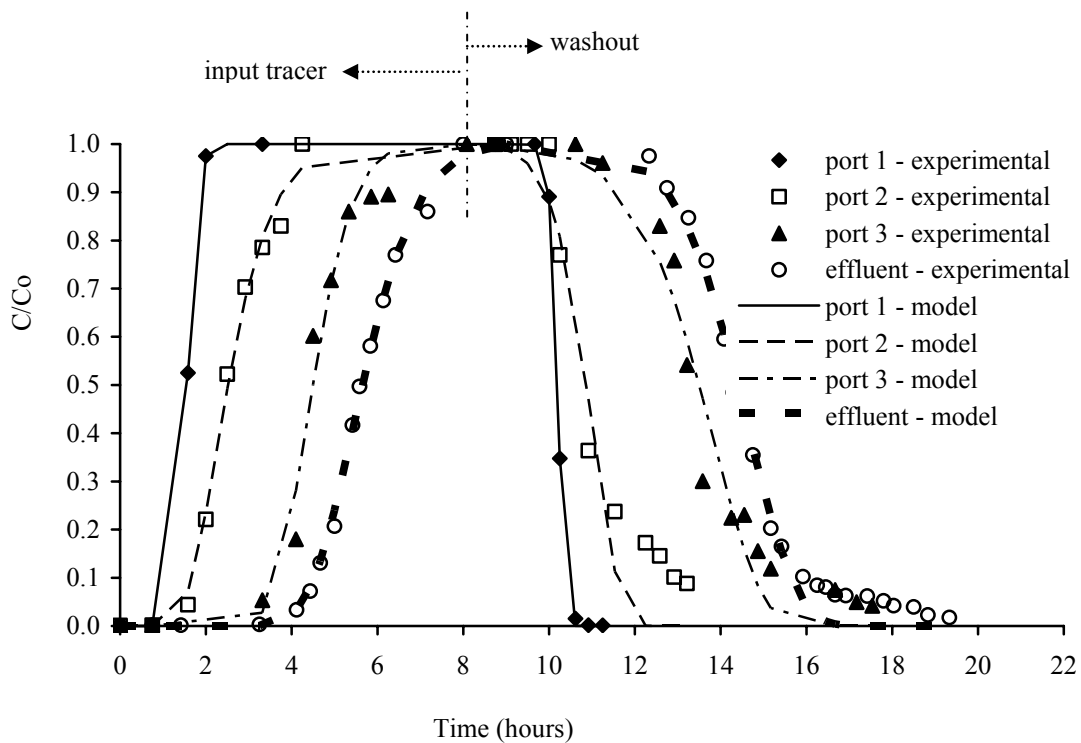
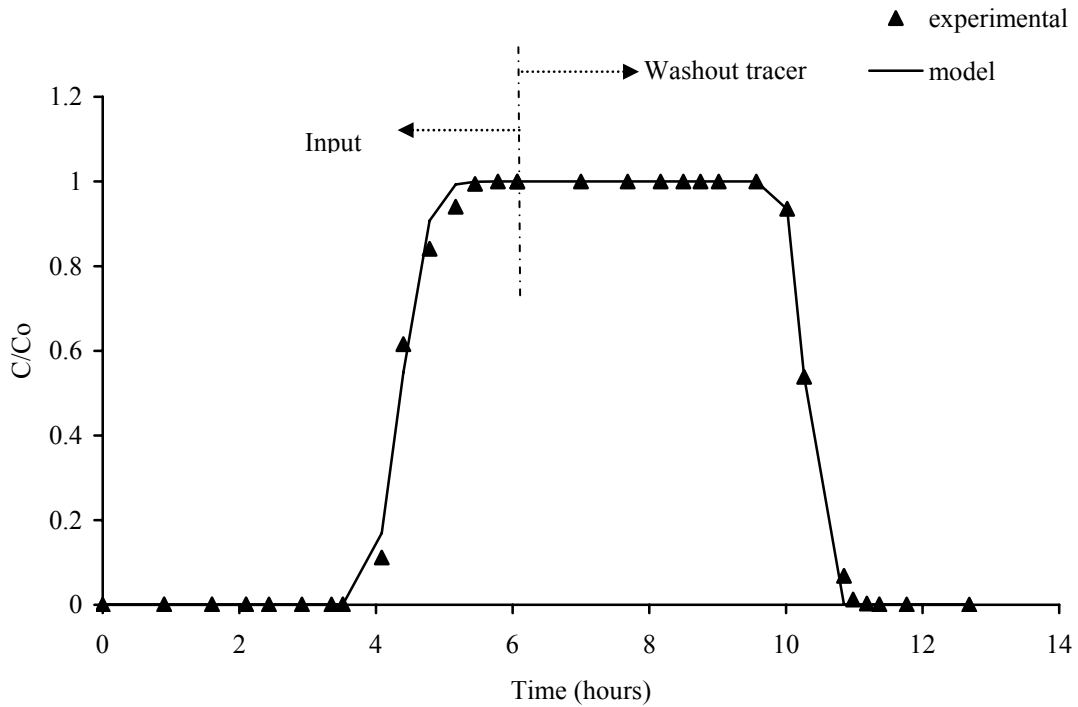
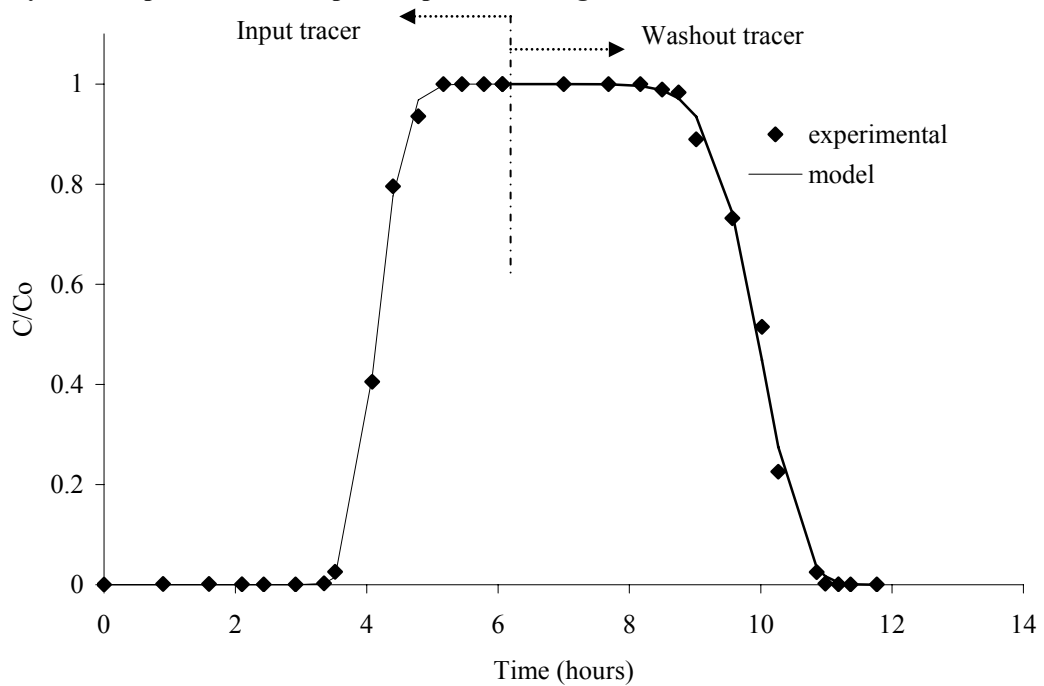


Figure A. 6. Observed and modeled bromide tracer breakthrough and washout curves for the 40% Dickerson Precipitator fly ash / 60% sand column. Each experimental data point represents a single measurement.



**Figure A. 6. Observed and modeled bromide tracer breakthrough and washout curves for the 40% Potomac River fly ash / 60% sand column. The sampling was conducted at the effluent port only. Each experimental data point represents a single measurement.**



**Figure A. 6. Observed and modeled bromide tracer breakthrough and washout curves for the 40% Brandon Shores fly ash / 60% sand column. The sampling was conducted at the effluent port only. Each experimental data point represents a single measurement.**

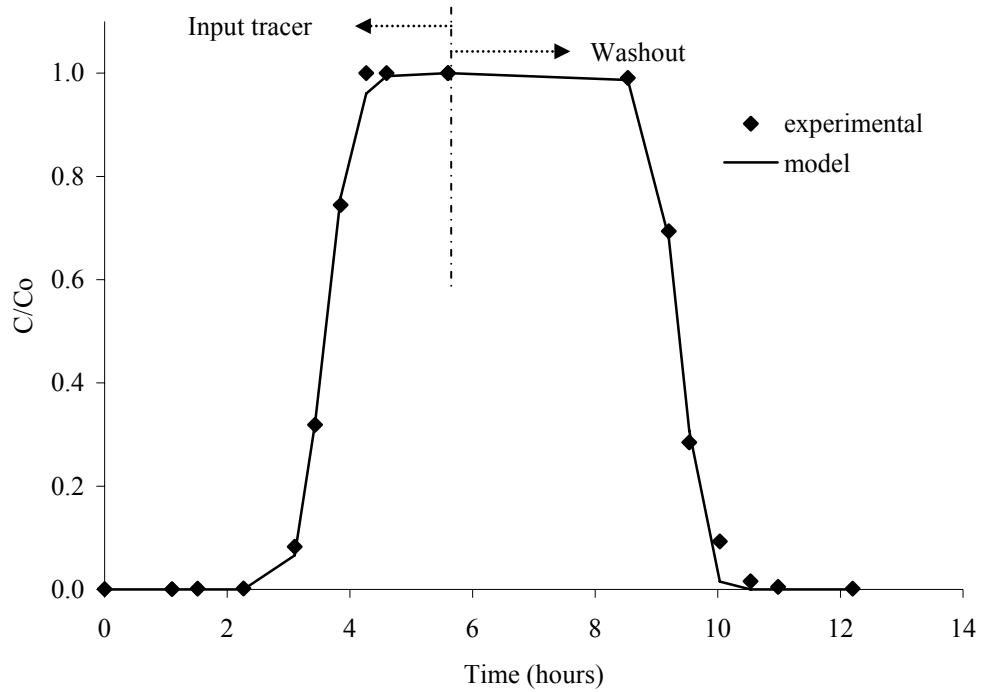


Figure A. 6. Observed and modeled bromide tracer breakthrough and washout curves for the 40% Chalk Point fly ash / 60% sand column. The sampling was conducted at the effluent port only. Each experimental data point represents a single measurement.

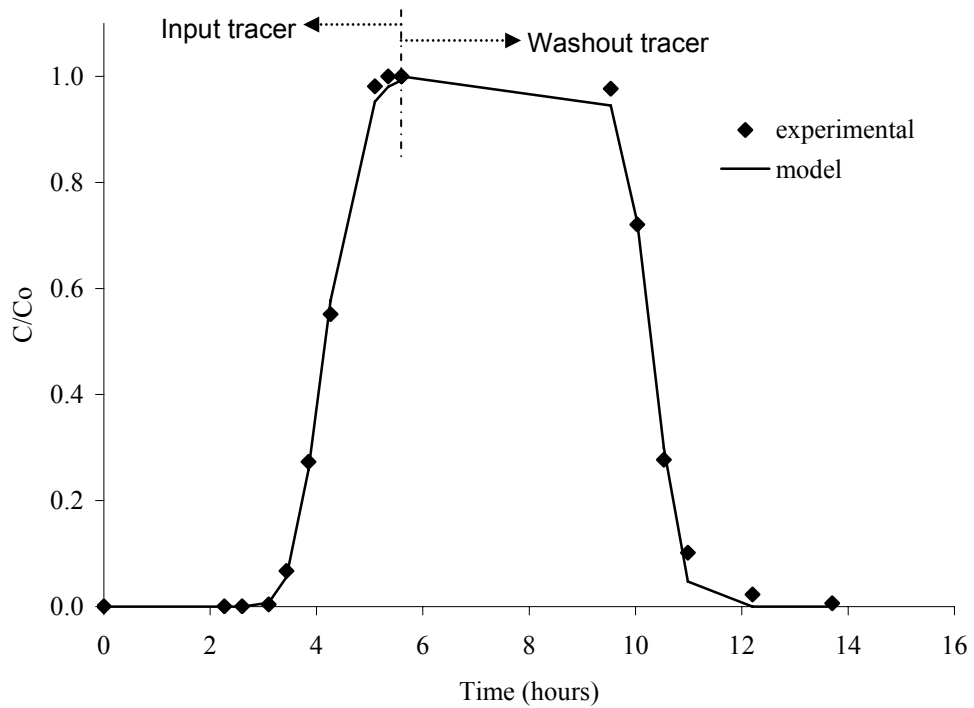


Figure A. 6. Observed and modeled bromide tracer breakthrough and washout curves for the 40% Dickerson Baghouse fly ash / 60% sand column. The sampling was conducted at the effluent port only. Each experimental data point represents a single measurement.

## REFERENCES

- Adamson, A.W. and Gast A.P. (1997) “Physical Chemistry of Surfaces”, *Wiley-Interscience, New York*.
- Agency for Toxic Substances and Diseases Registry –Toxicological profile website  
<http://www.atsdr.cdc.gov/toxpro2.html>
- Alesii, B.A., Fuller, W.H., and Boyle, M.V., (1980). “Effect of leachate flow rate on metal migration through soil”, *Journal of Environmental Quality*, Vol. 9pp. 119-126.
- Aislabie, J., Saul, D.J., Foght, J.M., (2006). “Bioremediation of hydrocarbon contaminated polar soils”, *Extremophiles*, Vol. 10, No. 3, pp. 171–179.
- Alkorta, I., and Garbisu, C., (2001). “Phytoremediation of organic contaminants in soils”, *Bioresource Technology*, Vol. 79, Issue 3, pp. 273-276.
- Allen, H.E., Perdue, E.M., and Brown, D.S., (1993). “Metals in Groundwater”, *Lewis Publishers, Chelsea, Miami*, pp. 1-36.
- ASTM C 618 – 05, (2005). Standard specification for coal fly ash and raw or calcined natural pozzolan for use in concrete. *In the Annual Book of ASTM Standards, 2005, Philadelphia, PA*.
- ASTM D 3987-85. (1992). “Standard test method for shake extraction of solid waste with water,” *Annual Book of ASTM Standards*, Vol. 04.01.
- Badr, T., Hanna, K., and de Brauer, C., (2004). “Enhanced solubilization and removal of naphthalene and phenanthrene by cyclodextrins from two contaminated soils”, *Journal of Hazardous Materials*, Vol. B 112, pp. 215–223.
- Benner, S. G., Blowes, D. W. and Ptacek, C. J. (1997). “Porous reactive wall for prevention of acid mine drainage: results of full-scale field demonstration.” *International Containment Technology Conference and Exhibition, February 9-12, St. Petersburg, Florida*.
- Berselli, S., Benitez, E., Fedi, S., Zannoni, D., Medici, A., Marchetti, L., Fava F.,(2006). “Development and assessment of an innovative soil-washing process based on the use of cholic acid-derivatives as pollutant-mobilizing agents”, *Biotechnology and Bioengineering*, Vol. 93, Issue 4, pp.761-770.

- Bilski, J.J., and Alva, A.K., (1995). "Transport of heavy metals and cations in a fly ash amended soil", *Bulletin of Environmental Contamination and Technology*, Vol. 55, pp. 502-509.
- Bin-Shafique, S., Benson, and C.H., Edil, T.B., (2002). "Leaching of heavy metals from fly ash stabilized soils used in highway pavements", *Geo Engineering report No. 02-14, Department of Civil and Environmental Engineering, University of Wisconsin-Madison, Madison, Wisconsin*.
- Bin-Shafique, S., Benson, C.H., Edil, T.B., and Hwang K., (2006). "Leachate concentrations from water leach and column leach tests on fly ash stabilized soils", *Environmental Engineering Science*, Vol. 23, No. 1, pp. 53-67.
- Blowes, D. W., Ptacek, C. J., Cherry, J. A., Gillham, R. W. and Robertson, W. D. (1995). "Passive remediation of groundwater using in situ treatment curtains." *Geoenvironment 2000, "Characterization, Containment, Remediation, and Performance in Environmental Geotechnics."* New York, American Society of Civil Engineers. 1588-1607.
- Bowders, J. J., Gidley, J. S. & Usmen, M. A. (1990) Permeability and Leachate Characteristics of Stabilized Class F Fly Ash. *Transportation Research Record No. 1288*, pp. 70-77.
- Braida, W.J., and Ong, S.K., (2001). "Air sparging effectiveness: laboratory characterization of air-channel mass transfer zone for VOC volatilization", *Journal of Hazardous Materials*, Vol. 87, No. 1-3, pp. 241-258.
- Brusseau, M.L., Jessup, R.E., and Rao, P.S.C., (1989). Modeling the transport of solutes influenced by multi process nonequilibrium", *Water Resources Research*, Vol. 25, No. 9, pp. 1971-1988.
- Bruseau, M.L., (1994). "Transport of reactive contaminants in heterogeneous porous media", *Reviews of Geophysics*, Vol. 32, No. 3, pp.285-314.
- Brusseau, M. L. (1996). "Evaluation of Simple Methods for Estimating Contaminant Removal by Flushing." *Ground Water*, Vol. 34 (1), pp. 19-22.
- Chang, Y.Y., and Corapcioglu, M. Y., (1998). "Plant-Enhanced Subsurface Bioremediation of Nonvolatile Hydrocarbons", *Journal of Environmental Engineering*, Vol. 124, No. 2, pp. 162-169.
- Cheng, X., Kan, A.T., and Tomson M.B., (2004). "Naphthalene adsorption and desorption from aqueous C<sub>60</sub> fullerene", *Journal of Chemical Engineering Data*, Vol. 49, pp. 675-683.

- Chichester, D.L., and Landsberger, S., (1996). "Determination of the leaching dynamics of metals from municipal solid waste incinerator fly ash using a column test", *Journal of Air and Waste Management Association*, Vol. 46, pp. 643-649.
- Chu, T.Y.J., Ruane, R.J., Krenkel, P.A., (1978). "Characterization and reuse of ash pond effluents in coal-fired power plants", *Journal of Water Pollution Control*, Vol. 50, Issue 11, pp. 2494-2508.
- Coates, J.D., Phillips, E.J.P., Lonergan, D.J., Jenter, H., and Lovley, D.R., (1996). "Isolation of *Geobacter* species from diverse sedimentary environments", *Applied Environmental Microbiology*, Vol. 62, pp. 1531-1536.
- Cockrell, C.F., and Leonard, J.W., (1970). "Characterization and utilization studies of limestone modified fly ash," *Coal Research Bureau*, Vol. 60.
- Cornelissen, G., Van Noort, P.C.M., and Govers H.A.J., (1998). "Mechanism of slow desorption of organic compounds from sediments: A study using model sorbents", *Environmental Science and Technology*, Vol.32, pp. 3124-3131.
- Creek, D.N., (1991). "Effect of flow rate on leaching of metals from fly ash and stabilized fly ash", *MS. Thesis, Department of Civil Engineering, Colorado State University, Fort Collins, Colorado*.
- Creek, D.N., and Shackelford, C.D., (1992). "Permeability and leaching characteristics of fly ash liner materials," *Transportation Research Record* 1345.
- Culver, T.B., Hallisey, S.P., Sahoo, D., Deitsch, J.J., and Smith J.A., (1997). "Modeling the desorption of organic contaminants from long-term contaminated soil using distributed mass transfer rates", *Environmental Science and Technology*, Vol. 31, No. 6, pp. 1581-1588.
- Dankwarth, F., Gerth, J., (2002): Abschätzung und Beeinflussbarkeit der Arsenmobilität in kontaminierten Böden. *Acta hydrochimica et hydrobiologica*, Vol. 30, pp. 1-8.
- Demirkan, M.M., (2008). "Remediation of petroleum hydrocarbons from subsurface environment using high carbon content fly ash", *Ph.D. Dissertation, Department of Civil and Environmental Engineering, University of Maryland, College Park, Maryland*.

- Demirkan, M.M., Morar, D.L., Aydilek, A.H., Seagren, A.E., Tsai, A., (2008). "Remediation of petroleum-contaminated groundwater using high carbon content fly ash", *Annual Congress of the Geo-Institute of ASCE, GeoCongress 2008: "The Challenge of Sustainability in the Geoenvironment"*, March 9-12, 2008, Sheraton New Orleans, New Orleans, Louisiana.
- DiGioia, A. M. and Nuzzo, W. L. (1972). "Fly Ash as Structural Fill," *Journal Power Division, ASCE, New York*, Vol. 98 (1), pp. 77-92.
- DiTorro, D.M., Mahony, J.D., Kirchgraber, P.R., O'Byrne, A.L., Pasquale, L.R., and Piccirilli, D.C., (1986). "Effect of nonreversibility, particle concentration, and ionic strength on heavy metal sorption", *Environmental Science and Technology*, Vol. 20, No. 1, pp. 55-61.
- Dudas, M.J., and Warren, C.J., (1986). "Submicroscopic model of fly ash particles", *Geoderma*, Vol. 40, No. 1-2, pp. 101-114.
- Dunnivant, F.M., Jardine, P.M., Taylor D.L., and McCarthy, J.F., (1992). "Cotransport of Cadmium and Hexachlorobiphenyl by Dissolved Organic Carbon through Columns Containing Aquifer Material", *Environmental Science and Technology*, Vol. 26, pp. 360-368.
- Edil, T.B., Sandstorm, L.K. and Berthouex, P.M., (1992). "Interaction of inorganic leachate with compacted pozzolanic fly ash," *Journal of Geotechnical Engineering*, Vol.118 (9), pp. 1410-1430.
- Eykholt, G.R., and Davenport, D.T., (1998). "Dechlorination of the chloroacetanilide herbicides alachlor and metolachlor by iron metal", *Environ. Science and Technology*, Vol. 32, pp. 1482-1487.
- Farrel, J., and Reinhard M., (1994). "Desorption of halogenated Organics from model solids, sediments, and soil under unsaturated conditions.1.Isotherms", *Environmental Science and Technology*, Vol. 28, pp. 53-62.
- Farrel, J., and Reinhard M., (1994). "Desorption of halogenated Organics from model solids, sediments, and soil under unsaturated conditions.2.Kinetics", *Environmental Science and Technology*, Vol. 28, pp. 63-72.
- Fenske, P.R., (1973). "Hydrology and radionuclide transport, monitoring well HT-2m. Tatum Dome, Mississippi", *Project Report 25, Technical report NVD-1253-6. Center for Water Resources Research, Desert Res. Inst. University of Nevada System, Reno.*
- Fisher, G.L., and Natusch,D.F.S., (1979). "Size dependence of the Physical and chemical properties of coal fly ash", In: *Analytical Methods of Coal and Coal Products, III, I.E. Karr, (Ed.), Academic Press. New York, 1979.*

- Francis, A.J., and Dodge, C.J., "Remediation of soils and wastes contaminated with uranium and toxic metals", *Environmental Science and Technology*, Vol. 32, No. 24, pp. 3993 -3998.
- Fry, V.A., and Istok, J.D., (1993). " An analytical solution to the solute transport equation with rate-limited desorption and decay", *Water Resources Research*, Vol. 29, No., 9, pp. 3201-3208.
- Fytianos, K., Tsaniklidi, B., and Voudrias, E., (1998). "Leachability of heavy metals in Greek fly ash from coal combustion", *Environment International*, Vol. 24, No. 4, pp. 477-486.
- Gelhar, L.W., C. Welty, and K.R. Rehfeldt. 1992. A critical review of data on field-scale dispersion in aquifers. *Water Resources Research*, Vol. 28, No. 7, pp. 1955–1974.
- Genç-Fuhrman, H., Mikkelsen, P.S., and Ledin, A., (2007). " Simultaneous removal of As, Cd, Cr, Cu, Ni and Zn from stormwater: Experimental comparison of 11 different sorbents", *Water Research*, Vol. 41, pp. 591-602.
- Ghosh, A., and Subbarao, C., (1998). "Hydraulic Conductivity and Leachate Characteristics of Stabilized Fly Ash", *Journal of Environmental Engineering*, Vol. 124, No. 9, pp. 812-820.
- Grathwohl, P., Gewalt, T., Pyka, W. and Schüth, C., (1993). "Determination of pollutant release rates from contaminated aquifer materials", In: Arendt, F., Annokkée, G.J., Bosman, R. and Van der Brink, W. J. (eds), *Contaminated Soil '93*, Kluwer, Dordrecht, The Netherlands, pp. 175–184.
- Gunasekara, A.S., and Xing, B., (2003). "Sorption and desorption of naphthalene by soil organic matter: Importance of aromatic and aliphatic components", *Journal of Environmental Quality*, Vol. 32, pp. 240-246.
- Harmon, T.C., and Roberts P.V., (1994). "Comparison of Intraparticle Sorption and Desorption Rates for a Halogenated Alkene in a Sandy Aquifer Material", *Environmental Science and Technology*, Vol. 28, pp. 1650-1660.
- Headley, J.V., Boldt-Leppin, B.E.J., Haung, M.D., and Peng, J., (2001). "Determination of diffusion and adsorption coefficients for volatile organics in an organophilic clay-sand-bentinite liner", *Canadian Geotechnical Journal*, Vol. 38, pp. 809-817.
- Hermosin, M.C., Cornejo, J. and Pérez-Rodríguez, J.L., (1987). "Adsorption and desorption of maleic hydrazide as a function of soil properties", *Soil Science*, Vol 44, pp. 250-256.



- Hoehn, E., (1983). "Geological interpretation of local-scale tracer observations in a river groundwater infiltration system", *Draft report, Swiss Federal Institute for Reactor Research (EIR), Würenlingen, Switzerland.*
- Hurt, R.H., Suuberg, E.M., Gao, Y.M., Lilly W.D., Külaots, I., and Smith, K., (1998). "Fundamental study of low-NO<sub>x</sub> combustion fly ash utilization", *Third semi-annual report (October 1, 1997 – April 30, 1998) - Division of Engineering Brown University, Providence, Rhode Island, 02912.*
- Jang, A., Choi, Y.S., and Kim, I.S., (1998). "Batch and column tests for the development of an immobilization technology for toxic heavy metals in contaminated soils of closed mines", *Water Science Technology*, Vol. 37, pp. 81–88.
- Jorgensen, K.S., Puutinen, J., and Suortti, A.M., (2000). "Bioremediation of petroleum hydrocarbon-contaminated soil by composting in biopiles", *Environmental Pollution*, Vol. 107, pp. 245–254.
- Kan, A.T., Fu, G., and Tomson, M.B., (1994). "Adsorption/desorption hysteresis in Organic Pollutant and soil/sediment interaction", *Environmental Science and Technology*, Vol. 28, pp. 859-867.
- Kan, A.T., Fu, G., Hunter, M., Chen, W., Ward, C.H., and Tomson, M.B., (1998). "Irreversible sorption of neutral hydrocarbons to sediments: Experimental observations and model predictions", *Environmental Science and Technology*, Vol. 32, pp. 892-902.
- Kan, A.T., Chen, W., and Tomson M.B., (2000). "Desorption of neutral hydrophobic organic compounds from field-contaminated sediment", *Environmental Pollution*, Vol. 108, pp. 81-89.
- Kandpal, G., Srivastava, P.C., and Ram, B., (2005). "Kinetics of desorption of heavy metals from polluted soils: Influence of soil type and metal source", *Water, Air and Soil Pollution*, Vol. 161, pp. 353-363.
- Kanungo, S.B., and Mohapatra R. (2000). "Leaching behavior of various trace metals in aqueous medium from two fly ash samples", *Journal of Environmental Quality*, Vol. 29, pp. 188-196.
- Karickhoff, S.W., and Morris, K.R. (2001). "Sorption dynamics of hydrophobic pollutants in sediment suspension", *Environmental Toxicology and Chemistry*, Vol. 4, Issue 4, pp. 469–479.

- Keijzer, T.J.S., Middeldorp, P.F., Van Alphen, M., Van Der Linde, P.R., and Loch J.P.G., (2002). "Desorption behavior of polycyclic aromatic hydrocarbons in harbor sludge from the port of Rotterdam, the Netherlands", *Water, Air and Soil Pollution*, Vol. 136, pp. 361-385.
- Kelly, W.P. 1948. Cation-exchange in soils. A.C.S. *Monograph No.109. Reinhold, New York.*
- Khan, Z., and Anjaneyulu, Y. (2005). "Influence of soil components on adsorption-desorption of hazardous organics-development of low cost technology for reclamation of hazardous waste dumpsites." *Journal of Hazardous Materials*, Vol. 118(1-3), pp. 161-169.
- Khodadoust, A.P., Lei, L., Antia, J.E., Bagchi, R., Suidan, M.T., Tabak, H.H., (2005). "Adsorption of polycyclic aromatic hydrocarbons in aged harbor sediments", *Journal of Environmental Engineering* © ASCE, Vol. 131, No. 3, pp. 403-409.
- Kim, J.Y., Edil, T.B., and Park, J.E. (1997). "Effective porosity and seepage velocity in column tests on compacted clay," *Journal of Geotechnical and Geoenvironmental Engineering*, Vol. 123 (12), pp. 1135-1142.
- Kinraide, T.B., and D.R. Parker. 1987. "Cation amelioration of aluminum phytotoxicity in wheat", *Plant Physiology*, Vol. 83, pp. 546- 551.
- Kinraide, T.B., (1998). "Three mechanisms for the calcium alleviation of mineral toxicities" *Plant Physiology*, Vol. 118, pp. 513-520.
- Kommalapati, R.R., Valsaraj, K.T., and Constant, W.D., (2002). "Soil-water partitioning and desorption hysteresis of volatile organic compounds from a Louisiana superfund soil", *Environmental Monitoring and Assessment*, Vol. 73, pp. 275-290.
- Külaots, I., Gao, Y.M., Hurt, R.H., and Suuberg, E.M., (1998). "Characterization of carbon in coal fly ash", *Report – Division of Engineering Brown University, Providence, Rhode Island.*
- Langenhoff, A.A.M., Zehnder, A.J.B., and Schraa, G., (1989). "Behaviour of toluene, benzene and naphthalene under anaerobic conditions in sediment columns", *Biodegradation*, Vol.7, No. 3, pp. 267-274.
- Lee, T., and Beson, C.H., (2002). "Using waste foundry sands as reactive media in permeable reactive barriers", *Geo Engineering report No. 02-01, Department of Civil and Environmental Engineering, University of Wisconsin-Madison, Madison, Wisconsin.*

- Lee, T.H., Byun, I.G., and Kim, Y.O., (2006). "Monitoring biodegradation of diesel fuel in bioventing processes using in situ respiration rate", *Water Science and Technology*, Vol. 53 (4-5), pp. 263-272.
- Li,P., Sun, T., Stagnitti, F., Zhang, C., Zhang, H., Xiong, X., Allinson, G., Ma, X., Allinson, M., (2002). "Field-Scale Bioremediation of Soil Contaminated with Crude Oil", *Environmental Engineering Science*, Vol. 19, No. 5, pp. 277-289.
- Liu, H. and Amy, G., (1993). "Modeling partitioning and transport interactions between natural organic matter and polynuclear aromatic hydrocarbons in groundwater", *Environ. Science and Technology*, Vol. 27, pp. 1553-1562.
- Long, J.M., (2003). "Leaching mechanisms: Batch, column, and stress induced leaching processes", *MS. Thesis, Department of Civil Engineering, University of The North Carolina, Charlotte, North Carolina.*
- Luo, Q.S., Zang, X.H., Wang, H., and Qian, Y. (2005). "Mobilization of phenol and dichlorophenol in unsaturated soils by non-uniform electrokinetics." *Chemosphere*, Vol. 59(9), pp. 1289-1298.
- Macek, T., Macková, M., Káš, J., (2000). "Exploitation of plants for the removal of organics in environmental remediation", *Biotechnology Advances*, Volume 18, Issue 1, pp. 23-34.
- Manz, O.E., (1999). "Coal fly ash: A retrospective and future look", *Fuel*, Vol. 78, No.2, pp. 133-136.
- Maxin, C.R., Kögel-Knabner,I., (1995). "Partitioning of polycyclic aromatic hydrocarbons (PAH) to water-soluble soil organic matter", *European Journal of Soil Science*, Vol. 46, Issue 2, pp. 193-204.
- McBride, M., (1994). "Environmental chemistry of soils", *Oxford University Press, New York.*
- McCarthy, K., Walker, L., Vigoren, L., Bartel, J. (2004). "Remediation of spilled petroleum hydrocarbons by in situ landfarming at an arctic site", *Cold Regions Science and Technology*, Vol. 40(31), pp. 2013-2039.
- Meckenstock, R. U., Annweiler, E., Michaelis, W., Richnow, H. H., Schink, B. (2000). "Anaerobic naphthalene degradation by a sulfate-reducing enrichment culture" *Applied Environmental Microbiology*, Vol. 66, pp. 2743-2747.
- Meegoda, J.N., and Ratnaweera, P., (1995). "Treatment of oil contaminated soils for identification and classification", *ASTM Geotechnical Testing Journal*, Vol. 18, No. 1, pp. 41-49.

- Miller, C.T., and Pedlt, J.A., (1992). "Use of a reactive surface-diffusion model to describe apparent sorption-desorption hysteresis and abiotic degradation of lindane in a subsurface material", *Environmental Science and Technology*, Vol. 26, pp. 1417- 1427
- Mitchell, J.K., (1976). "Fundamentals of soil Behavior", *John Wiley and Sons, Toronto*.
- Murphy, E. M., Ginn, T. R., Chilakapati, A., Resch, C. T., Phillips, J. L., Wietsma, T.W., and Spadoni, C. M. (1997). "The influence of physical heterogeneity on microbial degradation and distribution in porous media." *Water Resources Research*, Vol. 33, No. 5, pp.1087-1103.
- Naik, T.R., Singh, S.S., and Ramme, B.W., (2001). "Performance and leaching assessment of flowable slurry", *Journal of Environmental Engineering*, Vol. 127, Issue 4, pp. 359-368.
- Ogunro, V.O., and Inyang, H.I., (2003). "Relating batch and column diffusion coefficients for leachable contaminants in particulate waste materials", *Journal of Environmental Engineering © ASCE*, Vol. 129, Issue 10, pp. 930-942.
- Origgi, G., Colombo, M., De Palma, F., Rivolta, M., Rossi, P., Andreoni, V., (1997). "Bioventing of hydrocarbon-contaminated soil and biofiltration of the off-gas: results of a field scale investigation", *Journal of Environmental Science and Health*, Vol. A32(8), pp. 2298–2310.
- Padilla, I.Y., Yeh, T.C.J., and Conklin, M.H., (1999) "The effect of water content on solute transport in unsaturated porous media", *Water Resources Research*, Vol.35, No. 11, pp. 3303–3313.
- Parker, E.F., and Burgos, W.D., (1999). "Degradation patterns of fresh and aged petroleum-contaminated soils", *Environmental Engineering Science*, Vol. 16, pp. 21-29.
- Pavlostathis, S.G., and Mathavan, G.N., (1992). "Desorption kinetics of selected volatile organic compounds from field contaminated soils, *Environmental Science and Technology*, Vol. 26, pp. 532-538.
- Pignatello, J.J., (1990). "Slowly reversible sorption of aliphatic halocarbons in soils. 1. Formation of residual fractions", *Environmental Toxicology and Chemistry*, Vol. 9, pp. 1107–1115.
- Pignatello, J.J., and Xing, B., (1996). "Mechanisms of slow sorption of organic chemicals to natural particles", *Environmental Science and Technology*, Vol. 30, No. 1, pp.1-11.

- Powell, R. M. and Powell, P. D. 1998. "Iron Metal for Subsurface Remediation". *The Encyclopedia of Environmental Analysis and Remediation*. Robert A. Myers, ed. John Wiley & Sons, Inc., New York. 8:4729-4761.
- Powell, R. M. and R. W. Puls. July 1997a. "Permeable reactive subsurface barriers for the interception and remediation of chlorinated hydrocarbon and Chromium (VI) plumes in ground water". *U.S. EPA Remedial Technology Fact Sheet*. EPA/600/F-97/008.
- Praharaj, T., Powell, M.A., Hart, B.R., and Tripathy, S., (2002). "Leachability of elements from sub-bituminous coal fly ash from India", *Environment International*, Vol. 27, pp. 609-615.
- Punshon, T., Adriano, D.C. and Weber, J.T., (1999). "Restoration of Eroded Land using coal fly ash and biosolids", *Electrical Power research institute, Pal Alto, California*, TR-113940.
- Qiao, X.C., Poon, C.S., and Cheeseman, C., (2005). "Use of flue gas desulphurization (FGD) waste and rejected fly ash in waste stabilization/solidification systems", *Waste Management*, Vol. 26, Issue 2, pp. 141-149.
- Rathousky, J., and Zukal, A., (2000). "Adsorption of krypton and cyclopentane on C<sub>60</sub>: An experimental study", *Fullerene Science and Technology*, Vol. 8, No. 4, pp. 337-350
- Ricou, P., Lecuyer, I., and Cloirec, P. L. (1999). "Removal of Cu<sup>+2</sup>, Zn<sup>+2</sup>, and Pb<sup>+2</sup> by adsorption onto fly ash and fly ash/lime mixing," *Water Science Technology*, Vol. 39 (10-11), pp. 239-247.
- Robbins, G. A. (1989). "Methods for determining transverse dispersion coefficients of porous media in laboratory column experiments." *Water Resources Research*, Vol. 25, No. 6, pp. 1249-1258.
- Roberts, A. L., Totten, L. A., Arnold, W. A., Burris, D. R. and Campbell, T. J. (1996). "Reductive elimination of chlorinated ethylenes by zero-valent metals." *Environmental Science and Technology*, Vol. 30, No. 8, pp. 2654-2659.
- Roy, W.R., and Griffln, R.A., (1984). "Illinois Basin Coal Fly Ashes. 2. Equilibria relationships and qualitative modeling of ash-water reactions", *Environmental Science and Technology*, Vol. 18, pp. 739-742.
- Sajwan, K.S., Pushon, T., and Seaman J.C., (2006). "Production of coal combustion products and their potential uses", In: "*Coal Combustion Byproducts and Environmental Issues*", by Sajwan S., Twardowska, I., Pushon, T., and Alva, A.K., pp.3-9.

- Sangster Research Laboratories under auspice of the Canadian National Committee for CODATA sponsored by Canada Institute for Scientific and Technical Information CISTI website: <http://logkow.cisti.nrc.ca/logkow>
- Santhanam, C.J., Lunt, R.R., Johnson, S.L., Cooper, C.B., Thayer, P.S., and Jones, J.W., (1979). "Health and environmental impacts of increased generation of coal ash and FGD sludges", *Environmental Health Perspective*, Vol. 33, pp. 131-157.
- Sarkar, M., and Acharya, P.K., (2006). "Use of fly ash for the removal of phenol and its analogues from contaminated water", *Waste Management*, Vol. 26, pp. 559-570.
- Sato, S., and Comerford, N.B., (2006). "Assessing methods for developing phosphorus desorption isotherms from soils using anion exchange membranes", *Plant and Soil*, Vol. 279, pp. 107-117.
- Sauer, J.J., Benson, and C.H., Edil, T.B., (2005). "Metals leaching from highway test sections constructed with industrial byproducts", *Geo Engineering report No. 05-21, Department of Civil and Environmental Engineering, University of Wisconsin-Madison, Madison, Wisconsin*.
- Schaefer, C.E., Schüth, C., Werth, C.J., and Reinhard, M., (200). Binary desorption isotherms of TCE and PCE from silica gel and natural solids", *Environmental Science and Technology*, Vol. 34, pp. 4341-4347.
- Schicke, C. (1996). "Innovative evaluation methods for bioremediation: flow-cell construction and tracer analyses," *Northwestern University, Evanston, IL*.
- Shackelford, C.D., and Glade, M.J., (1997). "Analytical Mass leaching model for contaminated soil and soil stabilized waste", *Groundwater*, Vol. 35, No. 2, pp. 233-242.
- Shokes, T. E., and Möller, G., (1999). "Removal of dissolved heavy metals from acid rock drainage using iron metal", *Environmental Science and Technology*, Vol. 33, No. 2, pp. 282 -287.
- Smith, M.T, Berruti, F., and Mehrotra. A.K. (2001). "Thermal desorption treatment of contaminated soils in a novel batch thermal reactor", *Industrial Engineering and Chemical Research*, Vol. 40, pp. 5421-5430.
- Sočo, E., and Kalemekiewicz, J. (2007). "Investigations of sequential leaching behavior of Cu and Zn from coal fly ash and their mobility in environmental conditions." *Journal of Hazardous Materials*, Vol. 145, pp. 482-487.

- Su, C., and Puls, R. W., (2001). "Arsenate and arsenite removal by zero-valent iron: Kinetics, redox transformation, and implications for in situ groundwater remediation", *Environmental Science and Technology*, Vol. 35, No. 7, pp. 1487–1492.
- Theis, T.M., and Wirth, J.L., (1977). "Sorptive behavior of trace metals on fly ash in aqueous systems," *Environmental Science and Technology*, Vol. 11 (12), pp. 1096-1100.
- Twardowska, I., and Stefaniak, S., (2006). "Coal and coal combustion Products: Prospects for future and environmental issues", In: "*Coal Combustion Byproducts and Environmental Issues*" by Sajwan S., Twardowska, I., Pushon, T., and Alva, A.K.
- Vallejo, B.A., Izquierdo, and A., Blasco, R., (2001). "Bioremediation of an area contaminated by a fuel spill", *Journal of Environmental Monitoring*, Vol. 3(3), pp. 274-280.
- van der Hoek, E.E., and Comans, R.N.J., (1996). "Modeling arsenic and selenium leaching from acidic fly ash by sorption on iron (hydr)oxide in the fly ash matrix", *Environmental Science and Technology*, Vol. 30, pp. 517–523.
- van Genuchten, M. T., (1981). "Analytical solutions for chemical transport with simultaneous adsorption, zero-order production and first-order decay", *Journal of Hydrology*, Vol. 49, pp. 213-233.
- van Genuchten, M. T., and Wagenet, R. J., (1989). "Two-site/two-region models for pesticide transport and degradation: Theoretical development and analytical solutions", *Soil Science Society of America Journal*, Vol. 53, No. 5, pp. 1303-1310.
- van der Sloot, H.A., (1996). "Developments in evaluating environmental impact from utilization of bulk inert wastes using laboratory leaching tests and field verification", *Waste Management*, Vol. 16, No. 1, pp. 65-81.
- Yang, K., and Xing, B., (2007). "Desorption of polycyclic aromatic hydrocarbons from carbon nanomaterials in water", *Environmental Pollution*, Vol. 145, pp. 529-537.